SUMO: a heavyweight post- translational modification wrestling between plant stress responses.

MORRELL, REBECCA,ELIZABETH,SYLVIA

SUMO: a heavyweight post-translational modification wrestling between plant stress responses.

Rebecca Morrell

Thesis submitted for Degree of Doctor Of Philosophy

Department of Biosciences

Durham University

March 2021

Abstract

Post-translational modifications (PTMs) enable plants to modify proteins in response to environmental stimuli. Better understanding these PTMS is important to help crops adapt to the changing environment caused by climate change. This thesis has studied the role of a PTM called Small Ubiquitin Like Modifier (SUMO) which is stress induced. Conjugation of SUMO to target proteins alters the target protein, some of these proteins have been examined in this thesis.

The research has specifically examined the role of SUMO in the Abscisic Acid (ABA) pathway. The work has deduced the ABA sensitivity of SUMO protease knockout mutants. It has established the SUMOylation sites in the ABA negative regulator Protein Phosphatase 2CA (PP2CA) and generated transgenic *Arabidopsis thaliana* expressing both a SUMOylatable and non-SUMOylatable form of PP2CA to determine the ABA phenotype. ABA mediated root inhibition and expression of ABA response genes has indicated that SUMOylated PP2CA may aid ABA signalling. It was hypothesised this may be in part due to a SUMO Interacting Motif (SIM) site located in the PYLS, a SIM site was identified in PYL8 and was not present in PYL1. *Arabidopsis thaliana* transgenics were generated to enable further understanding of the role of SUMO in the ABA pathways.

Additionally the role of SUMO in root hair formation was examined, based on the double SUMO protease knockout mutant *ots1 ots2* being found to have longer and fewer root hairs. A transcription factor required for root hair development RHD-Six Like 4 (RSL4) was found to contain three SUMO sites. Transgenic *Arabidopsis thaliana* was generated to examine the role of SUMOylatable and SUMO site mutated RSL4, however this led to contradictory results. Protein stability indicated that SUMOylatable RSL4 may be more stable and/or transcribe more RSL4 promoted genes than SUMO site mutated RSL4, but has smaller root hairs when grown on ethylene supplemented media. These contradictory results may be due to different roles of the three SUMO sites in RSL4.

Lastly research was continued on a project that had been started by Dr Vivek Verma, who had determined that a SUMO site in the GRAS domain of DELLA protein, Gibberellic Acid Insensitive (GAI) altered interactions with transcription factors. A SIM site was identified in Phytochrome Interacting Factor 4 (PIF4), which may be responsible for increased interaction of PIF4 when GAI is SUMOylated. Wild-type and SIM mutated PIF4 transgenic *Arabidopsis thaliana* was generated to understand the role of SUMO in GAI PIF4 interactions. The GAI SUMO site mutated transgenic *Arabidopsis thaliana* which had been generated by Dr Vivek Verma were analysed for Jasmonic acid phenotype and hypocotyl elongation phenotype.

Contents

List of publications

1. Morrell R, Sadanandom A. (2019) Keeping Up With the Pathogens: The Role of SUMOylation in Plant Immunity 2019b SUMOylation and Ubiquitination: Current and Emerging Concepts (Edited by: Van G. Wilson). Caister Academic Press, U.K. Pages: 489-5002
2. Morrell R, Sadanandom A. (2019) Dealing with stress: A Review of plant SUMO proteases. Front. Plant. Sci. 10:1122. doi: 10.3389/fpls.2019.01122.
3. Verma V, Srivastava A K, Gough C, Campanaro A, Srivastava M, Morrell R, Joyce J, Bailey M, Zhang C, Krysan P J, Sadanandom A. (2021) SUMO enables substrate selectivity by mitogen-activated protein kinases to regulate immunity in plants. PNAS 9;118(10):e2021351118. doi: 10.1073/pnas.2021351118

List of figures

List of tables

Abbreviations

- ABA — Abscisic Acid
- ACC — 1-Aminocyclopropane-1-Carboxylic Acid
- bHLH — Beta Helix-Loop-Helix
- BLAST — Basic Local Alignment Search Tool
- Bp — Base Pair
- cDNA — Complementary DNA
- Col-0 — Colombia-0
- Desi — deSUMOylation isopeptidase
- DNA — Deoxyribonucleic Acid
- GA — Gibberellic Acid
- GAI — GIBBERELLIC ACID INSENSITIVE
- gDNA — Genomic DNA
- GFP — Green Fluorescent Protein
- GID1 — GIBBERELLIN INSENSITIVE DWARF 1
- GRAS — GA INSENSITIVE (GAI), REPRESSOR of *ga1-3* (RGA), and SCARECROW (SCR)
- HA — Hemagglutinin of Influenza Virus
- IAA — Indole-3-Acetic Acid
- JA — Jasmonic Acid
- JAZ — JASMONATE ZIM DOMAIN
- kDa — Kilo Dalton
- KO — Knockout

- MAMP — Microbial Associated Molecular Pattern
- MS — Murashige & Skoog (media)
- OTS1/2 — OVERLY TOLERANT TO SALT 1/2
- PAMP — Pathogen Associated Molecular Pattern
- PCR — Polymerase Chain Reaction
- Pi — Phosphate
- PIF — PHYTOCHROME INTERACTING FACTORS
- PP2CA — PROTEIN PHOSPHATASE 2CA
- Pst — *Pseudomonas syringae* DC3000
- PTM — Post Translational Modification
- PYL8 — PYR1-LIKE 8
- RHD6 — ROOT HAIR DEFECTIVE 6
- RNA — Ribonucleic Acid
- RSL4/2- — RHD-SIX LIKE 4/6
- SA — Salicylic Acid
- SIM — SUMO Interacting Motif
- SIZ1 — SAP & MIZ1
- SnRK2 — SNF1-RELATED PROTEIN KINASE 2
- SPF1/2 — SUMO PROTEASE RELATED TO FERTILITY 1/2
- SUMO — SMALL UBIQUITIN-LIKE MODIFIER
- USPL — UBIQUITIN-SPECIFIC PROTEASE-LIKE

Declaration

This thesis is submitted to the University of Durham in support of my application for the degree of Doctor of Philosophy. It has been composed by myself and has not been submitted in any previous application for any degree. The work (including data generated and data analysis) was carried out by the author except where explicitly states otherwise.

Becky Morrell

Statement of copyright

Acknowledgements

First off I would like to thank my supervisor Ari Sadanandom, thanks for all the ideas, enthusiasm and knowledge on SUMO. Also thanks very much for all the help proofreading my thesis!

I am really grateful to everyone in the lab who has helped me throughout my phd. Thanks so much to Beatriz for first showing me around the lab and helping me with the dreaded IPs, I really appreciate your time. Thanks as well to my bench mates Vivek and Moumita for really helping to show me what to do, also big thanks to Anjil for all your help and advice. I hope you guys appreciated all the music and sorry for annoying you guys by constantly leaving my timer for you guys to turn off. I also need to thank Cunjin for your help, TV recommendations and Chinese lessons. I hope to be your PA for a few more years to come! Also a massive thanks to everyone else in the lab who has come and gone throughout the years Linda, Daniel, Mahsa, Fen, Jack and Gary, I really enjoyed working with you guys and was sad when you all left! Thanks also to current lab members Luke, Catherine, Navi, Alberto and all the new team in the lab as well thanks for your help!

Thanks also to the 12 oclock lunch team, although we haven't been able to have lunch together for over a year now it was always a highlight of the day and I hope we can go back to it soon! I also need to thank lab 1 (Elaine, Fieka, Jack and the old members) who first introduced me to lab science in my masters and gave a bench to work at during covid and job after. I'm so happy to be reintroduced to the 11 oclock coffee!

I also need to thank the other staff in the department that have kept everything running and helped me with my research including the microscopy facility staff and the technicians that grow all the plants! Thanks so much for helping my research run more smoothly!

I also want to thank the cool cats and kittens facebook chat, I really enjoy our weekly chats and I'm so glad covid has kept us in better contact! I've appreciated the distractions from work and checking if my plants are growing ok. With a special thanks to Alicia and Matt for help proofreading! Sorry the draft I sent was so bad! Also a special thanks to Sara it was so much fun living together in first year and I'm so grateful you introduced me to Gilmore Girls!

I also need to say a big thanks to my lovely family Mum, Dad, Thomas, Nan and Nan thank you for being so helpful and reassuring and supporting me through everything I love you guys.

Lastly thanks to Oliver who has fed me, motivated me, been as enthusiastic about Rupaul's Drag Race UK as me and still thinks all I do all day is count seeds. Shantay you stay.

Chapter 1

Introduction

1.1 SUMOylation

Proteins participate in nearly all cellular activities, capable of carrying our catalytic, regulatory, signalling and structural functions. Most proteins in the proteome (the complete set of proteins expressed by an organism) become post-translationally modified through their lifetime. Post-translational modifications (PTMs) include small functional groups or complex biomolecules conjugating to amino acid side chains or cleavage, splicing and cyclising the protein backbone. These transformations alter protein structures, destinations, interactions and activities and enable a wider variety of diversity and complexity in the proteome, than would be predicted by the number of protein-coding sequences in the genome. PTMs are mostly dynamic, to enable cells to rapidly respond to the environment (Conibear, 2020).

Small Ubiquitin-like MOdifier (SUMO) is a small polypeptide PTM that is critical for normal functions in eukaryotes, being conserved amongst the domain. Deleting the only SUMO isoform, SMT3, from a yeast (*Saccharomyces cerevisiae)* cell, causes a loss of cell viability (Meluh and Koshland, 1995; Giaever et al., 2002) and deletion in

Arabidopsis thaliana (Arabidopsis hereafter) of SUMO1 and SUMO2 is embryo lethal (Saracco et al., 2007; van den Burg et al., 2010), highlighting the critical role of SUMO in cell biology.

SUMOylation, the reversible attachment of SUMO onto a target lysine (K), is considered to be a stress response mechanism as SUMO conjugation to proteins is induced by heat, ethanol, drought and oxidative stress. This is conserved across many species, including *Arabidopsis, Drosophila*, and *Caenorhabditis elegans* to humans (Saitoh and Hinchey, 2000; Kurepa et al., 2003; Augustine et al., 2016). Due to its response to stress SUMOylation is highly dynamic and SUMO is quickly cycled between conjugated and free forms enabling accurate, rapid, specific responses to stimuli. *Arabidopsis* is predicted to have 5660 SUMOylated proteins, on a par with other major PTMs (post-translational modifications) like phosphorylation and ubiquitylation (Drabikowski et al., 2018; Miller et al., 2019).

However, in addition to stress responses SUMO is also implicated in many essential cellular responses. In *C. elegans* SUMOylated proteins are involved in genome stability, cell cycle progression, chromatin maintenance and modification, transcription, translation, RNA splicing, and ribosome biogenesis (Drabikowski et al., 2018). However, despite the large number of proteins that can be SUMOylated it has been observed that commonly, only a small percentage of target proteins are SUMO modified at a given time, entitled the "SUMO enigma" by Hay (2005).

SUMO is named due to its similarity to a well-studied post-translational modifier Ubiquitin, both contain a β-fold grasp (characterised by β-sheet with five anti-parallel β-strands and a single helical element between strands β-4 and β-5). However, they harbour low amino acid sequence similarity, resulting in different biochemical properties causing altered functions in the cell. The primary role of Ubiquitin is to destabilise and ultimately degrade proteins via the 26s proteasome, regulating protein stability in response to molecular stimuli. SUMO, in contrast, regulates protein function using a number of different mechanisms (figure 1.1).

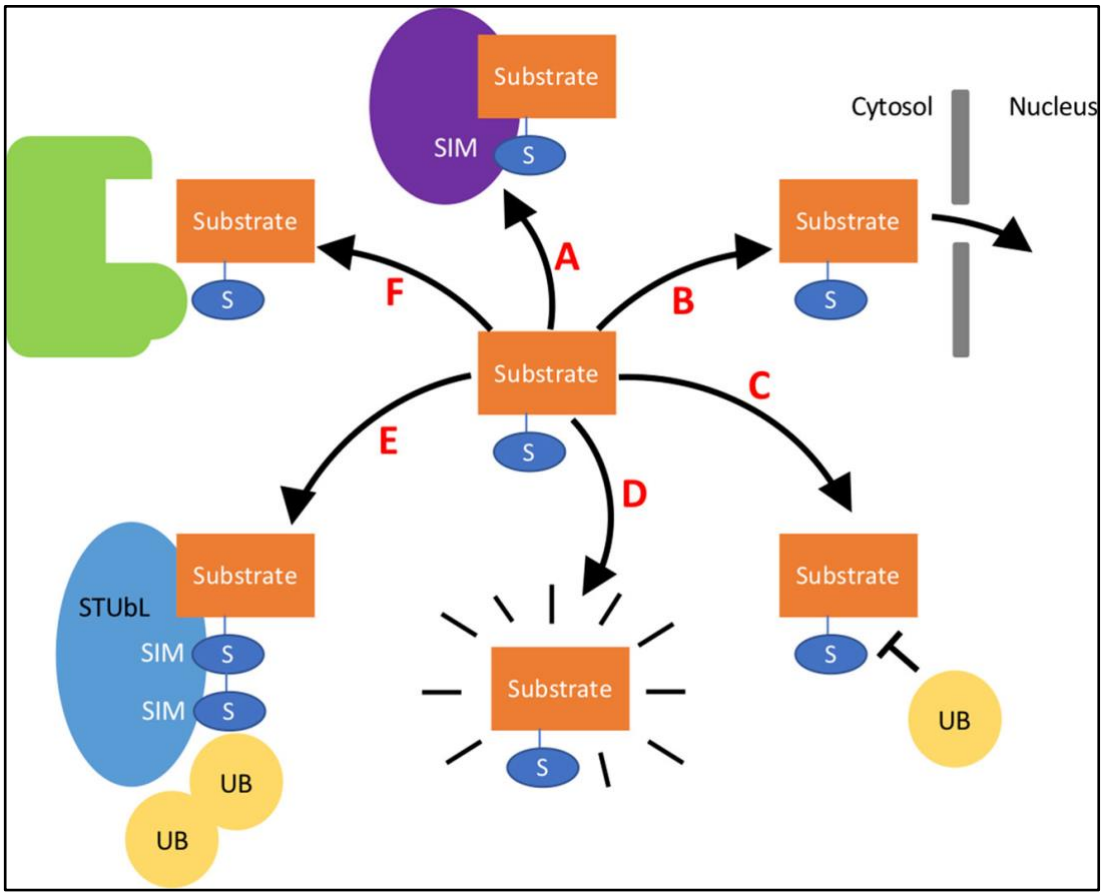

Figure 1.1 The variety of effects SUMO can have on its substrates. ***A****- SUMO (blue oval containing S) can aid interaction with proteins containing a SUMO interacting motif (SIM) site.* ***B****- SUMO can change the cellular localisation of a protein—for example, directing the protein to the nucleus.* ***C****- SUMO can protect substrates from degradation by blocking lysine residues in substrates that may be Ubiquitinated (yellow circle containing UB).* ***D****- SUMO binding to a protein can alter its structure, activating the protein.* ***E****- SUMOylated proteins can signal to STuBL proteins to target for degradation via ubiquitination.* ***F****- SUMO can block interaction with proteins by blocking binding sites.*

If a SUMO chain forms it can result in protein degradation via SUMO-Targeted Ubiquitin Ligases (STUbLs) culminating in Ubiquitination and degradation by the 26S proteasome (Elrouby et al., 2013). However, SUMOylation of target proteins can also result in enhanced interaction with a protein harbouring a SUMO Interacting Motif (SIM) site. SUMO can also block interaction with proteins by steric interference. In addition, SUMO binding to a target protein can signal the protein to change cellular location within a cell. Additionally, due to both SUMO and Ubiquitin attaching via a di-glycine motif to lysine residues in target proteins, SUMOylation can protect proteins from Ubiquitination by protecting lysine residues prone to Ubiquitination. Finally, SUMO binding to a protein can confer conformational changes to modified proteins altering its activity levels (Johnson, 2004; Wilkinson and Henley, 2010).

The outcome of SUMOylation is largely target dependent and altered by the location and number of SUMO substrates on a target (Wilkinson and Henley, 2010). Indeed, target protein substrates can have single SUMO monomers covalently attached to a lysine, multiple SUMO monomers attached to multiple lysines, or a polySUMO chain from one lysine. This results in a high complexity of different SUMO patterns that can form on one protein altering the molecular consequences of the SUMOylation. For example, SUMOylation at one site may stabilise the protein by protecting the lysine from ubiquitination and SUMOylation at a second site may promote interaction with a protein harbouring a SIM site that usually the substrate does not interact with.

1.1.1 SUMOylation pathway

Despite the difference in the biochemical properties of Ubiquitin and SUMO, the two protein families share very similar biochemical steps that catalyse conjugation onto target proteins (figure 1.2). Firstly, mature SUMO is generated by a SUMO peptidase cleaving 10 amino acids, exposing a carboxyl-terminal diglycine motif (Johnson, 2004). SUMO is activated by an E1 activation heterodimer of SAE1/2 (SUMO-Activating Enzyme). SAE1 has two isoforms SAE1a and SAE1b; either can be used to create the E1 heterodimer with SAE2, using ATP (Adenosine TriPhosphate) the complex forms SUMO-AMP. The AMP (Adenosine MonoPhosphate) is released from the SUMO-AMP resulting in the formation of a high-energy thioester bond between the sulfhydryl group of the catalytic cysteine residue in SAE2 and the carboxyl group of glycine in SUMO.

Activated SUMO is transferred from the SAE2 to a cysteine residue in SCE1 (SUMO Conjugating Enzyme), an E2 conjugation enzyme, in a transesterification reaction to form SUMO-SCE1 thioester complex. This complex catalyses the reaction of SUMOylation onto a lysine in the target substrate *via* an isopeptide bond between the SUMO carboxyl terminal glycine and the ε-amino group of lysine (K). The lysine, typically, is part of the SUMOylation consensus motif ψKXE/D; ψ denotes a large hydrophobic residue, K the acceptor lysine, X any amino acid, and E/D glutamate or aspartate.

SUMO E3 ligases are SCE1-interacting proteins that also help aid the transfer of SUMO from SCE1 to the target substrate. There are two identified E3 ligases in *Arabidopsis* SIZ1 (SAP and MIZ1) and HPY2 (High PloidY2)/MMS21 (Methyl Methanesulfonate Sensitivity 21), these complex proteins require a number of domains including nuclear localisation and SIM sites. However, SUMOylation of a target residue can occur without the presence of E3 ligases (Castano-Miquel et al., 2011); it is as yet unclear how essential E3 ligases are, they may enhance and amplify SUMO conjugation (Okada et al., 2009; Gareau and Lima, 2010). An additional catalytic step has been identified involving E4 ligases, that promote SUMO chain formation in a SCE1-dependent manner; two E4 ligases have been identified in *Arabidopsis* PIAL1 and 2 (Protein Inhibitor of Activated STAT-Like 1/2) (Tomanov et al., 2014).

Finally, SUMOylation is a cyclical process due to SUMO proteases, which carry out two main functions in the SUMO system. First, they cleave SUMO from target substrates, providing a pool of free SUMO, making SUMO a reversible modification (isopeptidase activity). Secondly, they mature newly synthesized SUMO by cleaving a c-terminal peptide from the immature SUMO (hydrolase/peptidase activity). These sources of SUMO are believed to be critical in the SUMO cycle as the cellular pools of unconjugated SUMO are very low (Johnson, 2004). In yeast, there are two SUMO proteases ULP1 and 2 (Ubiquitin-Like Protease 1/2); the *ulp1-1* mutant is lethal, demonstrating the critical role of SUMO proteases in cell function. Conversely 16 SUMO proteases have been identified in *Arabidopsis*, so far only *Arabidopsis* mutants in up to two SUMO proteases at a time have been generated.

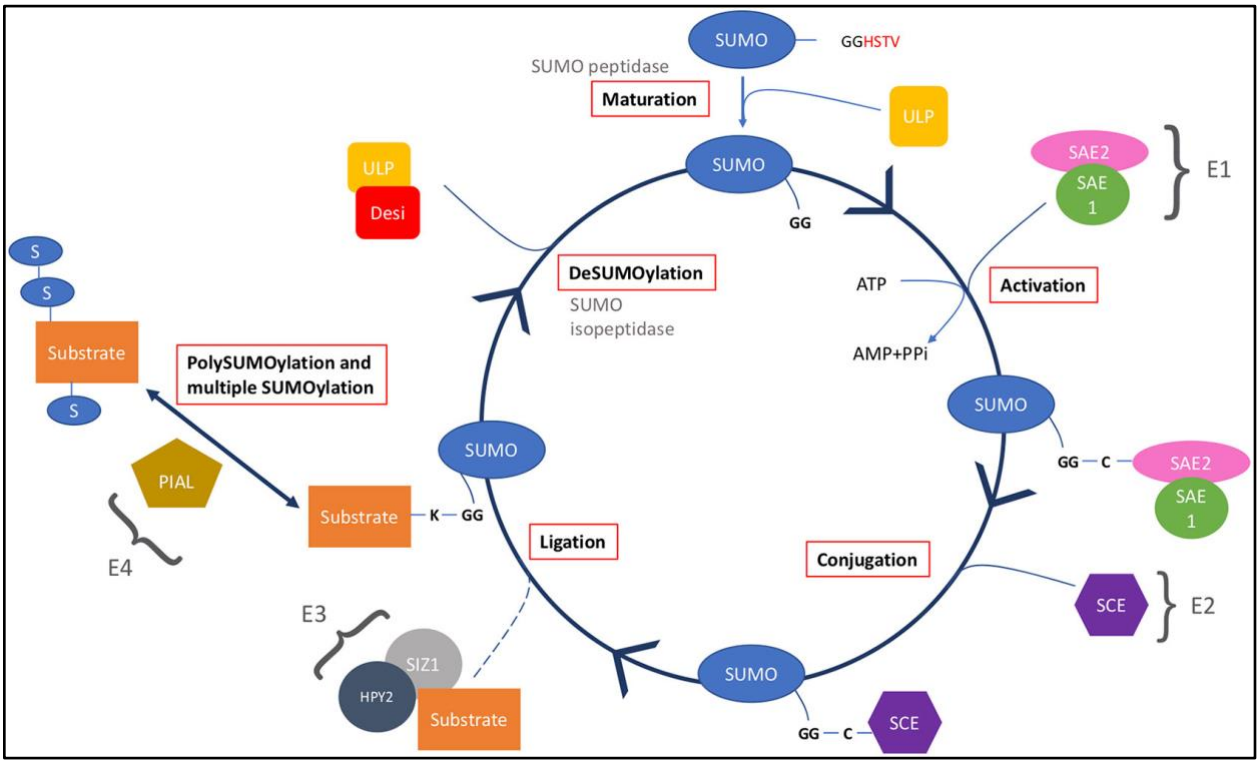

Figure 1.2 The mechanism of SUMOylation in Arabidopsis. *The SUMO cycle starts with maturation of immature SUMO by cleaving off the C-terminus using a SUMO peptidase. Mature SUMO is then activated using ATP and a heterodimer of SAE1 and SAE2. The SUMO is then passed to SCE in a conjugation step, and using a SUMO ligase is ligated onto the substrate. This substrate can then be SUMOylated at more than one SUMO site or from a polySUMO chain. Lastly, in the deSUMOylation step, SUMO is removed from the substrate using a SUMO isopeptidase to generate free SUMO.*

In the ubiquitin system, it is assumed that the ubiquitin E3 ligases provide the specificity in the system due to the large number of E3 ligases. However, in the SUMO system, two SUMO E3 ligases have been identified. In contrast, a relatively larger number of SUMO proteases have been identified, which display specificity to the target proteins,

suggesting that they may provide specificity in the SUMO system (Chosed et al., 2006; Colby et al., 2006; Yates et al., 2016; Benlloch and Lois, 2018).

1.1.2 SUMO proteases

In *Arabidopsis* there are two main classes of SUMO proteases which possess variable ability to mature SUMO and cleave SUMO from target substrates. The SUMO proteases currently identified in eukaryotes are all cysteine proteases. Cysteine proteases are named after the cysteine residue (in their active site triad or dyad), which is used as a nucleophile to break the thioester bond between the SUMO and target protein (Rawlings et al., 2008). Also present in the active site is a histidine that functions as a general base, and additionally, in some cases, there is an extra base that is required for stability. The orientation of the cystine, histidine, and stabilising amino acid can differ (Rawlings et al., 2008). Additionally all the SUMO proteases identified contain a papain fold, which characterises all ubiquitin-specific and UBL-specific cysteine proteases characterised so far (Gillies and Hochstrasser, 2012).

The ULP (Ubiquitin Like Protease) SUMO protease family, first identified in plants due to their similarity to yeast ULP1/2 proteases, belong to the same cysteine protease clan CE and family C48. The CE clan is characterised as having a catalytic triad with residues in the order histidine, glutamine (or asparagine), and then cysteine (figure 1.3). Currently, eight ULPs have been predicted in *Arabidopsis*; six have been characterised as SUMO proteases (Table 1.1).

However, two new classes of SUMO proteases have since been identified, whilst all the SUMO proteases are cysteine proteases surprisingly they are members of different clans and families. The different clan classifications show evolutionary relationships and are based on the different amino acids and the order of the amino acids required for the active site. Within the clan, the proteases are further characterised into families which shows a statistically significant relationship in amino acid sequence to at least one other family member.

Shin et al. (2012) identified a novel type of SUMO protease in mouse; the two proteins were named DeSI1 (DeSUMOylating Isopeptidase1) and DeSI2 and lacked sequence similarity to ULP enzymes. They are members of the CP clan, C97 family, the CP clan has a catalytic dyad composed of histidine and cysteine (figure 1.3): in the DeSI active site, no third residue is required (Suh et al., 2012). Orosa et al. (2018) identified eight putative DeSI proteases in *Arabidopsis* based on sequence similarity to human DeSI1/2 and functionally characterised one protein, DeSI3a.

Another SUMO protease recently identified in humans is called USPL1 (Ubiquitin-Specific Protease-Like1) (Schulz et al., 2012); two homologues have been predicted, via bioinformatic techniques, however, they have not been characterised in *Arabidopsis* (Morrell and Sadanandom, 2019a). USPL is a clan CA C98 cysteine protease family

member (Rawlings et al., 2008). The CA clan is characterised as having the catalytic triad in the opposite orientation to that of CE clan with the residues cysteine, histidine, and asparagine (or Aspartic acid) (figure 1.3).

Table 1.1 The SUMO proteases currently identified in Arabidopsis.

Name	Cysteine protease clan	Cysteine protease family	Tair accession	Characterised?	Reference
Overly Tolerant to Salt 1 (OTS1) (ULPd)	CE	C48	At1G60220	Yes	Kurepa et al., 2003, Chosed et al., 2006, Colby et al 2006
Overly Tolerant to Salt 2 (OTS2) (ULPc)	CE	C48	At1g10570	Yes	Kurepa et al., 2003, Chosed et al., 2006, Colby et al 2006
Early in Short Days4 (ESD4)	CE	C48	At4g15880	Yes	Murtas et al., 2003
ESD4 Like SUMO protease 1 (ELS1) (ULP1a)	CE	C48	At3g06910	Yes	Kurepa et al., 2003
ESD4 Like SUMO protease 2 (ELS2) (ULP1b)	CE	C48	At4g00690	Yes	Kurepa et al., 2003
Fourth ULP Gene 1 (FUG1)	CE	C48	At3g48480	No	Lois 2010
SUMO Protease related to Fertility 1 (SPF1) (ASP1/ULP2like2)	CE	C48	At1g09730	Yes	Novatchkova et al., 2004, Liu et al., 2017, Kong et al., 2017
SUMO Protease related to Fertility 2 (SPF2) (ULP2like1)	CE	C48	At4g33620	No	Novatchkova et al., 2004, Liu et al., 2017, Kong et al., 2017
DeSI 1	CP	C97	At3g07090	No	Orosa et al., 2018
DeSI 2A	CP	C97	At4g25660	No	Orosa et al., 2018
DeSI 2B	CP	C97	At4g25680	No	Orosa et al., 2018
DeSI 3A	CP	C97	At1g47740	Yes	Orosa et al., 2018
DeSI 3B	CP	C97	At2g25190	No	Orosa et al., 2018
DeSI 3C	CP	C97	At5g25170	No	Orosa et al., 2018

DeSI 4A	CP	C97	At4g17486	No	Orosa et al., 2018
DeSi 4B	CP	C97	At5g47310	No	Orosa et al., 2018

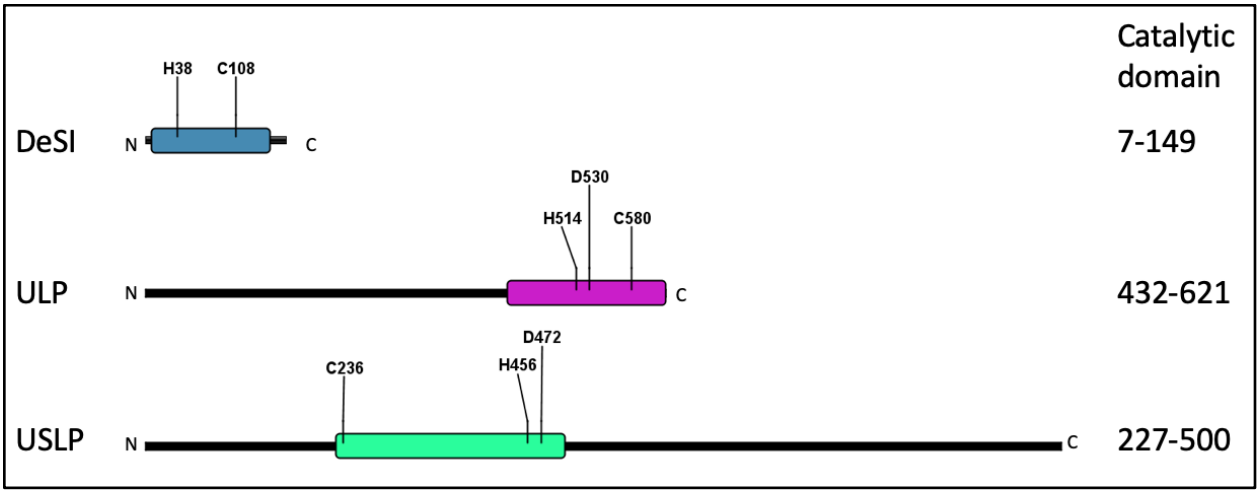

Figure 1.3 The domain organisation and length (in amino acids) of the SUMO proteases family class. *The DeSI catalytic domain is shown in blue, the ULP catalytic domain in pink and the USPL catalytic domain in green. The key residues in the catalytic triad/dyad are shown along with the amino acid number position they are located in, in the human DeSI1, yeast ULP1 and human USPL1 proteins.*

The ULP SUMO proteases are evolutionarily distinct from the DeSI SUMO proteases (Figure 1.4). The ULP SUMO proteases have a phylogenetic origin that can be traced to green algae and other eukaryotes including yeast ULP1 and ULP2 (Castro et al., 2018), whereas the DeSI proteases have not been identified in yeast. The evolutionary classification of the proteases has proved difficult due to the high amino acid sequence divergence. Initially, the ULP SUMO proteases was classified on similarity to the yeast *Sc*ULP1 or *Sc*ULP2 based on the location of the active site in the protein (Figure 1.3) (Novatchkova et al., 2004; Lois, 2010). However, a different classification was found based on amino acid conservation (Castro et al., 2018). The current classification in use was carried out by Novatchkova et al. (2012), who conducted an in-depth phylogenetic analysis, including *Arabidopsis*, tomato, grapevine, and poplar genomes. They generated a novel grouping of the ULP proteases into four groups in *Arabidopsis*, namely, A, B1, B2, and C (Novatchkova et al., 2012). The classification system was also adopted by Benlloch and Lois (2018) and Castro et al. (2018), with the latter changing the naming system which is being used in this thesis. Class I ELS type of homologues is believed to have evolved from ScULP1 including ESD4, ELS1, and ELS2. Three different subdivisions have evolved from ScULP2 including class II OTS-type homologues including OTS1 and OTS2 and class III SPF-type homologues, including SPF1 and SPF2 and class IV FUG type that is yet to be characterised as a SUMO protease.

However, the relationship of FUG1 to the other SUMO protease groups strongly suggests that it has the same activity (Novatchkova et al., 2012). FUG1, unlike the other ULPs is absent from early plant taxa, being present in flowering plants (Castro et al., 2018).

The DeSI proteins are not as well studied evolutionarily due to their very recent identification in *Arabidopsis*; however, due to the similarities in some of their sequences, it can be hypothesised that they may share functional redundancy (Orosa et al., 2018), but this is yet to be determined. If USPL1 homologues are found in *Arabidopsis*, it is likely that they will share more evolutionary similarity with the ULP proteases as clan CE proteases are hypothesised to share sequence similarity with clan CA proteases.

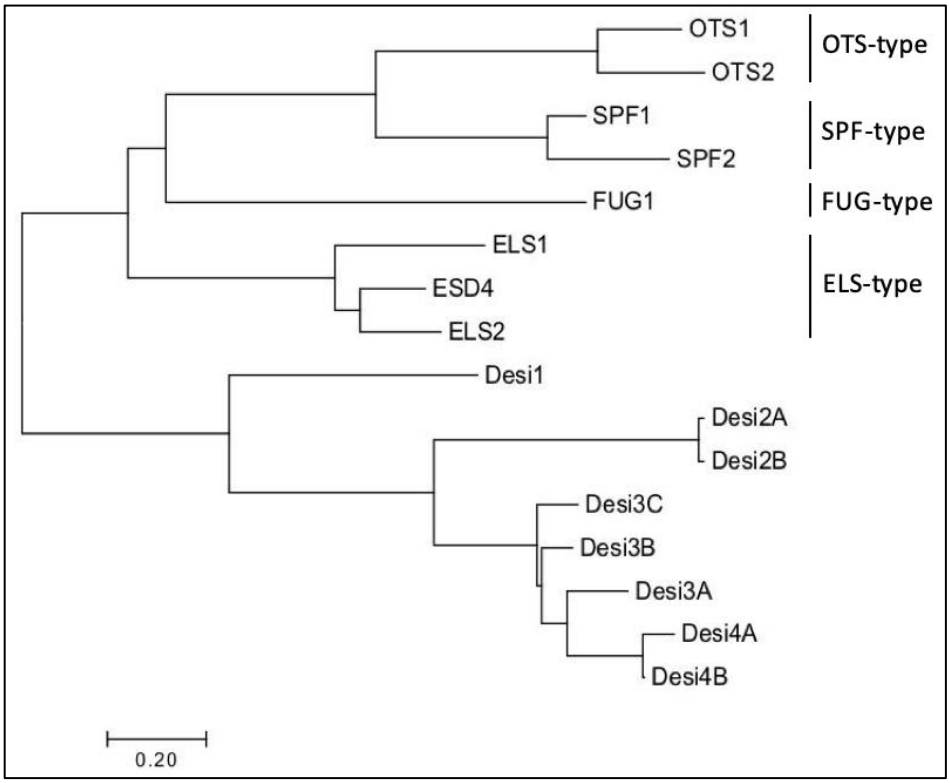

Figure 1.4 Phylogenetic tree of currently identified SUMO proteases in Arabidopsis. *The proteases cluster according to their catalytic triad. Alignments were made using ClustalX and visualized in Jalview. Bootstrap neighbor-Joining trees were made using ClustalX and visualized using MEGA7. OTS1 (At1g60220), OTS2 (At1g10570), SPF1 (At1g09730), SPF2 (At4g33620), FUG1 (At3g48480), ELS1 (At3g06910), ESD4 (At4g15880), ELS2 (At4g00690), Desi1 (At3g07090), Desi2A (At4g25660), Desi2B (At4g25680), Desi3A (At1g47740), Desi3B (At2g25190), Desi3C (At5g25170), Desi4A (At4g17486), Desi4B (At5g47310).*

1.1.3 SUMO-interacting motifs (SIMs)

A key effect SUMO can have on a protein is by altering protein interactions through SUMO-interacting motifs (SIM) sites, first identified by Minty et al., 2000. These are hydrophobic patches on a protein's beta sheet, flanked by acidic amino acids that enable non-covalent interaction with the β-grasp fold in SUMO that contains an α-helix and β-sheets. The β-sheet in the protein harbouring the SIM site slots between the α-helix and β-sheet in the SUMO in an anti-parallel manner. This enables proteins containing SIM sites to interact more readily with SUMOylated proteins (Hecker et al., 2006) depending on the SUMO-isoform, as SIMs display SUMO-isoform specificity.

In addition to a lot of SIMs being present in the general proteome (Conti et al., 2014; Srivastava et al., 2018) SIMs are also important components in the SUMO cascade, found in E2 and E3 enzymes in addition to the SUMO proteases. SIM sites in the E2 enzyme enable the enzyme to transfer the activated E1-SUMO complex to the target protein (Duda et al., 2007). The SIM site in the E3 enzyme facilitates binding to the SUMO-E2 complex to aid SUMOylation on target proteins (Yang and Sharrocks, 2010). Some SIM sites are located near the SUMOylatable lysine in target proteins to also facilitate binding to the SUMO-E2 complex and aid SUMOylation on the protein (Lin et al., 2006). For similar reasons some of the SUMO proteases have been predicted to contain SIM sites as this aids recognition and binding to proteins that require deSUMOylation (Hickey et al., 2012; Peek et al., 2018).

1.1.4 The role of SUMO in plants

In *Arabidopsis* eight isoforms of SUMO have been identified using bioinformatic techniques (Novatchkova et al., 2004). In *Arabidopsis*, SUMO1, 2, 3, and 5 are expressed (Benlloch and Lois, 2018), but only the 11-kDa SUMO1 and 2 are expressed at high levels (Castaño-Miquel et al., 2011), suggesting the remaining SUMOs may be pseudogenes or do not play a significant role in the cell. *At*SUMO1 and 2 share 83% amino acid sequence identity and are functionally similar to human SUMO2/3 these SUMOs have similar functions and are influenced by stress conditions. *At*SUMO3/5 are weakly expressed non-conserved isoforms containing approximately 35% sequence similarity to *At*SUMO1/2 (Castaño-Miquel et al., 2011). SUMO in *Arabidopsis* is critical, as deletion in *Arabidopsis* of *sumo1sumo2-1* is embryonic lethal (Saracco et al., 2007; van den Burg et al., 2010). In addition to SUMO playing critical roles in cell biology and being required for cell viability, SUMO also plays many important roles in hormone pathways and stress responses in *Arabidopsis*.

The auxin response factor ARF7 responds to dry environments in the soil, when a root surface is in contact with water ARF7 promotes the formation of lateral roots. This process relies on SUMOylation, in wet environments ARF7 is not SUMOylated and is capable of binding to DNA and promotes translation of LBD16 (Lateral organ Boundaries Domain 16), required for lateral root formation. However, on the dry side of the root ARF7 is SUMOylated, the

SUMOylation is required to recruit the auxin repressor protein IAA3 which inhibits lateral root formation (Orosa-Puente et al., 2018).

The *Arabidopsis* mutant deficient in the SUMO E3 ligase MMS21/HPY2 has shorter roots caused by deficient elongation zones in the root. The *mms21-1* mutant has reduced responses to external cytokinin and reduced expression of cytokinin-induced genes *ARR3, ARR4, ARR5* and *ARR7*. Expression of the cytokinin receptor and positive regulator of cytokinin signalling, *CRE1* (Cytokinin REsponse1) and *ARR1*, respectively, is reduced in the *mms21-1* mutants. Whilst the protein target of MMS21 has not been found, it is likely that one of its targets is in the cytokinin signalling cascade (Huang et al., 2009).

In tomato (*Solanum lycopersicum*) ethylene is an important hormone, employed by plants upon infection with *Xanthomonas euvesicatoria* (*Xcv*). Upon infection ethylene responsive transcription factor SlERF4 (*Solanum* Ethylene Responsive transcription Factor4) is SUMOylated, stabilising the protein. This enables the protein to promote transcription of ethylene response genes and increase ethylene levels. To aid its disease progression, *Xcv* injects into plant cells effector molecules. One effector XopD (Xanthomonas Outer Protein D) has SUMO protease activity and desSUMOylates SlERF4 to destabilise the protein and reduce ethylene production and plant immunity (Kim et al., 2013).

Srivastava et al (2018) discovered that the JA repressor protein JAZ contains a SUMO site that is SUMOylated upon necrotrophic infection, due to degradation of OTS1, but deSUMOylated upon biotrophic infection. The SUMOylation of JAZ under necrotrophic infection prevents COI1-mediated degradation of JAZ, resulting in accumulation of the JA repressor, preventing JA signalling. Conversely, upon biotrophic infection OTS1 accumulates and deSUMOylates JAZ, enabling binding with COI1 and ubiquitin mediated degradation, resulting in downstream signalling of JA response genes (Srivastava et al., 2018). The jasmonic acid (JA) and salicylic acid (SA) pathways are both important in pathogen defence, however SA acts antagonistically with JA. SUMOylation or deSUMOylation of the JA repressor protein enables *Arabidopsis* to switch between the prominent defence hormones in pathogen defence, dependent on the pathogen lifestyle traits (Srivastava et al., 2018).

The role of SUMO in salicylic acid (SA) signalling was first discovered in mutants defective in the SUMO E3 ligase SIZ1 (Salt Induced Zinc finger1). *siz1* mutants had higher levels of SA and constitutively active pathogen defence responses, callose deposition, increased resistance to pathogens, cell death and early flowering (Lee et al., 2007; Jin et al., 2008). Like the *siz1-1* mutant the ESD4 SUMO protease mutant *esd4-1* mutant shows a similar dwarf mutant. Mutation of ICS1 (IsoChorismate Synthase1), an SA biosynthesis gene, in the *esd4-1* mutant background results in partial recovery of the phenotype (Hermkes et al., 2010; Villajuana-Bonequi et al., 2014) suggesting the elevated SA levels contribute to the phenotype of *esd4-1* similar to *siz1-1.* The double *sumo1 sumo2* mutant is embryo lethal, whereas silencing SUMO2 in *sumo1-1* mutants (*sumo1-1amiR-SUMO2*) is viable. These mutants lead to accumulation of SA derivatives and activated SA-dependent defence responses, resulting in resistance to *Pseudomonas syringae*

(*Pst*) (van den Burg et al., 2010). Confusingly in addition to mutating SUMO, overexpressing SUMO1 or SUMO2 or conjugation deficient mutants both result in an increase in SA levels and activated defences compared to wild type (van den Burg et al., 2010). The SUMO protease OTS1 and OTS2 double mutant *ots1-1 ots2-1* also have higher endogenous levels of SA, which may be caused by increased expression of *ICS1* which causes enhanced resistance to *Pst*. The presence of SA results in degradation of OTS1/2 in turn promoting accumulation of SUMO1/2 conjugates, suggesting a feedback loop in SA signalling. SUMO1/2 conjugates may play a positive role in SA-mediated signalling (Bailey et al., 2016).

The SUMO protease ULP1A/ELS1 mutant has reduced sensitivity to salt, a stress which is known to inhibit brassinosteroid signalling. The brassinosteroid transcription factor BZR1 is SUMOylated in the nucleus, stabilising the protein as the SUMO blocks interaction with BIN2, preventing its degradation. During salt stress *Arabidopsis* arrests growth by deSUMOylating BZR1 in the cytoplasm and promoting accumulation of ULP1a, which deSUMOylates BZR1. Conversely ULP1a destabilises in the presence of brassinosteroids, enabling SUMOylated BZR1 to accumulate and promote growth. The *ulp1a* mutants are insensitive to BRZ (BRassinaZole), that inhibits biosynthesis of brassinosteroid. BRZ stimulates salt stress, reduced signalling of brassinosteroids results in accumulation of ULP1a, however the mutant accumulates SUMOylated BRZ1 and does not cease growing. There is no phenotypic difference between *ulp1a* mutants and Col-0 in growth promoting BL (epi-BrassinoLide), as this results in degradation of ULP1a and SUMOylation of BRZ1, which occurs in the *ulp1a* mutants (Srivastava et al., 2020).

SUMO conjugates are known to increase when a plant is subjected to a heat stress (Kurepa et al., 2003). E3 SUMO ligase T-DNA insertion mutant *siz1-2* and *siz1-3* show freezing and chilling sensitivities. It was identified that SIZ1 aids the SUMOylation of ICE1 (Inducer of CBF/DREB1 Expression1) a MYC-like basic helix-loop-helix (bHLH) transcription factor that activates expression of *CBF/DREB1* (C-repeat Binding Factor/Dehydration Responsive Element Binding1) in low temperatures that enhances the plants freezing tolerance and provides cold acclimation. SUMOylation of ICE1 stabilised the protein preventing ubiquitination and degradation of the protein. In the *siz1-2* and *siz1-3* mutants, due to reduced SUMOylation of ICE1, there is reduced expression of *CBF/DREB1* and particularly CBF3/DREB1A resulting in cold sensitive mutants (Miura et al., 2007). The transcription factor DREB2A is stabilised in heat shock via SUMOylation. Upon high heat DREB2A SUMOylation blocks interaction with BPM2 (BTB-POZ and MATH domain), a ubiquitin ligase, enabling transcription of genes to provide thermotolerance (Wang et al., 2020). In addition, overexpressing tomato SIZ1 enhances tomato tolerance to heat stress by reducing reactive oxygen species and increasing heat shock transcription factors and heat shock proteins (Zhang et al., 2017).

Two SUMO protease mutants (*ots1-1 ots2-1* double mutant and *esd4-1* single mutant) and an E3 SUMO ligase mutant (*siz1-1*) result in early flowering phenotype (Conti et al., 2008; Murtas et al., 2003; Jin et al., 2008). In the *esd4* and *ots* mutants, the molecular mechanism of the early flowering phenotype has not been examined (Conti et al., 2008; Murtas et al., 2003). SIZ1, however, has been found to facilitate SUMOylation of FLD (Flowering Locus D) a

demethylase. Non SUMOylatable FLD mutants results in reduced expression of FLC (Flowering Locus C), a floral repressor, and reduced acetylation of histone 4 at FLC chromatin. The evidence suggests that SIZ1 is required for full activation of FLC and suppression in flowering (Jin et al., 2008). In addition to FLD being SUMOylated, FLC is also SUMOylated and results in suppression of flowering (Son et al., 2014).

Plants possess phytochrome proteins that are photoreceptors sensing the light, providing information of diurnal and seasonal time, important for photosynthesis and controlling development and photomorphogenesis. Phytochromes interact with downstream transcription factors controlling gene expression to respond to the light. Plants lacking photoreceptor PHYtochrome-B (phyB) show hyposensitivity to red light, with an increased red light fluence rate, the hypocotyl length does not change, whereas the WT hypocotyl length decreases with an increase in red light fluence rate. The SUMO protease knockout mutant *ots1-1 ots2-1* is also hyposensitive to red light, however the phenotype is less extreme than the photoreceptor mutant. This is due to photoreceptor phyB being SUMOylated at the C-terminus, this SUMOylation is increased in red light in the middle of the day. SUMOylation of phyB inhibits binding of PIF5 (Phytochrome Interacting Factor5), this transcription factor promotes skotomorphogenesis. The OTS SUMO proteases deSUMOylate phyB enabling interaction with PIFs resulting in degradation and inhibition of skotomorphogenesis and promotion of photomorphogenesis. SUMOylation of phyB negatively regulates light signalling (Sadanandom et al., 2015).

FLS2 (FLagellin Sensitive2) is an important Pattern Recognition Receptor (PRR) that detects MAMPs/PAMPs (Microbial/Pathogen Associated Molecular Pattern) on the surface of cells triggering immune responses. Orosa et al. (2018) identified a SUMO site in FLS2, which was SUMOylated in the presence of flagellin and aided the release of BIK1 (Botrytis Induced Kinase1) a kinase that activates downstream signalling of immunity genes. On infection with virulent bacterial pathogen *Pseudomonas syringae pv. tomato* (*Pst*) the non-SUMOylatable $FLS2^{K/R}$ was found to be more susceptible to the infection. SUMO is required for flagellin dependent release of BIK1 which results in downstream signalling. The non-SUMOylatable $FLS2^{K/R}$ mutant is less capable of producing oxidative bursts and inducing MPK6/3 protein production due to less BIK1 being released from FLS2, resulting in reduced immunity. The SUMO protease Desi3A was identified as the SUMO protease that de-SUMOylates FLS2. The *desia3a-1* mutants show enhanced flagellin susceptibility, high ROS (reactive oxygen species) burst, increased protein production of MPK3/6 and resistance to bacterial infection of *Pst*. This is due to FLS2 being highly SUMOylated resulting in more free BIK1 capable of activating its downstream signalling components (Orosa et al., 2018).

Another example of the SUMO systems role in plant immunity arises from the pathogens causing infection. In order to overcome Pathogen Triggered Immunity (PTI) pathogens use their type III secretion systems to insert effectors into plant cells, encoded by Avirulence (*Avr*) genes, triggering ETS (Effector Triggered Susceptibility). As has been mentioned earlier some of these effector molecules are capable of disrupting the SUMO status of proteins in plants, reducing the plant immune response. Some effector molecules have SUMO protease functions (Kim et al., 2013;

Orth et al., 1999, 2000; Deslandes et al., 2003; Roden et al., 2004; Bartetzko et al., 2009; Hotson et al., 2003; Hotson and Mudgett 2004; Morrell and Sadanandom 2019b) and deSUMOylate host target proteins preventing hypersensitive response. In addition to harbouring SUMO protease function, two different necrotrophic fungal pathogens *Botrytis cinerea* and *Plectosphaerella cucumerina* were found to result in post-transcriptional downregulation of SUMO conjugation enzymes SCE1 and SAE2. *Arabidopsis* mutants containing a mutated SAE2 protein that inhibits SUMO conjugation is more susceptible to necrotrophic infection (Castano-Miquel et al., 2017).

Plant Effector Triggered Immunity (ETI) is triggered upon detection of pathogen *Avr* genes and is established when a plant protein encoded by an R (resistance) gene interacts with the pathogen effector protein. A type of R protein, NB-LRR (Nucleotide-Binding and a Leucine Rich Repeat) protein SNC1 (Suppressor of NPR1 Constitutive1) is SUMOylated and in the E3 SUMO ligase mutant *siz1-1* mutant SNC1 is activated/over-accumulated. Overexpressing an F-box protein CPR1 (Constitutive expresser of PR gene 1), that degrades SNC1, in the *siz1-1* mutant background was able to restore the *siz1-1* mutant phenotype of disease resistance. This suggests that SIZ1 may have a role in the active levels of SNC1 mediated by the SUMOylation status caused by SIZ1 (Gou et al., 2017).

As mentioned above SUMO is involved in various aspects of plant development and hormone responses. Not mentioned, however, was the role of SUMO in modifying proteins in the hormone pathways abscisic acid (ABA) and gibberellins (GA) and the role of the PTM on proteins in the root hair development pathway. These three different projects are explored throughout the thesis and the background of each project will be explored in the next three subchapters.

1.2 ABA

In addition to SUMO playing a role in the hormone pathways mentioned above, SUMO is also involved in the abscisic acid (ABA) hormone pathway. The ABA pathway is one of five major hormone pathways in plants. It plays a key role in many physiological and developmental aspects in plants. ABA as a repressor of growth accumulates in the seed to initiate and maintain dormancy; mutants in ABA signalling produce non dormant seeds (Rodríguez-Gacio et al., 2009). ABA also accumulates in water deficit, triggering responses for homoeostasis such as stomatal closure to limit transpiration and mediates gene expression to protect photosynthetic machinery (Vishwakarma *et al*., 2017). ABA also works to inhibit the switch from vegetative to reproductive growth. Furthermore, ABA is implicated in wounding and stomatal regulation, seed maturation, environmental stress such as cold, salinity and pathogens and sensitivity to other plant hormones like ethylene and JA (Finkelstein 2013).

ABA also has different effects on disease susceptibility depending on the pathogen present and stage of infection. Initially ABA is beneficial in pathogen defence as high levels of ABA closes the stomata preventing pathogen invasion, particularly from bacteria, which are mainly capable of infiltration through the stomata. Additionally ABA promotes callose deposition which can prevent infiltration of fungi and oomycetes into the plant tissue (Ton *et al.,* 2009). However, if the pathogen gains entry to the cells ABA biosynthesis becomes a negative regulator. Pathogens secrete into cells effectors that interfere with host signalling promoting ABA signalling. It is beneficial to a pathogen upon infiltration to enhance ABA signalling because ABA inhibits JA and SA signalling. SA is beneficial to a plant infected with a biotrophic or hemibiotrophic pathogen as it establishes systemic acquired resistance (SAR). JA and ethylene is beneficial to a plant infected with a necrotrophic pathogen (Ton *et al.,* 2009).

1.2.1 The ABA signalling cascade

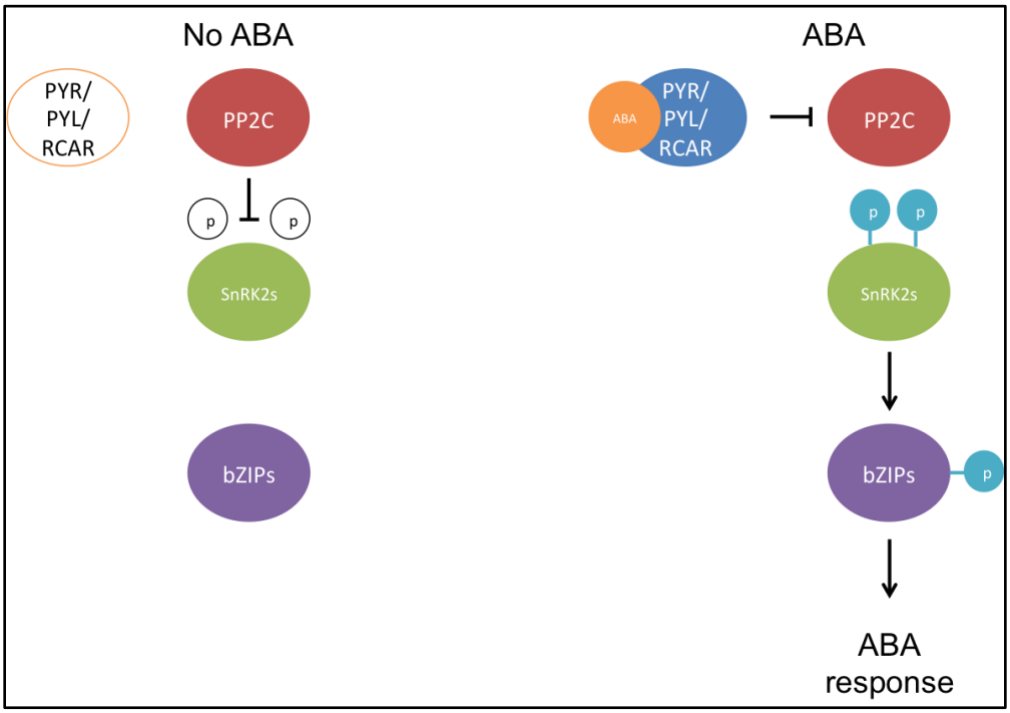

Figure 1.5 The ABA signalling cascade. *In the absence of ABA the PP2Cs are constitutively active, dephosphorylating the SnRK2s, leaving them inactive. When ABA is present it binds to the PYLs, forming a co-receptor with the PP2Cs inactivating the PP2Cs. This enables the SnRK2s to autophosphorylate and activate themselves and phosphorylate the bZIP transcription factors and other ABA responsive transcription factors. This results in expression of ABA responsive genes, causing an ABA response.*

ABA signalling can redirect the expression of one-tenth of the *Arabidopsis* genome and the levels of ABA present in a cell can vary by two orders of magnitude between stress and non-stress conditions (Nemhauser *et al*., 2006), this highlights the importance of correctly regulating the ABA signalling pathway. The ABA pathway is controlled, like most phytohormone pathways in plants, by negative regulators, the PP2Cs (Clade A Protein Phosphatases 2C), in a 'relief of repression' model. In the absence of ABA, the PP2Cs are constitutively dephosphorylating the SnRK2s (SNF1-Related protein Kinase 2), inactivating their phosphorylation activity, blocking ABA signal transduction (Ma et al., 2009; Park et al., 2009; Santiago et al., 2009) (figure 1.5). However when ABA is present in the cell it binds to the PYR/PYLs (PYrabactin Resistance/PYR-Like), they are considered to be co-receptors as the ABA binding affinities of the PYLs/PYRs is enhanced when they interact with the PP2Cs (Melcher *et al*., 2009). The conformational change induced in the PYLs/PYRs by ABA binding results in a gate and latch formation of two β-loops closing over the ABA in the ligand-binding pocket. This creates a surface that enables the ABA-bound PYL to bind to the active site of PP2Cs forming a heterodimer and blocking any activity (Antoni *et al*., 2012; Melcher et al., 2009; Miyazono et al., 2009). This results in the PP2Cs being unable to dephosphorylate the SnRK2s, which auto-phosphorylate, activating themselves. This enables the SnRK2s to phosphorylate downstream transcription factors, such as AREBs/ABFs (ABRE-Binding/ABRE-Binding Factors), which promotes transcription of ABA responsive genes resulting in an ABA response.

1.2.2 The PP2C family

Like many other hormone pathways in plants, in the ABA pathway there is a standard relief of repression, where signalling of the pathway relies on removing the repression (Cutler et al., 2010). PP2Cs in *Arabidopsis* are the negative regulators in the ABA pathway. There are currently nine identified PP2Cs in *Arabidopsis*; ABI1 (ABscisic acid Insensitive1), ABI2, HAB1 (Hypersensitive to ABA1), HAB2, PP2CA, HAI1 (Highly ABA Induced1), HAI2, HAI3 and AHG1 (ABA-Hypersensitive Germination1). The first PP2Cs were identified by screening for ABA insensitive mutants (Koornneef et al., 1984; Leung et al., 1994, 1997; Meyer et al., 1994; Rodriguez, et al., 1998), others were found based on sequence homology (Saez et al., 2004). The HAI mutants, identified later, do not show an ABA-hypersensitive phenotype in seed germination like other PP2C mutants, however they do in post-germination growth (Bhaskara et al., 2012).

The PP2Cs are Ser/Thr phosphatases that are Mg^{2+} dependent and their expression is induced by high ABA levels or stress inducing conditions (Fujita et al., 2009, 2011). The PP2Cs act redundantly (Rubio et al., 2009; Saez et al., 2006), however they have distinctive roles in different tissues and organs. The differing PP2Cs have different expression patterns, subcellular localisation patterns and expression at different developmental stages. As mentioned above the PP2Cs are inhibited by PYLs, this interaction results in ubiquitination and degradation of the PP2Cs via the 26S proteasome (Wu et al., 2016; Kong et al., 2015).

The PP2Cs physically interact with numerous cytosolic and nuclear proteins, interacting with many proteins and altering ABA downstream signalling (Cherel et al., 2002; Saez et al., 2008; Brandt et al., 2012). In the absence of ABA the PP2Cs interact and dephosphorylate key residues in the activation loop of the SnRK2s, which is required for autoactivation of the kinase (Ng et al., 2011; Yunta et al., 2011). The binding site in the PP2Cs is the same location for binding the PYLs and the SnRK2s requiring the same amino acids that are conserved among the clade A PP2Cs are required to coordinate the binding (Soon et al., 2012; Miyazono et al., 2009; Santiago et al., 2012). However in addition to binding to the PYLs and the SnRK2s the PP2Cs interact with many other proteins to control ABA responses. ABI1 has been demonstrated to bind to homeodomain transcription factors AtHB6 (Himmelbach et al., 2002), it is also capable of interacting with directly and dephosphorylating guard cell S-type anion channel SLAC1 (SLow Anion Channel associated 1), which increases intracellular Ca^{2+} levels in guard cells to close the stomata (Brandt et al., 2012). ABI1 and ABI2 interact with some Protein Kinase S (PKS) proteins including SOS2 (Salt Overly Sentitive 2); this family of proteins is involved in DNA damage repair and replication block checkpoint kinases, the proteins also go on to interact with calcium binding proteins (Ohta et al., 2003). ABI2 also interacts physically with the preprotein of the plastid-associated lipid-binding protein fibrillin, via PTM, ABI2 increases fibrillin abundance, mediated by ABA (Yang et al., 2006). Finally, HAB1 binds to ATP chromatin remodelling complex protein SWI3B (Saez et al., 2008).

1.2.3 The PYL family

The PYL family of soluble ABA receptors were identified by two independent research groups based on different approaches (Ma et al., 2009; Park et al., 2009). There are 14 identified PYR/PYL proteins (called PYLs herein for simplicity), but they are also known as RCARs (Regulatory Components of ABA Receptors); PYR1 and PYL1-13, which have high sequence and structural conservation. They are members of the START (StAR-related lipid-Transfer domain) protein family also known as the Bet v 1 superfamily (Park et al., 2009). They localise to the cytoplasm (Yu et al., 2019; Rodriguez et al., 2014) or nucleus (Li et al., 2014; Rodriguez et al., 2014).

ABA binding in the ligand-binding pocket in PYLs, surrounded by conserved loops CL1-4, results in conformational rearrangements leading to the formation of a PYL-PP2C heterodimer (Yin et al., 2009). However, the PYLs can be further classified based on their ABA sensitivity and oligomserisation status. Generally, monomeric PYLs are more likely to be able to interact with PP2Cs in the absence of ABA (Hao et al., 2011). PYR1 and PYLs 1-4 are obligatory ABA-dependent inhibitors of PP2Cs, they are all constitutive dimers except PYL3 where there is a faster equilibrium between dimer and monomer (Hao et al., 2011) and PYL4 which is solely a monomer. PYLs 5-12 are mostly monomeric, except PYL 7, 11 and 12, they inhibit the phosphatase activity of PP2Cs in the absence of ABA. However complete inhibition of PP2Cs by these PYLs is achieved at much lower concentrations when ABA is added (Hao et al.,

2011). PYL13, however has been suggested by one group to be unresponsive to ABA (Li et al., 2013). PYL13 was found to differ from the other PYLs in key residues that affect ABA perception, mutating these residues results in a partially functional ABA receptor (Zhao et al., 2013). However the same group found overexpressing PYL13 resulted in ABA sensitivity and mutated PYL13 plants showed ABA insensitivity. Additionally PYL13 interacted with PP2CA in a yeast-two-hybrid assay in an ABA-dependent manner. However unlike other PYLs PYL13 also interacts with and antagonises other PYLs negatively regulating their ABA responses (Zhao et al., 2013; Fuchs et al., 2014).

Mutants deficient in up to 12 PYLs are insensitive to ABA in seed germination, seedling growth, stomatal closure and gene expression. A mutant with all the PYRs/PYLs knocked out is severely impaired in growth and fails to produce seeds (Zhao et al., 2018). ABA activation of SnRK2s was blocked, however surprisingly, in the mutant, osmotic stress activation of SnRK2s was enhanced. The results demonstrated that the PYLs negatively regulate ABA-independent SnRK2 activity by interacting and inhibiting osmotic stress-activated SnRK2 protein kinases (Zhao et al., 2018), a subclass of SnRK2s that is not directly targeted by the PP2Cs.

Some PYLs can also mediate between different hormone pathways. PYL8 interacts with transcription factors MYB44, MYB73 and MYB77. Interaction of PYL8 with MYB77 increases MYB77 binding to the MBSI motif promoter in multiple auxin-responsive genes. *pyl8* mutant lateral roots are more sensitive to ABA and the recovery of lateral root growth was delayed in the presence of ABA but was rescued in presence of IAA (Zhao et al., 2014). Additionally *pyl8 pyl9* double knockout mutants have a prolonged quiescent phase that is reversed in the presence of IAA (Xing et al., 2016).

1.2.4 The SnRK2 family

The SnRK2s were identified as ABA-activated kinases, homologous to human AMPK (AMP-activated Kinase). Plant SnRKs are grouped into 3 categories. SnRK2s are unique to plants and composed of 10 kinases. They can be further subclassed into 3 groups; not responsive to ABA, weakly activated by ABA and strongly activated by ABA, SnRK2.2, 2.3 and 2.6 fall into this latter category. SnRK2 members are activated by osmotic stress; mutants lacking all 10 SnRK2s are hypersensitive to osmotic stress (Fuji et al., 2011). Mutants lacking the three strongly ABA activated SnRK2s are impaired in almost all ABA responses demonstrating these kinases are central to ABA signalling (Fuji et al., 2009; Fujita et al., 2009; Nakashima et al., 2009).

SnRK2s contain a well-conserved kinase catalytic domain and a C-terminal regulatory region that encompasses two sub-domains. Domain I, which is also known as the SnRK2 box, is conserved in all SnRK2s and is required for kinase activity. At the C-terminus domain II is a highly acidic region. In the absence of ABA PP2Cs physically interact with

this domain, which is only conserved among the ABA-responsive members; it is thus also known as the ABA box (Belin et al., 2006; Yoshida et al., 2006).

In the presence of ABA the released SnRK2s are activated by autophosphorylation or phosphorylation via other kinases. ABA-induced reactivation of PP2C-dephosphorylated SnRK2 kinases requires phosphorylation by MAPKK-kinases (M3Ks). M3K triple knock-out plants show reduced ABA-sensitivity and impaired rapid osmotic-stress-induced SnRK2 activation (Takahashi et al., 2020). The SnRK2s phosphorylate downstream transcription factors including AREBs/ABFs and S-type anion channels to induce ABA responses and close stomata (Vahisula et al., 2008).

The SnRK2s are believed to be the most evolutionarily conserved part of the ABA pathway. The third subclass of SnRK2s, that are strongly activated by ABA were discovered in moss *Physcomitrella patens.* Additionally in the moss an upstream Raf-like kinase (ARK) is present; together they work to protect the moss from drought. The SnRK2s identified in *Physcomitrella patens* were capable of binding ABA, which modern day *Arabidopsis* SnRK2s are unable to do. *Arabidopsis* subclass III SnRK2s (strongly activated by ABA SnRK2.2, 2.3 and 2.6) were capable of complementing the moss, deficient of its native SnRK2s *snrk2*$^{-}$. However the other *Arabidopsis* subclass I SnRK2s were incapable of complementing *snrk2*$^{-}$. It is thought the *Arabidopsis* subclass 3 SnRK2s (composed of SnRK2.2, 2.3 and 2.6) along with ABA and ARK evolved from the earliest land plants to regulate pre-existing dehydration responses. Subclass I SnRK2s evolved later in vascular plants from the third subclass, conferring osmostress protection independent from the ancient system (Shinozawa et al., 2019).

1.2.5 The ABA pathway and SUMO

The role of SUMO in the ABA pathway was first discovered in *Arabidopsis* overexpressing SUMO1 and SUMO2. These SUMO overexpressing transgenics roots had reduced ABA sensitivity on ABA plates, however the ABA responsive gene, *RD29A*, expression was increased in the overexpressing SUMO transgenics (Lois et al., 2003).

Miura et al., 2009 demonstrated that ABI5, an ABA responsive transcription factor is SUMOylated by SIZ1, a SUMO E3 ligase. When ABI5 is SUMOylated the protein becomes inactive, when deSUMOylated the protein is activated and capable of transcribing ABA responsive genes. The *siz1-1* mutant is more sensitive to ABA and has increased expression of ABA-induced gene expression. A later study found that SIZ1 also aids SUMOylation of R2R3-type transcription factor MYB30. The MYB30 transgenic plants, that are not capable of being SUMOylated, showed increased ABA sensitivity compared to MYB30 WT transgenics. The double *siz1-2 myb30-2* mutant exhibited enhanced ABA sensitivity compared to either single mutant. SUMOylation of MYB30, in the presence of SIZ1 during ABA treatment stabilised MYB30, these results indicate that SUMOylation of MYB30 is critical for functioning in ABA signalling (Zheng et al., 2012).

In addition to SUMO E3 ligases being implicated in the ABA signalling pathway SUMO protease mutants also show ABA phenotypes. SUMO protease SPF1 also called ASP1 (*Arabidopsis* SUMO Protease1) mutant *asp1-1* has an ABA-insensitivity phenotype in early seedling development and has been shown to accumulate in ABA treatment (Wang et al., 2018).

In contradiction to the SPF1 ABA phenotype, T-DNA SALK OTS1 OTS2 insertional mutants (*ulp1c-2*; SALK_050441 *ulp1d-2*; SALK_029340) displayed an ABA sensitive phenotype showing reduced root length, germination and stomatal aperture in response to ABA (Castro et al., 2016). OTS1 and OTS2 were identified as positive regulators of osmotic stress and stomatal closure. The difference in ABA sensitivity between SPF1 and OTS SUMO proteases may be due to the OTS SUMO proteases targeting and deSUMOylating different proteins in the ABA pathway. Gene expression is also altered in *ots1 ots2* SUMO protease mutants particularly in genes associated with drought dependent transcriptional regulation (Walsh, PhD Thesis, 2017).

Currently only two transcription factors in the ABA pathway, ABI5 and MYB30 have been identified as being modified by SUMO (Miura et al., 2009; Zheng et al., 2012). SUMO has been identified as an important PTM modifying many crucial proteins in hormone signalling cascades from DELLA to JAZ proteins, resulting in fine-tuning of hormone signalling. Due to the identification of several SUMO protease mutants and SUMO overexpression transgenics having ABA phenotypes (Castro et al., 2016; Wang et al., 2018; Lois et al., 2003), and SUMOs ability to fine tune signalling cascades (Verma et al., 2018), we speculated that additional proteins in the ABA pathway, upstream of ABA transcription factors may be SUMO modified. In chapter 3 and 4 of this thesis work was undertaken to determine if other proteins in the ABA pathway, upstream of ABA transcription factors were SUMOylated and to understand if the SUMOylation altered downstream signalling transduction.

1.3 Root hairs

SUMO is involved in the development of different plant organs, such as flowers and responding to environmental cues. Important environmental cues plants must respond to is in soil substrates, as substrates are not uniform, roots have to respond to nutrient and water availability in the soil. As previously mentioned SUMO regulates hydropatterning of roots (development of lateral roots when in contact with water) (Orosa-Puente et al., 2018). Like lateral roots, root hairs also develop in response to environmental cues and aid nutrient acquisition, particularly of inorganic nutrients such as phosphate, Mn, Fe and Zn (Ma et al., 2001; Muller and Schmidt 2004) however, they also function to anchor plants into substrates. Furthermore, root hairs play an important role in modulating and providing an interaction interface for beneficial microbes that perform essential roles for plants. Root hairs play an important

role in root exudation of inorganic acids, amino acids, proteins, mucilage, phenolics and secondary metabolites. These exuded components function in mineral weathering, mobilisation of nutrients, metal detoxification and growth inhibition of pathogenic bacteria, invertebrates, herbivores or neighbouring plants. Root hairs also are involved in forming nitrogen-fixing nodules in legumes by curling around attached rhizobia bacteria (Oldroyd and Downie 2008; Olroyd and Dixon 2014).

Arabidopsis root hairs are cells that are approximately 10 µm in diameter, grow rapidly from the root epidermis at more than 1 µm/min and can be over 1 mm in length (Grierson and Schiefelbein, 2002). Whilst they provide plants with numerous advantages, they are not essential for plant viability; the double *rsl2 rsl4* hairless mutant has no other morphological phenotype other than a lack of root hairs (Yi et al., 2010). Domesticated plants have abundant and long root hairs, which is a desirable trait in modern crop breeding (Brown et al., 2013). Root hairless mutants of *Arabidopsis* and barley (*Hordeum vulgare* L.) grown in low phosphate conditions display severe nutrient stress symptoms (Bates and Lynch 2000; Gahoonia and Nielsen 2003). Crop varieties with relatively long root hairs typically absorb more phosphate and potassium from the soil than those with relatively short hairs (Gahoonia et al. 1997; Hogh-Jensen and Pedersen 2003; Yan et al. 2004). The biggest environmental factor affecting root hairs is phosphate availability; low phosphate results in increased length and number of root hairs (Bates and Lynch 1996; Fohse and Jungk 1983; Ma et al., 2001). *Arabidopsis* accessions *Co* and *C24* have high densities of longer root hairs and are more efficient at acquiring phosphate (Narang et al., 2000). Iron deficiency also increases hair density and length; iron-deficient roots produce ectopic hairs and hair length doubles (Schmidt et al., 2000), manganese and zinc (Ma et al., 2001) also affect root hair development.

These single cell extensions grow from the root epidermis in the differentiation zone of young roots of most angiosperms. In most eudicots the first sign of root hair development is the formation of a bulge on the outer periclinal wall of an epidermal cell (Clowes 2000; Pemberton et al., 2001). In type 1 root hair development all epidermal cells are morphologically identical before hair initiation and any cell can differentiate to be a hair or non-hair cell. Some epidermal cells progress to form hair cells, separated from other hair cells by non-hair cells, the environmental condition determines the number of hair cells. This type of development of hair cells developing from morphologically equivalent cells, type 1 development, is typically seen in rice (figure 1.6).

Type 2 and type 3 root hair development is characterised by specialised epidermal cells, called trichoblasts, that are morphologically different from other epidermal cells (atrichoblasts) and develop to form root hairs. Trichoblasts differ from atrichoblasts by having a smaller size, greater rate of division, being more densely cytoplasmic, a lower rate of vacuolation, unique cell surface ornamentation and distinct cell wall epitopes (Berger et al., 1998a, 1998b, Dolan et al., 1994, Masucci et al., 1996, Galway et al., 1994, Freshour et al., 1996; Grierson et al., 2014). Type 2 hair cell development arises from trichoblasts alternating with atrichoblasts along longitudinal epidermal cell file, this is

typically seen in grass species such *Brachypodium*, whereas type 3 hair cells develop in a separate longitudinal file from atrichoblasts (figure 1.6).

Type 3 development of trichoblasts and atrichoblasts are organised into longitudinal files, this differentiation occurs early in development in the rootward region of the meristem. In *Arabidopsis,* like most Brassicaceae and related families like Capparaceae, Tovariceae and Resedaceae, root hair development follows type 3 development, where the root hairs form in a longitudinal file, determined by the position of the cell to the underlying cortex. Epidermal cells in a cleft between two cortical cells differentiate into a root hair cell, cortical cells either side of the cleft differentiate into a non-hair cell. Immature hair cells can be differentiated from non-hair cells in their size, cytoplasmic density, rate of cell division, vacuolation and chromatin organisation. The genes that are expressed to determine root hair cell fate are expressed and active in the embryo suggesting in embryogenesis epidermal cells perceive the positional information and adopt their specific cell fate (Berger et al. 1998a, 1998b; Costa and Dolan 2003). This positional information continues post embryonic root growth to ensure correct spatial pattern of epidermal differentiation.

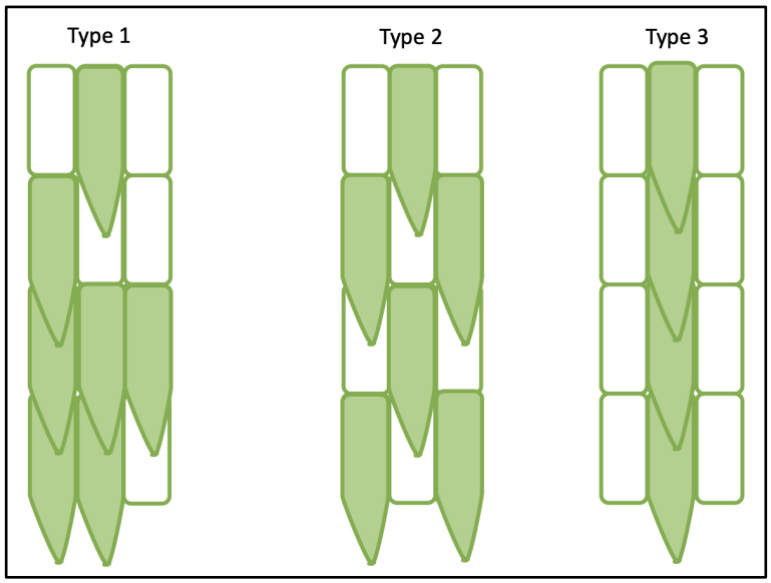

Figure 1.6 Types of root hair epidermal patterning. *In type I, any root epidermal cell can produce a root hair. In type II, root hairs derive from asymmetric cell divisions after which the larger cell enters the non-hair cell fate whereas the smaller cell develops into a root hair. Type III is characterised by alternating files of root hair and non-root hair cells. (Adapted from Salazar-Henao et al., 2016).*

1.3.1 The root hair signalling cascade

Cells in the epidermis determine if they should develop into atrichoblasts and trichoblasts early on in the development of the cell in the meristematic region of the root, however this information is then further reinforced in a signalling cascade from surrounding cells. In two studies it was shown that introducing novel cells into regions, such as by laser ablation, could alter the cell fate of neighbouring cells from atrichoblasts to trichoblast and visa versa. The newly introduced cells expressed marker genes and exhibited cellular characteristics that are appropriate for their new position (Berger et al., 1998a, 1998b). This demonstrates some positional cues that determine cell fate specification may rely on extracellular cues. These cues arise not only from neighbouring trichoblasts and atrichoblasts, but also from the underlying cortical cells. Epidermal cells in contact with two cells in the underlying cortical layer develop into root hair cells, whereas epidermal cells that are only in contact with one cortical cell enter the non-hair cell developmental programme (Grierson et al., 2014).

The genes that control root hair cell fate specification are varied and broad and there is still much debate over the role of individual genes. The first gene identified that is present in non-hair cells (epidermal cells that do not go on to form hair cells) and not present in hair cells was *GL2* (GLabra 2), this gene encodes a homeodomain transcription factor protein (Rerie et al., 1994; DiCristina et al., 1996). A GL2 enhancer-trap GFP construct cell line showed expression of GL2 in non-hair epidermal cells located outside the periclinal cortical cell wall (i.e. the normal GL2 root-expression pattern) in the meristematic region of the root. The reporter lines suggest that the patterning information may be provided and cell fates defined within or one cell beyond the epidermal/lateral root cap initials (Masucci et al., 1996; Berger et al., 1998a). Other gene regulators that are thought to be involved in non-hair cell fate and are expressed in these cells include the homeodomain transcription factor the WD40-repeat protein TRANSPARENT TESTA GLABRA (TTG), the bHLH transcription factors GLABRA3 (GL3) and a paralog of GL3 ENHANCER OF GLABRA3 (EGL3) and an R2R3-type MYB transcription factor WEREWOLF (WER) (DiCristina et al., 1996; Bernhardt et al. 2003; Galway et al. 1994; Lee and Schiefelbein 1999; Masucci et al. 1996; Rerie et al. 1994; Walker et al. 1999). The role of TTG is not clear but it is thought to activate an *Arabidopsis* homolog of the maize R (a basic helix-loop-helix transcriptional activator) (Ludwig et al., 1989). These genes were identified by mutations resulting in root hairs in almost every epidermal cell. Conversely genes that are expressed in and promote root hair cell fate are the R3 MYB-like proteins CAPRICE (CPC) and functional paralogs TRIPTYCHON (TRY) or ENHANCER OF CPC (ETC) (Kirik et al. 2004; Schellmann et al. 2002; Simon et al. 2007; Wada et al. 1997; Schiefelbein et al., 2014). Again, mutants of these genes produce roots with no hair cells supporting these genes pivotal roles in hair cell formation.

The molecular mechanism determining hair cell fate is thought to be lateral inhibition with feedback (figure 1.7). A complex of WER/TTG/GL3-EGL3 located in non-hair cells promotes GL2 expression, which in turn is a positive regulator of non-hair cell fate, mutations in WER and TTG abolishes and reduces respectively GL2 promoter activity. In trichoblasts, the expression of *WER* is reduced by a positional signal induced by JACKDAW (JKD) that comes from

the cortex (Hassan et al., 2010). This difference in WER expression drives formation of distinct epidermal cell fates by unbalancing the transcriptional gene network that regulates epidermal patterning (Kwak and Schiefelbein 2007, 2008). The JKD signal is greater in hair cells and is perceived by the leucine-rich repeat receptor-like kinase (LRR-RLK) SCRAMBLED (SCM) (Kwak et al., 2005), resulting in WER repression. The mutant of SCM forms hair and non-hair cells randomly (Kwak et al., 2005). In hair cells CPC competes with WER for binding to the TTG/GL3-EGL3 complex, the reduced abundance of WER (when JKD is perceived by SCM) enables the TTG/GL3/EGL3 complex to form with CPC instead. The WER/TTG/GL3-EGL3 complex also regulates CPC/ETC/TRY expression and mediates the movement into neighbouring hair cells. The GL2 mutant is epistatic to CPC, CPC is thought to act in the WER/TTG/GL2 pathways as a negative regulator of GL2. CPC encodes a Myb-like DNA binding domain but without a typical transcriptional activation domain (Wada et al., 1997), this has led to the theory that CPC inhibits GL2 transcription by binding to the promoter and blocking its activation. CPC also binds to the WER/TTG/GL3-EGL3 complex reducing expression of GL2, promoting formation of a hair cell. CPC also reduces expression of WER and induces expression of GL3-EGL3 which moves to the neighbouring non-hair cells, forming a second lateral feedback loop (figure 1.7).

Accumulation of the WER/TTG/GL3-EGL3 complex in non-hair cells induces accumulation of GL2 and CPC but also reduces GL3-EGL3 resulting in preferential expression in hair cells. Furthermore the activator complex also promotes expression of a functional paralog of WER, MYB23 (Kang et al., 2009). A negative-feedback loop between the activator complex and *SCM* also exists, leading to reduced *SCM* expression in non-root hair cells (Kwak and Schiefelbein, 2008). The resulting intercellular feedback loops cause a mutual dependence mechanism between neighbouring epidermal cells reinforced by protein movement and protein complex formation generating epidermal patterning (figure 1.7).

Moreover, in *try* but not in *cpc* mutants a reduction of SCM protein is observed, implying positive feedback via TRY on the preferential accumulation of SCM in trichoblasts (Kwak and Schiefelbein, 2014). Interestingly, the activator complex promotes the expression of both positive regulators (GL2) and inhibitors (CPC, ETC1 and TRY) of non-hair cell fate (Schiefelbein et al., 2014).

Ultimately the model can be shortly summed up as 2 competing transcription factors, WER and CPC competing to form a complex with TTG and GL3-EGL3. Immature epidermal cells have a high level of WER present leading to expression of GL2 and non-hair cell differentiation, immature epidermal cells with a high level of CPC present have repression of GL2 enabling hair cell differentiation, however it is not clear how the different levels of WER and CPC are generated.

Epidermal patterning is modulated by hormonal signalling (Dolan 2001; Pitts et al. 1998; Van Hengel et al. 2004; Zhu et al. 2006), environmental factors (Muller and Schmidt 2004; Schmidt and Schikora 2001; Zhang et al. 2003) and chromatin organization (Caro et al. 2007; Costa and Shaw 2006), but little is known about how these processes

interact with the epidermal gene regulatory network to control cell differentiation in the *Arabidopsis* root epidermis. Once the hair cell fate has been determined by the cells they undergo differentiation, with hairs emerging.

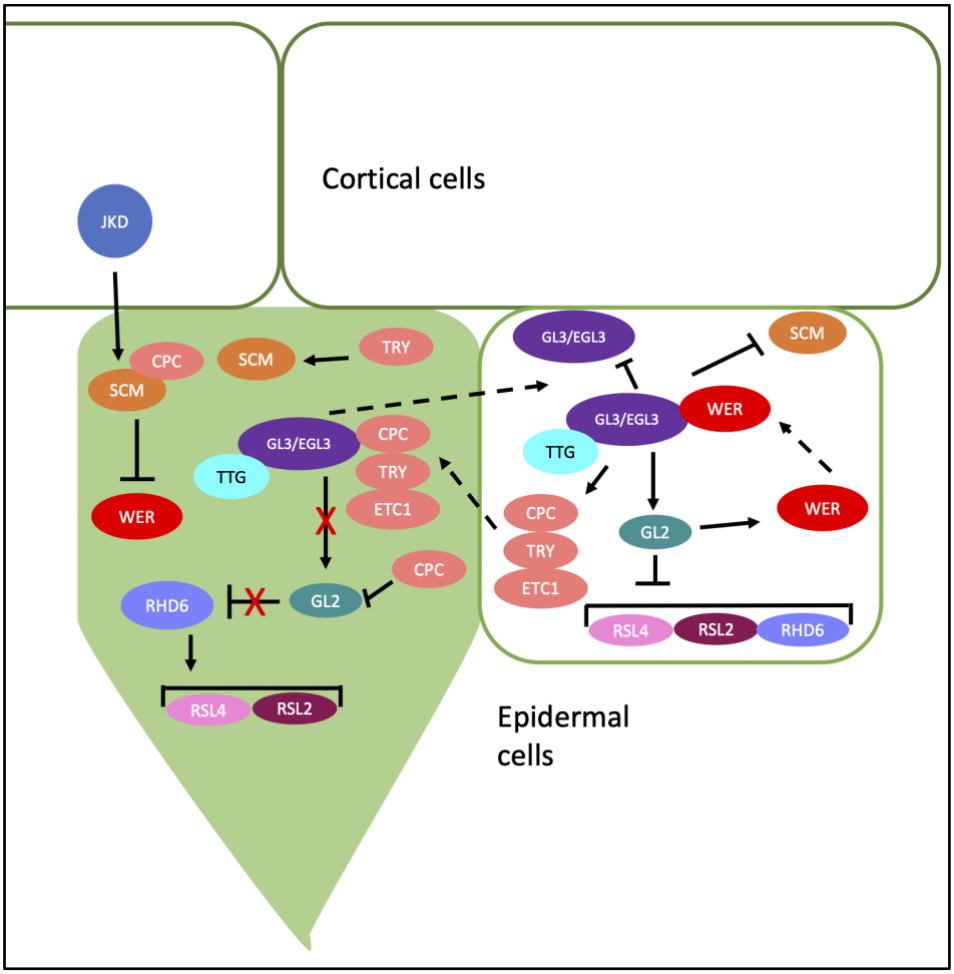

Figure 1.7 Position-dependent cell fate specialisation in the Arabidopsis root epidermis. *Transcriptional activation is indicated by arrows; blunted lines indicate transcriptional repression. Dashed lines indicate intra/intercellular protein movement. (Adapted from Salazar-Henao et al., 2016).*

1.3.2 Root hair formation

Root hair differentiation is classed into two phases, root hair initiation and elongation. The root hair initiation phase begins with a complex auxin-mediated process that determines the initiation site, called planar polarity determination (Balcerowicz et al., 2015). In *Arabidopsis* this is restricted to the rootward region of the cell and is controlled by auxin and microfilaments such as actin. The epidermal cells switch from expanding anisotropically to polar growth (Balcerowicz et al., 2015).

Once the position of the outgrowth is determined, the polar initiation site, a disc-shaped area of the cell wall forms a bulge about 22 µm across, the pH of the cell wall decreases (Bibikova et al., 1998) and other physiological changes occur. The cell wall loosens and expands enabling growth at the root hair tip, the cell also ceases to elongate longitudinally. Small GTP-binding proteins from the ROP (Rho Of Plant) family appear at the bulge and remain at the tip of the developing hair until growth ends (Molendijk et al., 2001). As the bulge enlarges the endoplasmic reticulum condenses and actin accumulates, under optimal conditions, it takes about 30 minutes for a root hair swelling to form on the surface of the cell (Bibikova et al. 1999; Baluska et al., 2000).

RHD6 (Root Hair Defective), a bHLH transcription factor, is required to initiate root hair formation (Masucci and Schiefelbein, 1994). Mutants of *rhd6* produce few and misplaced root hairs that develop in a more shootward position in the epidermal cell compared to wild type. Occasionally the *rhd6* mutant develops two root hairs from a single epidermal cell (Masucci and Schiefelbein, 1994). This suggests that RHD6 is involved in a mechanism that encourages hair formation at the apical end of the cell and by controlling the establishment and number of swellings. RHD6 also regulates expression of other genes encoding bHLH transcription factors that control later events of initiation and tip growth including RSL4 (RHD-Six Like) (Yi et al., 2010).

When the hair is growing, the extreme tip has dense cytoplasm, with a large number of secretory vesicles containing cell wall and membrane components that are trafficked from the golgi complex to the plasma membrane to fuse. Throughout tip growth actin is concentrated at the tip (Baluska et al., 2000). The Golgi complex, along with the endoplasmic reticulum and mitochondria, comprise the organelle rich zone that lies in the sub-apical region of the growing root hair cell. These organelles are responsible for the synthesis and transport of macromolecules that sustain tip-growth. The basal region of the cell is vacuolated (Carol and Dolan 2002; Foreman and Dolan 2001). The nucleus moves from the cell body to the root hair where it maintains a distance from the growing tip. An experiment performed by Ketelaar et al., 2002 moved the nucleus away from the tip, this blocked root hair elongation, demonstrating the importance of having the nucleus located near the expanding region.

The other components required in root hair elongation include transporters for moving ions (potassium, calcium) and auxin, cytoskeleton (microtubules and actin) and cell wall modifications (Grierson et al., 2014), composing of genes that process the network of polysaccharides and structural proteins. The growing tip requires a calcium concentration of 1 µM Ca^{2+} to control the direction of the growth (Schiefelbein et al., 1992). Other osmotic ions the growing hair cell imports, such as K^+ and Cl^- is to ensure turgor is maintained in the cell. Turgor ensures the cytoplasm fits against the cell wall, if contact between the plasma membrane and wall is jeopardised the root hair growth stops (Grierson et al., 2014).

RSL4 (RHD-SIX LIKE 4) encodes a bHLH transcription factor that was identified as a direct target of RHD6 and found to be an important regulator of root hair growth. Plants with mutations in *RSL4* developed fewer and shorter root hairs while gain-of function plants resulted in constitutive growth leading to the development of very long root hairs

(Yi et al. 2010). Together, these observations demonstrate that RSL4 is necessary for root hair growth. Microarray studies indicate that RSL4 regulates hair cell elongation by controlling the expression of genes involved in a number of cellular processes that affect cell growth, such as cell wall modification, endomembrane trafficking and ion transport (Yi et al. 2010), RSL4 expression is also increased by auxin.

When the hair stops growing the cytoplasm at the tip disperses and the vacuole enlarges into the dome, ROP proteins (Molendijk et al., 2001), the calcium gradient (Wymer et al., 1997), and calcium channel activity (Schiefelbein et al., 1992; Very and Davies, 2000) are lost from the tip. However no mechanisms have yet been established to determine how the root hair stops growing.

1.3.3 Hormones and root hairs

There are numerous ethylene and auxin signalling mutants that exhibit a root hair phenotype. AVG (AminoethoxyVinylGlycine) an ethylene biosynthesis inhibitor or Ag^{+} (an inhibitor of ethylene perception) blocks root hair formation (Masucci and Schiefelbein, 1994; Tanimoto et al., 1995). ACC (1-Amino-Cyclopropane-1-Carboxylic acid), an ethylene precursor, induces some ectopic root hair cells in *Arabidopsis* (Tanimoto et al., 1995). Furthermore, mutations affecting the CTR1 *(*Constitutive Triple Response 1) locus, which encodes a Raf-like protein kinase is thought to negatively regulate the ethylene signal transduction pathway (Kieber et al., 1993) causing root hairs to form on epidermal cells that are normally hairless (Dolan et al., 1994). Additionally auxin resistant mutants *dwf* (DWarF) and *axr2/IAA7* (AuXin Resistant/Indole-3-Acetic Acid), a putative transcriptional regulator of auxin-responsive genes (Nagpal et al., 2000), are hairless (Mizra et al., 1984; Wilson et al., 1990), and show a similar phenotype to the hairless mutant *rhd6*, which can be reversed by including in the growth media IAA (an auxin) (Masucci and Schiefelbein, 1994).

Treating *rhd6* mutants with an ethylene precursor also restores the position of hair emergence to normal, implicating ethylene in this process. This is supported by the phenotypes of *etr1* (EThylene Response1) and *eto1* (EThylene Overproducer1) mutants. *etr1* mutants perceive ethylene poorly because they have a mutated ethylene receptor. Like *rhd6* hairs, *etr1* hairs emerge nearer to the basal end of the hair cell. *eto1* plants produce more ethylene than wild type and root hairs form closer to the apical end of the cell (Masucci and Schiefelbein, 1996). A small proportion of cells on *rhd6* and *axr2* plants have extra hairs (Masucci and Schiefelbein, 1994), suggesting that the growth regulators auxin and ethylene may also be involved in mechanisms that control the number of swellings. The *axr1,* a component of the auxin signalling machinery, *aux1 (*AUxin Resistant*)*, an auxin influx carrier and *etr1* mutants have short root hairs so all of these genes are required for root hairs to achieve wild-type length (Pitts et al., 1998). The short hairs of these mutant plants suggest that ethylene and auxin signalling stimulate elongation (Pitts et al., 1998).

In the case of ethylene this is supported by the phenotype of *eto1* mutants, which synthesise more ethylene and have longer root hairs than wild type plants (Pitts et al., 1998).

Current research suggests that the hormones do not have an impact on the TTG/GL2 pathways (Masucci and Schiefelbein, 1996) and other studies have suggested auxin and ethylene promote root hair outgrowth after epidermal cell type has been established (Masucci and Schiefelbein, 1996; Cao et al., 1999). Taken together, the results suggest that the WER/TTG/GL2/CPC pathway acts upstream of, or independently from, the ethylene/auxin pathway to define the pattern of cell types in the root epidermis.

1.3.4 Root hair formation and SUMO

The role of SUMO in root hair formation was first determined in T-DNA insertional mutants of *siz1*, a SUMO E3 ligase. These mutants showed hypersensitivity in low phosphate (herein called Pi) and produced many, longer root hairs (Miura et al., 2005). The *siz1* mutants also showed greater transcript abundance of three genes, *PT2*, *PS2* and *RNS1* that are induced upon Pi starvation when grown in Pi-sufficient medium, suggesting these genes are negatively regulated by SIZ1 in Pi-sufficient conditions. Conversely initially upon Pi starvation two genes that are induced upon Pi starvation *IPS1* and *RNS1*, had reduced expression compared to WT (wild type), however after 2-3 days the expression levels were more similar. This suggests that SIZ1 can positively regulate these two genes at the initial stages of Pi limitation. The MYB transcription factor PHR1 is required for expression of *IPS1* and *RSN1*, this protein contains two SUMO sites and can be SUMOylated *in vitro* by SIZ1 (Miura et al., 2005). Using *Japonica* subspecies of *O. sativa* mutants *OsSIZ1* showed a similar phenotype to the *Arabidopsis siz1* mutant of an increase in root hair number (Wang et al., 2011).

Previous work conducted by Walsh (PhD thesis, 2017) had indicated that the double SUMO protease mutant, *ots1 ots2*, showed longer and fewer root hairs, compared to WT. Chapter 5 in this thesis first tested the hypothesis of *ots1 ots2* harbouring longer and fewer root hairs, compared to WT. Root hair specification, initiation and elongation is a relatively rapid response to external stimuli, SUMO has been well characterised in being involved in responding to such stimuli (Orosa-Puente et al., 2018; Huang et al., 2009; Srivastava et al., 2020). Furthermore a large number of proteins are involved in root hair specification, initiation and elongation. This led us to speculate that more than one protein (PHR1) maybe SUMOylated in the root hair signalling pathways. Using inhouse software these proteins were scanned to identify SUMO sites, the proteins were tested for SUMOylation status and the role of SUMO on the proteins examined.

1.4 Gibberellins

In addition to the role of SUMO in the hormone pathways previously mentioned, SUMO is also involved in the Gibberellic acid (GA) pathway. GA was first identified in the 1920s and 1930s from a rice pathogenic fungus which induced a disease phenotype of plants, that grow so tall they were not capable of supporting their own weight. Later it was discovered plants can synthesise their own GA (Schwechheimer, 2012). Gibberellins are important hormones in plants known for their growth promoting properties. The hormone pathway regulates growth in response to a wide variety of environmental cues and regulates a diverse number of processes including floral and seed development, leaf and root growth, seed germination, bolting and crosstalk with other hormone pathways (Locascio et al., 2013).

The GA pathway has been studied extensively due to its ability to improve crop yield and quality and the critical role the hormone played in the 'green revolution'. The 'green revolution' was coined to encompass massive yield increases in global cereal production, which has been able to more than keep up with food demand from a population which doubled in 40 years. This was possible due to high-yielding varieties of wheat and rice in addition to applications of fertiliser and pesticides. The high-yielding crop varieties were generated by introducing dwarfing genes, this shortened and strengthened stems, providing increased support for the heavy grain of high-yielding varieties reducing lodging of plants, which occurs in wind and rain, causing large yield losses. An additional advantage of shorter stems meant that a greater assimilate partitioned into the grain as opposed to the stem (Hedden, 2003). The dwarfing genes identified in rice and wheat were found to be mutated DELLA proteins which are more stable due to a mutation in the DELLA domain preventing interaction with the GA receptor and consequential degradation (Hedden, 2003). Stabilised DELLAs repressed the GA pathway transcription factors, preventing growth.

1.4.1 The GA signalling cascade

As with ABA, the GA pathway operates a similar 'relief of repression model', the DELLAs are the group of transcriptional repressor proteins which are degraded by the GA receptor GID1 (Gibberellin Insensitive Dwarf 1) in the presence of GA. The DELLAs restrain growth and developmental processes that are regulated by GA by inhibiting transcription factors and promoting stress resistance. In the presence of GA, GID1 interacts with DELLA, inducing degradation via the SCF^{SLY1} or SCF^{SNE} (SKP1-CULLIN-F-BOX complex with the F-box protein subunit SLEEPY1 or SNEEZY) E3 ubiquitin ligases and the 26S proteasome. This inhibits the DELLA repression on the transcription factors enabling GA signalling (figure 1.8).

In response to GA, DELLAs also act as central regulators that integrate internal and external signals (Sun 2011, Xu et al., 2014; Daviere and Achard 2016). Initially DELLAs were thought to regulate gene expression as transcription

factors, however they lack a canonical DNA-binding domain. Instead they interact with and regulate transcription factor function. There are many known DELLA interacting proteins including basic helix-loop-helix (bHLH) transcription factors including PIFs (Phytochrome Interacting Factors) that control hypocotyl growth regulated by light signalling (De Lucas et al., 2008). DELLAs also interact with GRAS proteins including SCL3 (ScareCrow-Like3) which promotes GA-induced root and hypocotyl elongation and radial patterning (Zhang et al., 2011). Another group of known DELLA interacting proteins is the JA signalling repressor JAZ proteins. DELLAs binding inhibit JA-mediated root growth inhibition and plant defence by preventing interaction of JAZ with MYC2, a transcription factor that promotes expression of JA responsive genes (Hou et al., 2010). DELLAs also regulate ethylene signalling by interacting with EIN3 (Ethylene INsensitive3), an ethylene signalling activator. DELLAs inhibit the EIN3 preventing the formation of the ethylene-induced apical hook (An et al., 2012). Lastly DELLAs also inhibit brassinosteroid-induced hypocotyl elongation by binding to BZR1, a BR activator, blocking DNA binding of BRZ1 with target gene promoters (Bai et al., 2012). DELLA also blocks DNA binding to the target gene promoters of PIFs and EIN3, in addition to BRZ1. Another transcription factor with which DELLAs interact is GAF1 (GAI-Associated Factor 1) transcription factor. This protein triggers a negative feedback loop that activates GA biosynthesis and DELLA degradation (Fukazawa et al., 2017).

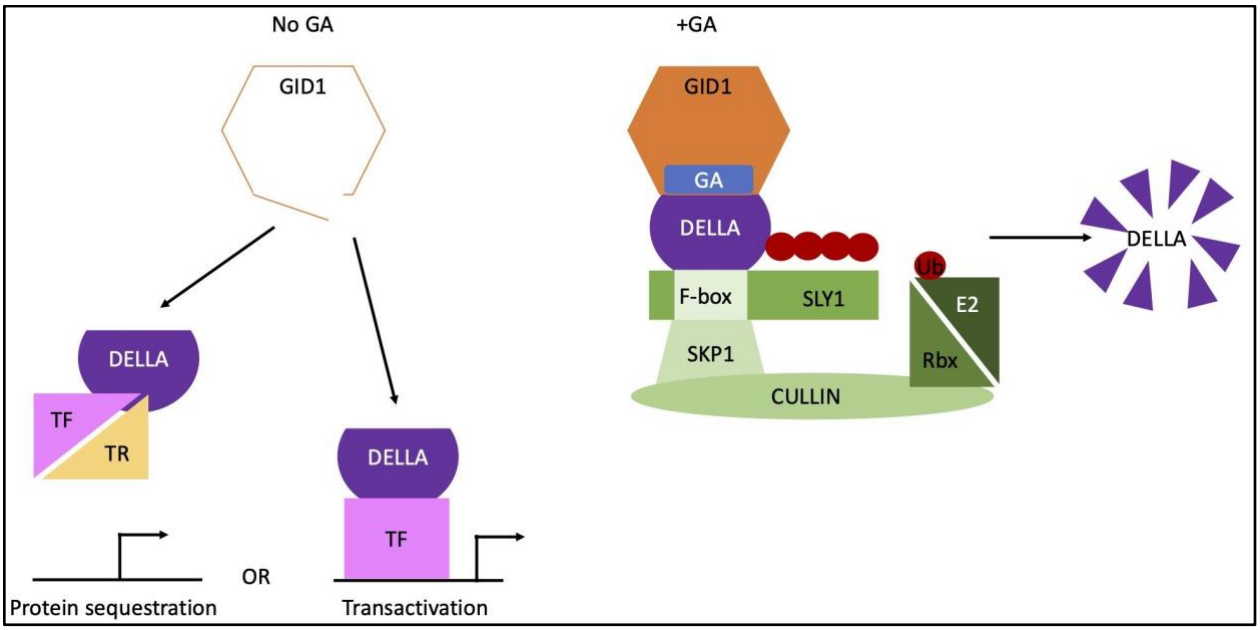

Figure 1.8 The GA signalling cascade. *In the absence of GA the DELLA proteins are active, binding to transcription factors and transcriptional repressors resulting in protein sequestration or transactivation. When GA is present in the cell it binds to the GA receptor, GID1 which forms a complex with DELLA. This results in recognition and ubiquitination of DELLA by the SCF^{SLY1} E3 ligase. Polyubiquitination results in degradation of the DELLA protein via the 26S proteasome.*

1.4.2 The GID family

The GA receptor, GID1 was identified through map-based cloning in a GA-insensitive mutant in rice in 2005 (Ueguchi-Tanaka et al., 2005). Rice was found to have one GID1 gene, whereas *Arabidopsis* has three functional homologs. Loss of all three genes is required for a complete loss of GA response and unlike GA biosynthesis mutations, is not rescued by GA application (Griffiths et al., 2006; Willige et al., 2007).

GID1 localises mainly to the nucleus but also localises in the cytoplasm (Ueguchi-Tanaka et al., 2005; Willige et al., 2007). GID1 has a domain that binds GA and a second N-terminal 'lid' domain that interacts hydrophobically with the lactone ring of GA and upon binding folds over the GA-binding pocket. This conformational change that occurs upon binding GA causes the GID1 N-terminal helical lid domain to behave like a molecular glue and interact with the DELLA repressor proteins (Ueguchi-Tanaka etal., 2005; Murase et al., 2008). DELLA is also thought to stabilise the GID1-GA hormone as the GID1-GA-DELLA complex binds GA with a higher affinity than GID1 alone.

1.4.3 The DELLA family

Some monocot and dicot species only have one DELLA protein, such as rice or tomato, whereas *Arabidopsis* has five DELLA proteins; RGA (Repressor of GAI1-3), GAI (GA-Insensitive), RGL1 (RGA-Like1), RGL2, RGL3. The DELLA proteins are nuclear localised and composed of two main protein domains. The N-terminal portion of the protein is the regulatory 'DELLA' domain and contains the conserved amino acid sequence Asp-Glu-Leu-Leu-Ala. The DELLA motif is recognised by GID1, which regulates the stability of the protein. The N-terminal domain is intrinsically disordered and upon GID1 binding folds and becomes structured. The TVHYNP region, which is near the DELLA domain, enables binding of the GID1 receptor, mutations in the region results in semi dominant GA-insensitive dwarf phenotype, caused by the inability to regulate the DELLA repressor. The other region in the DELLA regulatory domain is the Ser/Thr/Val-rich domain which is involved in phosphorylation. The C-terminal portion of the protein is the GRAS (GAI, RGA and SCARECROW) domain, which is found in a large number of protein classes (Bolle, 2004). The GRAS domain forms the interaction interface with many different proteins and is responsible for the repressive effects of the DELLA proteins. The GRAS domain contains PFYRE and SAW regions which help form secondary interactions with GID1.

DELLAs are degraded by ubiquitin via the 26S proteasome pathway resulting in activation of GA responses. However in addition to ubiquitination, DELLA proteins undergo other post-translational modifications to provide further dynamic regulation of the DELLAs. DELLAs are phosphorylated at several residues, predominantly in the GRAS domain, there is also a phosphorylation site at the C-terminus of the PolyS/T region. These sites provide protein stability and activity (Hussain et al., 2005). Another layer of regulation which has been identified is *O*-linked

glycosylation. This is a dynamic and reversible posttranslational reaction carried out by SEC (SECret agent) on multiple sites in the N-terminus and in the PolyS/T region. A close homolog of SEC is SPY (SPindlY), both proteins contain an N-terminal tetratricopeptide repeat domain, involved in protein-protein interaction and C-terminal putative *O*-linked *N*-acetylglucosamine (*O*-GlcNAc) transferase (OGT) catalytic domain, which transfers *O*-GlcNAc from UDP-GlcNAc to Ser and Thr residues of proteins. The *spy* mutants were originally identified in a genetic screen for negative regulators of GA signalling. The loss of function mutants are capable of germinating in the presence of paclobutrazol (inhibitor of GA biosynthesis) and capable of rescuing the dwarf phenotype of GA-deficient mutants (Jacobsen and Olszewski, 1993) it was thought that both SPY and SEC could carry out *O*-GlcNAcylation. However, using mass-spectrometry analysis, *O*-GlcNAcylation in DELLA were lost in *sec-3* mutant plants, but not in *spy-8* mutants (Zentella et al., 2016).

SPY was identified to be a *O*-fucosyltransferase, a protein that catalyses the transfer of fucose from GDP-fucose to the hydroxyl groups of Ser and Thr. There are several *O*-fucosylation sites in the RGA protein which cluster in the same region as the *O*-GlcNAcylation sites. Using mass-spectrometry, it was identified the level of *O*-fucosylation decreased in *spy-8* mutants, but was unaltered in *sec-3* mutants (Zentella et al., 2017).

SPY and SEC are thought to compete to modify DELLA, suggesting they have opposing roles (Zentella et al., 2017). The binding affinity of DELLA interacting partners was examined when DELLAs were *O*-GlcNAcylated, compared to being *O*-fucosylated. *O*-GlcNAcylated RGA reduced interaction with essential growth regulators BZR1 and PIFs, leading to growth arrest, conversely *O*-fucosylated RGA increased interaction with BZR1 and PIFs. This was further corroborated by the *sec-3* and *spy-8* phenotype. The GA responsiveness and dwarf phenotype of the GA-deficient *ga1-3* mutant can be partially rescued by the *spy-8* (*spy-8 ga1-3*) mutation, whereas the growth and GA responsiveness is further reduced in the *sec-3* mutant (*ga1-3 sec-3*) (Zentella et al., 2016; Zentella et al., 2017). It has been suggested that SPY and SEC may activate and repress DELLA, respectively, via conformational transition enhancing/preventing binding with interaction partners (Camut et al, 2017).

1.4.4 DELLA and SUMO

Conti et al., (2014) found in *Arabidopsis* the levels of SUMOylation of RGA and GAI are increased under salt stress conditions and they are deSUMOylated by OTS1. When SUMO protease double knockout plants *ots1-1 ots2-1* (herein called *ots ko)* plants are placed in salt stress conditions there is increased DELLA accumulation, compared to Col-0. Initially it was thought that SUMOylation of the DELLA proteins blocked GID1 mediated degradation, however only a small pool of DELLA was SUMOylated, which could not explain the accumulation of unmodified DELLA proteins. Conti et al., 2014 proposed a model whereby SUMOylated DELLA binds to GID1 but is not degraded, however it is capable of sequestering GID1, preventing it from targeting the pool of unmodified DELLA proteins for degradation,

thus inhibiting GID1. Furthermore the SUMO site, in the N-terminal helical switch region of the DELLA protein, where GID1 binds to ubiquitinate DELLA, may provide a physical barrier to GID1. SUMOylated DELLA is capable of sequestering GID1 through the SIM site in the lid region of GID1, that covers the GA docking pocket, this interferes with GA access to GID1, blocking GID1 access to DELLAs. This enables GID1-DELLA interaction in the absence of GA allowing SUMOylated DELLA to "mop up" GID1 protein preventing ubiquitination of DELLA. This process occurs in stress conditions, the post-translational modification of SUMOylation occurs faster than downregulation of GA and may provide a fast response system to cease GA signalling (Conti et al., 2014).

Gonçalves et al., 2020 recently demonstrated that the single rice DELLA protein, SLR1, is SUMOylated at a different residue than the K65 residue which Conti et al., 2014 identified in *Arabidopsis*. Instead SLR1 is SUMOylated at the second residue in the protein K2 and not at K60, the residue counterpart to the *Arabidopsis* K65. The group generated an expression construct to constitutively express a genetic fusion of mature SUMO to the K2 residue of SLR1 ($SUMO1_{GG}$::$SLR1_{K2}$) to examine if salt tolerance was increased. The SUMO1SLR1-OX lines showed less stress to salt treatment. However, this could not be attributed to increased accumulation of SLR1 as the SLR1-OX lines had similar protein levels. The group assumed the increased salt tolerance was due to the SUMO attached to SLR1 and performed RNA-seq analysis on a SUMO1SLR1-OX line and a SLR1-OX line. The SUMO1SLR1-OX line had increased expression of *GA20ox2* and *GA2ox3*. These enzymes control the synthesis and inactivation of active GA_4. SLR1 could affect the transcription of *GA20ox2* by interacting with transcription factor YAB4 and repressing expression of *GA20ox2*. Using a yeast two-hybrid system and biomolecular fluorescence complementation (BiFC) to examine the interaction of SLR1 and SUMO1SLR1 with YAB4, SUMO bound to K2 was found to block the interaction. Furthermore the interactions of six other transcription factors was found to be disrupted or reduced, demonstrating that SUMO represents a novel mechanism to disrupt interaction with several transcription factor families and modulate DELLA activity (Gonçalves et al., 2020).

Conti et al., (2014) reported on a SUMO site in the N-terminus identified using a bacterial system (Conti et al., 2014), however the group also identified a SUMO site in the C-terminus of DELLA, that was not reported at the time. The objective of chapter 6 of this thesis was to research the role and effect on DELLA of SUMOylation at the C-terminus.

1.5 Study objectives

Arabidopsis is predicted to have 5660 SUMOylated proteins, (Miller et al., 2019), SUMOylated proteins have been identified in nearly every hormone pathway. SUMOylated proteins are also found in pathways responding to environmental stimuli and in pathways that alter plant development. This thesis can be broadly broken down into

three separate projects, carrying out research into the role of SUMOylated proteins involved in the ABA hormone pathway, root hair development and the GA hormone pathway. The aim of each project was to further understand the role of SUMO in three main areas as follow:

- Initial screens had indicated that an *Arabidopsis* mutant with two SUMO proteases knocked out (*ots1 ots2*) was ABA hypersensitive. This led to scanning the key components of the ABA signalling cascade with software that predicts SUMO sites to identify the SUMOylated proteins the SUMO proteases target. The ABA negative regulator PP2CA was identified as harbouring SUMO sites. The aim of the project was to determine the role of SUMO in the function of the PP2CA protein.
- Another screen conducted with *Arabidopsis* mutant (*ots1 ots2*) examined if the mutant had a root hair phenotype. The mutant was found to harbour fewer, longer root hairs, compared with control. This led to scanning the key proteins involved in root hair formation with software that predicts SUMO sites to identify SUMOylated proteins. A transcription factor RSL4, that is required for root hair formation was identified as harbouring SUMO sites. The aim of the project was to determine the role of SUMO in the function of the RSL4 protein.
- Previous work in the lab had determined that the negative regulator of the GA pathway DELLA harboured two SUMO sites, the first site provides protein stability (Conti et al., 2014). Work had demonstrated that the second SUMO site in the GRAS-domain altered interactions with transcription factors. The aim of this project was to determine if an interacting transcription factor PIF4 harboured a SIM site and to determine the biological phenotype of the GRAS-domain SUMO site in DELLA.

Chapter 2

Materials and methods.

2.1 Materials

The chemicals used for the practical work in this thesis were brought from Sigma-Aldrich, Fisher Scientific, VWR or Melford, unless stated otherwise.

2.1.1 Buffers

All buffers were made with ultrapure deionised water.

TE buffer: 0.01% Tris-HCl pH 7.5, 0.001% EDTA

SOC: 2% tryptone, 0.5% yeast extract, 0.05% NaCl, 0.019% KCl, pH NaOH, after autoclaving 0.036% glucose, 0.001% $MgCl_2$

TAE buffer: 2 M Tris, 5.71% Glacial acetic acid, 0.06 M Disodium EDTA

Genomic DNA extraction buffer: 0.2% Tris-HCl (pH 7.5), 0.25% NaCl, 0.025% EDTA, 0.5% Sodium dodecyl sulphate (SDS).

DEPC water: 1 ml DEPC in 1 litre of sterile water left overnight then autoclaved at 121oC for 20 minutes.

SDS-PAGE running gel: 0.38 M Tris-HCl (pH 8.8 at 25˚C), 0.1% Sodium dodecyl sulphate (SDS), 8-15% (w/v) 29:1 Acrylamide:Bis-acrylamide, 0.05% (w/v) Ammonium persulphate (APS), 0.07% (v/v) Tetramethylethylene-diamine (TEMED).

SDS-PAGE stacking gel: 132 mM Tris-HCl (pH 6.8 at 25˚C), 0.1% SDS, 4% (w/v) 29:1 Acrylamide:Bis-acrylamide, 0.05% (w/v) APS, 0.15% (v/v) TEMED.

4x SDS Loading Buffer: 200mM Tris-HCl (pH 6.8 at 25°C), 8% (w/v) SDS, 50mM EDTA, 20mg Bromophenol blue, 4% w/v β-mercaptoethanol, 40% (v/v) glycerol.

10x SDS-PAGE RunningBuffer: 250mM Tris-HCl (pH 8.3 at 25°C), 1.9M glycine, 1% (w/v) SDS.

Coomassie Stain: 0.25% (w/v) Coomassie Brilliant Blue R-250, 10% (v/v) MeOH, 10% (v/v) glacial acetic acid.

Coomassie Destain: 10% (v/v) MeOH, 10% (v/v) glacial acetic acid.

1x Transfer Buffer: 25mM Tris, 190mM glycine, 20% (v/v) MeOH.

10x TBS: 500mM Tris (pH 7.4 at 25°C), 9% (w/v) NaCl.

1x TBST: 50mM Tris (pH 7.4 at 25°C), 0.9% (w/v) NaCl, 0.1% (v/v) Tween20.

Blocking Solution: 5% (w/v) non-fat milk powder in 1xTBST.

SUMO Extraction Buffer: 50mM NaCl, 50mM Tris-HCl (pH 8 at 25°C), 1mM EDTA, 1% (v/v) NP-40, 0.5% (w/v) Sodium deoxycholate, 0.2% (w/v) SDS, 20mM NEM, 1 per final 10ml protease inhibitor cocktail.

CO-IP Buffer: 150mM NaCl, 50mM Tris-HCl (pH 8 at 25°C), 5mM EDTA, 10% (v/v) glycerol, 0.1% (v/v) Triton-X, 10mM DTT, 1 per final 10ml protease inhibitor cocktail.

Ponceau S Stain: 0.5% (w/v) Ponceau S, 1% (v/v) glacial acetic acid

Binding buffer: 140nM NaCl, 2.7mM KCl, 10mM Na2HPO4, 1.8mM KH2PO4, pH 7.4.

Elution buffer: 50mM Tris base, 20mM Reduced glutathione, pH 8.0

2.1.2 Enzymes

Polymerases MyTaq Red Mix - Bioline

Q5® Hot Start High-Fidelity DNA Polymerase - New England BioLabs

Brilliant III Ultra-Fast SYBR QPCR - Agilent technologies

Gateway Life Technologies pENTR D-TOPO - Thermo Fisher

Life Technologies Gateway cassette LR clonase II - Thermo Fisher

Reverse Transcription Invitrogen SuperScript® II Reverse Transcriptase - Thermo Fisher

Invitrogen RNaseOUTTM Recombinant Ribonuclease Inhibitor - Fisher Restriction Enzymes

T4 DNA ligase- New England BioLabs

DNase I- Zymo

Restriction enzymes; DpnI HF, NcoI HF, NotI HF, SalI HF, XhoI HF, KpnI HF, NruI HF, PvuI HF and MluI HF - New England BioLabs.

2.1.3 Antibiotics

Table 2.1 Stock solution and working concentration of antibiotics used in the study.

Antibiotic	Stock solution (mg/ml)	Working concentration (µg/ml)	Supplier
Kanamycin	50	50	Melford
Rifampicin	12.5	12.5	Duchefa Biochemie
Gentamicin	25	25	Melford
Spectinomycin	50	50	Melford
Carbenicillin	50	50	Melford
Chloramphenicol	34	34	Duchefa Biochemie

2.1.4 Kits

ZR Plasmid Miniprep™ isolation kit- Zymo

Direct-zol RNA Miniprep kit- Zymo

Gel DNA recovery kit- Zymo

pENTR/D-TOPO Cloning kit- Thermo Fisher

MACS® microbead system- Miltenyi Biotech

2.1.5 Ladders

DNA hyperladder™ 1KB plus- BioLine

PageRuler™ Plus Prestained Protein ladder- Thermo Fisher

2.1.6 Vectors

Table 2.2 Vector size and antibiotic resistance used.

Vector	Size (bp)	Resistance	Promoter	Tag	Purpose
pENTR D-TOPO	2580	Kanamycin	N/A	N/A	Gateway entry vector
pENTR4 dual	3757	Kanamycin	N/A	N/A	Entry vector
pMDC107	11,744	Kanamycin	N/A	C-terminal mGFP6	Destination vector
pAlligator2	~10,300	Spectinomycin	Enhanced 35S promoter	N-terminal 3XHA and E-GFP	Destination vector
pGWB17	17,407	Kanamycin	35S promoter	C-terminal 4XMyc	Destination vector
pEarleygate104	12,505	Kanamycin	35S promoter	N-terminal E-YFP	Destination vector

pEarleygate201	11,779	Kanamycin	35S promoter	N-terminal HA	Destination vector
pGWB15	17,358	Kanamycin	35S promoter	N-terminal 3XHA	Destination vector
pEarleygate103	12,411	Kanamycin	35S promoter	C-terminal mGFP5 and 6XHis	Destination vector

2.1.7 Bacterial strains

Table 2.3 List of bacteria used in this study.

Organism	Strain	Resistance	Purpose
Escherichia coli	DH5	None used	Laboratory strain, plasmid maintenance and propagation
Agrobacterium tumefaciens	GV3101:pMP90	Rifampicin and Gentamicin	*Arabidopsis* transformation and Benthamiana transient transformation
Escherichia coli	CCDB+		Propagation of empty plasmids
Pseudomonas syringae	DC300	Rifampicin	Pathotest

2.1.8 Antibodies

Table 2.4 List of primary antibodies

Antibody	Host	Working concentration (TBST)	Supplier-order number
Anti-Ha	Rat	1:10,000	Roche
Anti-His	Rat	1:10,000	Roche
Anti-SUMO1	Rabbit	1:5000	Manufactured inhouse
Anti-GFP	Rabbit	1:8000	Abcam
Anti-GST	Rat	1:5000	Abcam
Anti-Myc	Rabbit	1:5000	Abcam

Table 2.5 List of secondary antibodies.

Antibody	Host	Working concentration (TBST)	Supplier-order number
Anti-Rat-Hrp	Goat	1:20,000	Sigma
Anti-Rabbit-Hrp	Donkey	1:20,000	Sigma

2.1.9 Arabidopsis

Table 2.6 List of Arabidopsis mutants.

Mutant	Gene ID	Code	Ecotype
ots ko (*ots1-1 ots2-1*)	AT1G60220 AT1G10570	SALK 022798 SALK 001579	Col-0

spf ko (spf1-1 spf2-2)	AT1G09730 AT4G33620	SALK 040576 SALK 090744	Col-0
pp2ca-1	AT3G11410	SALK 028132	Col-0
p3 (*pp2ca-1 hab1-1 abi1-2*)	AT3G11410 AT1G72770 AT4G26080	SALK 028132 SALK 002104 SALK 72009	Col-0
pyl458 (*pyl4-1 pyl5-1 pyl8-1*)	AT2G38310 AT5G05440 AT5G53160	SAIL_517_C08 SM3_3493 SAIL_1269_A02	Col-0
rsl ko (rsl2-1 rsl4-1)	AT4G33880 AT1G27740	SAIL_514_C04 / CS874457/N874457 GT_5_105706/N168205	Col-0
pifq (*pif1-1 pif3-3 pif4-2 pif5-3*)	AT2G20180 AT1G09530 AT2G43010 AT3G59060	SAIL_256_G07 (Huq et al 2004) SALK (monte et al 2004) SAIL_1288_E07 SALK_087012.41.25	Col-0
della ko (*rga-24 gai-t6*)	AT2G01570 AT1G14920	rga-24 gai-t6	Ler

2.1.10 Media

Media was autoclaved until sterile and either kept in a conical flask, if liquid culture was required, or poured into circular or square plates in a flow hood.

MS: 0.22% Murashige & Skoog Modified Basal Salt Mixture (Melford) 0.8% phytoagar (if required), pH to 5.7 with KOH.

Low and high phosphate MS: 0.22% Murashige & Skoog Modified Basal Salt Mixture (Phytotech lab) 0.8% phytoagar (if required), 3 µM/312 µM KH_2PO_4, pH to 5.7 with KOH or KCl.

LB: 2% LB broth (Lennox) 1.2% microagar (if required), pH to 7.2 with NaOH.

Kings B broth: 1% Peptone, 0.075% K_2HPO_4, 0.6% micro agar (if required), 0.5% glycerol, after autoclaving 0.3% 1M $MgSO_4$.

2.2 Plant growth and treatment

2.2.1 Benthamiana growth

Seeds were sown directly onto moist Levington F2 plus sand compost in a tray. The tray was covered with a lid to maintain humidity until the seedlings had been established. The pots were kept in a growth room with a temperature of 21˚C and a 16/8 hour light/dark programme. Seedlings were transplanted after 1 week into individual 10 cm pots where they were left to grow under the same conditions until the plants had produced approximately 6-10 leaves.

2.2.2 Arabidopsis seed sterilisation for tissue culture

Arabidopsis seeds were sterilized in a closed box in a fume hood using chlorine gas generated from the addition of 3 ml concentrated hydrochloric acid to 100ml of 13% hypochlorite solution. The seeds were left for 12 hours before being ventilated to render the box safe and placed on plates under sterile conditions (laminar flow hood). The 1⁄2 MS plates were then sealed with micropore tape (3M) and stratified for two days at 4°C. The plates were then placed vertically at room temperature in a 16/8 hour light/dark programme to induce germination and growth in a Sanyo Growth cabinet.

2.2.3 Arabidopsis thaliana tissue culture, plant medium

All *Arabidopsis* seedlings used were grown on 1⁄2 MS medium (Melford) and 0.8% agar. Media was allowed to cool to 50°C before adding hormone treatments or selective agents.

2.2.4 Arabidopsis thaliana hormone treatment

The following hormone and herbicide stock solutions were made:

Table 2.7 Hormone and herbicide stock solution concentrations

Hormone	Solvent	Stock Conc.
ABA	DMSO	100 mM
MeJa	Water	500 mM
GA_3	Water	100 mM
ACC	Water	100 mM
IAA	Water	10 mg/ml
Hygromycin	Water	25 mg/ml
BASTA (glufosinate-ammonium)	Water	20 mg/ml

Four to five days after germination on standard 1⁄2 MS plates, seedlings were transferred to the hormone-supplemented plates. The plates were then placed vertically at room temperature in a 16/8 hour light/dark programme in a Sanyo GROWTH CABINET. After five to seven days, images of the seedlings were taken and the images analysed in ImageJ, which allowed accurate measuring of the roots whilst equilibrating the scale of each picture to the ruler. The measurements were then analysed statistically using a Student's T-test or ANOVA, and averages calculated and plotted on a bar chart. Additionally, after photographs were taken, several seedlings that represented the mean of each genotype were placed together on a single plate for comparison.

2.2.5 Arabidopsis thaliana growth

Arabidopsis seeds were sown in moist Levington F2 plus sand compost treated with Calypso SC 480 insecticide (Bayer). The seeds were then stratified for 3 days at 4°C before being transferred to growth rooms. The plants were grown under long day conditions: 16 light hours at 22°C and 8 dark hours at 20°C with a constant relative humidity of 70%.

2.2.6 Floral dipping of Arabidopsis thaliana

A. tumefaciens (GV3101 pMP90) transformed with the constructs were used to transform *Arabidopsis* plants by the floral dip method (Clough and Bent 1998). In brief, agrobacterium was initially grown on agar plates with rifampicin, gentamicin and kanamycin. 10 ml of liquid LB with equivalent selection was inoculated from freshly grown plates and grown overnight at 28°C with shaking at 200 rpm. *Agrobacterium* was inoculated into 500 ml of liquid LB with appropriate selection and grown as before for 24 hours. The cells were centrifuged at 4500 rpm for 10 minutes and the supernatant disposed. The cells were resuspended in 400 ml 5% (w/v) of sucrose in sterile water. Silwett-L77® was added to a concentration of 0.02% before dipping the unopened inflorescence of bolted *Arabidopsis* (4-5 week old grown under long day conditions) for 30 seconds with agitation. Dipped plants were laid down in trays and placed into an autoclave bag for 24 hours before standing upright and allowing to set seed.

2.2.7 Selection of transgenic Arabidopsis thaliana

Primary transformants were either selected for by spreading seed on soil soaked with 0.1% Glufosinate (marketed as Basta, Bayer) and stratified for two days at 4˚C. After 14 days, resistant seedlings were pricked out onto fresh soil with no selection and grown under long day conditions. Hygromycin resistant transformants were selected by sterilising seeds and aseptically spreading on 1/2 MS plates supplemented with 25µg/ml final concentration hygromycin. The plates were sealed with micropore tape (3M) and the seeds stratified at 4°C for two days. The plates were then moved to growth cabinets and grown for 10 days, resistant seedlings were pricked out on soil with no selection and grown under long day conditions. Once siliques formed, the plants were bagged individually and allowed to set seed.

Secondary transgenic seed was sterilized and spread aseptically on 1⁄2 MS plates supplemented with 20µg/ml final glufosinate-ammonium or 25µg/m final concentration hygromycin. The plates were sealed with micropore tape (3M) and the seeds stratified at 4°C for two days. The plates were then moved to growth cabinets and grown for 10 days. The seedlings were then screened for resistance at a ratio of 3:1 (resistant : susceptible) in order to select for transgenics containing a single transformation insert. Selected lines were then pricked out onto fresh soil with no selection. Again, individual plants were bagged to collect seed once siliques had formed.

Tertiary transgenic seed was sterilised and spread aseptically on 1⁄2 MS plates supplemented with 20µg/ml final glufosinate-ammonium or 25µg/ml final concentration hygromycin. The plates were sealed with micropore tape (3M) and the seeds stratified at 4°C for two days. The plates were then moved to growth cabinets and grown for 10 days. Plants were then screened for complete resistance, indicating homozygous transgenics. Selected lines were

then pricked out onto fresh soil with no selection. Again, individual plants were bagged to collect seed once siliques had formed.

2.2.8 Infections

Pseudomonas syringae DC3000 (Pst) were grown on plates containing King's B agar and incubated in the dark for two days at 28°C. After this time, King's B liquid media was inoculated from the plate and placed on a shaker and grown overnight at 28°C. The bacteria was then centrifuged at 4000 rpm for 10mins at room temperature. The pellet was resuspended in sterile water and spun again under the same conditions previously described. $1X10^8$ cfu/ml was reached through serial dilution of the sample. From each 4 week-old plant, 4 leaves were dipped in the solution for 5 seconds and placed in the back in the same growth conditions as before (short day). After 2, 3, 4 or 5 days, 1cm2 leaf discs were cut from infected leaves and crushed with 240ml of sterile water. The sample was then serially diluted along the microtiter plate, taking 40ml of the initial/previous sample and diluting 1 in 5 each new well. Taking 10µl of each dilution, the samples were then droplet spotted on a King's B agar plates and left to air dry for 10mins. They were then transferred to a 25°C room for 36 hours before pictures were taken for colonies to be counted. For each genotype this was repeated on 3 plates for each time point (Katagiri *et al*., 2002).

2.3 Microbiological procedures

2.3.1 Generation of chemically competent E coli

The selected E. coli strain (e.g. DH5α) was streaked out onto a fresh LB agar plate with no selection and incubated at 37°C for 24 hours. A single colony was selected using a sterile loop and used to inoculate 10ml of LB liquid. The culture was grown for 16 hours at 37°C. 1ml of the culture was then used to inoculate 200ml of LB liquid, with shaking at 220rpm, at 37°C for a further 6 hours. The culture was transferred to chilled centrifuge tubes and centrifuged at 4000rpm for 15 minutes at 4°C. The supernatant was removed and the cells resuspended in 10ml of ice-cold TE buffer. The culture was re-centrifuged under the same conditions, the supernatant removed and the cells resuspended in 20ml of ice-cold liquid LB. The cells were then stored at -80°C in 100µl aliquots.

2.3.2 Generation of chemically competent Agrobacterium tumefaciens

The selected *Agrobacterium* strain (e.g. GV3101) was streaked out onto a fresh LB agar plate with rifampicin and gentamicin selection and incubated at 28°C for 48 hours. A single colony was selected using a sterile loop and used to inoculate 10ml of LB liquid plus rifampicin and gentamicin. The culture was grown for 24 hours at 28°C. 1ml of the culture was then used to inoculate 200ml of LB liquid plus rifampicin and gentamicin and incubated, with shaking at 220rpm, at 28°C for a further 18 hours. The culture was transferred to chilled centrifuge tubes and centrifuged at 4000rpm for 15 minutes at 4°C. The supernatant was removed and the cells resuspended in 10ml of ice-cold TE buffer. The culture was re-centrifuged under the same conditions, the supernatant removed and the cells resuspended in 20ml of ice-cold liquid LB. The cells were then stored at -80°C in 200µl aliquots.

2.3.3 Transformation of chemically competent bacterial cells

Transformation and growth of bacterial cells with recombinant plasmids were used to 'bulk up' and select said plasmids (using E.coli strain DH5α), to express recombinant protein (using E.coli strain BL21 (DE3)) or to act as a vector in transient expression systems (using *Agrobacterium* strain GV3101).

For a typical transformation 100 – 200ng Plasmid DNA was added to 40/200µl chemically competent *E. coli*/*Agrobacterium*, respectively.

Cells were thawed on ice for 10 min, plasmid DNA was then added. The cells were flash frozen in liquid nitrogen for 3 mins. Then the cells were transferred to 37°C for 3 min then returned to ice for a further 5min. 1ml of SOC (at RT) was added and the cells were incubated in an orbital shaker at 220rpm for 1 hour at 37°C or 2 hours at 28˚C for *E. coli* and *Agrobacterium*, respectively..

The culture was centrifuged at 4,000 rpm for 2 mins and the majority of the supernatant removed. The cells were resuspended in the remaining 50µl supernatant and was spread upon an LB plate with antibiotic selection. The plates were incubated overnight at 37°C for E. coli and over a period of two days at 28°C for *Agrobacterium*. Colony PCRs were then performed to check for the presence of the recombinant gene (see 2.4.2).

2.3.4 Recombinant plasmid purification

Recombinant plasmids were purified from 10ml E. coli DH5α cultures incubated overnight at 37°C using a ZR Plasmid Miniprep Kit - Classic (Zymo Research). The amount of DNA obtained was then quantified using a NanoDrop™ One (Thermo Scientific).

2.4 DNA/RNA analysis

2.4.1 Oligonucleotides

The Arabidopsis Information Resource (TAIR) was used to retrieve *Arabidopsis thaliana* gene coding DNA sequences, or in the case of plasmid sequences, from online repositories, such as addgene. Primers were designed to gene targets using SnapGene Viewer software, or the National Center for Biotechnology Information (NCBI) primer BLAST web application (Geer et al., 2010).

2.4.2 Polymerase chain reaction

Colony PCR:

Six colonies per transformation were screened for successful recombinants. Individual bacterial colonies were picked using pipette tips and incubated in the PCR mix for 2 mins. The PCR was carried out using vector specific primers corresponding to the vector combined with gene specific primers to check for the recombinant gene insert after bacterial transformation.

Table 2.8 Colony PCR setup.

Component	Per reaction
2X Bioline MyTaq Red Mix	5 µl
Forward primer (10pm/µl)	0.4 µl
Reverse primer (10pm/µl)	0.4 µl
DNA template	10-20 ng
Sterile water	To 10 µl

Table 2.9 Colony PCR cloning conditions A table showing the cycling programmes used during colony PCR.

Temperature	Time	Number of cycles
95˚C	3 min	-
95˚C	30 sec	x30
58˚C	30 sec	
72˚C	30 sec per kb	
72˚C	7 mins	-
10˚C	∞	-

Whole PCR reactions were run on an agarose gel to check that PCR products were the correct size, corresponding to the gene insert size plus the vector region.

Cloning PCR:

Q5™ (NEB) cloning polymerase was used to amplify the different genes and promoter regions and cause site directed mutagenesis using primers with CACC added to the 5' end of the forward primer for cloning using pDTOPO cloning system. Primers with the correct restriction sites added were used for cloning with the pENTR4 cloning strategy. The template DNA used to clone the genes and promoters were cloned from cDNA and genomic DNA (see 2.4.2). Primers were tested on DNA with a gradient across the heat cycler for the annealing step.

Table 2.10 Q5 PCR setup A table showing the composition of cloning and site-directed mutagenesis PCRs

Component	Per Reaction
5x Q5™ reaction buffer	10 µl
10 mM dNTPs	1 µl

Forward primer (10 pM/µl)	2.5 µl
Reverse primer (10 pM/µl)	2.5 µl
Template DNA	100-200 ng
Q5™	0.5 µl
Sterile water	Up to 50 µl

Table 2.11 Q5 PCR cloning conditions the cycling programmes used during cloning and site directed mutagenesis.

Temperature	Time	Number of cycles
98˚C	3 min	-
98˚C	30 sec	x25
58˚C	30 sec	
72˚C	30 sec per kb	
72˚C	7 mins	-
10˚C	∞	-

Gene amplification was observed using agarose gel electrophoresis. Cloning and mutagenesis PCR gene products of the correct size were then cut from the gel using a sharp scalpel and the DNA purified using a Zymoclean Gel DNA Recovery Kit (Zymo).

Genotyping PCR:

Primers were designed which straddle either side of T-DNA insertion sites or amplify a region of interest. Primers were tested on wild-type genomic DNA with a gradient across the heat cycler for the annealing step.

Table 2.12 Arabidopsis genotyping PCR setup the compositions of Arabidopsis thaliana genotyping PCR.

Component	Per reaction
2X Bioline MyTaq Red Mix	5 µl
Forward primer (10pm/µl)	0.4 µl
Reverse primer (10pm/µl)	0.4 µl
Arabidopsis gDNA	3 µl
Sterile water	To 10 µl

Table 2.13 Arabidopsis thaliana genotyping PCR cycling programme

Temperature	Time	Number of cycles
95˚C	3 min	-
95˚C	30 sec	x30
58˚C	30 sec	
72˚C	30 sec per kb	
72˚C	7 mins	-
10˚C	∞	-

Once the optimal annealing temperature was determined, the specificity of the primers was confirmed using genomic DNA from mutant *Arabidopsis* lines alongside wild-type positive control template.

Mutation PCR:

The PCR was carried out using forward and reverse primers covering the same region containing the mutation to amplify the whole vector. As few cycles as possible was used to reduce the number of errors in the finished product and the PCR product was run on an agarose gel to confirm amplification. Following the mutation PCR the PCR product was digested with DpnI. After digestion for 1 hour at 37˚C the digestion was incubated at 80˚C for 20 minutes then the 10 µl product was transformed into DH5α.

Table 2.14 Restriction digestion setup of a mutation PCR the components used in a standard restriction digest of a mutation PCR product.

Component	Per reaction
10x compatible NEB buffer	1 µl
PCR reaction	1 µl
DpnI (NEB)	0.5 µl
Sterile water	7.5 µl

2.4.3 Agarose gel electrophoresis

Agarose was added to the 1xTAE buffer to make a 0.6-1% solution. The solution was then microwaved at full power until the agarose had dissolved. The solution was allowed to cool before ethidium bromide was added to a final concentration of 0.0001%. The solution was then poured into an appropriate sized gel mould, a 8/20 well comb added and the solution allowed to set. The gel was then placed into an electrophoresis tank filled with 1xTAE. Samples were loaded into the wells along with Hyperladder 1kb Plus (Bioline) and the gels were run at 70-120V, dependent upon agarose percentage used. The gels were imaged using a BioRad Gel Doc 2000.

2.4.4 Agarose gel purification

Cloning and mutagenesis PCR gene products of the correct size were cut from the gel using a sharp scalpel and the DNA purified using a Zymoclean Gel DNA Recovery Kit (Zymo).

2.4.5 pENTR/D-TOPO reaction

A pENTR/D-TOPO reaction with clean PCR product, purified using Gel DNA Recovery Kit containing the recombinant gene was performed following the instructions provided in the supplied kit (Invitrogen). The reaction contents were then transformed into E. coli DH5α.

2.4.6 pENTR4 cloning

Clean PCR product, amplified to contain restriction sites, not found in the DNA fragment to correspond with a restriction site in pENTR4 was purified using Gel DNA Recovery Kit. The purified PCR product and pENTR4 was then digested with the relevant restriction enzymes for 1 hour at 37˚C. The digested product was run on a 0.6% agarose gel and the correct sized fragment and pENTR4 backbone was cut from the gel using a sharp scalpel and the DNA purified using a Zymoclean Gel DNA Recovery Kit. The digested products were then ligated together using T4 DNA ligase overnight at 18˚C, 10 µl of the reaction was then transformed into E. coli DH5α.

2.4.7 Restriction digestion

Restriction digestion of purified DNA was used to remove template DNA from mutagenesis PCR products (DpnI (NEB)), to cut the pENTR/D-TOPO vector ready for LR reaction (NruI and PvuI (NEB)) and for restriction cloning into the pENTR4 vector. For a standard restriction digest the reactions were incubated at 37˚C temperature on a shaker for 1 hour. The digestion products were then run on an agarose gel.

Table 2.15 Restriction digestion setup components in standard restriction digest with NEB enzymes.

Component	Per reaction
10x compatible NEB buffer	5 µl
DNA	1 µg

Restriction endonuclease (NEB)	5 U per µg DNA
Sterile water	Up to 50 µl

2.4.8 T4 DNA Ligase reaction

T4 DNA ligase reactions were carried out to anneal two DNA fragments after restriction digestion containing corresponding restriction digestion sites. For a standard ligase reaction however the ratio of vector to insert varied depending on the size (in kb) of each fragment. The reactions were incubated at room temperature for 1 hour or 16˚C overnight. 10 µl reaction was then transformed into E. coli DH5α.

Table 2.16 Ligase reaction setup components for T4 DNA ligase

Component	Per reaction
10x T4 DNA Ligase Buffer	2 µl
Vector DNA	50 ng
Insert DNA	37.5 ng
T4 DNA ligase	1 µl
Sterile water	Up to 20 µl

2.4.9 LR Reaction into Gateway® Destination Vectors

pENTR4/D-TOPO vector containing the recombinant gene was digested with NruI and PvuI (NEB), ensuring the gene of interest was not also digested. The LR reaction was performed following the instructions provided in the supplied

kit (Invitrogen) with an appropriate Gateway® Destination Vector for protein expression in E. coli BL21 (DE3) or *Agrobacterium.* The reaction contents were then transformed into E. coli DH5α.

2.4.10 gDNA Extraction from Arabidopsis thaliana

A single leaf disc was cut using the end of a p10 pipette tip. The disc was ground briefly in a 1.5ml Eppendorf tube using a mini-pestle. 150µl of extraction buffer was added and the mix ground again until homogenous. The sample was centrifuged at 13,300 rpm for 5 minutes. 100µl of the supernatant was transferred to a fresh tube and 100µl of neat isopropanol was added and mixed via inversion. The mixture was incubated at room temperature for 5 minutes. Samples were centrifuged at 13,300 rpm for 10 minutes and the supernatant discarded. The pellet was mixed gently with 500µl of 70% EtOH and centrifuged at 13,500 rpm for 5 minutes. The supernatant was discarded and the pellet left to air-dry for 15 minutes. The dry pellet was then dissolved in 50µl of 10mM Tris (pH 8.5 at 25°C). The quality of the gDNA extraction was then checked via PCR using ACTIN2 primers.

2.4.11 RNA Extraction from Arabidopsis thaliana

Frozen plant tissue was ground into a fine powder using a pre-cooled Eppendorf and micro pestle. The ZR zymo RNA extraction Kit (ZYMO) was used to extract RNA. All extractions were performed following the instructions provided in the supplied kit. RNA was eluted into DEPC water and quantified by measuring absorbance at λ260nm and λ280nm using a NanoDrop™ One (Thermo Scientific).

2.4.12 cDNA Synthesis

1µl of oligo dT (500µg/ml) and 1µl dNTP mix (10µM each) was added to the reaction and incubated at 65°C for a further 5 minutes. The reaction was then chilled briefly on ice and spun down. 4µl 5X First Strand Buffer, 2µl 0.1M DTT and 1µl RNaseOUT was added to the reaction and mixed gently. The reaction was incubated at 42°C for 2 minutes before 1µl SuperScript® II Reverse Transcriptase was added to the reaction. The reaction was then incubated at 42°C for a further 50 minutes. Finally, the reaction was heated to 70°C for 15 minutes to terminate the reaction. The resultant cDNA was made up to 100µl using ultra-pure water. The quality of the resultant cDNA was tested by PCR with ACTIN2 primers.

2.4.13 Quantitative PCR

Quantitative PCR primers were either obtained from published literature (stated in the results chapters) or designed to gene targets using the NCBI primer BLAST (Geer et al., 2010) and primer annealing was tested using gradient PCR. Optimal cDNA concentration analysis was not conducted. 10 µl reactions consisting of components listed in table 2.17 were run in Qiagen RotorGene® Q under programme conditions stated in table 2.18.

Relative expression was compared between genotypes and treatments using target primers and primers to the housekeeping gene ACTIN2 (At3g18780) for normalisation (the in-house standard housekeeping gene). Technical repeats were conducted in triplicate for each sample and comparisons were performed using the comparative quantification $2^{-\Delta\Delta CT}$ method (Warton et al., 2004) using the software provided by Qiagen. Melting curve analysis for each reaction was conducted using the software provided by Qiagen.

Table 2.17 QPCR setup.

Component	Per reaction
SYBR green	5 µl
Forward primer (10pm/µl)	0.5 µl
Reverse primer (10pm/µl)	0.5 µl
Template cDNA	0.5 µl
Sterile water	To 10 µl

Table 2.18 Programme for QPCR using Rotor-Gene Q machine.

Temperature	Time	Number of cycles
95˚C	3 min	-
95˚C	10 sec	X40

58˚C	30 sec	
72˚C	2 min	

2.4.14 Constructs made

Table 2.19. Constructs made.

Entry vector	Insert	Size of insert (bp)	Template	Destination vector	Purpose	Map of construct
pENTR D-TOPO	PP2CA WT	1200	cDNA	pEG104	SUMO IPs, interaction co-IPs	A.2.1, A.2.2
pENTR D-TOPO	$PP2CA^{2K/R}$	1200	cDNA	pEG104	SUMO IPs, interaction co-IPs	A.2.1, A.2.2
pENTR D-TOPO	$PP2CA^{K260R}$	1200	cDNA	pEG104	SUMO blot	A.2.1, A.2.2
pENTR4	$PP2CA_{pro}$;;$PP2CA^{WT}$	4144	cDNA and genomic DNA	pMD107	Stable Arabidopsis transformation	A.2.3, A.2.4
pENTR4	$PP2CA_{pro}$;;$PP2CA^{2K/R}$	4144	cDNA and genomic DNA	pMD107	Stable Arabidopsis transformation	A.2.3, A.2.4
pENTR D-TOPO	$PYL1^{WT}$	666	cDNA	pGWB17	SIM IPs and interaction co-IPs	A.2.5, A.2.6
pENTR D-TOPO	$PYL4^{WT}$	624	cDNA	pGWB17	SIM IPs and interaction co-IPs	A.2.7, A.2.8
pENTR	$PYL8^{WT}$	567	cDNA	pGWB17	Interaction co-IPs, SIM IPs	A.2.9,

D-TOPO					and stable Arabidopsis transformation	A.2.10
pENTR D-TOPO	PYL13^{WT}	495	cDNA	pGWB17	SIM IPs and interaction co-IPs	A.2.11, A.2.12
pENTR D-TOPO	PYL8$^{VM/AA}$	567	cDNA	pGWB17	Interaction co-IPs, SIM IPs and stable Arabidopsis transformation	A.2.9, A.2.10
pENTR4	RSL4^{WT}	777	cDNA	pEG104	SUMO IPs and stable Arabidopsis transformation	A.2.13, A.2.14
pENTR4	RSL4$^{3K/R}$	777	cDNA	pEG104	SUMO IPs and stable Arabidopsis transformation	A.2.13, A.2.14
pENTR D-TOPO	PIF4^{WT}	1293	cDNA	pEG104	SIM IPs, interaction Co-IPs and stable Arabidopsis transformation	A.2.15, A.2.16
pENTR D-TOPO	PIF4$^{VM/AA}$	1293	cDNA	pEG104	SIM IPs, interaction Co-IPs and stable Arabidopsis transformation	A.2.15, A.2.16

2.5 Protein analysis

2.5.1 SDS-PAGE

Acrylamide gel electrophoresis is used to separate and visualise proteins that differ in molecular weight. The tertiary structure of the loaded proteins is denatured by SDS, which coats the protein in a negative charge, allowing for separation by size alone. The application of an electric field upon a gel causes separation of the proteins into discrete

bands that can be seen using Coomassie staining or transferred to a PVDF membrane for western blotting. The gels consist of a stacking, in which the protein is loaded and a running gel, in which the protein bands are resolved, which can vary in acrylamide percentage depending on the weight of proteins that require separation.

Lysed samples were mixed with 2x or 4x SDS Loading Buffer to give a 1x concentration, heated to 95C for 5min and loaded onto a gel. Gels were run at 50-90V to resolve the proteins.

2.5.2 Western blotting

Western blotting is used to visualise specific proteins within homogenised cell or tissue extracts. A PVDF membrane was submersed in methanol for 1 min then soaked in 1x transfer buffer for up to 15 min with blotting paper and sponges. The blotting cassette was prepared and proteins transferred overnight at 25V at 4°C from an SDS-PAGE gel onto the membrane. The membrane was incubated in a blocking solution for 1 hour to prevent non-specific binding of the primary antibody (Bergendahl et al 2003). The membrane was washed 1xTBST and incubated with primary antibodies in 1x TBST. The membrane was washed with 1xTBST and incubated with secondary antibodies (HRP). The membrane was washed again with 1xTBST and developed using an ECL solution.

2.5.3 Infiltration of Nicotiana benthamiana

Agrobacterium containing recombinant plasmid was incubated overnight in an orbital incubator shaker at 28°C and 220rpm. The cells were pelleted at RT at 5000rpm and resuspended in 20ml 10mM sterile MgCl2. The cells were diluted using 10mM sterile MgCl2 to an OD600 0.1-1 and infiltrated into a single Nicotiana benthamiana leaf using a 1ml sterile syringe. The plant was then kept at 20°C on a long day cycle for 3 days.

2.5.4 Protein Extraction from Nicotiana benthamiana Leaves

1g of infiltrated Nicotiana benthamiana leaves were cut at the stem from the plant, wrapped in aluminium foil and flash frozen in liquid nitrogen. The leaves were then powdered in a liquid nitrogen-cooled mortar and pestle and 1g of PVPP added.

For SUMO:

2ml of ice-cold SUMO buffer was added to the powdered tissue and ground further using the mortar and pestle to form a paste. Upon melting, the now liquid paste was then transferred to a pre-cooled Eppendorf tube. The tubes

were centrifuged at 4°C and 8,000rpm for 12 min. The supernatant was transferred to a fresh pre-cooled tube and was either prepared for loading onto an SDS-PAGE gel by the addition of 1xSDS Buffer or immunoprecipitated using the MACS® microbead system (Miltenyi Biotech) as per the instructions included in the kit. The tubes were incubated on a rotator at 4˚C for 25 minutes and the SUMOylated protein extracted using a µMACs multi-stand and separator. The eluted protein was then loaded onto an SDS-PAGE gel for western blotting.

For CO-IP and SIM IP:

The IP for a CO-IP and SIM IP is similar as for SUMO the differences as the buffer used. The only difference is the tubes are centrifuged at 4°C and 10,000rpm for 10 min.

2.5.5 Arabidopsis protein extraction

Total protein

Frozen leaf tissue was ground to a fine powder with a chilled pestle and mortar. Extraction buffer was added 1:1 (weight/ volume). The mixture was centrifuged at 13500rpm at room temperature for 10 minutes. Samples were diluted 1:5 adding 4X protein sample buffer then loaded onto an SDS-PAGE gel for western blotting.

IP

Frozen leaf tissue was ground to a fine powder with a chilled pestle and mortar and ice-cold SUMO buffer was added. Upon melting, the now liquid paste was then transferred to a pre-cooled Eppendorf tube. The tubes were centrifuged at 4°C and 8,000rpm for 12 min. The supernatant was transferred to a fresh pre-cooled tube and was either prepared for loading onto an SDS-PAGE gel by the addition of 1xSDS Buffer or immunoprecipitated using the MACS® microbead system (Miltenyi Biotech) as per the instructions included in the kit. The tubes were incubated on a rotator at 4˚C for 25 minutes and the SUMOylated protein extracted using a µMACs multi-stand and separator. The eluted protein was then loaded onto an SDS-PAGE gel for western blotting.

2.6 Imaging

2.6.1 Confocal microscopy

Leaf sections were cut (approximately 0.5cm2) and placed on a microscope slide (Fischer Scientific), a droplet of water added before covering the leaf section with a 22x22mm cover slip (Menzel-Glaser, Waltham, USA). The slide was placed on the stage of a Zeiss LSM 880 Airyscan confocal microscope (Zeiss, Oberkochen, Germany). A 64x objective oil lens was used for viewing and an Ar-Ion gas laser was used to excite YFP at 514nm and GFP at 488nm.

2.7 Software packages

2.7.1 Sequence analysis, primer design and plasmid map preparation

Snap Gene Viewer version 5.2.4 ©2004-2021 GSL Biotech

2.7.2 Image capture

Quantity One 1-D Analysis Software Version 4.6.5 © Bio-Rad Laboratories

2.7.3 Figure preparation

Image J Version 1.47.

UCSF Chimera Version 1.14 (Petterson et al., 2004)

Mega X Version 10.1.7 1993-2021 (Kumar et al., 2018).

Clustal X Version 2.1 (Larkin et al., 2007)

2.7.4 Phylogenetic tree construction

TAIR (https://www.arabidopsis.org/) was used to retrieve protein sequences for the *Arabidopsis* SUMO proteases. NCBI-blast (p-blast) (https://blast.ncbi.nlm.nih.gov/Blast.cgi) was used, under standard parameter settings, to identify proteins from different plant species for bioinformatic analysis to determine the conservation of predicted SUMO binding sites. Alignments were made using ClustalX (https://www.ebi.ac.uk/Tools/msa/clustalo/) and

visualised using Jalview (http://www.jalview.org/). Bootstrap Neighbor-Joining trees were made using ClustalX and visualised using MEGAX (https://www.megasoftware.net/).

2.7.5 Protein modelling using Chimera

To visualise the 3D structures of PP2CA and PYL13 the atomic coordinates were downloaded from the Protein Data Bank (https://www.rcsb.org/) under the accession number 4N0G (Li et al., 2013). The proteins were visualised and the protein chains and amino acid regions of interest were coloured using Chimera (https://www.cgl.ucsf.edu/chimera/).

2.7.6 Software for determining SUMO sites and SUMO interaction motifs

SUMO and SIM site predictions were carried out using in-house experimental software developed using similar algorithms to GPS-SUMO (http://sumosp.biocuckoo.org/online.php). The software was developed by Stuart Nelis (PhD thesis 2014). Protein sequences used with the software were retrieved from TAIR (https://www.arabidopsis.org/).

2.8 Data analysis

2.8.1 Statistical analysis

Data were expressed as means ± SEM. Statistical differences were tested with a Student's T-test when appropriate to compare the differences between two groups e.g. comparing a mutant phenotype to WT (Col-0). ANOVA with Tukey test post hoc was used when appropriate to compare the means between three + groups. The values $P < 0.05$ were considered statistically significant. Statistical analysis was done using software (https://astatsa.com/OneWay_Anova_with_TukeyHSD/) and (https://www.graphpad.com/quickcalcs/ttest1.cfm). The mean of each group was compared to the mean of every other group in pairwise comparisons which identified groups which had a Tukey HSD significance p-value below .05 alpha level. The pairwise comparisons that identified two groups that had a p-value below .05 alpha level are given different letters in figures where ANOVA with Tukey test post hoc analysis has been conducted. Groups with more than two letters have more than one group where the means do not have a significance p-value below .05 alpha level.

Chapter 3

The role of SUMO in the ABA hormone pathway.

3.1 Introduction

As has already been mentioned two transcription factors in the ABA pathway, ABI5 and MYB30 have been identified as being modified by SUMO (Miura et al., 2009; Zheng et al., 2012). *Arabidopsis* transgenics with mutations in SUMO proteases and *Arabidopsis* transgenics overexpressing SUMO have also been identified as having ABA phenotypes (Castro et al., 2016; Wang et al., 2018; Lois et al., 2003).

SUMO has been identified as an important PTM modifying many crucial proteins in hormone signalling cascades from DELLA to JAZ proteins, resulting in fine-tuning of hormone signalling. We speculated that additional proteins in the ABA pathway, upstream of ABA transcription factors that have already been identified as being SUMO modified, may also be SUMOylated.

In this chapter different components of the ABA signalling pathway were scanned with in-house software to identify SUMO sites. Using this software the negative regulator of the ABA pathway PP2CA was predicted to harbour SUMO sites, the prediction was further supported by the SUMO sites being conserved in the protein from different plant species and the location on the protein 3D structure. PP2CA is one of nine protein phosphatase type 2Cs (PP2Cs) that negatively regulate the ABA pathway. When active the PP2Cs negatively regulate the ABA pathway by dephosphorylating and de-activating ABA-signalling components including the b-ZIP transcription factors, ABF

transcription factors and SLAC1 anion channel. The PYLs are the positive regulators of the ABA pathway. The PYLs bind to the active site of the PP2Cs inhibiting their phosphatase activity, relieving PP2C induced inhibition of the ABA-signalling components resulting in activation and downstream ABA signalling. In order to test whether PP2CA is SUMOylated in this chapter the lysines in PP2CA that SUMO attaches to were identified, and plant expression constructs of SUMOylatable $PP2CA^{WT}$ and non-SUMOylatable $PP2CA^{2K/R}$ were generated

After demonstrating PP2CA SUMOylation work to identify the SUMO proteases, which cleave SUMO from PP2CA was started. As has already been mentioned two different classes of SUMO proteases have been identified in plants; the ULP type SUMO proteases and the more recently identified DESI type proteases (Morrell and Sadanandom, 2019). There have been 8 identified ULP type proteases including OTS1, OTS2, FUG1, SPF1, SPF1, ELS1, ELS2 and ESD4 and 8 identified DeSI type proteases DeSI1, DeSI2A, DeSI2B, DeSI3A, DeSI3B, DeSI3C, DeSI4A and DeSI4B. Whilst the cellular localisation of a large number of the proteases has yet to be established current known cellular localisation includes the cell membrane, cytoplasm, nucleus, nuclear membrane and speckle like bodies in the nucleus (Morrell and Sadanandom, 2019). They are also known to be localised in different organs in the plant including flowers, seeds, roots, leaves, stomata and stems (Morrell and Sadanandom, 2019). Additionally the SUMO proteases are also known to be expressed and degraded under different stresses and hormones. This means each protease can target different proteins with great specificity to regulate the SUMOylated landscape. In order to determine the SUMO protease that deSUMOylates PP2CA the ABA phenotype of SUMO protease knockouts was examined. Additionally protein interaction between PP2CA and different SUMO proteases was tested.

3.2 PP2CA has predicted SUMO sites

Several key components of the ABA signalling pathway were scanned for potential SUMO binding sites using in-house bioinformatic software, HyperSUMO (Nelis, PhD thesis 2014) that predicts SUMO sites. The gene family which showed the strongest and most conserved SUMO sites were the negative regulators of the ABA pathway, the PP2Cs.

One of the PP2Cs, PP2CA has two predicted SUMO sites, of which Lys260 in PP2CA is conserved amongst the nine PP2Cs (figure 3.1). *Arabidopsis* PP2CA was identified in other plant species using BLASTp (Gish and States, 1993). These PP2CAs (from different plants species), identified by BLASTp, under the standard parameter settings, were aligned using Clustal Omega (Sievers et al., 2011) to determine the conservation of predicted SUMO binding sites (following the method in Orosa et al, (2018), Verma et al, (2021) and Srivastava et al, (2020)) from *C. sativa* (XP_010495429), *E. salsugeineum* (XP_006407450), *B. rapa* (XP_009146731), *O. sativa* (XP_015621342), *Z. mays* (PWZ53479), *S. tuberosum* (XP_006355694), *N. tabacum* (NP_001312664), and *C. annuum* (KAF3620585). The results

of this analysis demonstrate that in addition to the K260 SUMO site being conserved in different PP2Cs it is also conserved across species (figure 3.2). The second predicted SUMO site, K179 lysine, was not conserved in any of the other *Arabidopsis* PP2Cs. However, the K179 SUMO site was conserved amongst most of the different plant species, only not present in *S. tuberosum, N. tabacum* and *C. annuum*.

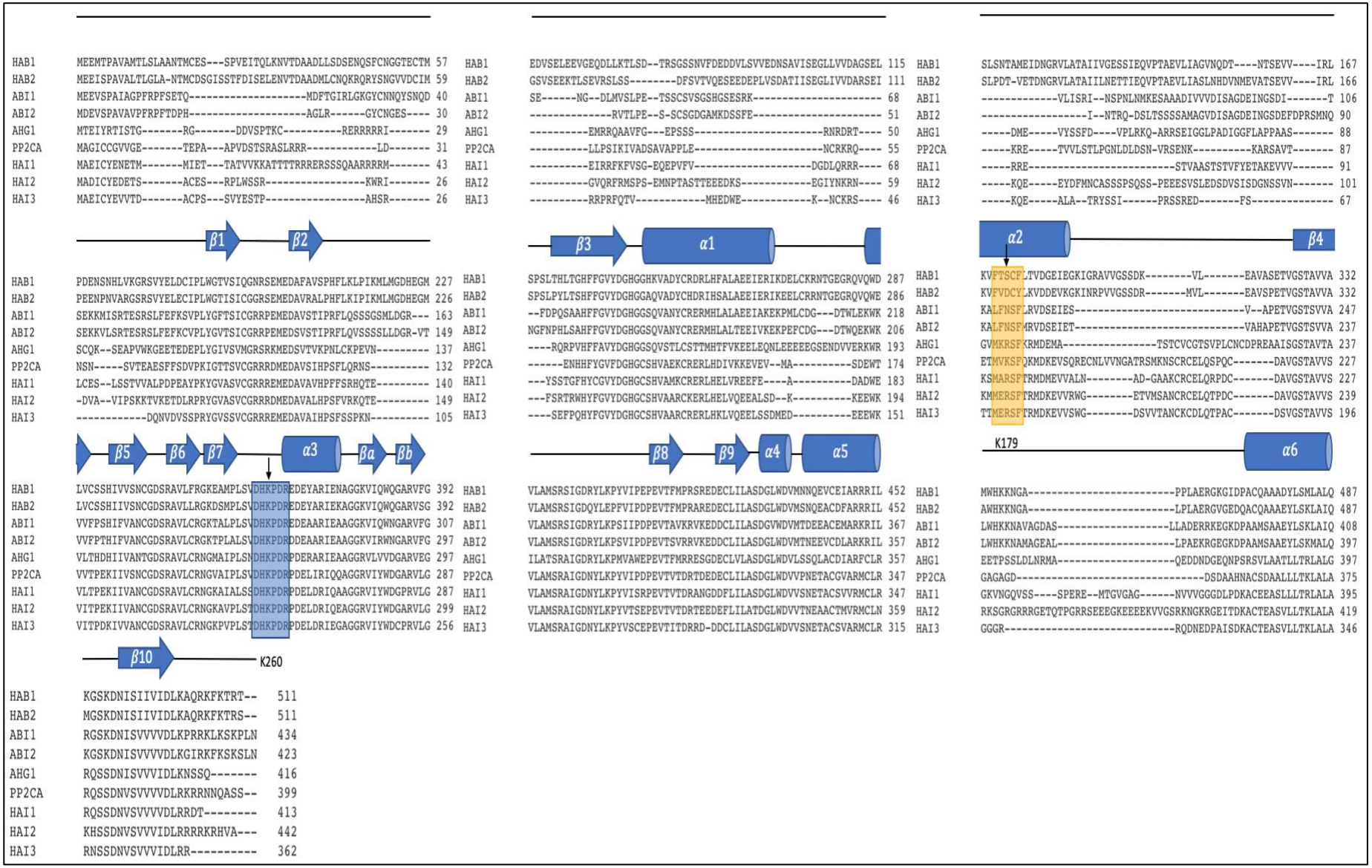

Figure 3.1 Predicted SUMO sites are conserved in different Arabidopsis PP2Cs. *The amino acid sequences, from TAIR, of the nine currently identified Clade A PP2Cs in Arabidopsis aligned using Clustal Omega website. The secondary elements of the core structure of PP2Cs are shown above the sequences (adapted from Li et al., 2013). Two SUMO sites were predicted with >80% confidence. One of the predicted SUMO sites, highlighted by the blue box, K260 is highly conserved in all nine Clade A PP2Cs, the second predicted SUMO site, K179, highlighted by the yellow box, is only conserved in PP2CA. The black arrows indicate the SUMOylatable lysine (K).*

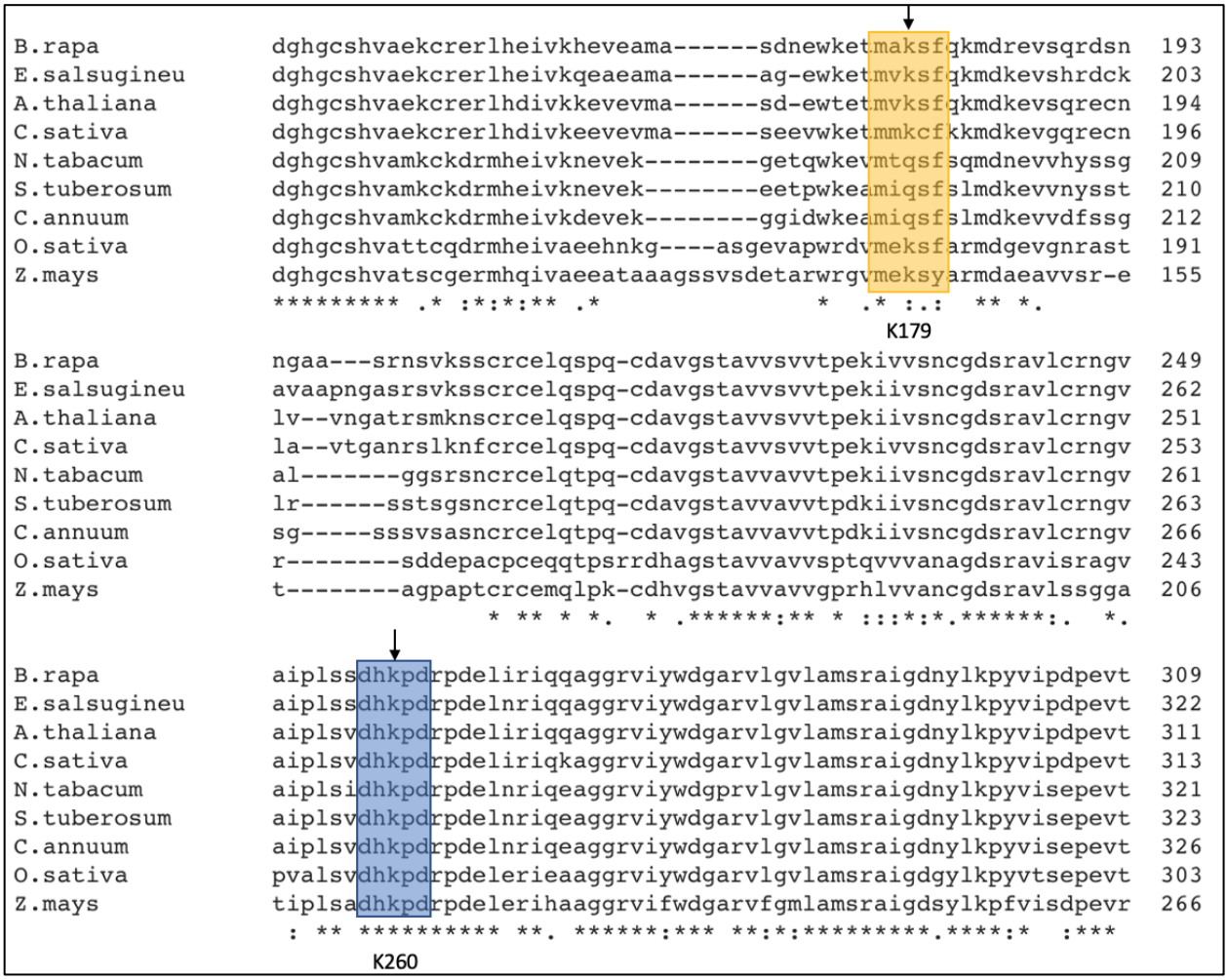

Figure 3.2 Predicted SUMO sites are conserved in PP2CAs from different species. *The amino acid sequences, from Uniprot, of PP2CAs from different species aligned using the Clustal Omega website. The predicted AtPP2CA K260 SUMO site, highlighted by the blue box, is highly conserved in all species homologs of PP2CA. The second predicted SUMO site, K179, highlighted by the yellow box, is not conserved amongst all the species that are aligned. The black arrows indicated the SUMOylatable lysine (K).*

Whilst primary protein sequence analysis by HyperSUMO is useful in identifying potential SUMO binding sites and searching for conservation of SUMO sites in gene families and species, it does not take account of the 3D structure of the protein. No matter how favourable the amino acid sequence of a SUMO sequence is, SUMO can only bind to lysine residues exposed to the external environment, that will not be rendered inaccessible through steric hindrance. The two predicted SUMO binding sites K179 and K260 were located on the crystal structure of the PP2CA-PYL13 complex (pdb file: 4NOG; Li et al., 2013) using the protein structure modelling software Chimera *(*Petterson et al., 2004*).* Both SUMO sites are exposed to the external environment (figure 3.3). K260 is located on a looped region,

between a beta sheet and an alpha helix, close to the interacting interface between PP2CA and the PYLs (figure 3.3). In fact the K260 SUMO site is within the active site of PP2CA and is close to the ABA binding site. Therefore SUMO attachment at the K260 residue may block ABA from binding at the active site. The K179 SUMO site is located on an alpha helix further away from the active site. The position of both SUMO sites on the exterior of the proteins renders both locations potentially suitable for SUMOylation.

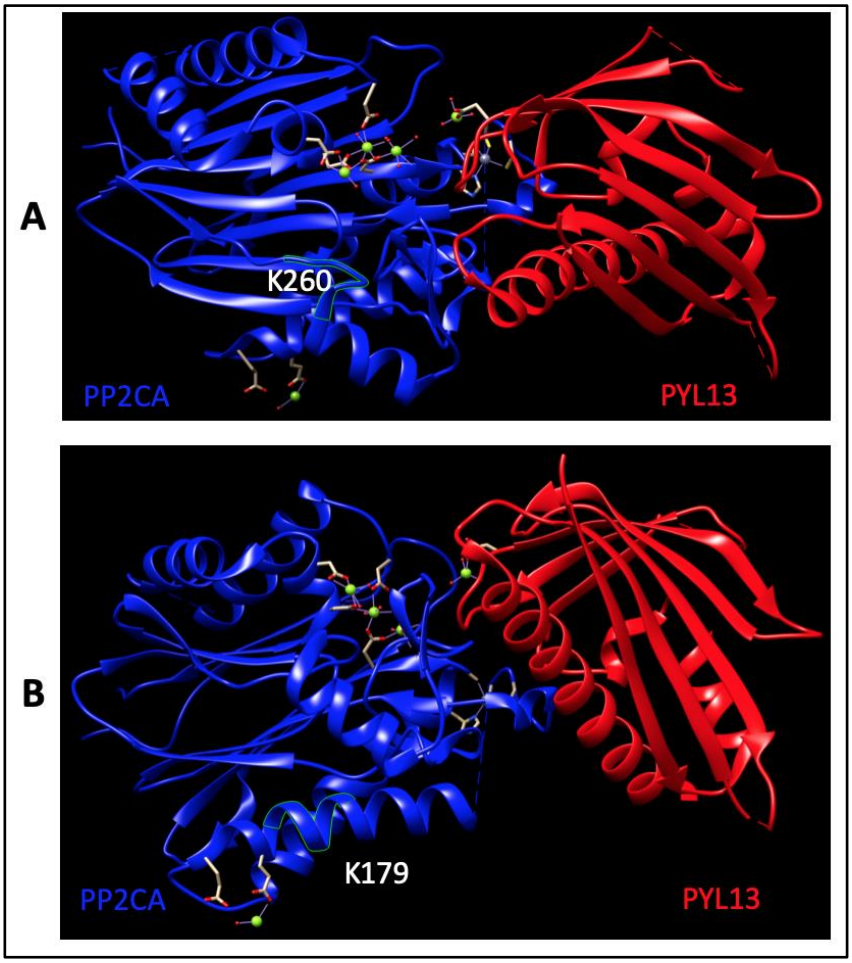

Figure 3.3 3D structure of PP2CA-PYL13 receptor complex depicting the locations of the SUMO sites in PP2CA. *PP2CA is shown in blue and PYL13 is shown in red. The identified SUMO sites in PP2CA are highlighted in yellow using the visual software to demonstrate the 3D location of the highlighted amino acids.* ***A)*** *shows the PP2CA K260 SUMO site.* ***B)*** *shows the same two proteins interacting, however the plane of the image has been changed to aid visualisation of PP2CA K179 SUMO site. The figure was generated in Chimera (Petterson et al., 2004) modelling software version 1.14 using co-ordinates from pdb file 4N0G (Li et al., 2013).*

After initial bioinformatic analysis had indicated two potential SUMO sites located on *At*PP2CA, this was then tested experimentally. Full length *At*PP2CA (1.2 kb) was amplified (figure 3.4) from Col-0 cDNA, using oligonucleotides

(appendix table 3.1) designed to amplify the whole predicted coding sequence. The PCR product was cloned into the entry vector *pENTR/D-TOPO* (Sigma) and transformed into *E. coli* DH5α. The colonies screened for successful clones by PCR and were sequenced via DBS genomics. A recombination reaction was carried out to transfer *At*PP2CA into the 35S N-terminal GFP-tag Gateway destination vector pEARLYGATE104. $PP2CA^{WT}$ in pEARLYGATE104, was identified via colony PCR (figure 3.4), isolated and used to transform *Agrobacterium* strain GV3101 for transient expression in *N. benthamiana*.

In order to identify the predicted SUMO binding sites involved in the conjugation of SUMO moieties to PP2CA, site directed mutagenesis was used to remove the predicted SUMO binding residue. Due to the complete conservation of the 260^{th} lysine in PP2CA this residue was mutated first to an arginine, using specially designed overlapping mismatch primers. Mutating lysine to arginine maintains the structural environment of the surrounding protein structure, due to both amino acids having similar biochemical properties (Grantham, 1974), however it prevents SUMO binding. The non SUMOylatable mutant K260R was amplified from purified recombinant PP2CA pENTR/D-TOPO. The template plasmid product was digested and transformed into *E. coli* DH5α. Mutant clones were identified through sequencing by DBS Genomics and transferred via recombination into the 35S N-terminal GFP-tag Gateway destination vector pEARLYGATE104. Confirmed $PP2CA^{K260R}$ clones in pEARLYGATE104 was identified via colony PCR, isolated and transformed into the *Agrobacterium* strain GV3101 for transient expression.

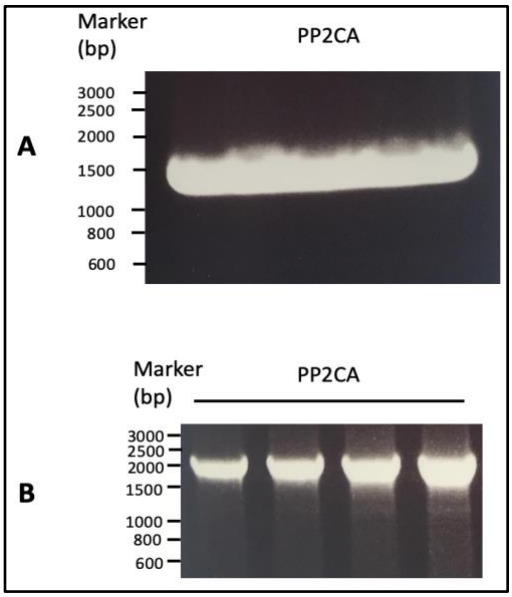

Figure 3.4 Cloning PP2CA from cDNA and transforming PP2CA into plant expression vector pEG104. *Image of DNA gel showing amplification of full length PP2CA from cDNA and PCR confirming PP2CA presence in plant expression vector.* ***A*** *shows the resulting PCR fragment analysed on an agarose gel by electrophoresis size separation (1200 bp).* ***B*** *shows the amplification of PP2CA from E.coli colonies that grow on selection media (2100 bp). A minimum of 4 colonies per construct were tested, all that were sampled tested positive for the desired band size. The 1kb DNA marker is labelled.*

A transient assay in *N. benthamiana* expressing 35S:GFP:PP2CA^{WT} and 35S:GFP:PP2CA^{K260R} was conducted to test the SUMOylation status of the ABA negative regulator. PP2CA^{WT} or PP2CA^{K260R} were co-infiltrated in *N. benthamiana* with 35S:SUMO1:HA. After three days the protein was extracted from *N. benthamiana*, 30 µl was run as an input and immunoblotted against α-HA, another 30 µl was run as input and immunoblotted against α-GFP. The rest of the extracted protein was immunoprecipitated (IP) against α-GFP. Two bands for PP2CA were observed in the IP sample lane, with more PP2CA^{K260R} being present than PP2CA^{WT} (figure 3.5), consistently PP2CA expressed in *N. benthamiana* using the pEG104 vector gave two bands for PP2CA. The lower of the two bands is the correct predicted size of PP2CA, 43 kDa plus 25 kDa for the GFP tag, the higher band was hypothesised to be phosphorylated PP2CA, however it was not run of a phospho tag gel to confirm. Due to PP2CA being weakly expressed PP2CA cannot be seen in the input lane. The SUMOylation status of the recombinant PP2CA was shown via western blotting with α-HA antibodies (Sigma). A smear, from ~70kDa to the top of the gel indicate many SUMO moieties bound to PP2CA. This SUMOylated smear however was seen in both PP2CA^{WT} and PP2CA^{K260R} indicating that PP2CA^{K260R} is still being SUMOylated. A GFP control was not used in this assay, however it was not repeated again to include a GFP control, instead the second SUMO site was mutated and another SUMO assay was conducted, including a GFP control.

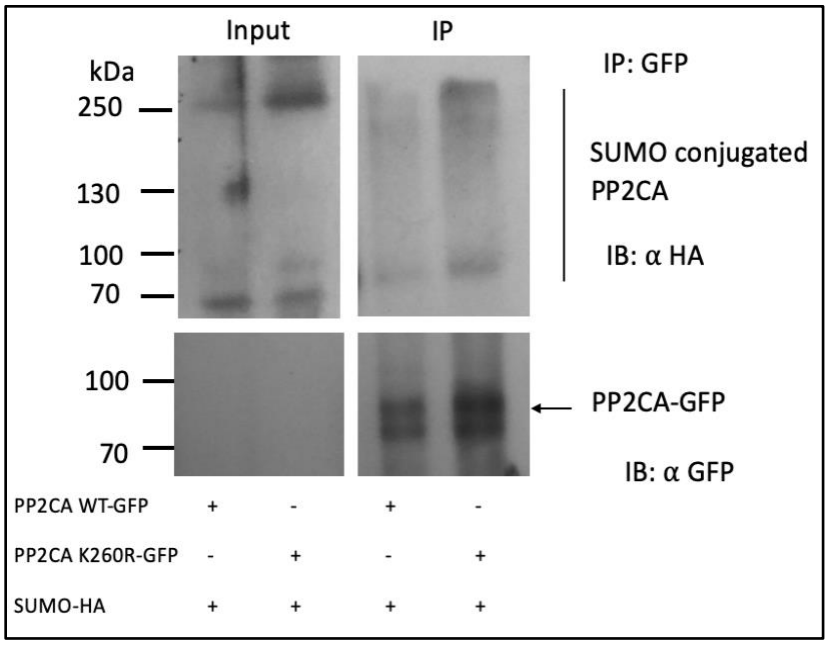

Figure 3.5 PP2CA^{K260} is still SUMOylated. *Transient expression was performed in N. benthamiana leaves co-expressing PP2CA^{WT}-GFP or PP2CA^{K260R}-GFP with SUMO1-HA (13 kDa). Total protein (input) was subjected to immunoprecipitation (IP: α-GFP) with α-GFP immunoaffinity beads followed by immunoblot analysis anti-GFP (IB: α-GFP) antibodies to detect PP2CA^{WT}/PP2CA^{K260R}-GFP and anti-HA (IB: α-HA) antibodies to detect SUMO1-HA. Total protein of all samples (input) was probed with anti-GFP antibodies and anti-HA antibodies to determine PP2CA and SUMO protein levels. Arrow indicates PP2CA-GFP (68 kDa).*

In order to test whether K179 is a SUMO site the second SUMO site in PP2CA, K179, was mutated. PP2CA$^{2K/R}$ was generated in the pEARLYGATE104 expression vector and transformed into the *Agrobacterium* strain GV3101 for transient expression. 35S:GFP:PP2CA^{WT} and 35S:GFP:PP2CA$^{2K/R}$ was transiently expressed in *N. benthamiana* to test the SUMOylation status of the ABA negative regulator. GFP was also used as a negative control for the IP. As has been seen previously (figure 3.5), two bands were observed in the PP2CA IP sample lanes, the lower of the two bands is the correct predicted size of PP2CA, 43 kDa plus 25 kDa for the GFP tag. The higher band was hypothesised to be phosphorylated PP2CA, however it was not run of a phospho tag gel to confirm. The two PP2CA proteins are also being degraded during immunoprecipitation, this can be observed in the protein bands beneath 70 kDa. Less PP2CA$^{2K/R}$ is present than PP2CA^{WT} (figure 3.6), PP2CA cannot be seen in the input due to low expression. The SUMOylation status of the recombinant PP2CA was shown via western blotting with α-HA antibodies (Sigma). A band at ~70kDa was present in PP2CA^{WT} but not PP2CA$^{2K/R}$ suggesting the loss of SUMOylation, as predicted, with the mutation of the SUMOylated lysine residues identified using the HyperSUMO software. However there is less PP2CA$^{2K/R}$ present in the IP lane and less SUMO-HA present in the input so PP2CA$^{2K/R}$ cannot be confirmed to completely remove SUMO, however, compared to PP2CA^{WT} there is a reduced level of SUMOylation of PP2CA$^{2K/R}$.

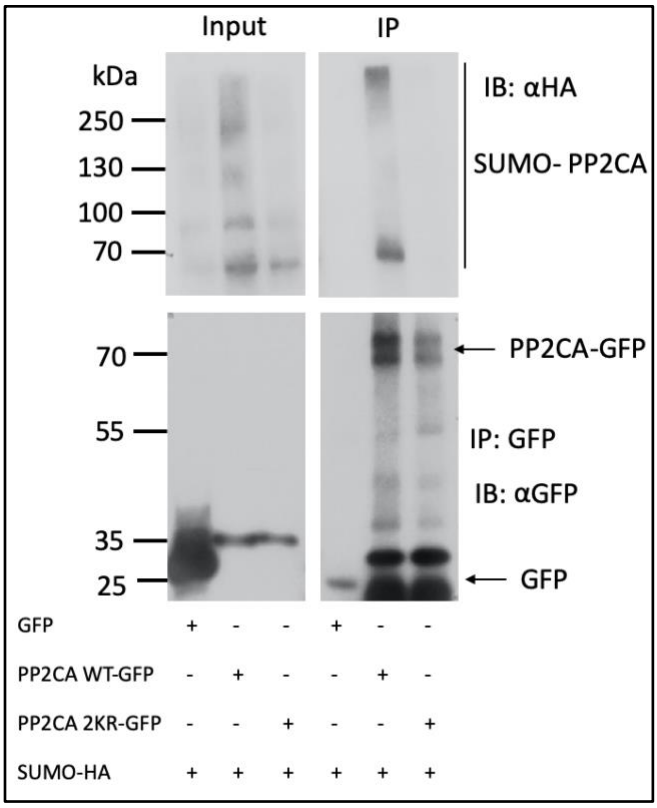

Figure 3.6 PP2CA$^{2K/R}$ is potentially not SUMOylated. *Transient expression was performed in N. benthamiana leaves co-expressing PP2CA^{WT}-GFP, PP2CA$^{2K/R}$-GFP, or GFP with SUMO1-HA (13 kDa). Total protein (input) was subjected to immunoprecipitation (IP: α-GFP) with α-GFP immunoaffinity beads followed by immunoblot analysis anti-GFP (IB: α-GFP) antibodies to detect PP2CA^{WT}/PP2CA^{K260R}-GFP/GFP and anti-HA (IB: α-HA) antibodies to detect SUMO1-HA. Total protein of all samples (input) was probed with anti-GFP antibodies and anti-HA antibodies to determine PP2CA/GFP and SUMO protein levels. Arrow indicates PP2CA-GFP (68 kDa) GFP (25 kDa). These western blots were repeated thrice, this figure is a representative of outcome of those experiments*.

3.3 PP2CA interaction with SUMO proteases

After putatively determining that PP2CA is SUMOylated the SUMO protease which may be responsible for deSUMOylating PP2CA was then examined by examining ABA phenotypes. One of the most well-characterised phenotypes linked to ABA is that of primary root length on ABA supplemented media. ABA produces a biphasic growth response: low concentrations of ABA cause an increase in root growth whilst high concentrations (1 µM+) inhibit root growth, in an additive effect (Mulkey et al., 1983; Ghassemian et al., 2000; Zeevaart and Creelman, 1988). The inhibitory effect of ABA on roots has long been established as inhibiting root cell elongation and resulting in smaller root cells (de la Torre et al., 1972).

Initially the effects of ABA on primary root length in a hyper-SUMOylated environment, such as that of the SUMO protease knock-out mutant line *ots1-1 ots2-1*, herein called *ots ko*, were studied. The *ots ko* mutant line was first tested as it is a well characterised mutant used in the lab that had been shown to be degraded in the presence of ABA in rice (Srivastava et al., 2017), additionally OTS1 and OTS2 plant overexpression vectors are available in the lab and RNA seq data had indicated *ots ko* has differentially expressed genes in response to ABA compared to Col-0 (Walsh, PhD Thesis, 2017). The T-DNA knockout loss of function transgenic *ots1-1 ots2-1* (SALK_022798 and SALK_001579) (Conti et al., 2008) called *ots ko* mutant line were kindly provided by Dr Beatriz Orosa.

In order to gauge if *ots ko* had an ABA sensitive or insensitive response the *ots ko* transgenic was grown along with mutants in the ABA pathway that generate a sensitive or insensitive response. As the SUMO status of PP2CA was being examined the T-DNA loss of function transgenic *pp2ca-1* (SALK_28132) (Kuhn et al., 2006), was examined. Due to the functional redundancy of the PP2Cs, single PP2C loss of function transgenics show only moderate ABA sensitivity compared to transgenics with multiple PP2Cs knocked out (Rubio et al., 2009). In addition to *pp2ca-1* a triple T-DNA insertion loss of function transgenic *pp2ca-1 hab1-1 abi1-2* (SALK_28132, SALK_2104 and SALK_72009) (Rubio et al., 2009) (herein called *p3*) was used as a more sensitive mutant to ABA than *pp2ca-1*. Additionally an ABA insensitive T-DNA loss of function transgenic *pyl4 pyl5 pyl8* (SAIL_517_C08, SM3_3493, SAIL_1269_A02) (Gonzalez-Guzman et al., 2012) (herein called *pyl458*) was also examined. *Pp2ca-1, p3* and *pyl458* were kindly provided by Dr Pedro Rodriguez.

In the absence of ABA the mean root lengths of Col-0, *ots ko, pp2ca-1* and *pyl458* was similar, with the mean root lengths of 4 cm, 3.3 cm, 3.2 cm and 3.1 cm respectively. However, as has been reported in Rubio et al., 2009, even in the absence of ABA *p3* is almost half the length of the other *Arabidopsis* genotypes. In the presence of ABA a significant difference in primary root length between Col-0 and the SUMO protease mutant line *ots ko* was observed (figure 3.7, 3.8). A reduction of primary root length was seen in both Col-0 and the *ots ko* mutant in response to ABA. However, the reduction in primary root length was significantly more severe in the *ots ko* line; this suggests that the *ots ko* mutant is more sensitive to ABA than WT. As expected, the ABA insensitive mutant *pyl458*, which is lacking three PYL receptors only has a small decrease in root length, compared to growth in the absence of ABA. Additionally, as has been reported (Rubio et al., 2009), the PP2C mutants plants *pp2ca-1* and *p3* have a reduction in root length on ABA, however only *p3* is statistically significantly shorter compared to Col-0 on ABA. Due to the functional redundancy of the PP2Cs the triple mutant knockout is significantly more sensitive to ABA than a single mutant (Merlot et al., 2001; Saez et al., 2006).

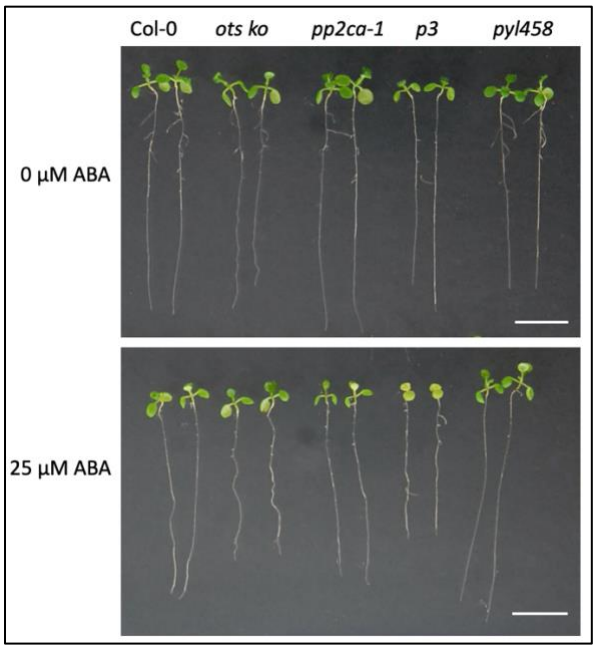

Figure 3.7 The ots ko mutant shows reduced primary root length in response to ABA. *Representative image of 11 day old seedlings, Col-0, ots ko, pp2ca-1, p3 and pyl458, germinated and grown for 5 days on 1/2 MS medium then transferred to either 1/2 MS or 1/2 MS with 25 µM (+)-ABA and grown for a further 6 days. Scale bar = 1 cm.*

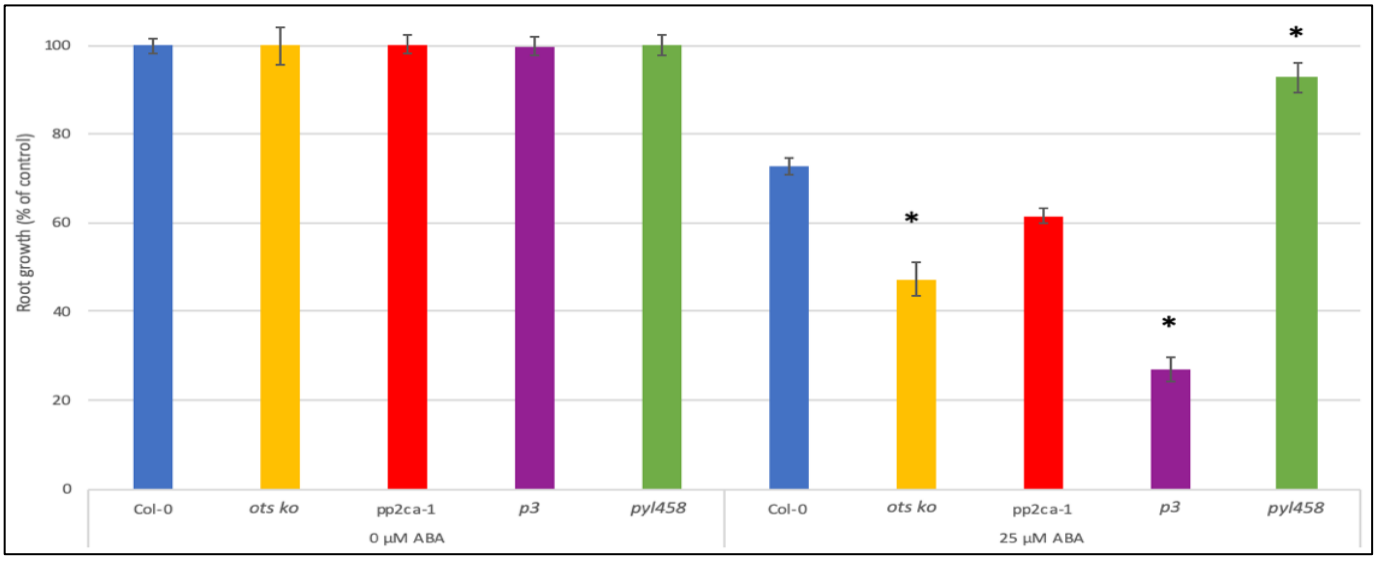

Figure 3.8 Quantification of ABA-mediated root growth inhibition of Col-0, ots ko, pp2ca-1, p3 and pyl458 mutants. *Five-day-old seedlings of the different genotypes were transferred to 1/2MS or 1/2MS with 25 µM (+)-ABA and grown for additional six days before root lengths were measured. Data is relative to growth on 0µM ABA. Data are means ± se (n = 100-30 each). Three repeats were conducted. A one-way ANOVA determined a statistical significance between the groups ($F(4,97) = 62.58$ $P < 0.00001$). A Tukey post hoc test revealed that the % root growth of ots ko (47.2% ± 3.9% p=0.001), p3 (26.9% ± 2.5% p=0.001) and pyl458 (92.7% ± 3.3% p=0.001) was statistically significantly (p<0.05) different compared to Col-0 indicated with an *. However whilst pp2ca-1 (61.5% ± 1.7% p=0.02) was different from Col-0 it was not significantly different. Three repeats conducted.*

In order to further explore the role SUMOylation plays in the ABA response, the *ots ko* mutant line seeds were also exposed to ABA, as ABA also has a well-characterised role in germination and seedling establishment. Mutants deficient in ABA are unable to establish dormancy (Karssen et al., 1983), whilst exogenous application of ABA prevents precocious germination of immature embryos (Zeevaart and Creelman, 1988). To further investigate the role of SUMOylation in the ABA response, the effects of ABA on seedling establishment in a hyper-SUMOylated environment, such as that of the SUMO protease knock-out mutant line *ots ko*, were studied.

The SUMO protease knockout mutant line, *ots ko*, along with a WT control (Col-0), an ABA insensitive mutant line *pyl458* and two ABA sensitive mutant lines *pp2ca-1* and *p3* seedling establishment was examined. In the absence of ABA all the lines studied had established by day 4, determined by the development of photosynthetic competence (green cotyledons) (figure 3.9 and 3.10).

In the presence of exogenous ABA the establishment became impaired (figure 3.9 and 3.10). The ABA insensitive mutant *pyl458* still exhibits 70% establishment, at day 4, as the mutant does not perceive the ABA as efficiently as Col-0, due to mutated ABA receptors. Conversely *p3* and *pp2ca-1* have respectively 5% and 30% establishment on 0.5 µM ABA, at day 4, due to being hypersensitive to ABA. Whilst *ots ko* is not as sensitive to ABA as the *p3* and *pp2ca-1* mutant lines its establishment rate on ABA is lower than Col-0 suggesting that the *ots ko* mutant line is more sensitive to ABA than Col-0.

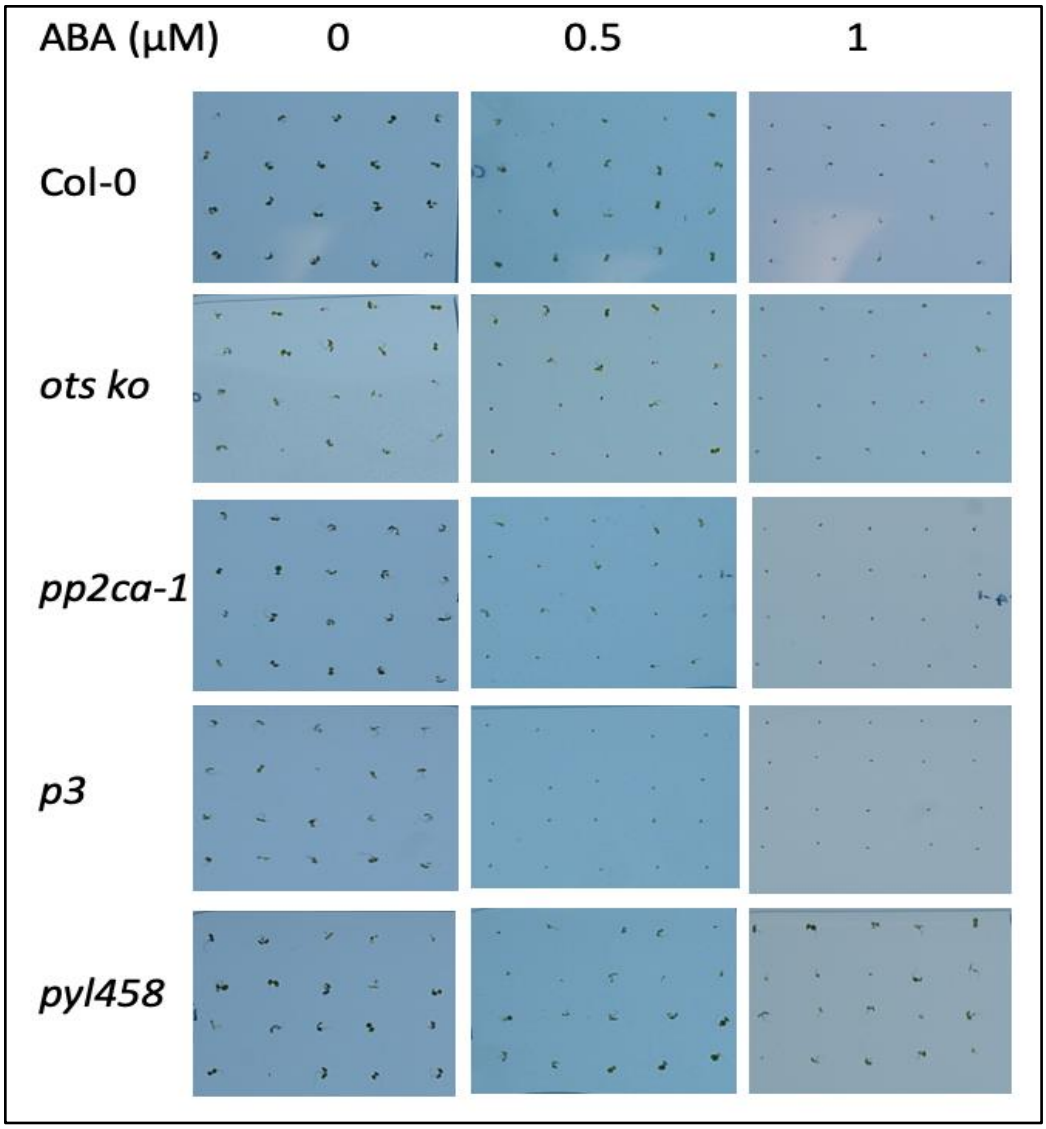

Figure 3.9 The ots ko transgenic shows increased ABA sensitivity in seedling establishment. *Approximately 30 seeds of each genotype (col-0, ots ko, pp2ca-1, p3 and pyl458) were stratified on moist filter paper at 4˚C for 2 days in the dark. They were then transferred to 1/2MS supplemented with differing concentrations of ABA, 0 µM ABA (left panel), 0.5µM ABA (middle panel) and 1µM ABA (right panel). Photographs were taken 4 days later and scored for cotyledon emergence.*

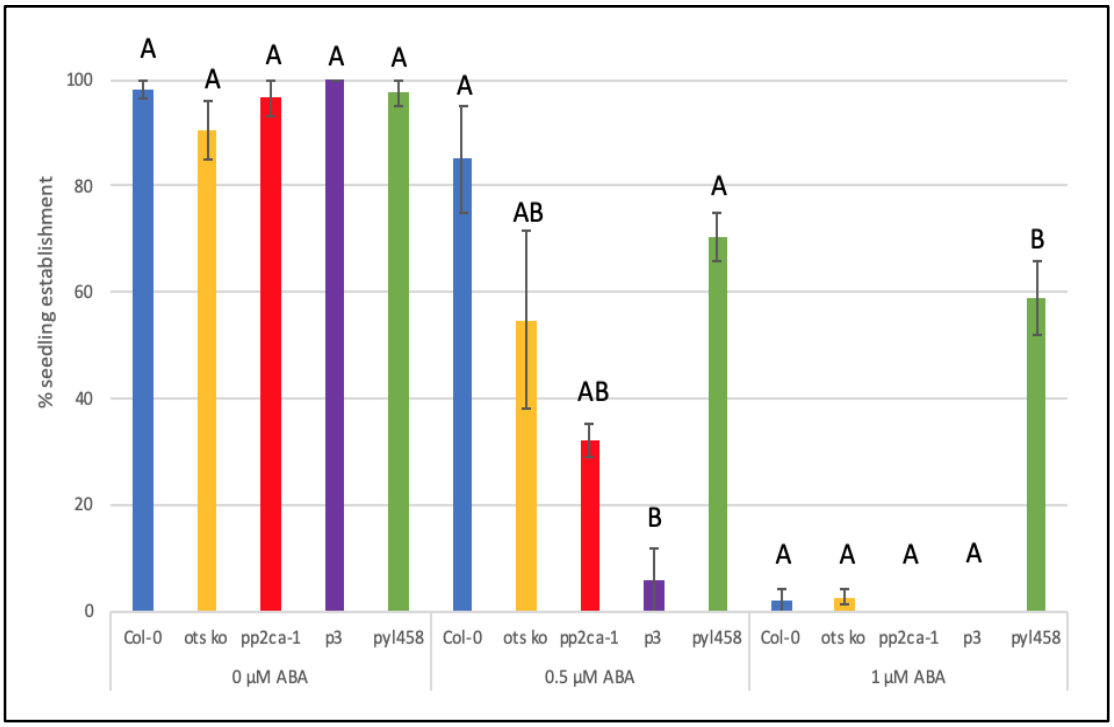

Figure 3.10 Quantification of ABA-mediated seedling establishment inhibition of Col-0, ots ko, pp2ca-1, p3 and pyl458 mutants. *Percentage of seeds that germinated and developed green cotyledons in the presence of the indicated concentrations of ABA. Approximately 40 seeds of each genotype were sowed on each plate and scored 4 days later. Data are means ± se (n = 40 each). Bars with different letters in each treatment were significantly different from others; p > 0.05; one-way ANOVA with post hoc Tukey test. Two repeats conducted.*

In order to understand more about the ABA phenotype of the *ots ko* mutant, quantitative PCR (qPCR) was used to measure basal gene expression of ABA related genes. The genes studied include ABA biosynthesis genes, *ABSCISIC ALDEHYDE OXIDASE 3* (*AAO3)*, *NINE-CIS-EPOXYCAROTENOID DIOXYGENASE 3* (*NCED3)* and *ZEAXANTHIN EPOXIDASE* (*ABA1/ZEP)* (Finkelstein, 2013), and ABA response genes, *RESPONSE TO DESICCATION 22* (*RD22), RESPONSE TO DESICCATION 29A (RD29A), RESPONSE TO DESICCATION 29B (RD29B)* and *RAB GTPASE HOMOLOG B18 (RAB18)* (appendix table 3.2) (Kasuga et al., 2004; Lang and Palva, 1992; Nakashima et al., 2009; Yamaguchi-Shinozaki and Shinozaki, 1993).

Relative to the housekeeping gene *ACTIN2* in Col-0 ABA biosynthesis genes were upregulated in response to 50 µM ABA as has been reported in Wu et al., 2016. One housekeeping gene was used following the method in Orosa et al, (2018). The *ots ko* mutant did not exhibit such a strong expression of ABA biosynthesis gene *AAO3* in response to ABA as Col-0. The two other ABA biosynthesis genes studied (ABA1 and NCED3) had the same expression levels in Col-0 and *ots ko* in both the presence and absence of ABA. In contrast, the *ots ko* double mutants showed a greater expression of ABA response genes *RD29A*, *RD29B* and *RAB18* in the absence of ABA, compared to Col-0. When ABA was applied, the expression levels of ABA response genes in *ots ko* double mutants was increased compared to Col-

0 of *RD22*, *RD29B* and *RAB18*, suggesting that in the presence and absence of ABA *ots ko* had increased ABA signalling (figure 3.11).

The results show that compared to Col-0 the *ots ko* double mutant has perturbed ABA expression of biosynthesis and response genes. The mutant may already be under ABA stress in the absence of ABA and exogenous application of ABA provides a further stress, resulting in the ABA hypersensitive phenotypes.

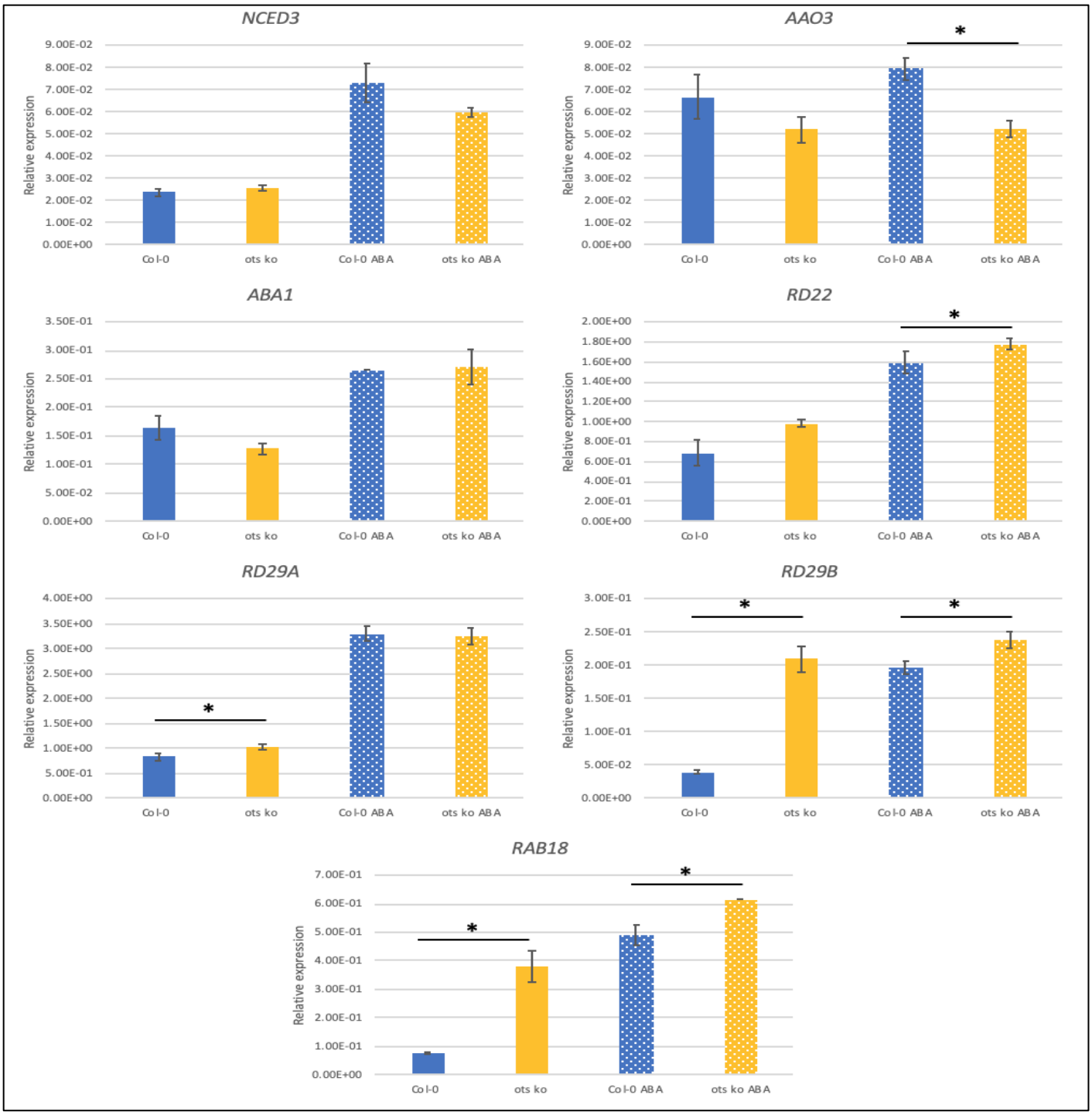

Figure 3.11 ABA responsive genes are upregulated in the ots ko mutant. *Quantitative PCR expression analysis of ABA synthesis (NCED3, ABA1 and AOO3) and responsive (RD22, RD29A, RD29B and RAB18) genes in Col-0 and ots ko. 10 day old seedlings were transferred to liquid MS containing DMSO (control) or 50 µM ABA for 3 hours, as in Wu et al., 2016. Seedlings were incubated for 3 hours then collected and total RNA was extracted, quality control checks were performed and cDNA synthesised. ACTIN2 transcript was analysed as the internal control. Error bars represent ±SE of 3 technical repeats. A one tailed T-test analysed the statistical significance of gene expression between each genotype comparing expression in the presence and absence of ABA independently. * p value < 0.05 (one tailed T-test).*

The *ots ko* phenotype indicates that the mutant is more sensitive to ABA than Col-0. This may be due to OTS1 interacting with PP2CA. To determine whether there is a physical interaction between PP2CA and OTS1 a transient pull down assay in *N. benthamiana* using 35S:GFP-PP2CA^{WT} and 35S:OTS1-HA was conducted. The OTS1-HA vector was kindly provided by Dr Vivek Verma. In addition to incubating OTS1 with PP2CA-GFP, OTS1 was also incubated with GFP as a negative control. Whilst this blot is far from optimal the single band observed in the IP sample lane showed that OTS1 was expressed in all lanes and successfully immunoprecipitated (figure 3.12). No interaction was observed between PP2CA-GFP and OTS1-HA, however a positive control was not also used in this assay, and should be used in repeat experiments. As has been stated previously PP2CA cannot be detected in the input due to weak expression. However this experiment could be repeated with immunoprecipitation with GFP beads.

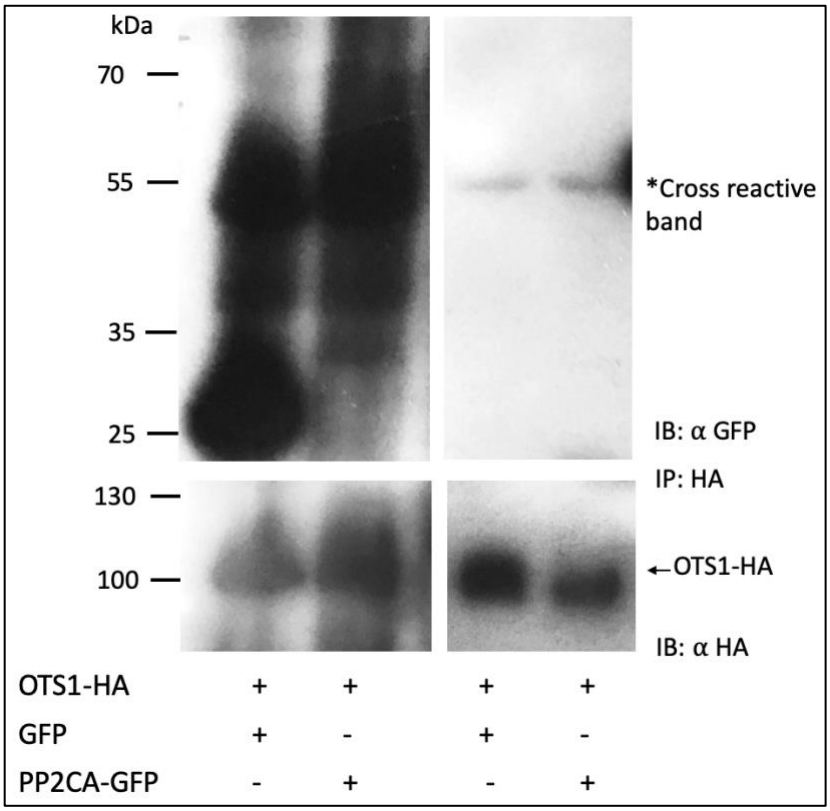

Figure 3.12 PP2CA does not appear to interact with SUMO protease OTS1 in co-immunoprecipitation protein assays. *Transient expression was performed in N. benthamiana leaves co-expressing PP2CA^{WT}-GFP (68 kDa) or GFP with OTS1-HA. Total protein (input) was subjected to immunoprecipitation (IP: α-HA) with α-HA immunoaffinity beads followed by immunoblot analysis anti-GFP (IB: α-GFP) antibodies to detect PP2CA/GFP and anti-HA (IB: α-HA) antibodies to detect OTS1-HA. Total protein of all samples (input) was probed with anti-GFP antibodies and anti-HA antibodies to determine PP2CA/GFP and OTS1 protein levels. Arrow indicates OTS1-HA (70 kDa) and GFP (25kDa). These western blots were repeated twice, this figure is a representative of outcome of those experiments.*

Due to the lack of interaction between OTS1 and PP2CA another SUMO protease was investigated to identify the protease that deSUMOylates PP2CA. Firstly the root length analysis on ABA of SUMO protease T-DNA loss of function transgenic, *spf1-1 spf2-2*, (SALK_040576 and SALK_090744) (Castro et al., 2018) herein called *spf ko*, along with Col-0, and an ABA sensitive mutant line *p3* was examined. The *spf ko* mutants were tested as it is a well characterised mutant used in the lab.

In the absence of ABA the mean root lengths of Col-0 and *spf ko* was similar, with mean root lengths of 3.2 cm. However, as mentioned earlier in the absence of ABA *p3* is almost half the length of the other *Arabidopsis* genotypes. In the presence of ABA a significant difference in primary root length between Col-0 and the SUMO protease mutant line *spf ko* was observed (figure 3.13, 3.14). A reduction of primary root length was seen in both Col-0 and the *spf ko* mutant in response to ABA. However, the reduction in primary root length was significantly more severe in the *spf ko* line on par with the triple PP2C knockout mutant *p3*; this suggests that the *spf ko* mutant is more sensitive to ABA than WT. As expected, the triple PP2C mutants *p3* has a reduction in root length on ABA, statistically significantly shorter compared to Col-0 on ABA.

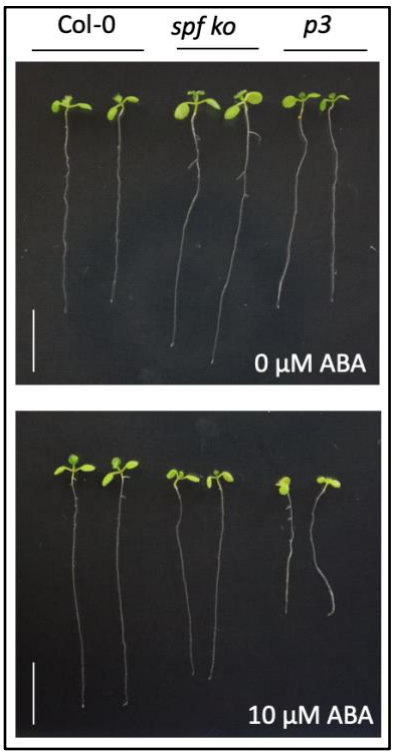

Figure 3.13 ***SPF double knockout mutants shows reduced primary root length in response to ABA, compared to Col-0.*** *Representative image of 11 day old seedlings, col-0, spf ko and p3, germinated and grown for 5 days on 1/2*

MS medium then transferred to either 1/2 MS or 1/2 MS with 25 µM (+)-ABA and grown for a further 6 days. Scale bar = 1 cm.

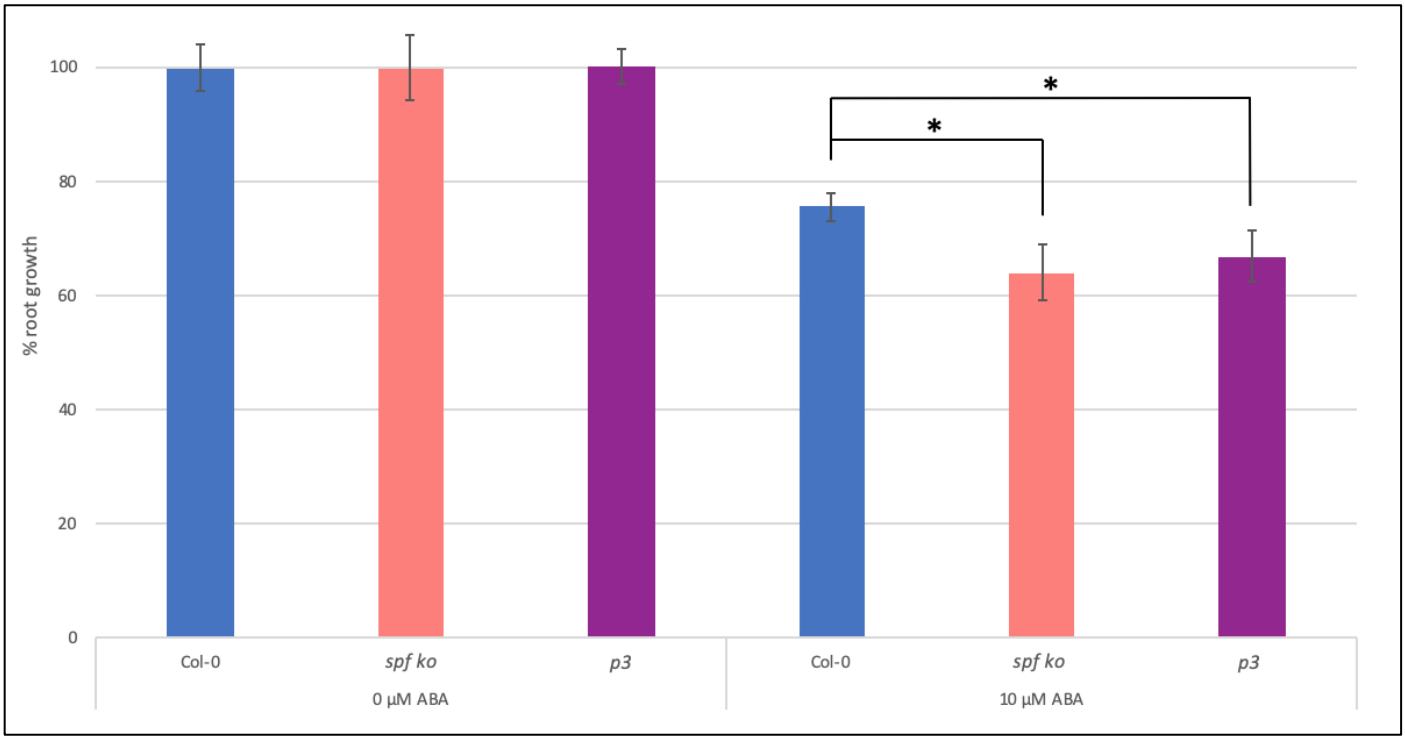

Figure 3.14 Quantification of ABA-mediated root growth inhibition of Col-0, spf ko and p3 mutants. *Five-day-old seedlings of the different genotypes were transferred to 1/2MS or 1/2MS with 25 µM (+)-ABA and grown for additional six days before root lengths were measured. Data is relative to growth on 0µM ABA. Data are means ± se (n = 19-20 each). A one-tailed T-test determined a statistical significance between Col-0 (75.6% ± 2.4%) and spf ko (64% ± 4.8%) genotype root lengths (t(18)= 2.18, p=0.02). * indicates a statistically significant difference (p<0.05). Two repeats conducted.*

In order to further explore the role of SUMO protease double mutant *spf ko (spf1 spf2)* in ABA responses the transgenic seeds were also exposed to ABA, for a seedling establishment assay. The SUMO protease knockout mutant line, *spf ko*, along with a Col-0 and two ABA sensitive mutant lines *pp2ca-1* and *p3* seedling establishment was examined. In the absence of ABA all the lines studied had germinated and established by day 4 (figure 3.15 and 3.16).

In the presence of exogenous ABA the seedling establishment became impaired (figure 3.15 and 3.16). The ABA negative regulator mutants, *p3* and *pp2ca-1* have respectively 5% and 30% establishment on 0.5 µM ABA, at day 4, due to being hypersensitive to ABA. Whilst *spf ko* is not as sensitive to ABA as the *p3* and *pp2ca-1* mutant lines its

establishment rate on ABA is lower than Col-0 suggesting that the *spf ko* mutant line is more sensitive to ABA than Col-0.

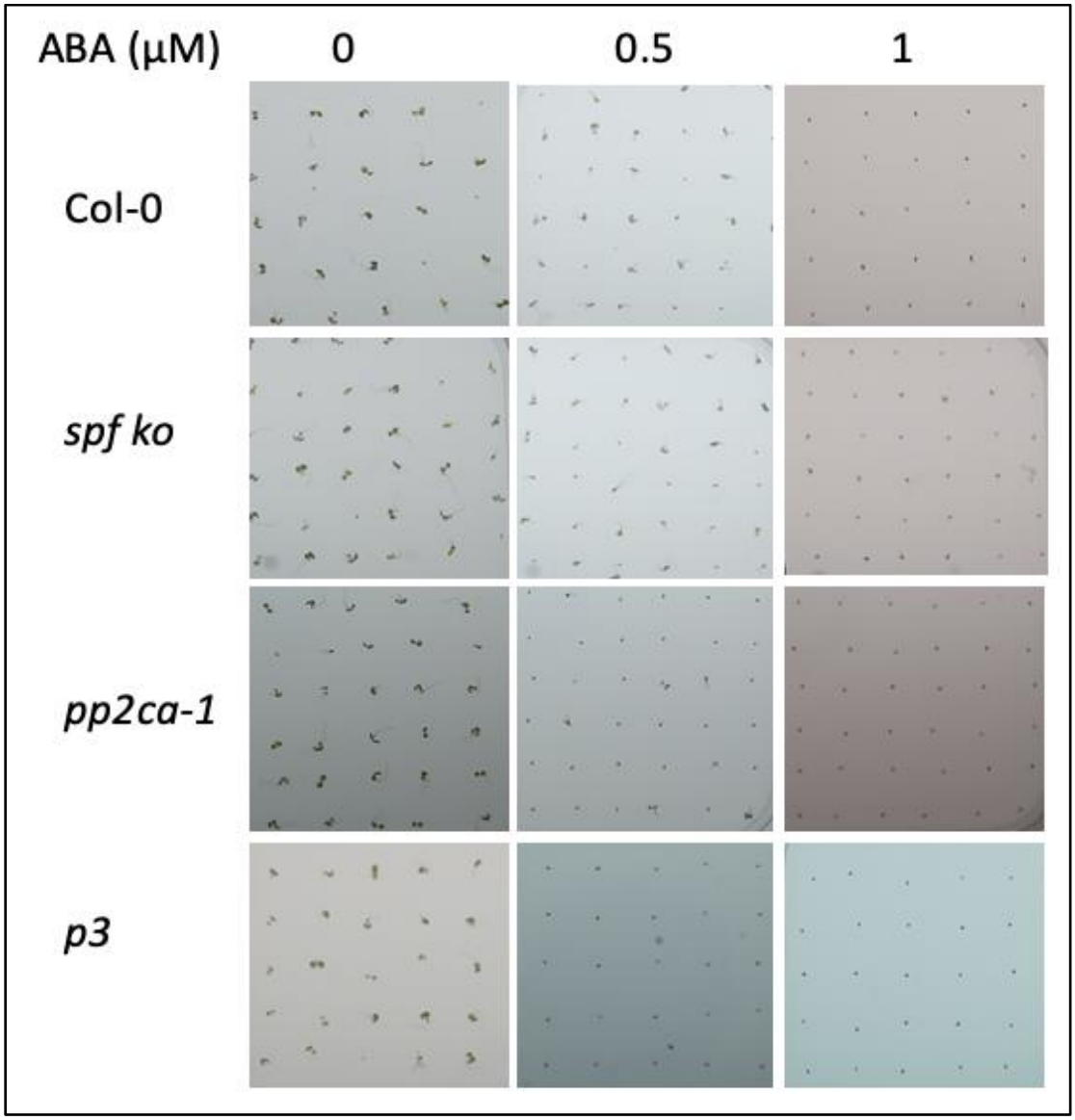

Figure 3.15 Representative photo of seedling establishment of Col-0, spf ko, pp2ca-1 and p3 mutants under ABA treatment. *Approximately 30 seeds of each genotype (Col-0, spf ko, pp2ca-1 and p3) were stratified on moist filter paper at 4˚C for 2 days in the dark. They were then transferred to 1/2MS supplemented with differing concentrations of ABA, 0 µM ABA (left panel), 0.5µM ABA (middle panel) and 1µM ABA (right panel). Photographs were taken 4 days later and scored for cotyledon emergence.*

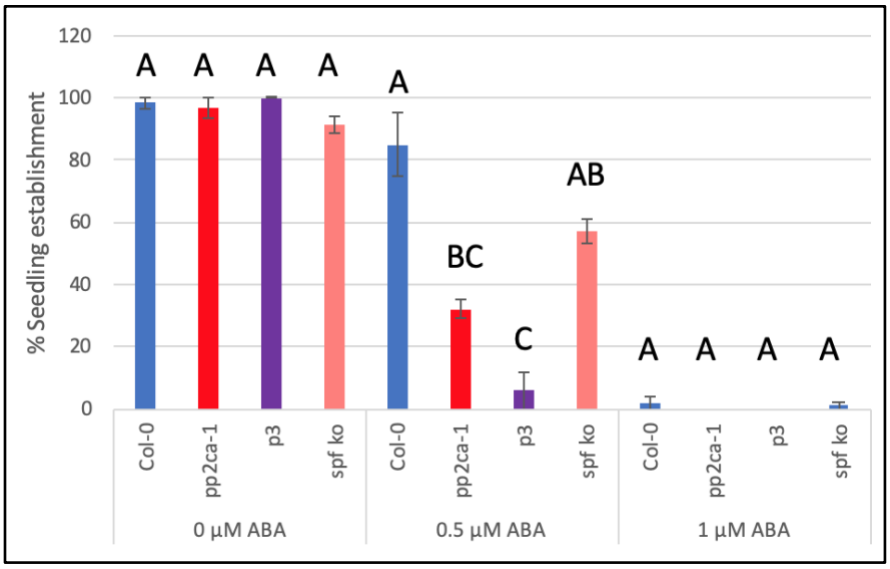

Figure 3.16 Quantification of ABA-mediated seedling establishment inhibition of Col-0, spf ko, pp2ca-1 and p3 mutants. *Percentage of seeds that germinated and developed green cotyledons in the presence of the indicated concentrations of ABA. Approximately 40 seeds of each genotype were sowed on each plate and scored 4 days later. Data are means ± se (n = 40 each). Bars with different letters in each treatment were significantly different from others; p > 0.05; one-way ANOVA with post hoc Tukey test. Two repeats conducted.*

The *spf ko* seedlings show a similar ABA phenotype to the *ots ko*, however, physical interaction between SPF1, SPF2 and PP2CA has to be examined. To determine if SPF1 or SPF2 interact with PP2CA a transient assay in *N. benthamiana* using 35S:GFP-PP2CA^{WT} and 35S:SPF1-HA was performed by Dr Anjil Srivastava. Figure 3.17 (data kindly donated by Dr Anjil Srivastava) shows that PP2CA does not interact with SPF1 or SPF2.

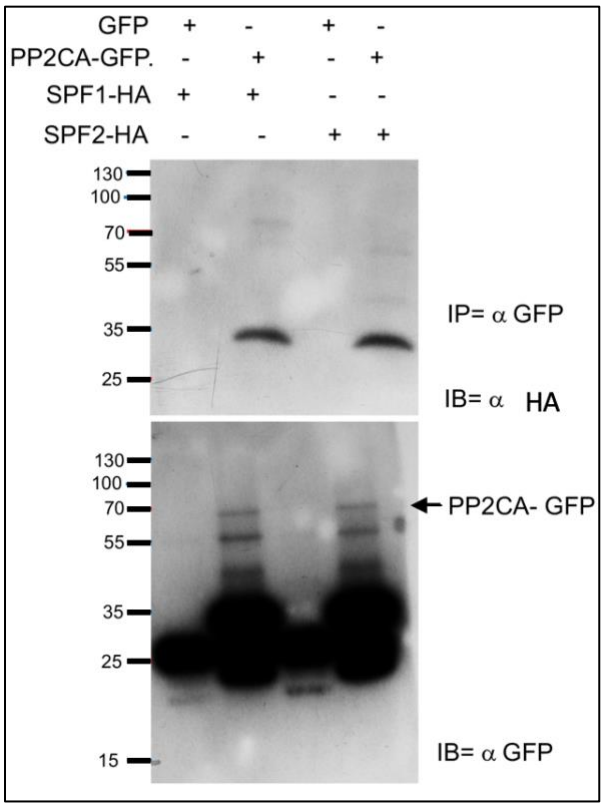

Figure 3.17 ***PP2CA does not interact with SUMO protease SPF1 or SPF2.*** *Transient expression was performed in Nicotiana benthamiana leaves co-expressing either GFP (25 kDa) or PP2CA-GFP with either SPF1-HA (113 kDa) or SPF2-HA (91 kDa). Total protein was subjected to immunoprecipitation (IP: α-GFP) with α-GFP immunoaffinity beads followed by immunoblot analysis anti-GFP (IB: α-GFP) antibodies to detect PP2CA-GFP/GFP or anti-HA (IB: α-HA) antibodies to detect SPF1-HA/SPF2-HA. Arrow indicates where PP2CA-GFP (68 kDa). This western blot was repeated thrice by Dr Anjil Srivastava, this figure is a representative of outcome of those experiments. Data kindly provided by Dr Anjil Srivastava.*

As it had been demonstrated that PP2CA does not interact with OTS1, SPF1 or SPF2 an interaction IP was set up to determine if PP2CA interacted with any of the Desi SUMO proteases. Desi3A was selected as a negative control, in addition to GFP alone, as Desi3A localises in the plasma membrane (Orosa et al., 2018), whereas PP2CA is known to mainly localise in the nucleus with some expression in the cytoplasm (Antoni et al., 2012), this should result in no interaction between Desi3A and PP2CA. Desi3B and Desi4A were selected due to their predicted expression in guard cells (Winter et al., 2017) and predicted expression in the nucleus and cytoplasm (Hooper et al., 2017).

A transient assay in *N. benthamiana* using 35S:HA-PP2CA^{WT} and 35S:Desi3A-GFP, 35S:Desi4A-GFP and 35S:Desi3B-HA-GFP was conducted, with the Desi constructs kindly provided by Dr Beatriz Orosa-Puenta and Ms Catherine Gough, PP2CA-HA was kindly provided by Dr Pedro Rodriguez. Whilst it is not ideal to co-infiltrate two proteins with the same tag (HA-PP2CA^{WT} and Desi3B-HA-GFP) a Desi3B-GFP vector was not available and due to time constraints it was not possible to generate one. The supernatant was probed with GFP beads, which would not select for PP2CA,

so any bands of PP2CA size in the IP probed with HA, could be assumed to have been pulled down from PP2CA interacting with Desi3B. The plant expressing PP2CA-HA and Desi3A-GFP did not express the two proteins, however the second negative control, GFP alone did express and no interaction between GFP and PP2CA was observed (figure 3.18). The HA blots of PP2CA-HA and Desi3B-HA-GFP show darker lanes than the other lanes, due to two HA-tagged proteins being expressed. PP2CA can be seen interacting with both Desi4A, with PP2CA being seen in the high exposure and Desi3B, clearer in the lower exposure. Whilst a single band was observed for PP2CA in the input, two bands appear in the Desi3B lane which may be caused by cross reactivity or degradation. PP2CA may interact with both Desi3B and Desi4A, with each protein deSUMOylating PP2CA in different situations. Further experiments are needed to elucidate if both proteins functionally deSUMOylate PP2CA, this could involve determining if the proteins co-localise using fluorescently tagged proteins expressed in *N. benthamiana,* determining if ABA increases or decreases interaction and conducting in vitro deSUMOylation assays.

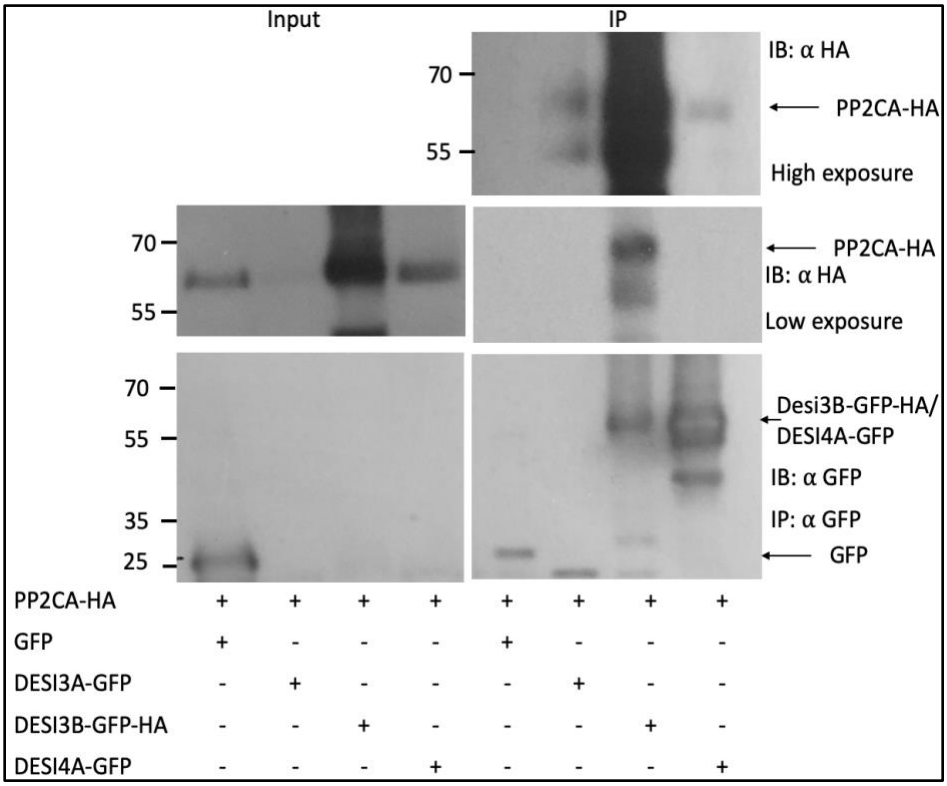

Figure 3.18 PP2CA interacts with Desi3B and Desi4A, but not with GFP. *Transient expression was performed in Nicotiana benthamiana leaves co-expressing GFP, DESI3A-GFP (56 kDa), DESI3B-GFP-HA or DESI4A-GFP with PP2CA-HA. Total protein (input) was subjected to immunoprecipitation (IP: α-GFP) with α-GFP immunoaffinity beads followed by immunoblot analysis with anti-GFP (IB: α-GFP) antibodies to detect GFP/DESI3A/DESI3B/DESI4A-GFP and anti-HA (IB: α-HA) antibodies to detect PP2CA-HA (high and low exposure). Total protein of all samples (input) was probed with anti-GFP antibodies and anti-HA antibodies to determine GFP/DESI3A/DESI3B/DESI4A and PP2CA protein levels. Arrow indicates PP2CA-HA (46 kDa), GFP (25 kDa) and DESI4A-GFP/DESI3B-GFP-HA (50/55 kDa respectively).*

3.4 Discussion

As has already been mentioned previous research has demonstrated the role of SUMO in the ABA pathway. Different SUMO proteases have been shown to alter ABA sensitivity and different ABA transcription factors have been shown to be SUMOyated (Miura et al., 2009; Zheng et al., 2012; Castro et al., 2016; Wang et al., 2018; Lois et al., 2003). This chapter has demonstrated another component in the ABA pathway the PP2C negative regulator PP2CA is SUMOylated and identified the two SUMO sites, where this SUMOylation occurs. Although not tested further work could be carried out to determine if other members of the PP2C family are SUMOylated, via the conserved SUMO site.

Following on from determining PP2CA is SUMOylated work was then conducted to establish which SUMO protease deSUMOylates PP2CA. Initially OTS1 and OTS2 were examined by establishing if the double mutant *ots ko* has an ABA phenotype. The OTS SUMO proteases were selected initially as work from the lab had determined that rice SUMO protease *Os*OTS1 is degraded in ABA (Srivastava et al., 2017). The *ots ko* mutant has an ABA hypersensitive phenotype showing increased ABA mediated inhibition of root lengths with a less clear germination phenotype. Additionally ABA responsive genes were upregulated in *ots ko* compared to Col-0 in both the presence and absence of ABA.

This is in conflict with results reported by Castro et al., 2016, who studied the ABA and osmotic stress response of OTS1 and OTS2, however they used different T-DNA lines which have insertions further upstream than the insertions present in *ots ko*. Castro et al., 2016 studied ULP1c (Ubiquitin like protease 1C, OTS2) and ULP1D (Ubiquitin like protease 1D, OTS1). The double SUMO protease transgenic *ulp1c-2 ulp1d-2* (SALK_050441, SALK_029340) harbours T-DNA insertion sites in the 4th exon and 4th intron respectively. Whereas the *ots ko* mutant used in this thesis uses *ots2-1 ots1-1* (SALK_022798, SALK_001579) which harbours T-DNA insertion sites in the 11th and 14th exons respectively. Castro et al., 2016 reported no ABA mediated inhibition of root length phenotype and reported a similar seed dormancy response to exogenous ABA between *ulp1c-2 ulp1d-2* and wild type plants. This is in conflict with the data generated in this thesis, however it may be due to the different T-DNA lines which were used in the studies. However, more in agreement with the work generated in this thesis Castro et al., 2016 reported differentially expressed ABA related and drought related genes in *ulp1c-2 ulp1d-2* when treated with ABA or drought. Similar results were found in RT-qPCR expression analysis of ABA response genes in *ots ko* treated with ABA. In addition the study reported increased root length sensitivity to PEG and mannitol, which lowers the osmotic potential of media, simulating low water potential. These water deficit phenotypes are associated with ABA mediated signalling (Castro et al., 2016). It may be the phenotypic differences found in ABA mediated inhibition of root length and ABA mediated seed dormancy may be the result of different T-DNA lines.

After establishing *ots ko* has an ABA sensitive phenotype an interaction assay was conducted using PP2CA and OTS1 in a co-immunoprecipitation, which could not establish protein interaction, suggesting that PP2CA does not interact with OTS1. Following on from this the ABA sensitivity of *spf ko* was analysed. The SUMO protease double mutant *spf ko* was shown to be ABA hypersensitive, with increased ABA mediated inhibition of root length. This phenotype was also conflicting with published literature. Using SUMO protease mutant *asp1-1* (a SPF1 knockout mutant) Wang et al., 2018 demonstrated the mutant was ABA insensitive (Wang et al., 2018). The *asp1-1* mutant has reduced seed dormancy sensitivity in response to exogenous ABA compared to wild type and reduced expression of ABA responsive genes in response to ABA (Wang et al., 2018). However the transgenic line used in this thesis used a double SPF SUMO protease, SPF2, which results in ABA hypersensitivity. Interaction assays of PP2CA with SPF1 and SPF2, kindly carried out by Dr Anjil Srivastava demonstrated that PP2CA does not interact with SPF1 or SPF2.

Further interaction assays have suggested that PP2CA may interact with Desi3B and Desi4A, selected due to their predicted expression in guard cells (Winter et al., 2017) and theorised expression in the nucleus and cytoplasm (Hooper et al., 2017). Unfortunately due to a lack of time, this interaction and ABA phenotype could not be further explored. Future work can be carried out to test the interaction of these proteins by examining subcellular localisation and using BiFC analysis to determine interaction. Additionally an in vitro deSUMOylation assay could be conducted using recombinantly expressed and purified Desi3B and Desi4A, incubated with recombinantly expressed SUMOylated PP2CA. Due to a lack of time the ABA sensitivity of these two SUMO proteases was not assayed, however future work should analyse the ABA response of these proteases in both overexpression and knockout transgenics, examining the effect of germination and root growth in response to ABA. Further ABA phenotypes tha could also be tested include stomatal opening and closing in response to ABA. Furthermore the stability of the SUMO protease should be analysed in response to ABA, as Srivastava et al., 2017 has demonstrated that rice SUMO protease *Os*OTS1 is degraded in ABA.

Chapter 4

The role of SUMO in regulation of PP2CA.

4.1 Introduction

The previous chapter demonstrated that PP2CA is SUMOylated using the *N. benthamiana* expression system. However it can be difficult to elucidate the role of SUMO in PP2CA in overexpression systems, because the proteins are not expressed in their native environment at normal concentrations. Generating own promoter transgenics enables the protein to be expressed at a similar time and location to the wild type protein. It also allows the role of SUMOylated PP2CA to be monitored throughout the development of *Arabidopsis* to determine if it plays a different role at different stages of development. Finally as SUMO is regarded as a stress induced post translational modification (Ghimire et al., 2020), it enables better understanding of the role of SUMO when the transgenics are subjected to stresses.

In order to determine the functional role SUMOylation of PP2CA may have on ABA signalling, in this chapter plant expression constructs of $PP2CA^{WT}$ and $PP2CA^{2K/R}$ have been generated. *Arabidopsis* stably expressing these two proteins under the native promoter; $PP2CA^{WT}$ and $PP2CA^{2K/R}$ have been analysed. The transgenics' sensitivity to ABA was examined to determine if SUMOylation of PP2CA aids ABA signalling. This has been tested by examining root growth inhibition in response to exogenous ABA, seed dormancy in response to exogenous ABA and RT-qPCR expression analysis of ABA response genes when treated with ABA.

Additionally a pathotest was conducted to determine if SUMO has a role in ABA mediated pathogen response. This was conducted due to SUMO being generally regarded as a rapid response, quickly modifying the proteome in response to acute environmental changes such as heat shock (Miller and Vierstra, 2011). However increases in ABA produced in drought and salinity are typically long lasting stresses that gradually produce ABA over time, which do not require a rapid response. However ABA is involved in rapid response to respond to pathogen attack. Within one hour after inoculation with pathogenic and non-pathogenic bacteria, plants can increase their resistance by closing stomata (Melotto et al., 2008). This defence response can be triggered upon the application of pathogen-associated molecular patterns (PAMPs), such as flg22. Conversely plants deficient in the ABA pathway fail to rapidly close stomata, indicating the important role ABA has in pathogen triggered stomatal closure (Ton et al., 2009).

Lim et al., 2014 found overexpressing PYL8, the ABA co-receptor, increased resistance to *Pseudomonas syringae* (*Pst)* in dip inoculation assays, where the bacteria must infiltrate through the stomata. In contrast, PYL8 overexpression transgenics had reduced resistance to *Pst* upon infiltration inoculation, as once the bacteria has penetrated the epidermis, ABA signalling enhances plant susceptibility to pathogen disease by suppressing callose deposition and SA-mediated pathogenesis-related genes. Conversely overexpressing PP2CA increased susceptibility to *Pst* in dip inoculation assays, whereas *pp2ca-1* knockout mutant lines had increased resistance to *Pst* in dip inoculation assays. Lim et al., 2014 found these disease phenotypes correlated with stomatal aperture. This led us to pathotest the transgenics using dip inoculation of *Pst* to determine if SUMO attachment to PP2CA altered the transgenics pathogen immunity/susceptibility.

Lastly as the PP2CA$^{2K/R}$ transgenics showed less ABA sensitivity than PP2CA^{WT} we speculated this may be due to reduced transduction of the ABA signal. PP2CA forms a co-receptor complex with the PYLs to bind ABA resulting in ABA signalling. We hypothesised the reduced ABA sensitivity of the PP2CA$^{2K/R}$ transgenics may be due to SUMO attachment of PP2CA aiding the formation of the PP2CA PYL complex. The PYLs were analysed using the in-house SUMO prediction software which identified SIM sites. To further examine the PYL SIM sites *Arabidopsis* transgenics stably expressing PYL8^{WT} and a SIM site mutated PYL8$^{VM/AA}$ were generated and the ABA sensitivity of these transgenics was initially examined.

4.2 Generation and characterisation of *Arabidopsis* stably transformed lines

In order to understand the role of SUMO in PP2CA stable *Arabidopsis* lines were generated by expressing PP2CA^{WT} and PP2CA$^{2K/R}$ under its native promoter. The full length of the *At*PP2CA promoter region (3 kb upstream from the initiator ATG as defined by Chérel et al., 2002) was amplified from Col-0 genomic DNA. It was then cloned into the

NcoI and *NotI* restriction sites of the entry clone *pENTR4* Dual Selection (gateway invitrogen) vector followed by sequencing. An overlap PCR was then carried out between the promoter and WT and 2K/R mutated PP2CA coding regions of the DNA to generate two own promoter PP2CA constructs without introns. Initially, the promoter region and the two coding regions were amplified in a PCR reaction with primers containing sections that overhang into the promoter and gene respectively. The second PCR was carried out using the generated PCR fragments plus after 10 cycles the promoter forward primer and the gene reverse primer both with the required restriction sites were added resulting in a fused PCR product (4.2kb) (figure 4.1 and 4.2, appendix table 4.1). These were then cloned into the *SalI* and *NotI* restriction sites of *pENTR4* dual selection entry (gateway invitrogen) vector followed by sequencing. The two promoter gene constructs (WT and 2K/R) were then sub-cloned upstream of GFP in the gateway destination vector *pMDC104* using Gateway LR Clonase.

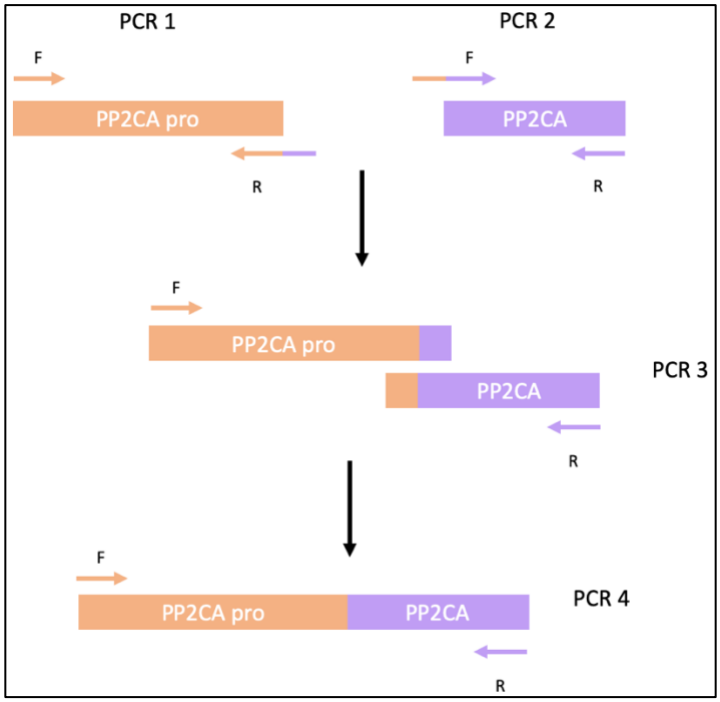

Figure 4.1 Model for generating overlap PCR. *Workflow for fusing together PP2CA coding region with PP2CA promoter. The first PCR amplifies the PP2CA promoter using a promoter forward primer (F) and an extended reverse primer that contains the beginning proportion of the PP2CA gene (R). The second PCR amplifies PP2CA, in two separate reactions for PP2CA^{WT} and PP2CA$^{2K/R}$. The PCR uses a PP2CA reverse primer and an extended forward primer that contains the end portion of the PP2CA promoter. The two PCRs generate fragments that overlap into the other, enabling in the third PCR the fragments to act as primers themselves. The PCR runs for 10 cycles before the PP2CA promoter forward primer and PP2CA reverse primer is added. The resulting PCR product joins two different PCR products. The fourth PCR amplifies the fused DNA region for restriction digestion into the entry vector.*

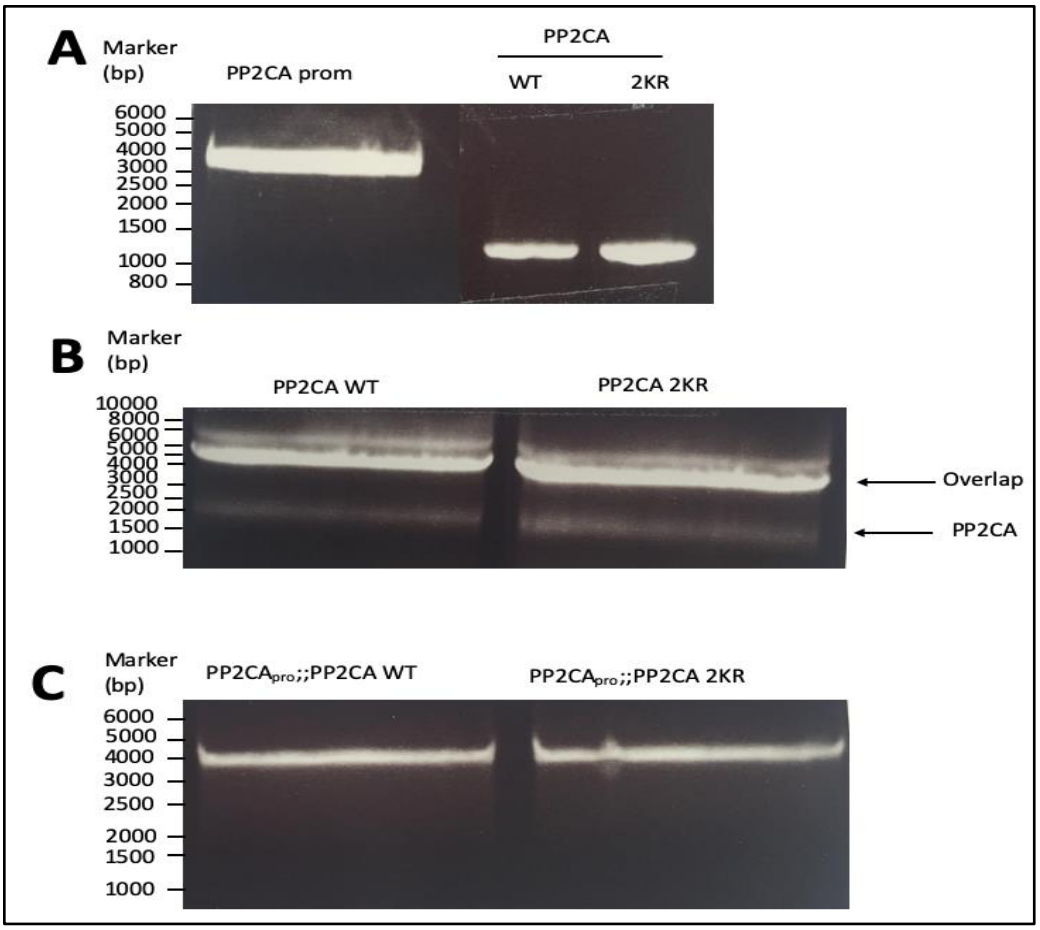

Figure 4.2 Generation of PP2CA$_{pro}$;;PP2CA WT/2KR constructs using an overlap PCR. *Image of DNA gel showing construction of own promoter PP2CA.* ***A)*** *Amplifying PP2CA WT, PP2CA 2K/R and PP2CA promoter (2947 bp) using overlapping primers were run on an agarose gel separated by electrophoresis.* ***B)*** *The products were then run in an overlap PCR containing the promoter and PP2CA fragments. The PCR products of the overlap PCR run on an agarose gel separated by electrophoresis. The arrow indicates PP2CA (1197 bp) and the overlap product (4144 bp)* ***C)*** *The products were then run in a PCR to amplify the overlapped product. The PCR product amplifying the overlapped product runs on an agarose gel separated by electrophoresis..*

These constructs were transformed into *Agrobacterium* strain *GV101* and the presence of the construct was confirmed by PCR (figure 4.3). These *Agrobacterium* strains were used to transform *Arabidopsis* plants (*pp2ca-1 and p3*) via the floral dip method (Clough and Bent 1998). It was decided to transform a single and triple PP2C knockout mutants; *pp2ca-1* was selected to determine if PP2CA^{WT} could reverse the phenotype. The triple *p3* transgenic was also selected because the PP2Cs have redundant functions and can mask the phenotype of single PP2C knockouts, we speculated this may mask the phenotype of PP2CA$^{2K/R}$ in a single PP2C knockout. Due to the increased ABA sensitivity in the *p3* transgenics, in addition to transforming the single *pp2ca-1* mutant the *p3* mutant was also transformed. The presence of the stable PP2CA^{WT} and PP2CA$^{2K/R}$ transgenes in the T3 generation was confirmed via PCR (figure 4.4).

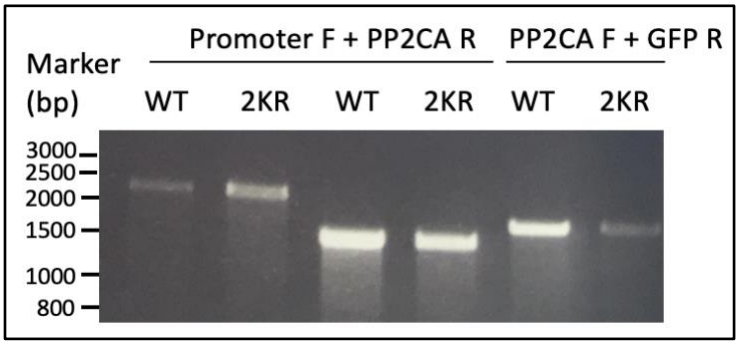

Figure 4.3 PP2CA$_{pro}$;;PP2CA WT and 2KR constructs transformed into Agrobacterium expression vector pMDC107. *Image of DNA gel showing amplification of fragments of PP2CA promoter and PP2CA from two Agrobacterium colonies, one containing PP2CA^{WT}, the other PP2CA$^{2K/R}$ that grows on selection media. Two different internal PP2CA promoter primers were used, resulting in two different sized bands generated (2173 bp and 1226 bp) plus a PP2CA and GFP primer (1572 bp).*

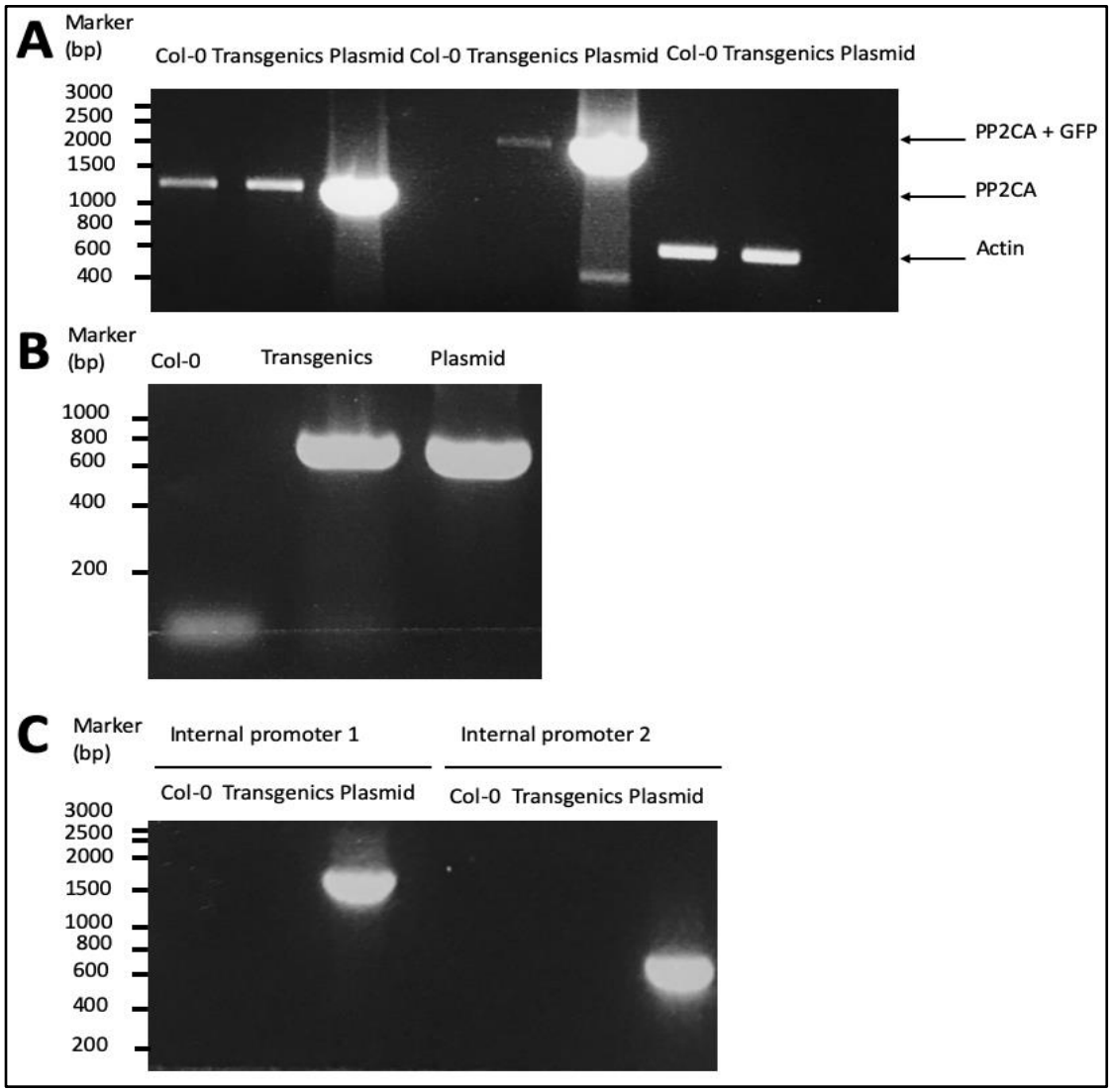

Figure 4.4 Genotyping plants dipped with $PP2CA_{pro}$;;$PP2CA^{WT}$ and $PP2CA^{2K/R}$ constructs. *Image of DNA gel showing amplification of fragments of PP2CA promoter and PP2CA from Arabidopsis transgenics cDNA. cDNA was also synthesised from Col-0 as a control, the pMDC107 plasmid used to transform the Arabidopsis was used as an additional control.* ***A)*** *The first three bands shows PCR amplification of PP2CA (1200 bp). The second three bands show PCR amplification of PP2CA-GFP (2106 bp). The last three bands show PCR amplification of ACTIN7 (546 bp).* ***B)*** *shows PCR amplification of GFP (735 bp)* ***C)*** *tests the quality of the cDNA to ensure the sample is not contaminated with DNA by amplifying sections of PP2CA promoter (1482 bp and 602 bp).*

In order to ensure the T3 transgenics were selected that had similar transgene expression levels to each other the expression levels of a minimum of 3 independent transgenic lines were analysed by real-time qPCR (figure 4.5 and 4.6). cDNA was synthesised from RNA, extracted from 10 day old seedlings grown on MS agar medium in a growth chamber. A minimum of two transgenic lines per construct, that showed similar levels of transgene expression to the other transgenics were selected for further analysis. Whilst this experiment was conducted to identify

transgenics with similar expression levels these RT-qPCRs should be repeated as it was only conducted with technical repeats not biological repeats, the expression of the *PP2CA* transcript should be analysed in Col-0, in addition to *pp2ca-1*/*p3* and the respective transgenics.

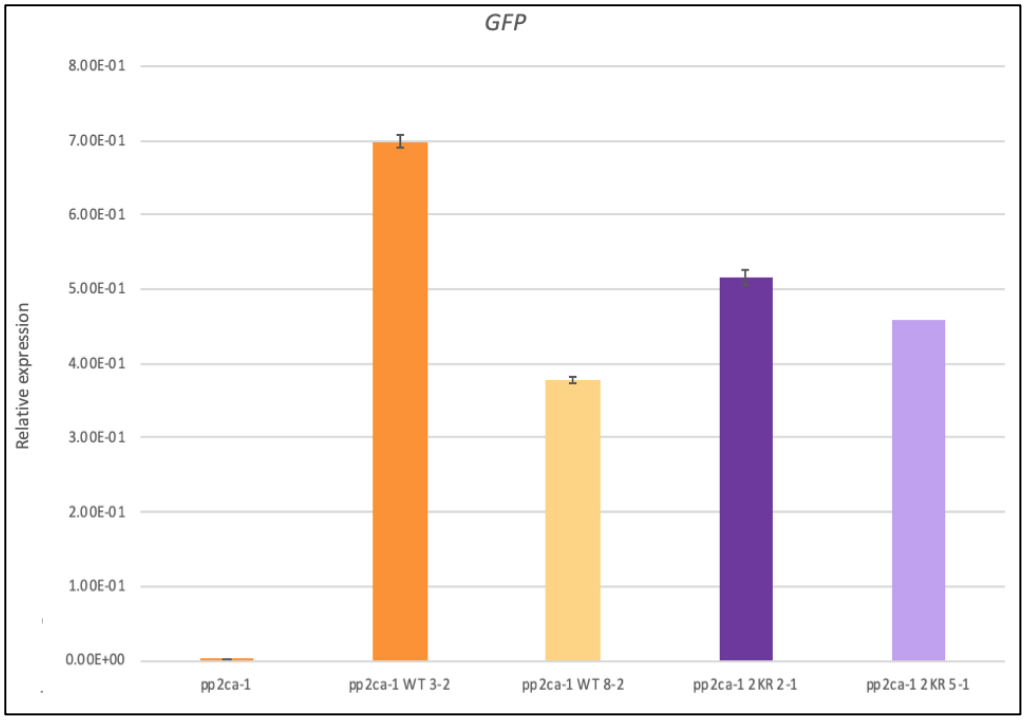

Figure 4.5 Expression analysis of GFP expression levels in different pp2ca-1 transgenic lines*. The expression levels of GFP in pp2ca-1 and different transgenic plant lines in the pp2ca-1 background expressing PP2CA^{WT} (3-2 and 8-2) and PP2CA$^{2K/R}$ (2-1 and 5-1) analysed by RT-qPCR. Relative GFP expression levels in 10 d old seedlings relative to ACTIN2. Error bars represent ±SE of 3 technical repeats.*

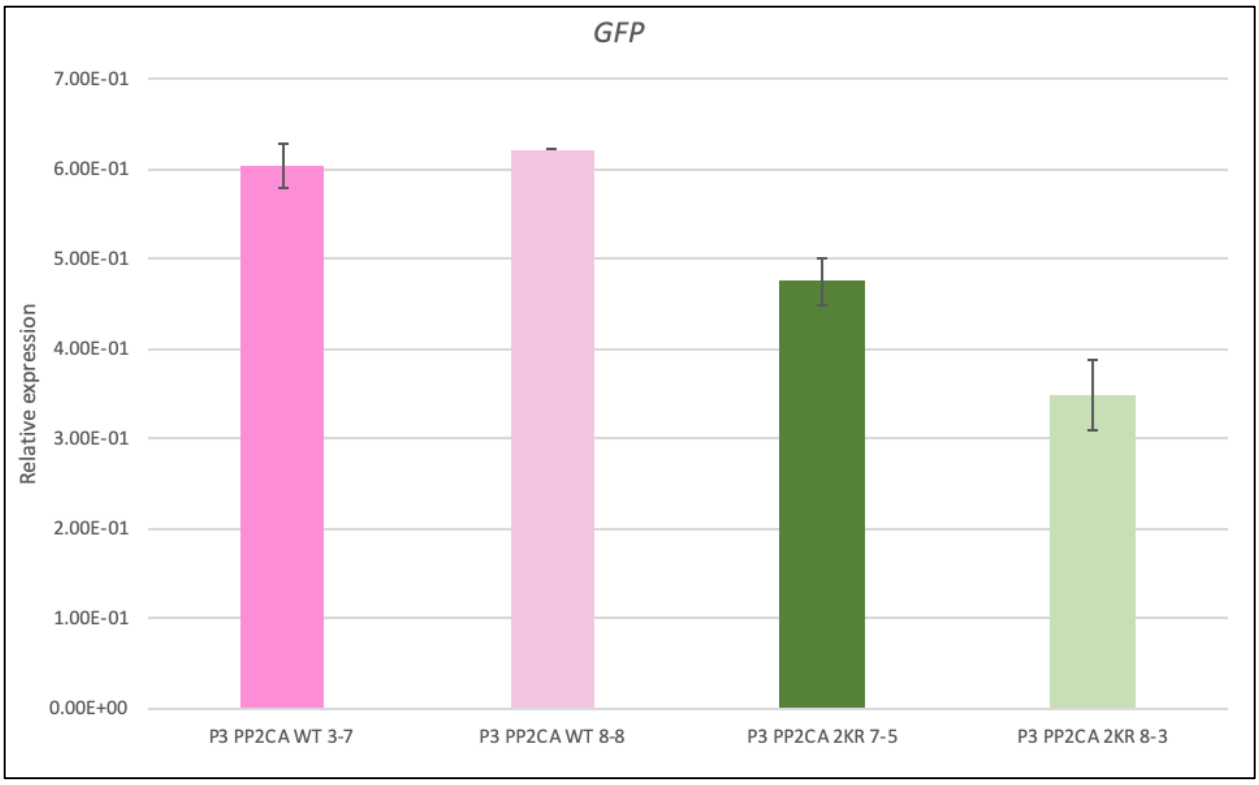

Figure 4.6 Expression analysis of GFP expression levels in different p3 transgenic lines*. The expression levels of GFP in different transgenic plant lines in the p3 background expressing PP2CA^{WT} (3-7 and 8-8) and PP2CA$^{2K/R}$ (5-7 and 8-3) analysed by RT-qPCR. Relative GFP expression levels in 10 days old seedlings relative to ACTIN2. Error bars represent ±SE of 3 technical repeats.*

Furthermore, to ensure the transgenic lines being assayed had similar protein levels the proteins were analysed by western blot (figure 4.7). Figure 4.7 shows PP2CA breakdown (bands at a lower molecular weight than PP2CA-GFP) particularly in the *pp2ca-1* knockout background, which may be due to the extraction technique. However PP2CA breakdown is also observed in the transgenics in the *p3* background. Two of the independent lines, *p3* PP2CA^{WT} 8-8 and *p3* PP2CA$^{2K/R}$ 8-3, show reduced protein abundance compared to the two other *p3* transgenic lines, however this may be due to less protein being present in the extraction, as shown in the loading control. Additionally *pp2ca-1* PP2CA^{WT} 3-2 has reduced protein abundance compared to the three other *pp2ca-1* transgenic lines. The stability of the transgenes should be examined using proteasome inhibitors and protein synthesis inhibitors, additionally stability in response to ABA should be examined, to determine if SUMOylation affects the stability of the proteins.

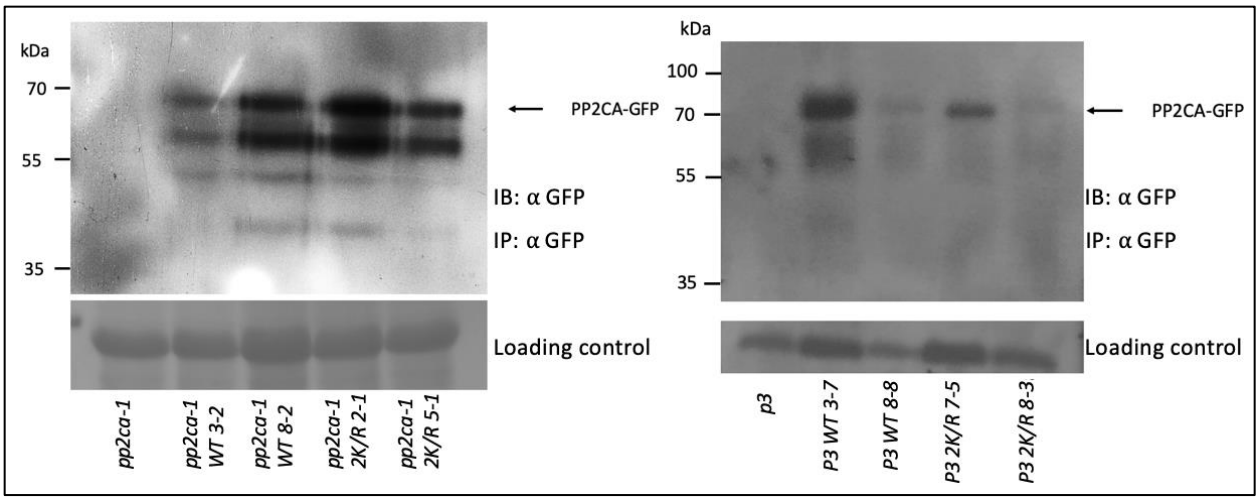

Figure 4.7 PP2CA^{WT} and PP2CA$^{2K/R}$ show similar protein abundance in both the pp2ca-1 and p3 knockout backgrounds. *The protein levels of PP2CA^{WT}-GFP and PP2CA$^{2K/R}$-GFP in different transgenic lines (p3 and pp2ca-1 backgrounds) were analysed by extracting total protein from each different line of transgenic Arabidopsis. Protein was also extracted from pp2ca-1 and p3 as negative controls. Total protein was immunoprecipitated (IP: α-GFP) with α-GFP immunoaffinity beads followed by immunoblot analysis with anti-GFP (IB: α-GFP) antibodies to detect PP2CA-GFP. Arrow indicates PP2CA-GFP (68 kDa). Below each blot is the ponceau-s stained rubisco loading control.*

Finally to determine if the proteins were being expressed correctly and localising where expected and to determine if the SUMO mutation was altering the localisation the *Arabidopsis* seedlings were examined using a fluorescence microscope (Zeiss SP5). As can be seen from the 5 day old seedling no difference can be observed between the seedlings expressing PP2CA^{WT} and PP2CA$^{2K/R}$, with both showing strong expression in the nucleus of the cells (figure 4.8) as was predicted (Antoni et al., 2012). However it is worth noting a nuclear stain was not used in this experiment, this work should be repeated again with this nuclear stain control. Future work could examine if the intensity of the fluorescence changes and if the localisation changes when the seedlings are exposed to exogenous ABA. However broadly figure 4.8 demonstrates the loss of the SUMOylatable lysines does not affect PP2CA localisation.

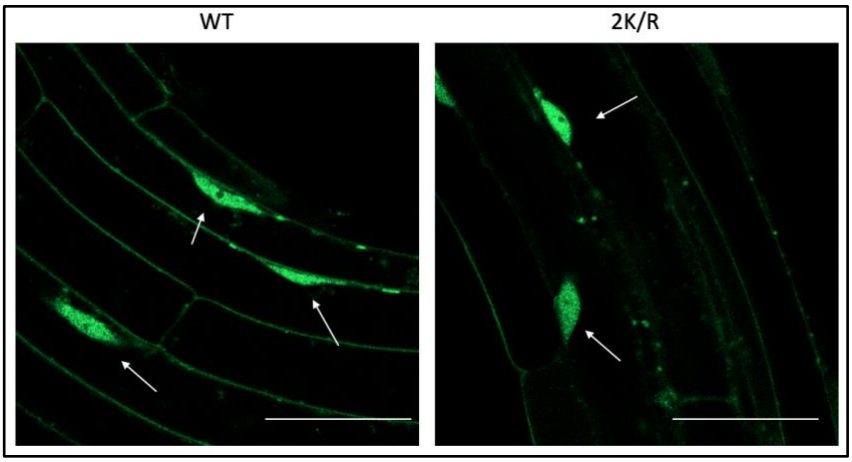

Figure 4.8 GFP tagged PP2CA protein localises in the nucleus of cells when stably expressed in Arabidopsis under its own promoter and is not altered by the loss of SUMOylated lysines. *Localisation of PP2CA^{WT}-GFP and PP2CA$^{2K/R}$-GFP fusion proteins in stably transformed 5 day old Arabidopsis roots was analysed by confocal laser scanning microscopy. The localisation pattern does not alter after mutation of lysine to arginine. The green signal indicates GFP. Strong expression of both PP2CA^{WT} and PP2CA$^{2K/R}$ can be seen in the nucleus of the cells (white arrow). Scale bar= 50 µm.*

4.3 Analysis of transgenic *Arabidopsis* stably expressing PP2CA

4.3.1 ABA sensitivity

To ascertain the function of SUMOylated PP2CA in the ABA pathway PP2CA^{WT} and PP2CA$^{2K/R}$ was expressed in *Arabidopsis* under its native promoter to determine if PP2CA$^{2K/R}$ exhibits an ABA sensitive or insensitive phenotype, compared to PP2CA^{WT}. Two independent transgenic lines of PP2CA$_{pro}$;;PP2CA^{WT} and two PP2CA$_{pro}$;;PP2CA$^{2K/R}$ in the *pp2ca-1* knockout background that showed similar levels of transcript expression and protein levels were assayed (figure 4.5 and 4.7). In addition to Col-0 and ABA sensitive mutant line *pp2ca-1* the root lengths of the different transgenics grown on 10 µM, 25 µM ABA or no ABA stimulus (control) were measured. In the absence of exogenous ABA, primary root lengths amongst the transgenics are not significantly different (figure 4.9 and 4.10).

In the presence of ABA, a significant difference in primary root length between the two independent transgenic lines of *pp2ca-1* PP2CA$_{pro}$;;PP2CA^{WT} and the two independent transgenic lines of *pp2ca-1* PP2CA$_{pro}$;;PP2CA$^{2K/R}$ was observed (figure 4.9, 4.10). A reduction of primary root length was seen in both *pp2ca-1* PP2CA$_{pro}$;;PP2CA^{WT} and *pp2ca-1* PP2CA$_{pro}$;;PP2CA$^{2K/R}$ transgenic lines. However, there was a greater reduction in primary root length in the *pp2ca-1* PP2CA$_{pro}$;;PP2CA^{WT} transgenic lines; this suggests that the *pp2ca-1* PP2CA$_{pro}$;;PP2CA$^{2K/R}$ transgenic lines are less sensitive to ABA than *pp2ca-1* PP2CA$_{pro}$;;PP2CA^{WT}. As expected, the PP2C mutant plants *pp2ca-1* were more sensitive to the exogenous ABA than Col-0, however *pp2ca-1* PP2CA$_{pro}$;;PP2CA^{WT} was not completely capable of

reversing the phenotype, whilst they were less sensitive to ABA than *pp2ca-1* they were not quite as insensitive as Col-0.

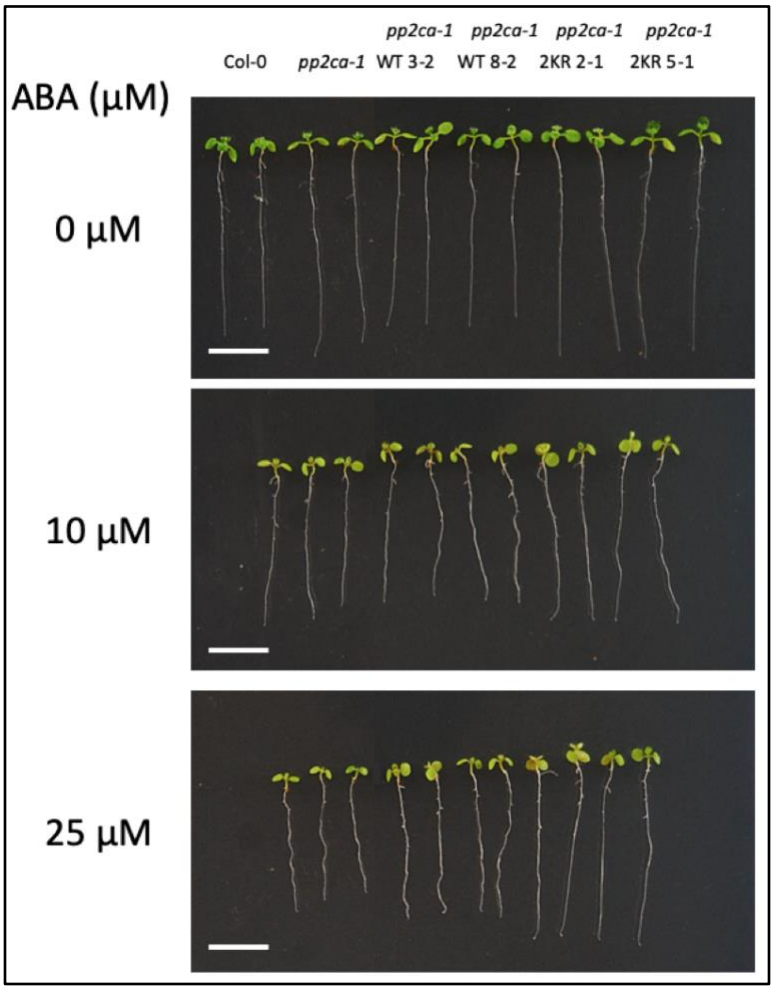

Figure 4.9 pp2ca-1 PP2CA^{WT} transgenics shows reduced primary root length in response to ABA, compared to pp2ca-1 PP2CA$^{2K/R}$ transgenics. *Representative image of 11 day old seedlings Col-0, pp2ca-1 and two independent transgenic lines of PP2CA^{WT} and PP2CA$^{2K/R}$ in the pp2ca-1 background, germinated and grown for 5 days on 1/2 MS medium then transferred to either 1/2 MS or 1/2 MS with 10 µM or 25 µM (+)-ABA and grown for a further 6 days. Scale bar = 1 cm.*

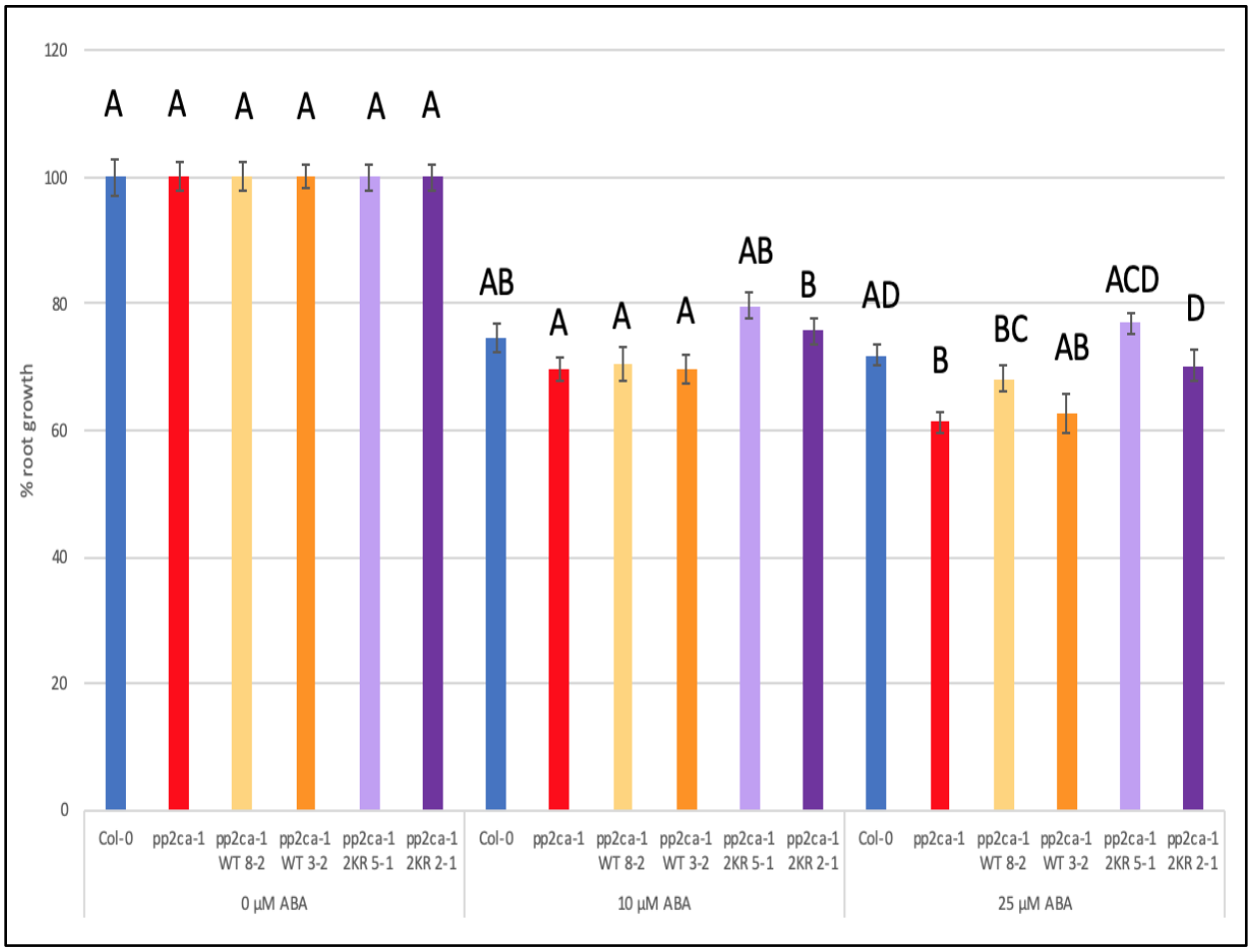

Figure 4.10 Quantification of ABA-mediated root growth inhibition of Col-0, pp2ca-1, pp2ca-1 WT 8-2, pp2ca-1 WT 3-2, pp2ca-1 2KR 5-1 and pp2ca-1 2KR 2-1 mutants. *Five-day-old seedlings of the different genotypes were transferred to 1/2MS, 1/2MS with 10 µM or 25 µM (+)-ABA and grown for additional six days before root lengths were measured. Data is relative to growth on 0µM ABA. Data are means ± se (n = 26-30 each). Bars with different letters in each treatment were significantly different from others; p > 0.05; one-way ANOVA with post hoc Tukey test. Two repeats conducted.*

Due to the functional redundancy of the PP2Cs the same assay was carried out again with the same constructs $PP2CA_{pro}$;;$PP2CA^{WT}$ and two $PP2CA_{pro}$;;$PP2CA^{2K/R}$ expressed in the triple mutant background *p3*. Two independent transgenic lines of $PP2CA_{pro}$;;$PP2CA^{WT}$ and two $PP2CA_{pro}$;;$PP2CA^{2K/R}$ in the *p3* triple mutant knockout background that showed similar levels of transcript expression and protein levels were assayed. In addition to Col-0 and an ABA sensitive mutant line *p3* the root lengths of the different transgenics grown on 10 µM or no ABA stimulus (control) were measured.

In the absence of exogenous ABA stimulation, primary root length amongst the transgenics are similar, (figure 4.11). In the presence of ABA a significant difference in primary root length between the two independent transgenic lines

of *p3* PP2CA$_{pro}$;;PP2CA^{WT} and the two independent transgenic lines of *p3* PP2CA$_{pro}$;;PP2CA$^{2K/R}$ was observed (figure 4.11, 4.12). A reduction of primary root length was seen in both *p3* PP2CA$_{pro}$;;PP2CA^{WT} and *p3* PP2CA$_{pro}$;;PP2CA$^{2K/R}$ mutant transgenic lines in response to ABA. However, the reduction in primary root length was significantly more severe in the *p3* PP2CA$_{pro}$;;PP2CA^{WT} transgenic lines; this suggests that the P3 PP2CA$_{pro}$;;PP2CA$^{2K/R}$ transgenic lines are less sensitive to ABA than *p3* PP2CA$_{pro}$;;PP2CA^{WT}. As expected, the PP2C triple mutant plants *p3* were more sensitive to the exogenous ABA than Col-0. However *p3* PP2CA$_{pro}$;;PP2CA^{WT} was more sensitive to ABA than *p3*. The replacement of a PP2C into the *p3* background should have reversed the ABA sensitivity, not increased it. This may be due to the location in the genome, where the PP2CA has been inserted.

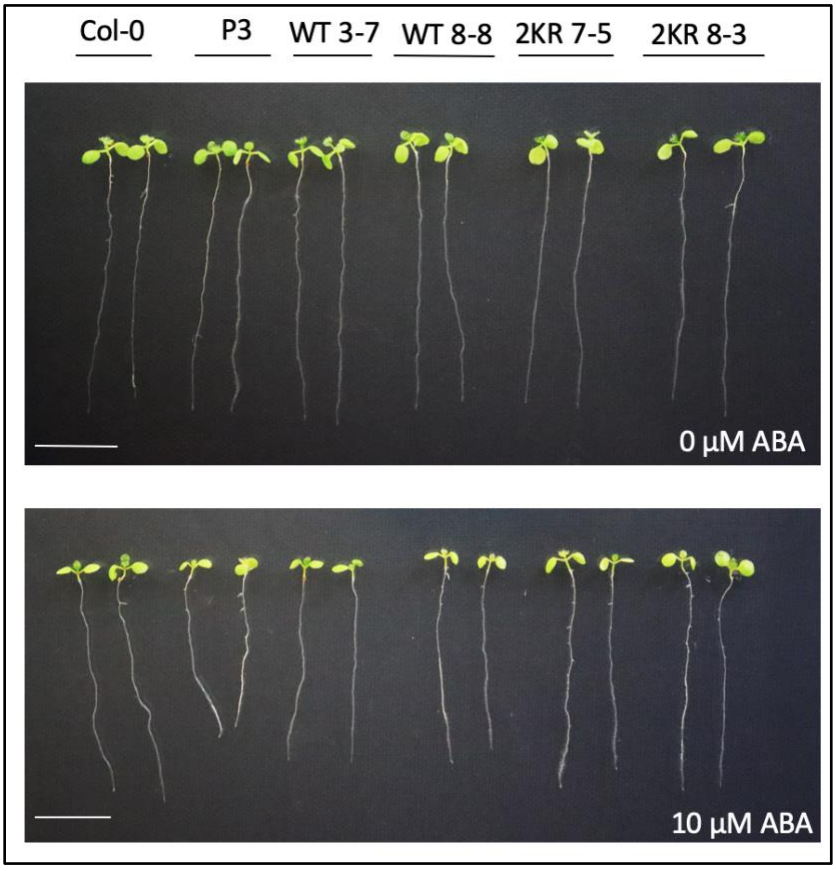

Figure 4.11 p3 PP2CA^{WT} mutants shows reduced primary root length in response to ABA, compared to p3 PP2CA^{2KR} mutants. *Representative image of 11 day old seedlings, col-0, pp2ca-1 and two independent transgenic lines of PP2CA^{WT} and PP2CA$^{2K/R}$ in p3 background, germinated and grown for 5 days on 1/2 MS medium then transferred to either 1/2 MS or 1/2 MS with 10 µM (+)-ABA and grown for a further 6 days. Scale bar = 1 cm.*

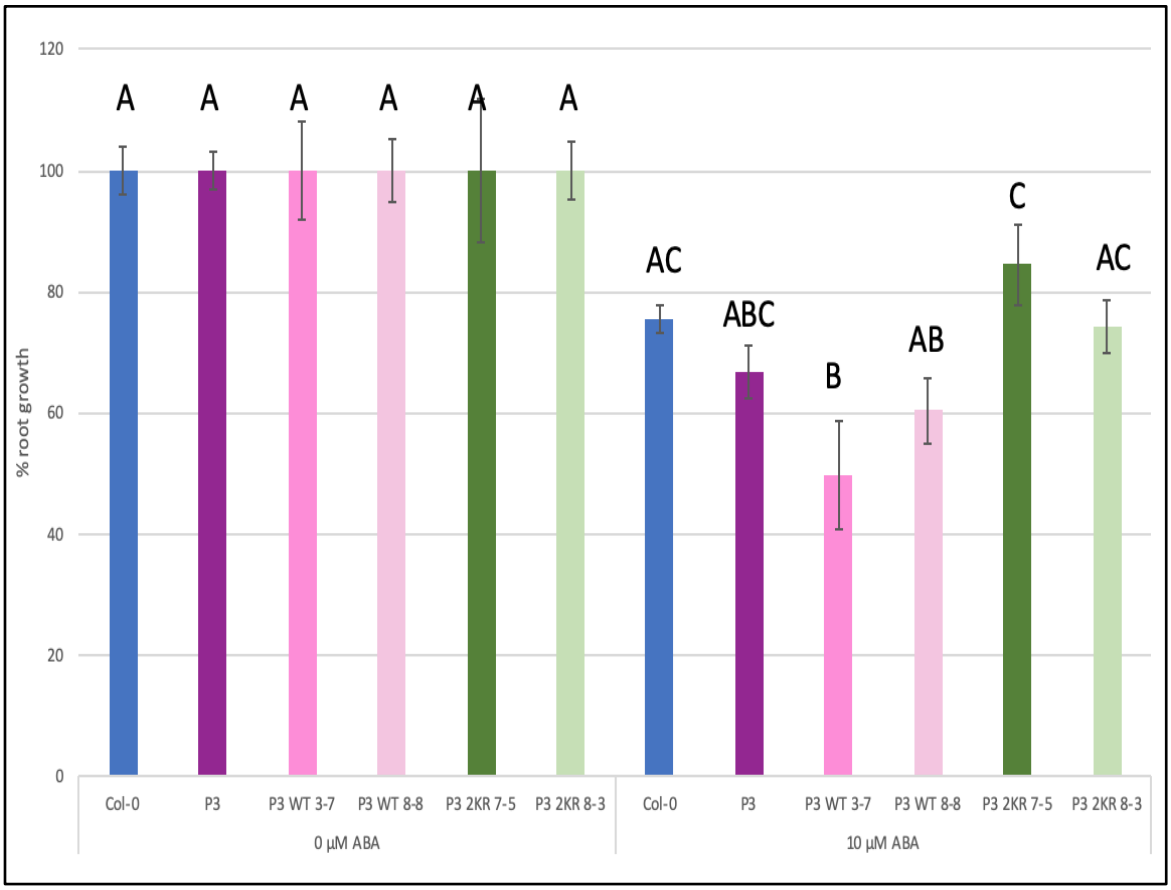

Figure 4.12 Quantification of ABA-mediated root growth inhibition of Col-0, p3, pp2ca^{WT} 3-7, pp2ca^{WT} 8-8, pp2ca^{2KR} 7-5 and pp2ca^{2KR} 8-3 transgenics. *Five-day-old seedlings of the different genotypes were transferred to 1/2MS or 1/2MS with 10 µM (+)-ABA and grown for additional six days before root lengths were measured. Data is relative to growth on 0µM ABA. Data are means ± se (n = 12-20 each). Bars with different letters in each treatment were significantly different from others; p > 0.05; one-way ANOVA with post hoc Tukey test. Two repeats conducted.*

In order to further explore the role of the differences between two lines of PP2CA$_{pro}$;;PP2CA^{WT} and two lines of PP2CA$_{pro}$;;PP2CA$^{2K/R}$ in ABA response the mutant line seeds were also exposed to ABA for a seedling establishment assay. The seedling establishment rate of two independent transgenic lines of PP2CA$_{pro}$;;PP2CA^{WT} and two PP2CA$_{pro}$;;PP2CA$^{2K/R}$ in the *pp2ca-1* knockout background that showed similar levels of transcript expression and protein levels were examined. In the absence of ABA all the lines studied had established by day 4 (figure 4.13 and 4.14).

In the presence of exogenous ABA the seedling establishment decreases (figure 4.13 and 4.14). The line that showed the least ABA sensitivity in seedling establishment was *pp2ca-1* PP2CA$_{pro}$;;PP2CA$^{2K/R}$ 2-1. The line that was most sensitive to ABA was *pp2ca-1* PP2CA$_{pro}$;;PP2CA^{WT} 3-2. However *pp2ca-1* PP2CA$_{pro}$;;PP2CA$^{2K/R}$ 5-1 and *pp2ca-1* PP2CA$_{pro}$;;PP2CA^{WT} 8-2 both showed similar levels of sensitivity to the ABA. Based on this data it is unclear if SUMO

plays a role in germination or seedling establishment, germination and further seedlings establishment experiments should be repeated to further understand the role of SUMO. The experiment should be repeated to provide biological repeats.

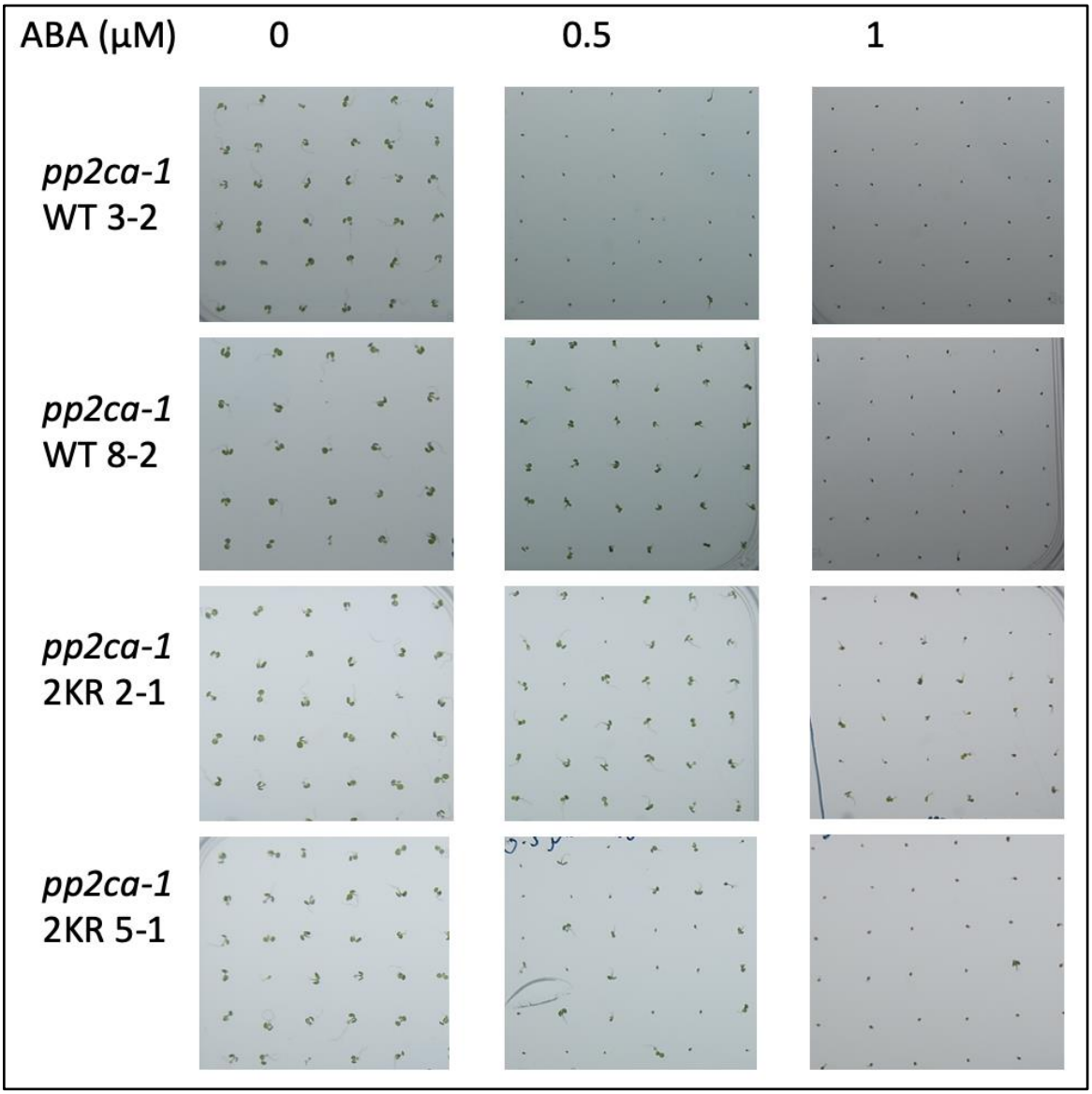

Figure 4.13 Representative photo of seedling establishment of pp2ca-1 PP2CA^{WT} and PP2CA$^{2K/R}$ mutants under treatment. *Approximately 30 seeds of each genotype (two independent transgenic lines of PP2CA^{WT} and PP2CA$^{2K/R}$ in pp2ca-1 background) were stratified on moist filter paper at 4˚C for 2 days in the dark. They were then transferred to 1/2MS supplemented with differing concentrations of ABA, 0 µM ABA (left panel), 0.5µM ABA (middle panel) and 1µM ABA (right panel). Photographs were taken 4 days later and scored for the seedling establishment.*

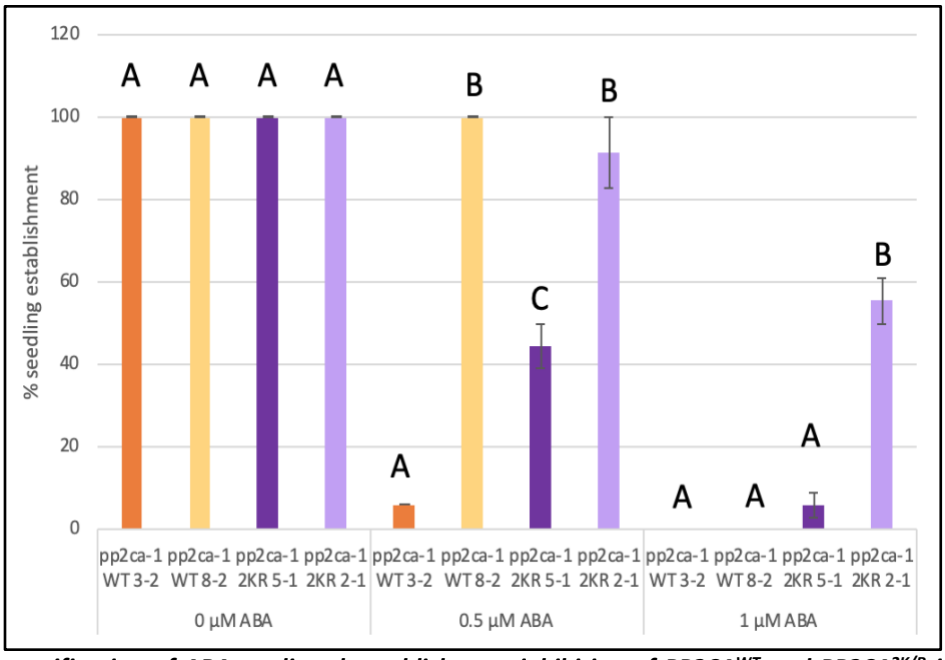

Figure 4.14 Quantification of ABA-mediated establishment inhibition of PP2CA^{WT} and PP2CA$^{2K/R}$ in the pp2ca-1 background. *Percentage of seeds that germinated and developed green cotyledons in the presence of the indicated concentrations of ABA. Approximately 40 seeds of each genotype were sowed on each plate and scored 4 days later. Bars with different letters in each treatment were significantly different from others; p > 0.05; one-way ANOVA with post hoc Tukey test..*

A seedling establishment assay was also conducted with two lines of PP2CA$_{pro}$;;PP2CA^{WT} and two lines of PP2CA$_{pro}$;;PP2CA$^{2K/R}$ expressed in the triple PP2C knockout background *p3.* However due to the transgenics being expressed in the *p3* background none of the seedlings established in 0.5 µM or 1 µM ABA (figure 4.15 and 4.16). The assay should be repeated again using lower ABA concentrations to determine if there is a germination phenotype. The seedling establishment data from the transgenics in the *pp2ca-1* background is unclear as to whether SUMOylated PP2CA plays a role in germination.

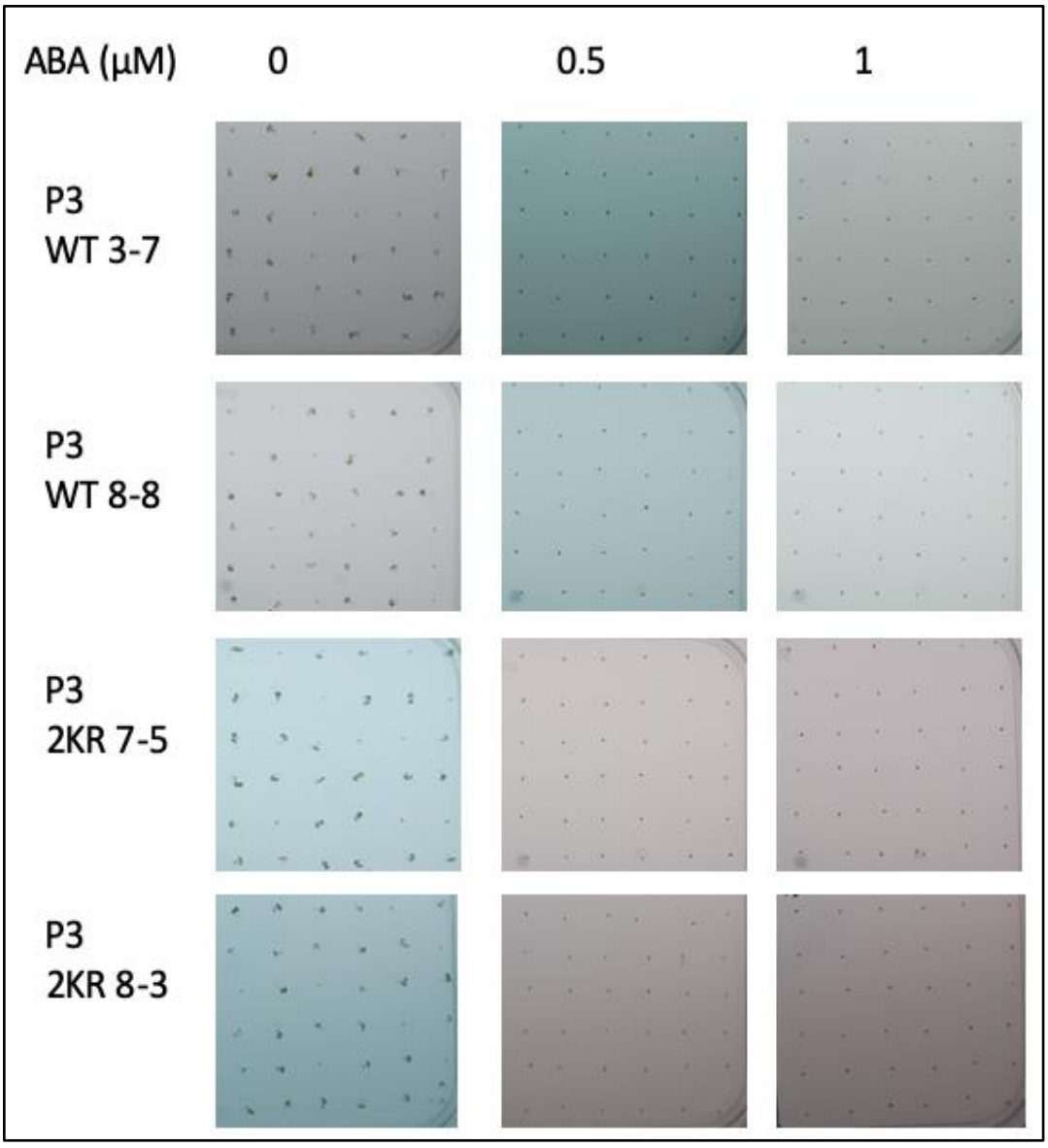

Figure 4.15 Representative photo of seedling establishment of p3 PP2CA^{WT} and p3 PP2CA$^{2K/R}$ mutants under treatment. *Approximately 30 seeds of each genotype (two independent transgenic lines of PP2CA^{WT} and PP2CA$^{2K/R}$ in p3 background) were stratified on moist filter paper at 4˚C for 2 days in the dark. They were then transferred to 1/2MS supplemented with differing concentrations of ABA, 0 µM ABA (left panel), 0.5µM ABA (middle panel) and 1µM ABA (right panel). Photographs were taken 4 days later and scored for the seedling establishment.*

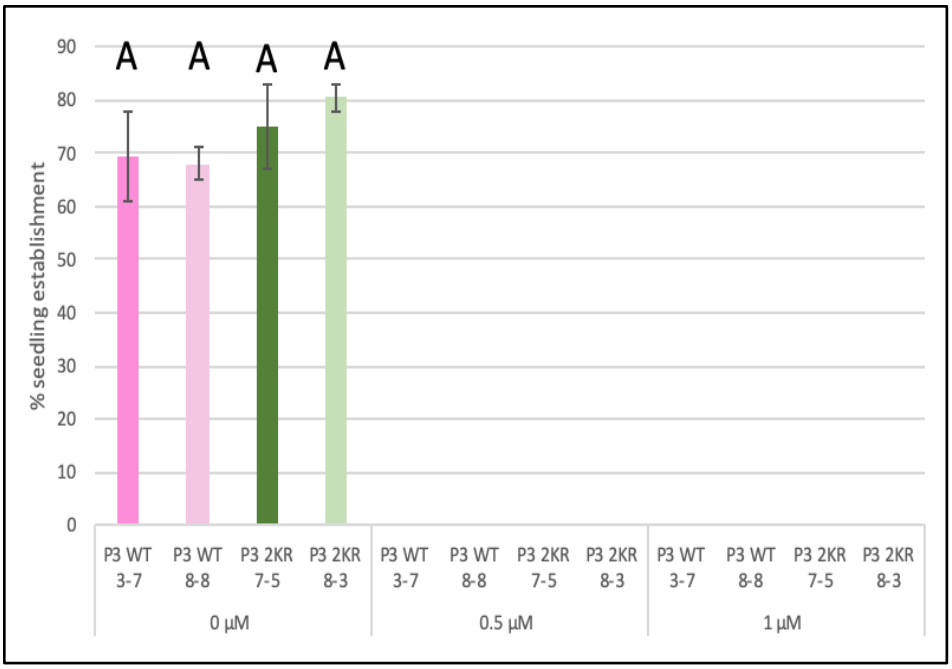

Figure 4.16 Quantification of ABA-mediated establishment inhibition of Col-0, spf ko and p3 mutants. *Percentage of seeds that germinated and developed green cotyledons in the presence of the indicated concentrations of ABA . Approximately 40 seeds of each genotype were sowed on each plate and scored 4 days later. Bars with different letters were significantly different from others; p > 0.05; one-way ANOVA with post hoc Tukey test.*

4.3.2 Role of SUMO in ABA expression genes

To further explore whether SUMOylation of PP2CA increases plants response to ABA and if the *Arabidopsis* transgenic mutants expressing PP2CA$^{2K/R}$ is less sensitive to ABA, the transcript level of downstream genes activated upon ABA was investigated. The genes studied include ABA biosynthesis genes, *AAO3, NCED3* and *ABA1/ZEP* (Finkelstein, 2013), and ABA response genes, *RD22, RD29A, RD29B* and *RAB18* (Kasuga et al., 2004; Lang and Palva, 1992; Nakashima et al., 2009; Yamaguchi-Shinozaki and Shinozaki, 1993) (appendix table 3.1).

As was expected most of the lines increase transcription of ABA biosynthetic genes in response to ABA as part of a positive feedback loop (figure 4.17) (Barrero et al., 2011). However interestingly the two *pp2ca-1* PP2CA$^{2K/R}$ mutant lines have lower expression of ABA biosynthetic gene *ABA1*, compared to *pp2ca-1* PP2CA^{WT} in the presence and absence of exogenous ABA. The two *pp2ca-1* PP2CA$^{2K/R}$ mutant lines had similar expression of *AAO3* to *pp2ca-1* PP2CA^{WT} 8-2, but a lower expression to *pp2ca-1* PP2CA^{WT} 3-2. In the presence of exogenous ABA the two *pp2ca-1* PP2CA$^{2K/R}$ mutant lines had a lower expression of *NCED3* compared to the *pp2ca-1* PP2CA^{WT} mutant lines. Figure 4.17 also demonstrates that the two PP2CA^{WT} lines are not completely capable of complementing *pp2ca-1* as would be predicted their expression of the studied transcripts should be similar to Col-0.

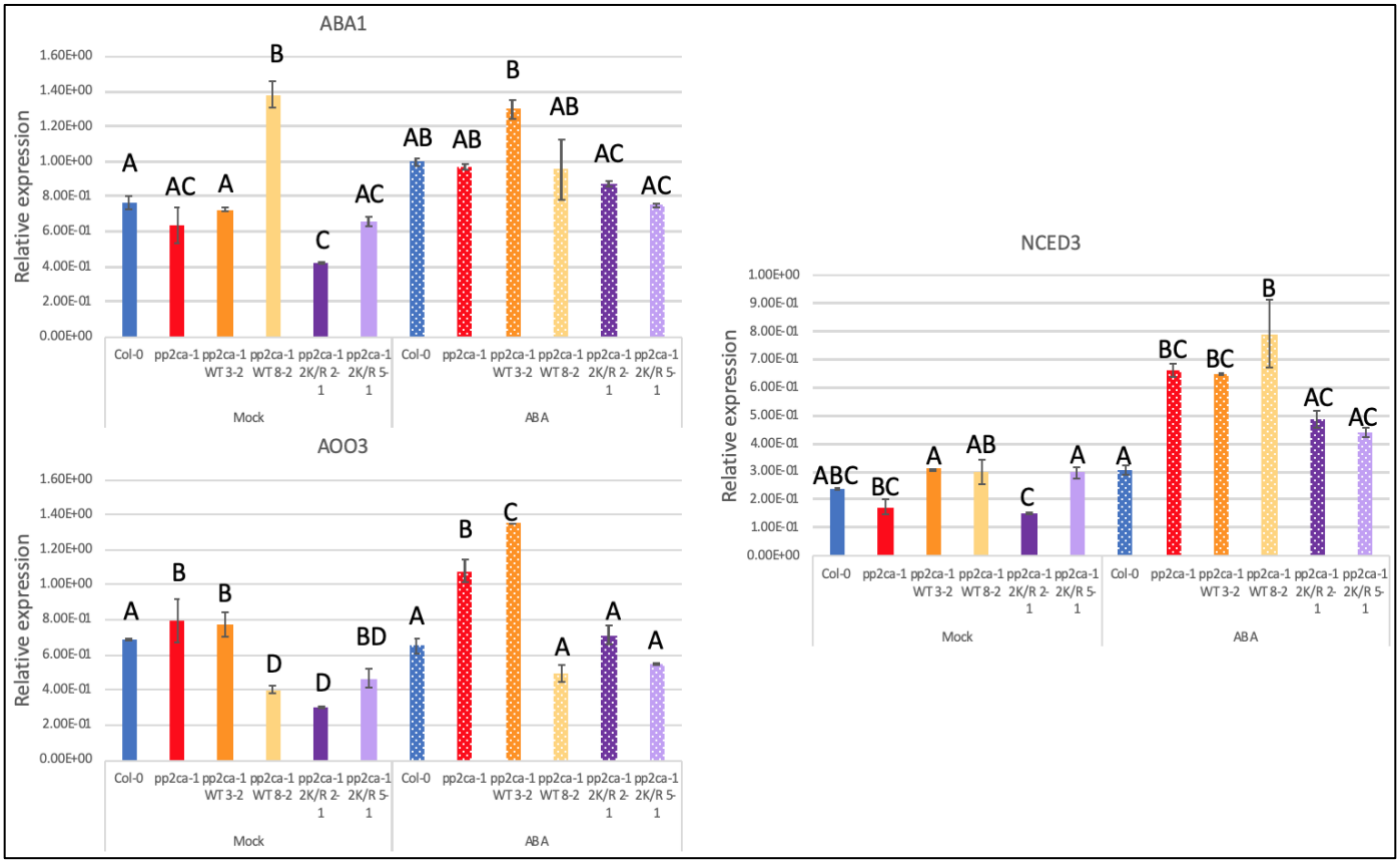

Figure 4.17 Quantitative RT-PCR analysis of gene expression of ABA biosynthetic genes before and after ABA treatment in the pp2ca-1 transgenics. *Quantitative PCR expression analysis of ABA biosynthesis genes in col-0, pp2ca-1 and two independent transgenic lines of PP2CA^{WT} (3-2 and 8-2) and PP2CA$^{2K/R}$ (2-1 and 5-1) in pp2ca-1 background. 10 day old seedlings were transferred to liquid MS containing DMSO (Mock) or 50 µM ABA for 3 hours, as in Wu et al., 2016. Seedlings were incubated for 3 hours then collected and total RNA was extracted, quality control checks were performed and cDNA synthesised. ACTIN2 transcript was analysed as the internal control, expression of ABA1, AOO3 and NCED3 was analysed. Error bars represent ±SE of 3 technical repeats. Error bars represent ± SEM of 3 technical repeats. Bars with different letters in each treatment were significantly different from others; p > 0.05; one-way ANOVA with post hoc Tukey test.*

There was greater variation in expression in the ABA responsive genes, with variation between the two *pp2ca-1* PP2CA^{WT} lines and the two *pp2ca-1* PP2CA$^{2K/R}$ lines (figure 4.18). However in the presence of exogenous ABA the two *pp2ca-1* PP2CA$^{2K/R}$ lines had reduced expression of *RD29A* and *RD29B* (figure 4.18). Additionally figure 4.18 also demonstrates that the two PP2CA^{WT} lines are not completely capable of complementing *pp2ca-1* as would be predicted their expression of the studied transcripts should be similar to Col-0, however as predicted *pp2ca-1* has increased expression of ABA response genes compared to Col-0. Future work should include a time course, to see how the levels of transcript change overtime and should repeat with biological repeats.

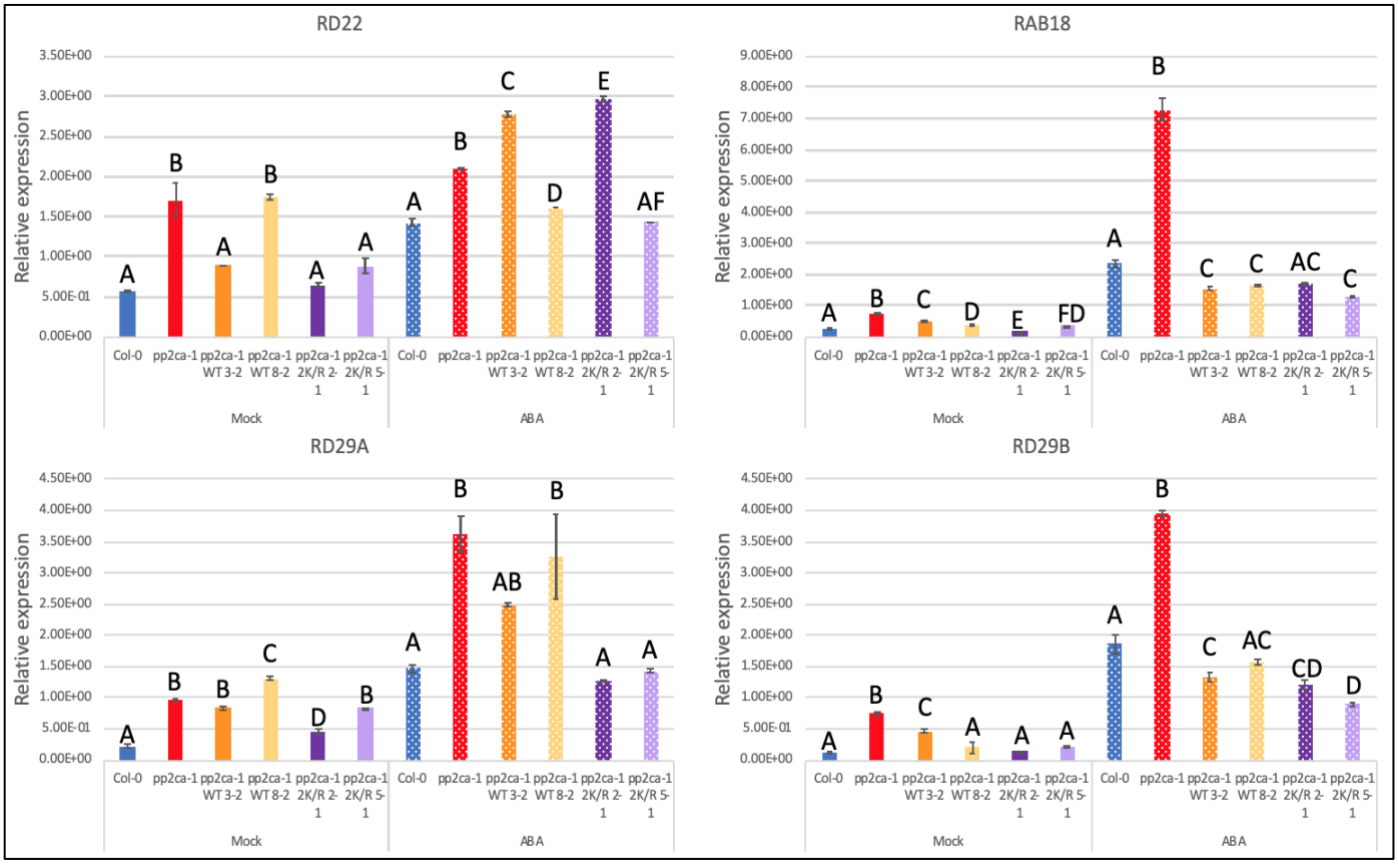

Figure 4.18 Quantitative RT-PCR analysis of gene expression of ABA response genes before and after ABA treatment in the p3 transgenics. *Expression analysis of ABA responsive genes in col-0, pp2ca-1 and two independent transgenic lines of PP2CA^{WT} and PP2CA$^{2K/R}$ in pp2ca-1 background. 10 day old seedlings were transferred to liquid MS containing DMSO (Mock) or 50 µM ABA for 3 hours, as in Wu et al., 2016. Seedlings were incubated for 3 hours then collected and total RNA was extracted, quality control checks were performed and cDNA synthesised. ACTIN2 transcript was analysed as the internal control, expression of RD22, RAB18, RD29A and RD29B was analysed. Error bars represent ±SE of 3 technical repeats. Error bars represent ± SEM of 3 technical repeats. Bars with different letters in each treatment were significantly different from others; p > 0.05; one-way ANOVA with post hoc Tukey test.*

4.3.3 Role of SUMO in ABA related pathogen response

To see if SUMO, a PTM capable of rapidly changing the proteome, was involved with the rapid pathogen triggered ABA response, *Pst* dip infection assays were carried out on 4-week-old plants. *Pst* was prepared as a liquid culture at a concentration of 1x10^{8} cfu mL−1, *Arabidopsis* was dipped for approximately 30 seconds. Dip infections were carried out as this would determine if changes in disease phenotype were caused by changes in stomatal aperture in response to the pathogen. Plants were allowed to grow normally and at 3 dpi (days post infection) leaf disks were

cut from the dipped leaves. The *Pst* was extracted and a serial dilution was carried out for quantification by plating 10ul of each dilution on plates containing kings-B media.

At 3 dpi Col-0 can be seen to be the most sensitive of the *Arabidopsis* genotypes tested (figure 4.19). This is expected as Lim et al., 2014 demonstrated *pp2ca-1* plants are more resistant to *Pst* than Col-0 due to hypersensitivity to ABA caused by the absence of the ABA negative regulator. As all the transgenics are either lacking two or three PP2C negative regulators it is expected that the Col-0 would be most sensitive to *Pst*. However *p3* is the second most sensitive which would not be predicted as this transgenic is lacking 3 PP2Cs, whereas the other four transgenics have had PP2CA returned. It was also unexpected that PP2CA$^{2K/R}$ would show a *Pst* resistant phenotype as PP2CA$^{2K/R}$ was less sensitive to ABA mediated root inhibition.

Due to time constraints this experiment was only conducted once and statistical significance cannot be conducted, this experiment should be completed twice more to confirm these results. However this first analysis can provide insights into possible roles of SUMOylated PP2CA in pathogen induced closure of stomata.

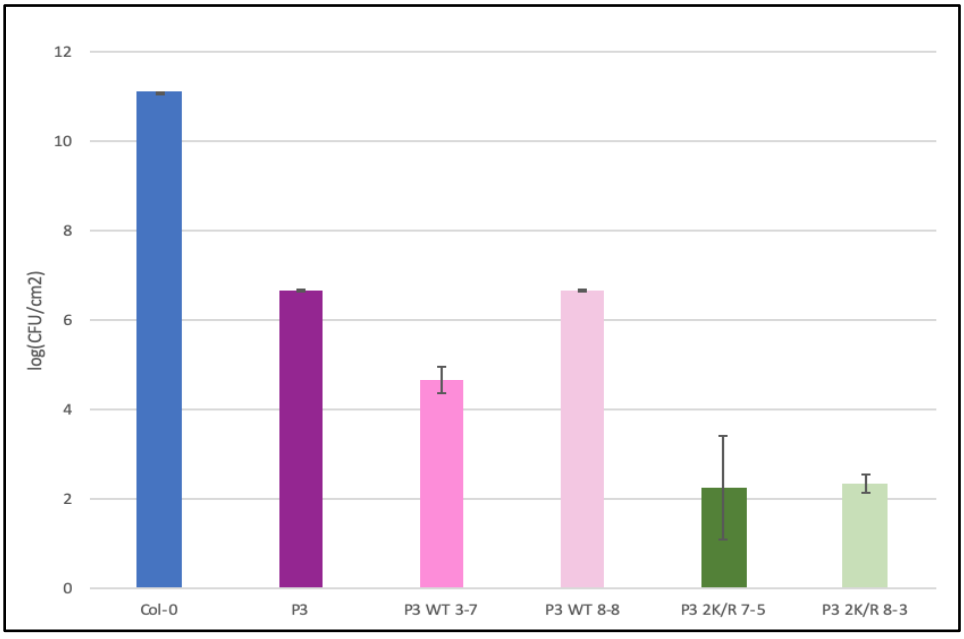

Figure 4.19 PP2CA$^{2K/R}$ plants are more resistant than PP2CA^{WT} plants to plant pathogen Pst. *Quantification of colony forming units (CFUs) from infected rosettes were counted 3 dpi. Pst was dipped into plants at a concentration of 10^8 cfu ml^{-1}. At 3 dpi bacterial growth in leaves from the different transgenics were quantified. Quantification was carried out in triplicate, each replicate used a leaf disc from three separate plants. Error bars represent ± SD of 3 replicates. Statistical analysis was not conducted as due to time constraints this experiment was only conducted once.*

Further work needs to be carried out to determine the disease phenotype of the transgenics. In addition to repeating this dipping experiment, the pathogen growth should also be monitored over several days. Having ABA hypersensitivity is advantageous to prevent the pathogen entering the stomata, however once in the cells ABA hypersensitivity increases pathogen virulence and aids disease progression by inhibiting salicylic acid signalling (Ton et al., 2009). Completing a time course would determine if $PP2CA^{WT}$ or $PP2CA^{2K/R}$ aids disease progression at different points of time. Syringe infiltrations of *Pst* are also required to determine if the phenotypes observed are due to changes in the stomata. In addition expression of PR genes and ABA-responsive genes should be analysed with and without pathogen or PAMP presence. Furthermore the SUMOylation status of PP2CA in response to pathogens or PAMPs should be studied to determine if as predicted SUMOylation of PP2CA increases upon perception of pathogens. Lastly the stomatal aperture should be measured in presence and absence of *Pst*, ABA, PAMP, flg22 and coronatine, a pathogen secreted virulence factor that induces stomatal reopening and inhibits ABA-mediated stomatal closure to overcome PAMP triggered immunity and stomatal defence (Underwood et al., 2007).

4.4 Generation and analysis of transgenic *Arabidopsis* expressing PYL8

Given that at least one SUMO site in PP2CA may be present in the interaction interface between PP2CA and the PYLs (figure 3.4) we speculated that a SUMO interaction motif (SIM) site may be present in the ABA co-receptors. The HyperSUMO programme (Nelis, PhD thesis 2014) that, in addition to predicting SUMO sites, also predicts SIM sites, scanned through the PYL gene family, which identified a SIM site that was conserved amongst most of the PYLs.

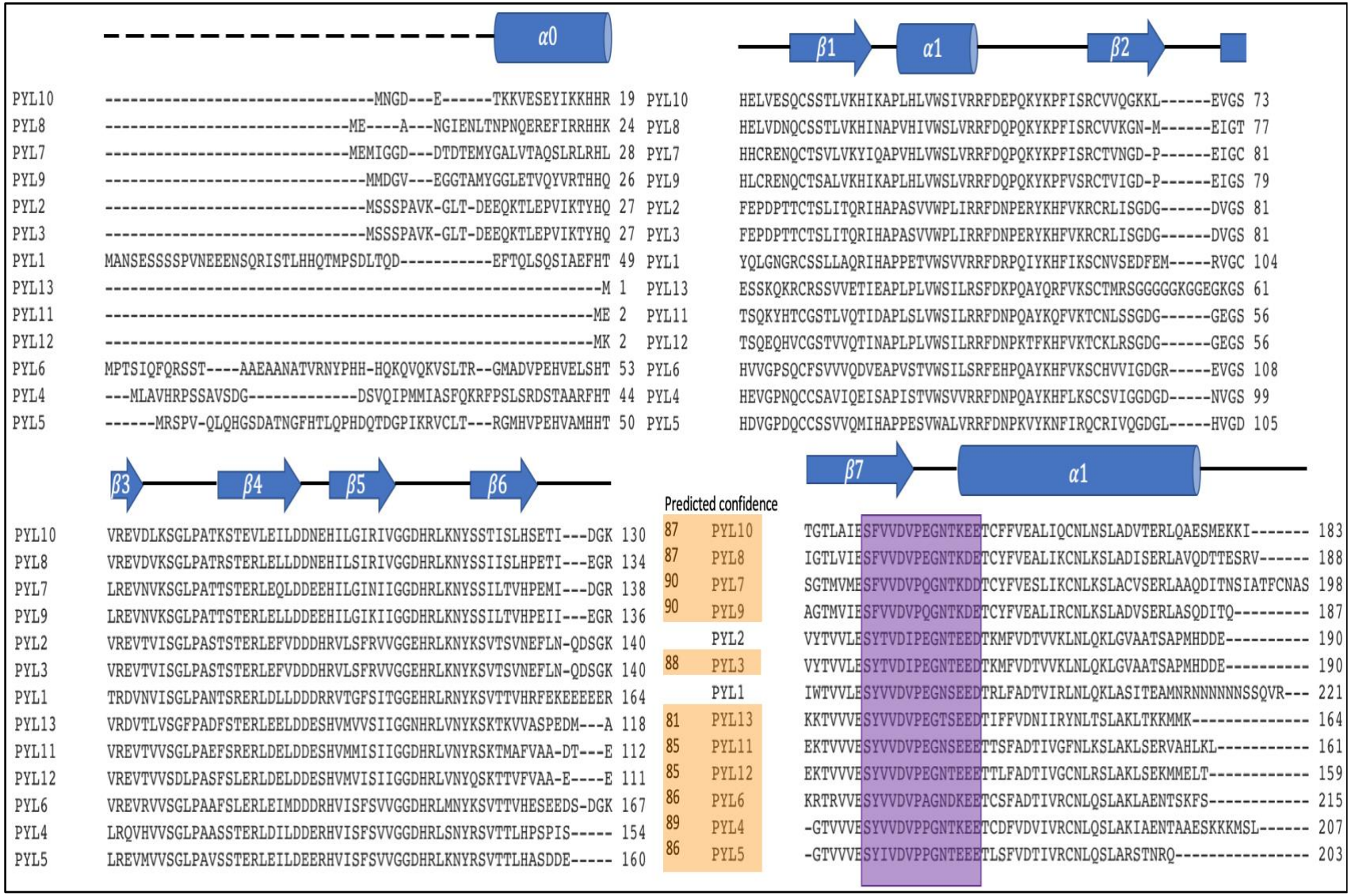

Figure 4.20 Location of the predicted SIM sites in PYLs, identified using in-house software. *The amino acid sequences, from TAIR, of the fourteen currently identified PYLs in Arabidopsis aligned using Clustal Omega website. The secondary elements are shown above the sequences, the N-terminal helix α0 is missing in PYLs 11-13 (Adapted from Li et al., 2013). The SIM site identified, highlighted in the purple box, were largely conserved and predicted with a >80% confidence, the confidence predicted for each PYL is listed in the yellow box.*

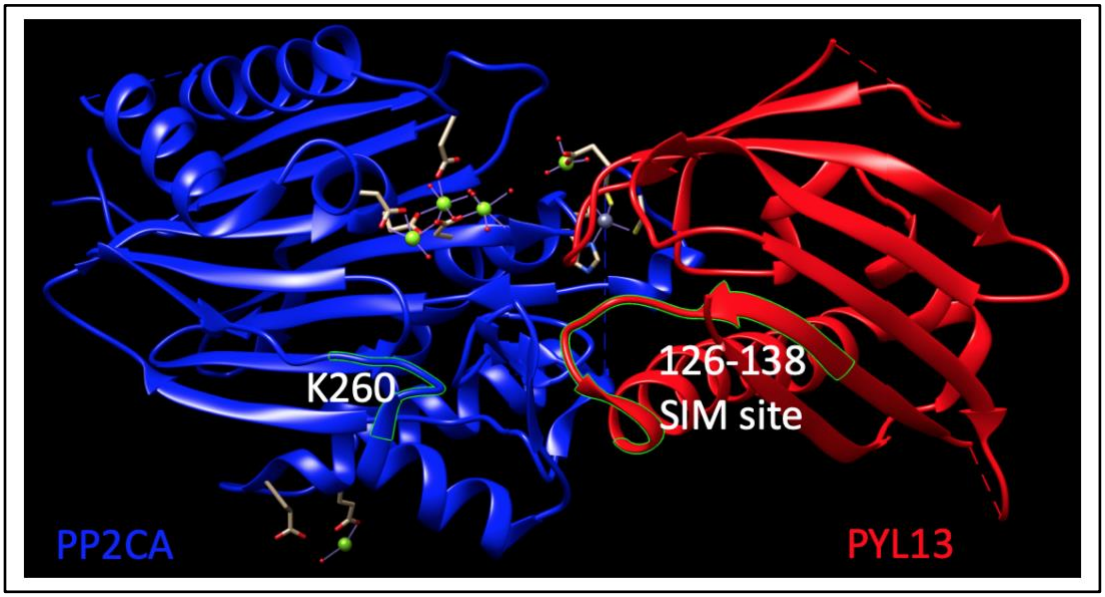

Figure 4.21 3D structure of PP2CA-PYL13 receptor complex depicting the locations of a SUMO site in PP2CA and a SIM site in PYL13. *PP2CA is shown in blue and PYL13 is shown in red, the ball and stick structures shows ligand interactions. The K260 SUMO site in PP2CA and SIM site in PYL13 are highlighted in yellow using the visual software to demonstrate the 3D location of the highlighted amino acids. The figure was generated in Chimera (Petterson et al., 2004) modelling software version 1.14 using co-ordinates from pdb file 4N0G (Li et al., 2013).*

As is the same for SUMO prediction, primary protein sequence analysis by HyperSUMO is useful in identifying potential SIM sites and searching for conservation of SUMO sites in gene families and species, but it does not take account of the 3D structure of the protein. True SIM sites have to be, as with SUMO sites, exposed to the external environment to enable interaction and also have to be located on a beta sheet as the beta sheet inserts in a groove in the SUMO protein between the beta sheet and alpha helix (Song et al., 2004). The predicted SIM site in the PYLs was located on the crystal structure of the PP2CA-PYL13 complex (pdb file: 4NOG; Li et al., 2013) using the protein structure modelling software Chimera *(*Petterson et al., 2004*).* The SIM site is exposed to the external environment and is located on a beta sheet (figure 4.20, 4.21). In fact, the PYL SIM site is located near the PP2CA SUMO site K260 and feasibly may be capable of interacting with SUMO attached at this residue (figure 4.21).

To test if the PYLs have SIM sites full length PYL1, PYL8 and PYL13 (666, 567 and 495 bp respectively) were amplified from Col-0 cDNA, using oligonucleotides (appendix table 4.2). The genes were cloned into the entry vector *pENTR/D-TOPO* (Sigma) (figure 4.22). Constructs were transferred via recombination into the 35S C-terminal 4XMyc-tag Gateway destination vector pGWB17. A colony PCR with a gene specific forward primer and vector specific reverse

primer (figure 4.23) confirmed positive clones. The vectors was then transformed into the *Agrobacterium* strain GV3101 for transient expression.

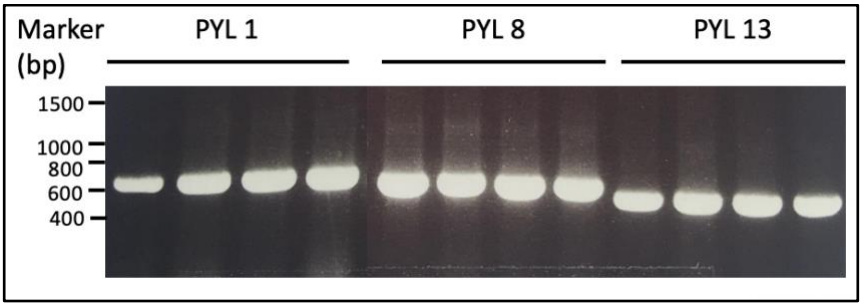

Figure 4.22 Cloning of Arabidopsis PYL1, PYL8 and PYL13 from cDNA. *Image of DNA gel showing cloning of PYL1 (666 bp), PYL8 (567 bp) and PYL13 (495 bp) from cDNA before transfer into pENTR™/D-TOPO™ Cloning Kit reaction. The resulting cDNA fragment of each gene analysed on an agarose gel by electrophoresis size separation. The 1kb DNA marker is labelled.*

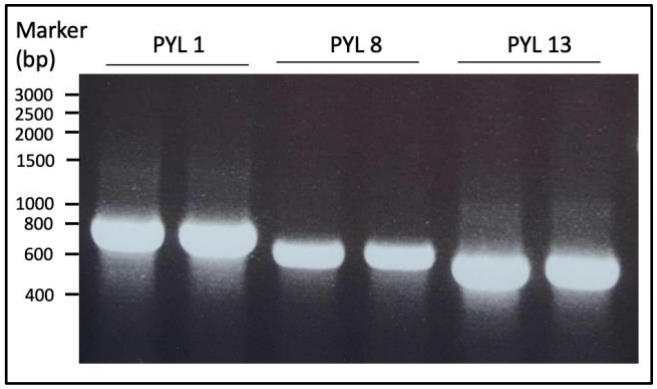

Figure 4.23 Arabidopsis PYL genes transformed into plant expression vector pGWB17. *Image of DNA gel showing the amplification of PYL genes from E.coli colonies that grow on selection media confirming PYL presence in plant expression vectors. For all the PYLs, labelled above, all the colonies that were sampled tested positive for the desired band size. The 1kb DNA marker is labelled.*

A transient assay in *N. benthamiana* using 35S:PYL1-Myc, 35S:PYL4-Myc, 35S:PYL8-Myc and 35S:PYL13-Myc was conducted to test whether the ABA co-receptors contain SIM sites, α-Myc monoclonal antibodies (Clonetech) were used to immunoprecipitate recombinant proteins. The single band observed in the IP sample lane showed that PYL1 has the greatest expression levels, followed by PYL8. PYL13 was weakly expressed, PYL4 was not expressed and was not studied further (figure 4.24). SUMO was only observed interacting with PYL8, suggesting that PYL8 harbours a SIM site that is not present in PYL1. However the SIM IP cannot determine if there is a SIM site in PYL13 or not as the expression of PYL13 was too weak to confirm either way.

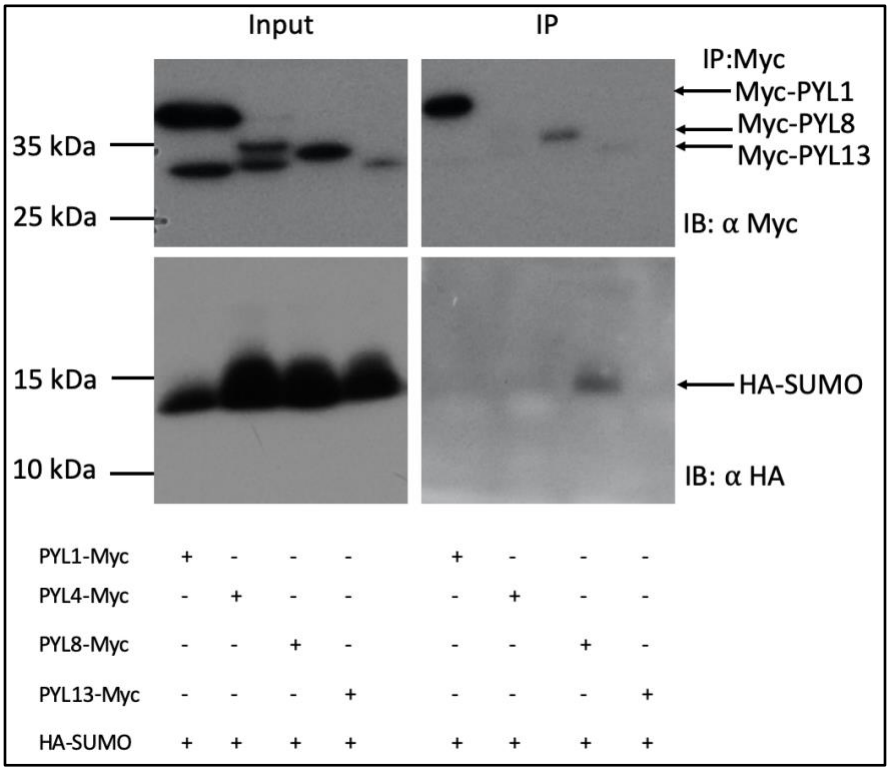

Figure 4.24 PYL8 contains a SIM-site, PYL1 does not bind SUMO. *Transient expression was performed in N. benthamiana leaves co-expressing PYL1-Myc, PYL4-Myc (23 kDa), PYL8-Myc or PYL13-Myc with SUMO1-HA. Total protein (input) was subjected to immunoprecipitation (IP: α-Myc) with α-Myc immunoaffinity beads followed by immunoblot analysis anti-Myc (IB: α-Myc) antibodies to detect PYL1/PYL4/PYL8/PYL13-Myc and anti-HA (IB: α-HA) antibodies to detect SUMO1-HA. Total protein of all samples (input) was probed with anti-Myc antibodies and anti-HA antibodies to determine PYL1/PYL4/PYL8/PYL13and SUMO protein levels. Cross reactivity can be seen in the PYL4 input lane. Arrows indicate PYL1-Myc (26 kDa), PYL8-Myc (22 kDa), PYL13-Myc (19 kDa) and SUMO1-HA (14 kDa). These western blots were repeated thrice, this figure is a representative of outcome of those experiments.*

The analysis of transgenic *Arabidopsis* expressing both $PP2CA^{WT}$ and $PP2CA^{2K/R}$ suggests the presence of SUMO plays a role in sensitivity to ABA. A putative SIM site has been identified in PYL8, which has been hypothesised to aid interaction with SUMOylated proteins. It is hypothesised that SUMOylated PP2CA aids interaction with PYLs harbouring SIM sites, which results in blocking PP2CA dephosphorylation of the Sn2RKs and degradation. The results from PP2CA expression in *Arabidopsis* suggest this may be the case, however to test this PYL transgenics have been generated, both WT PYL8 harbouring a SIM site, $PYL8^{WT}$ and PYL8 with the SIM site removed, $PYL8^{VL/AA}$.

Site directed mutagenesis was used to disrupt the predicted SIM site, by mutating amino acids harbouring hydrophobic side chains in the core of the SIM site to less charged alanine residues using specially designed overlapping mismatch primers as in Verma et al., 2021 (figure 4.25 appendix table 4.2). The mutation PCR used the

template PYL8 pENTR/D-TOPO, mutant clones were identified through sequencing and transferred via recombination into the 35S C-terminal 4XMyc-tag Gateway destination vector pGWB17 and identified via colony PCR (figure 4.25) then transformed into the *Agrobacterium* strain GV3101 for transient expression.

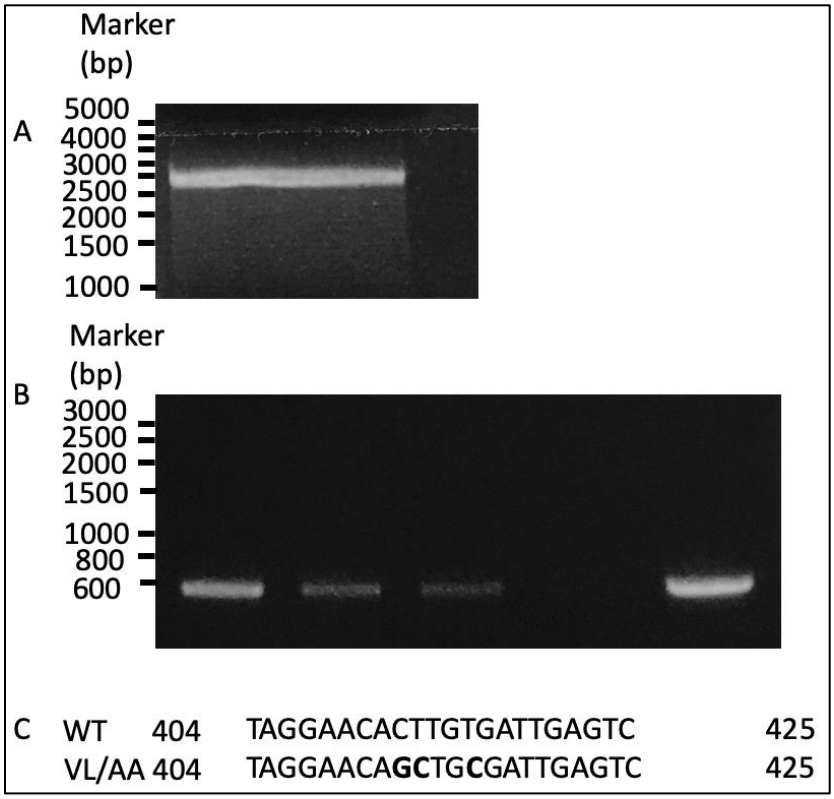

Figure 4.25 Mutation PCR of PYL8 WT and cloning into plant expression vector pGWB17. *Image of DNA gel showing* ***A)*** *amplification of PYL8 in a mutation PCR (3111 bp) and* ***B)*** *confirmation of presence of PYL8 in a plant expression vector (567 bp). All but one colony that was sampled tested positive for the desired band size. The 1kb DNA marker is labelled.* ***C)*** *Alignment of 22 bp region from 404-425 bp around the SIM site present in PYL8 WT (top line). The bottom line (VL/AA) shows the nucleobase changes from WT (shown in bold) resulting in altered amino acids.*

Ideally to ascertain if the mutation impairs SUMO binding to PYL8, a transient assay in *N. benthamiana* using 35S:PYL8^{WT}-Myc and 35S:PYL8$^{VL/AA}$-Myc would be conducted. However unfortunately due to lack of time this was not able to be completed. However a hydrophobicity plot has been charted that maps regions of hydrophobic and hydrophilic amino acids. SIM sites are known to be located on hydrophobic patches on beta sheets (Minty et al., 2000), disrupting the hydrophobic patches by mutating the hydrophobic amino acids to alanine can block SUMO interaction (Verma et al., 2021). To ascertain if the PYL8$^{VL/AA}$ SIM mutation reduced the hydrophobic patch in the predicted SIM site in the protein the amino acids were plotted using the Kyte-Doolittle Scale (figure 4.26). In PYL8^{WT}

the hydrophobicity of the β-7 sheet reached 2, however in the PYL8$^{VM/AA}$ SIM mutation the hydrophobicity reaches 1.5, showing the hydrophobicity has been reduced.

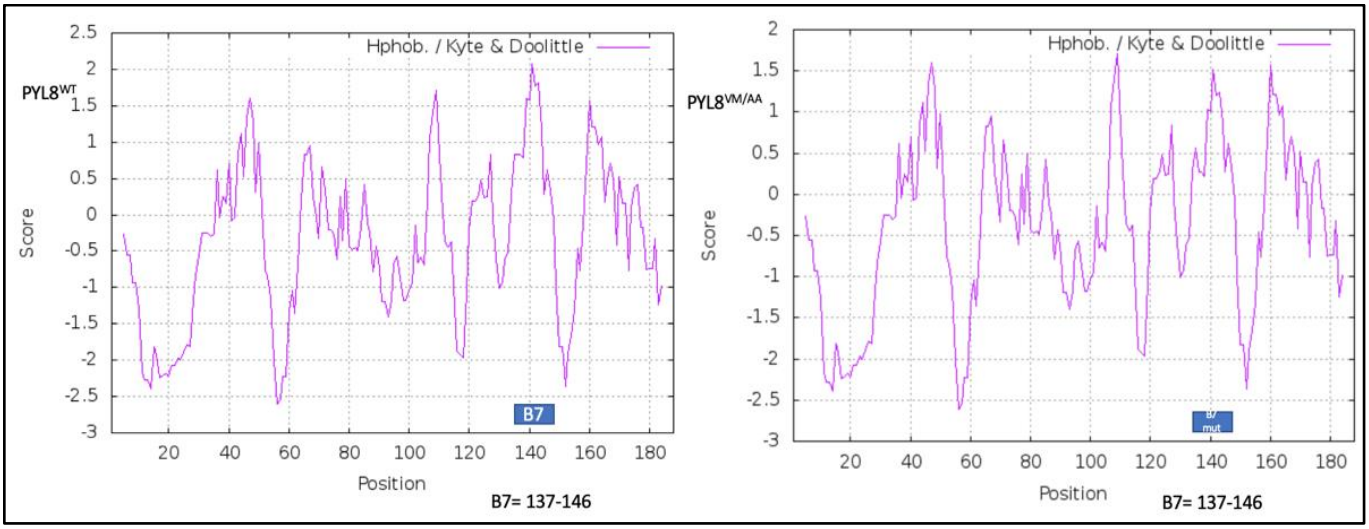

Figure 4.26 Hydrophobicity plot of PYL8^{WT} and PYL8$^{VM/AA}$. *Hydrophobicity plot of PYL8^{WT} (left) and PYL8$^{VM/AA}$ (right) with the location of the β-7 sheet marked on with a blue box.*

In order to determine if the SIM sites present in the PYLs aid interaction with SUMOylated PP2CA and enables downstream signalling of the ABA pathway transgenic *Arabidopsis* was generated to express either PYL8 harbouring a SIM site, PYL8^{WT} and PYL8 with hypothetically the SIM site removed, PYL8$^{VL/AA}$. The constructs that had been previously made for expressing in *N. benthamiana* were used, 35S C-terminal 4XMyc-tag Gateway destination vector pGWB17. These constructs were used to transform *Arabidopsis* plants *pyl4 pyl5 pyl8* herein referred to as *pyl458* via the floral dip method (Clough and Bent 1998). The presence of the transgene was confirmed via PCR (figure 4.27).

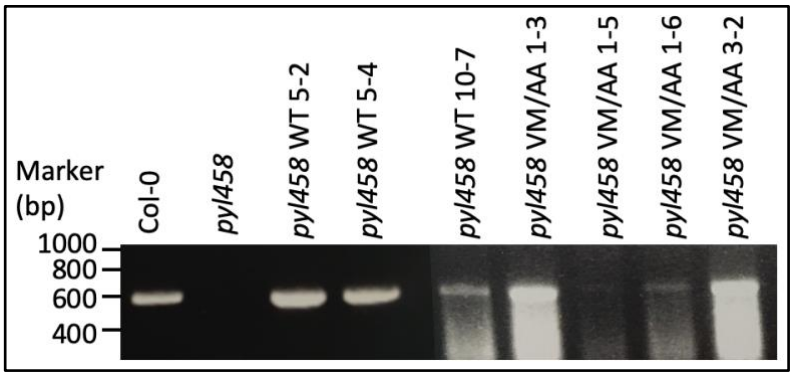

Figure 4.27 Transcript of PYL8 is detected by PCR in the pyl458 background. *Image of DNA gel showing amplification of PYL8 from Arabidopsis cDNA. RNA was extracted from eight transgenic lines expressing PLY8^{WT} and PYL8$^{VM/AA}$, in addition to Col-0 and pyl458 (negative control). The RNA was used to synthesise cDNA. No transcript was detected in the pyl458 as expected whereas Col-0, and the eight different PYL8 transgenics all displayed bands at the expected size for the PYL8 transcript (567 bp). The 1kb DNA marker is labelled.*

In order to ensure the T3 transgenics were selected that had similar transgene expression levels to each other the expression levels of a minimum of 3 independent transgenic lines were analysed by real-time qPCR (figure 4.28). cDNA was synthesised from RNA, extracted from 10 day old seedlings grown on MS agar medium in a growth chamber. A minimum of two transgenic lines per construct, that showed similar levels of transgene expression to the other transgenics were selected for further analysis. This was compared to Col-0, *PYL8* transgene expression in the transgenics overexpressing PYL8 in the *pyl458* background showed similar expression to Col-0. It would have been predicted that due to PYL8 being expressed under a constitutive 35S promoter *PYL8* expression in the transgenics should be higher than Col-0. This RT-qPCR should be repeated as it was only conducted with technical repeats not biological repeats, the expression of *PYL8* should be analysed in *pyl458*.

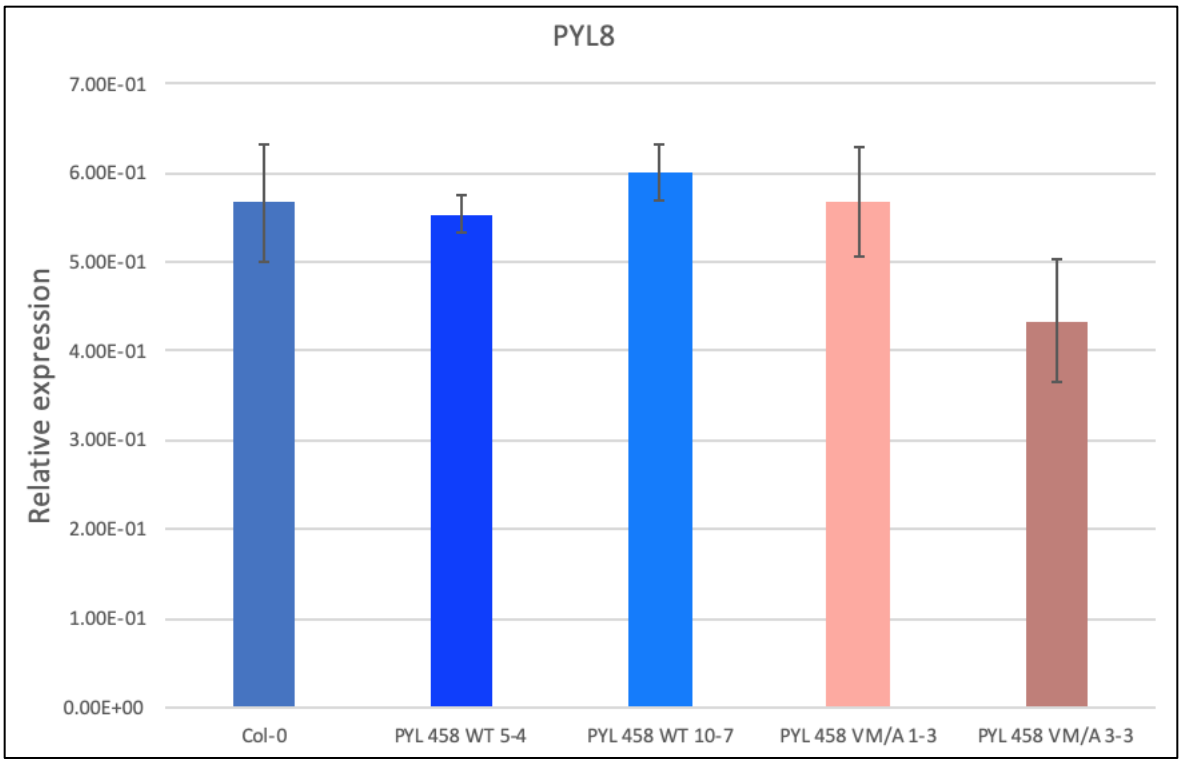

Figure 4.28 Analysis of PYL8 expression levels in different pyl458 transgenic lines*. The expression levels of PYL8 in Col-0 and different transgenic plant lines in the pyl458 background expressing PYL8^{WT} (5-4 and 10-7) and PYL8$^{VM/AA}$ (1-3 and 3-3) analysed by RT-qPCR. Relative PYL8 expression levels in 10 days old seedlings relative to ACTIN2. Error bars represent ±SEM of 3 technical repeats.*

To ascertain the role of the PYL8 SIM site two independent transgenic lines of PYL8^{WT} and PYL8$^{VM/AA}$ in the *pyl458* knockout background that showed similar levels of transcript expression to each other were grown on plates supplemented with ABA. In addition Col-0 and ABA insensitive mutant line *pyl458* were germinated on 1⁄2 MS plates and grown under long day growth conditions for four to five days. Four to five days after germination, the seedlings were then transferred to assay plates containing either 25 µM ABA or no ABA stimulus (control) and grown under long day light conditions for a further six to seven days.

Due to a lack of time and lack of seeds this experiment was only able to be repeated once, this experiment should be repeated again with a higher sample size. It is difficult to draw any initial conclusions from this experiment as both PYL8^{WT} root length % inhibition was similar on ABA to PYL8$^{VM/AA}$ 3-3, conversely PYL8$^{VM/AA}$ 1-3 was very sensitive to ABA, however this may be due to the low number of seedlings tested (Figure 4.29). This experiment should be repeated 2-3 times more to give a true insight of the role of the SIM site in PYL8.

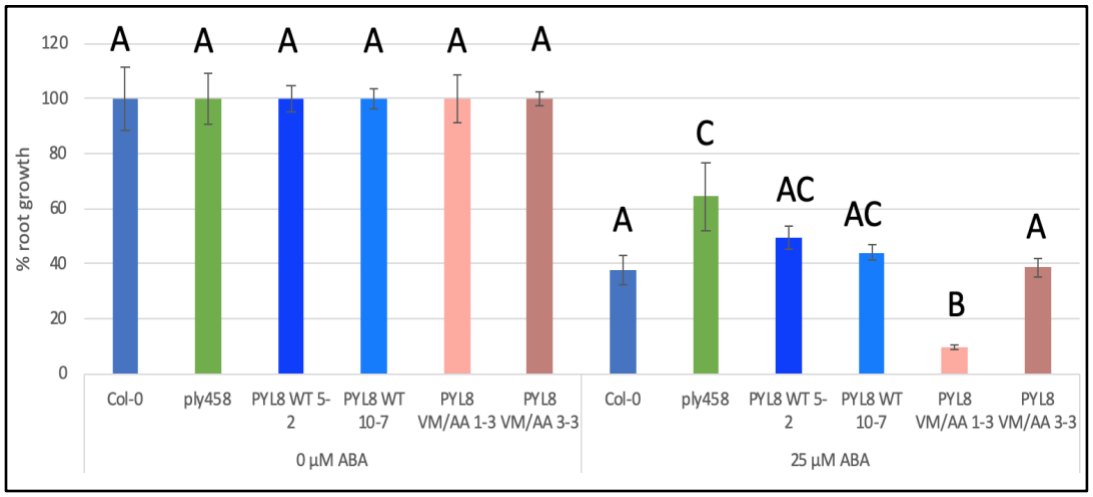

Figure 4.29 Quantification of ABA-mediated root growth inhibition of Col-0, pyl458, pyl458 PYL8^{WT} 5-2, pyl458 PYL8^{WT} 10-7, pyl458 PYL8$^{VM/AA}$ 1-3 and pyl458 PYL8$^{VM/AA}$ 3-3 mutants. *Five-day-old seedlings of the different genotypes were transferred to 1/2MS or 1/2MS with 25 µM (+)-ABA and grown for additional six days before root lengths were measured. Data is relative to growth on 0µM ABA. Data are means ± se (n = 6-18 each). A one-way ANOVA determined a statistical significance between the groups (F(6,64) = 8.54 P < 0.000003). Bars with different letters in each treatment were significantly different from others P>0.05; two-way ANOVA with post hoc Tukey test.*

Unfortunately due to time constraints the PYL8 SIM site analysis has only provided an insight into the potential role of SUMO. Initially a SIM IP should be conducted with PYL8^{WT} and PYL8$^{VM/AA}$ to determine if SUMO interacts with PYL8^{WT} and not PYL8$^{VM/AA}$. Additionally an interaction IP should be conducted to determine if the SIM mutation changes PYL8s interaction with PP2CA^{WT}. Conversely an additional interaction IP should be conducted to determine if PP2CA$^{2K/R}$ interacts less with PYL8^{WT}, compared to PP2CA^{WT}.

Additional analysis also has to be completed on the PYL8 expression transgenics. The protein level of the PYL8s in the transgenics needs to be ascertained and the stability of the proteins determined. Additionally the root length growth assay on ABA has to be repeated, furthermore the pathotest should be conducted with these transgenics, to determine if the phenotype matches the PP2CA transgenic phenotype. Based on the root length assays it would be predicted that as PP2CA^{WT} shows a more ABA sensitive phenotype compared to PP2CA$^{2K/R}$ it would be hypothesised that PYL8^{WT} would show a more ABA sensitive phenotype compared to PYL8$^{VM/AA}$.

4.5 Discussion

Arabidopsis lines expressing, PP2CA^{WT} and PP2CA$^{2K/R}$ under control of the native PP2CA promoter were generated in the single *pp2ca-1* and triple PP2C knockout *p3* background. The transgenic lines that were generated were analysed for transgene transcript expression (*GFP*) and protein abundance was examined by western blot. However the transcript expression of *PP2CA* should have been examined in the transgenics in addition to Col-0 and *pp2ca-1/p3.* Furthermore the western blot determining protein abundance should also be repeated. Once the transgenics had been selected they were used in root growth assays to determine the effects on root growth inhibition when exposed to ABA.

PP2CA^{WT} plants showed greater reduction in root growth when grown on media containing ABA, compared to PP2CA$^{2K/R}$. This trend of increased root inhibition of PP2CA^{WT} on ABA suggests that SUMOylation of PP2CA may aid inactivation of the PP2CA protein, it has been hypothesised that may be due to increased interaction with PYL co-receptors in the presence of ABA, though this is yet to be tested. PP2CA^{WT} transgenics in the *pp2ca-1* knockout background had higher expression of ABA biosynthesis and ABA responsive genes in the absence of ABA, which also suggest the transgenics are more sensitive to ABA, compared to PP2CA$^{2K/R}$. Whilst these experiments suggest that PP2CA SUMOylation may aid inactivation of PP2CA it also worth noting that PP2CA^{WT} expression in *pp2ca-1* and *p3* transgenic backgrounds was not capable of reversing the phenotypes suggesting that potentially the correct transgenic lines to study had not been selected.

Due to SUMO being involved in rapid responses (Miller and Vierstra, 2011) an ABA mediated response that requires a rapid response was tested. When plants detect pathogen PAMPs/MAMPs, prior to infection, plants rapidly close stomata to prevent pathogen invasion into the apoplastic space. We hypothesised, based on the ABA root insensitivity response of PP2CA$^{2K/R}$ grown on ABA, that upon detection of a pathogen PAMP/MAMP PP2CA may be rapidly SUMOylated to aid inactivation of the ABA negative regulator, to enable auto-phosphorylation of the SnRK2s and activation of transcription factors to transcribe genes resulting in an ABA response and closure of the stomata. To test this theory, the two independent lines of PP2CA^{WT} and PP2CA$^{2K/R}$ transgenics were dip-innoculated with *Pst*, to determine if the transgenics had increased or reduced disease resistance due to entry of the pathogen via the stomata. PP2CA$^{2K/R}$ showed greater disease resistance, compared to PP2CA^{WT}, suggesting the SUMOylation of PP2CA increased disease susceptibility, potentially by closing stomata slower. This result undermines the hypothesis that SUMOylation of PP2CA increases ABA sensitivity but needs repeating to be considered robust and to be statistically analysed. In addition to dipping the transgenics in *Pst* the pathogen should also be infiltrated into the leaves in a different experiment. Infiltrating *Pst* determines the role of SUMOylation of PP2CA once in the cells. Once the pathogen has entered the cells and is causing infection ABA signalling increases disease susceptibility, as ABA blocks SA, which provides resistance. If PP2CA^{WT} is more ABA sensitive, than PP2CA$^{2K/R}$ then once the pathogen is in the cell PP2CA$^{2K/R}$ may aid disease resistance. Additionally the SUMOylation status of PP2CA in response to pathogens should

be examined, to determine if SUMOylation increases/decreases in response to *Pst*. Finally an additional experiment that should be conducted is determining the size of the stomatal pores, in the PP2CA^{WT} and PP2CA$^{2K/R}$ transgenics, to determine if the pore size differs, in response to ABA or *Pst*.

Due to the ABA sensitivity of PP2CA^{WT} compared to PP2CA$^{2K/R}$ it was hypothesised that PP2CA SUMOylation may change interactions with the ABA co-receptors, the PYLs. PYL8 was found to have a SIM site (SUMO interacting motifs), whereas PYL1 did not. The other PYLs predicted to contain SIM sites were not tested for SUMO interaction, however this could be conducted in the future. The predicted SIM site was mutated, whilst there was not time to conduct an interaction assay to test whether PYL8^{WT} interacts with SUMO and PYL8$^{VM/AA}$ does not, a hydrophobic plot predicted that PYL8$^{VM/AA}$ hydrophobicity is reduced, compared to PYL8^{WT}. *Arabidopsis* seedlings expressing, SIM site PYL8^{WT} and non SIM site PLY8$^{VM/AA}$ under control of a 35S overexpressing promoter were generated and were used in root growth assays to determine the effects on root growth inhibition when exposed to ABA. Due to a lack of time the experiment was only able to be repeated once with a low number of replicates.

Future work should determine if PP2CA protein stability is affected by SUMO, this could be done by analysing protein stability after exogenous application of ABA over a time course. Furthermore the SUMOylation status of PP2CA^{WT} and PP2CA$^{2K/R}$ should be confirmed in the *Arabidopsis* transgenics. It should also be determined if the levels of SUMOylation in PP2CA increases or decreases in response to ABA.

Whilst there is still much work required to determine the role of SUMO in PP2CA initial analysis has suggested SUMOylated PP2CA may aid ABA sensitivity. An initial experiment has suggested the SUMOylated PP2CA may have a pathogen resistance phenotype, though this needs further work to test this. Lastly a SIM site has been identified in PYL8 and PYL8 transgenics have been generated for further analysing the role of this hypothetical SIM site.

Chapter 5

The role of SUMO in root hair formation.

5.1 Introduction

Root hairs are important subcellular extensions from root epidermal cells that increase the surface area, increasing the ability of plants to absorb nutrients. The density and length of root hairs is dependent on several factors including Pi content (Bates and Lynch, 2000), exposure to the ethylene precursor 1-aminocyclopropane-1-carboxylic acid (ACC) (Dolan, 1996) and auxin. The role of SUMO in root hair growth has already been reported, a SUMO E3 ligase mutant *siz1* produces more and longer root hairs compared to WT (Miura et al., 2005). This is thought to linked to Pi as the *siz1* mutant shows perturbed expression of Pi response genes. The *siz1* mutant shows greater transcript abundance in Pi-sufficient media of *PT2*, *PS2* and *RNS1* that is typically induced upon Pi starvation. Additionally the *siz1* mutant shows reduced expression of *IPS1* and *RNS1* upon Pi starvation, which in WT is increased (Miura et al., 2005). Using *Japonica* subspecies of *O. sativa* mutants *OsSIZ1* showed a similar phenotype to the *Arabidopsis siz1* mutant of an increase in root hair number (Wang et al., 2011).

Auxin plays a critical role in altering root hair length in response to Pi stress (Bhosale et al., 2018). Mutants in the auxin synthesis (*taa1*) and auxin transport (*aux1*) are unable to respond to low phosphate environments and elongate root hair length. Conversely *AUX1* expression in the lateral root cap and epidermal cells rescues the phenotype. Auxin transport to the differentiation zone promotes auxin-dependent hair response to low Pi. Low

external Pi results in induction of root hair expressed auxin-inducible transcription factors ARF19, RSL2 and RSL4 (Bhosale et al., 2018).

SUMO has already been implicated in changing root architecture in response to environmental stimuli and auxin. ARF7 an auxin response factor becomes SUMOylated in dry environments to prevent the formation of lateral roots. SUMOylated ARF7 recruits the auxin repressor protein IAA3 which inhibits lateral root formation. In wet environments ARF7 is not SUMOylated and is capable of binding to DNA and promoting translation of LBD16, required for lateral root formation (Orosa-Puente et al., 2018).

To investigate the role of SUMOylation in root hair growth this growth was studied in a hyper-SUMOylated environment i.e. in the SUMO protease double knock-out mutant line *ots ko*. Due to the evidence demonstrating that SUMO plays a role in root hair formation, this chapter aimed to elucidate further roles of SUMO in root hair formation, in particular to ascertain if *ots1-1 ots2-1* double mutant (herein called *ots ko*) has a root hair phenotype.

As *ots ko* was found to have a root hair phenotype different components of the root hair formation pathway were scanned to determine if they harboured SUMO sites. Transcription factors that control root hair polar growth in the initiation phase RHD6 and transcription factors that start the elongation phase RSL2/RSL4 (Menand et al., 2007; Yi et al 2010) were identified containing conserved SUMO sites. Hormonal and environmental cues converge to regulate the expression of RSL4 which controls the final size of the root hair cell (Yi et al., 2010; Datta et al., 2015; Song et al., 2016; Rymen et al., 2017; Franciosini et al., 2017). Due to the important role RSL4 harboured converging different environmental and hormonal cues we speculated this may be aided by SUMO modification. Work was conducted to determine if RSL4 is SUMOylated and the role of SUMO in regulating the bHLH transcription factor RSL4.

5.2 Characterisation of root hair formation in OTS SUMO protease mutants

To establish if *ots ko* has a root hair phenotype the root hair length and number were measured when grown on standard MS. The *ots ko* double mutant line (used in chapter 3) and loss of function double mutation *rsl2-1 rsl4-1* double mutant line (herein called *rsl ko*) were kindly provided by Dr Beatriz Orosa and Professor Liam Dolan (Oxford University) respectively. The *rsl2-1 rsl4-1* line was obtained by crossing the transfer DNA from GT_5_105706 into Col-0 plants and backcrossing to Col-0 for another four generations for *rsl4-1* and crossed with *rsl2-1* SAIL line 514C04 (Yi et al., 2010). The root hairless mutant, *rsl ko* has two bHLH transcription factors knocked out that regulate root hair development (Yi et al., 2010).

Seven-day-old seedlings from the SUMO protease mutant line, *ots ko,* produced significantly fewer root hairs per mm of root length in comparison to Col-0 (fig 5.1, and 5.2). This phenotype can be attributed to high levels of background SUMOylation. These findings further implicate the role SUMO has in root hair formation, which was observed in the knockout mutants of the SUMO E3 ligase *siz1* (Miura et al., 2005).

In addition to a decrease in root hair number, 7-day-old seedlings from the SUMO protease mutant line *ots ko* produced significantly longer root hairs in comparison to Col-0 (fig 5.1 and 5.3). Longer root hairs can be caused by stabilisation of transcription factors (Yi et al., 2010) or by changes in auxin homeostasis (Dharmasiri et al., 2005).

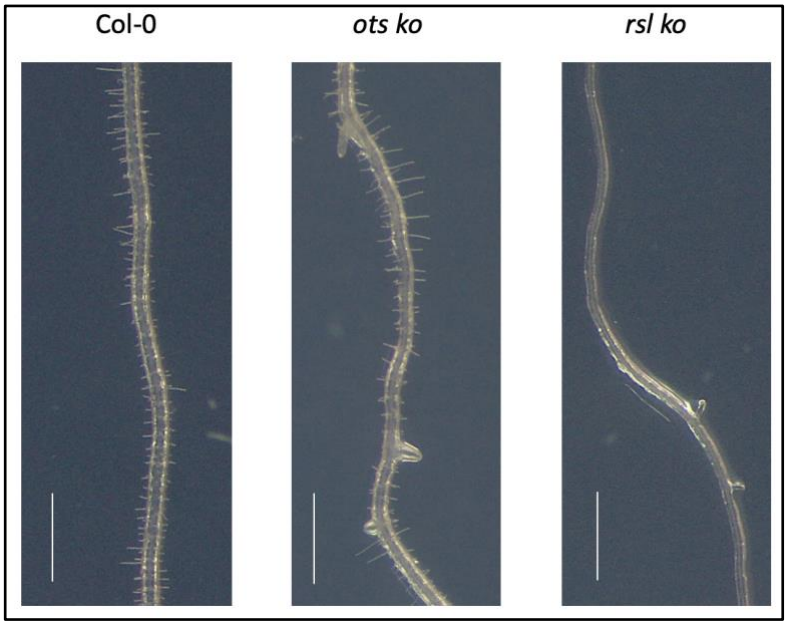

Figure 5.1 The ots ko mutant shows differences in root hair length and density in comparison to Col-0 on 0.1% sucrose. *A representative white light image of roots of 7 days old Col-0, ots ko and rsl ko seedlings showing different length and number of root hairs. Scale 1mm.*

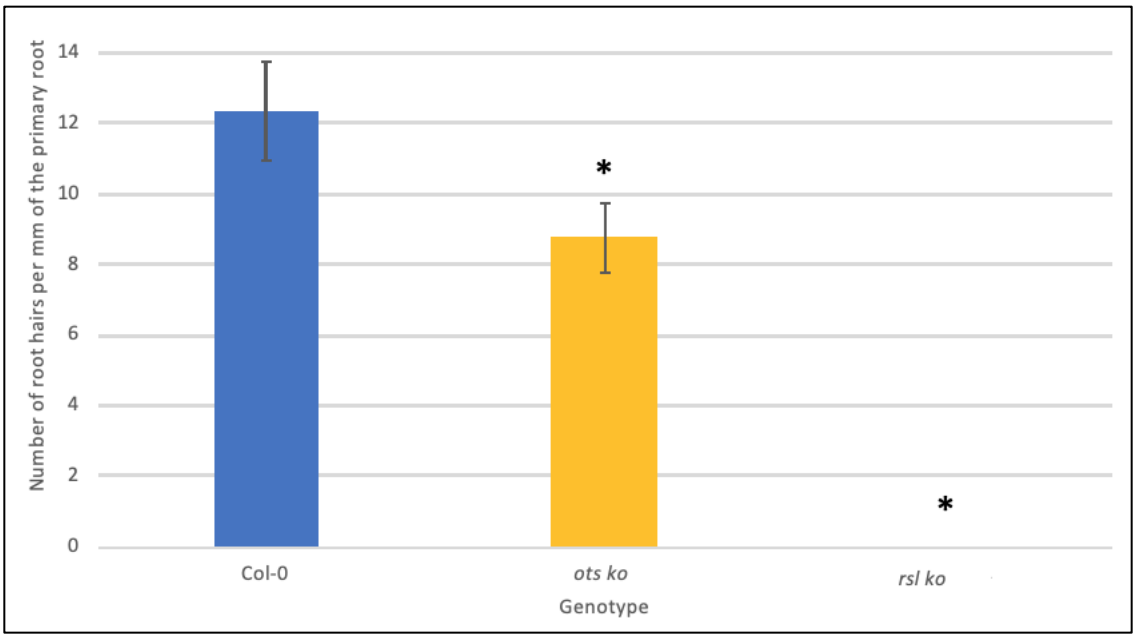

Figure 5.2 Quantification of the number of root hairs in ots ko and Col-0 on 0.1% sucrose. *Seedlings were germinated on 1/2MS and 0.8% phytoagar plates supplemented with 0.1% sucrose. Seedlings were then grown under long day light conditions for 7 days before the number of root hairs were counted. Data are means ± se (n = 20). A one-way ANOVA determined a statistical significance between the groups (F(2,57) = 43.43 P < 0.00001). A Tukey post hoc test revealed that the number of root hairs per mm in ots ko (8.78 ± 0.95 p=0.027), and rsl ko (0 ± 0 p=0.001) was statistically significantly (p<0.05) different compared to Col-0 (12.4 ± 1.4) indicated with an *. Two repeats conducted.*

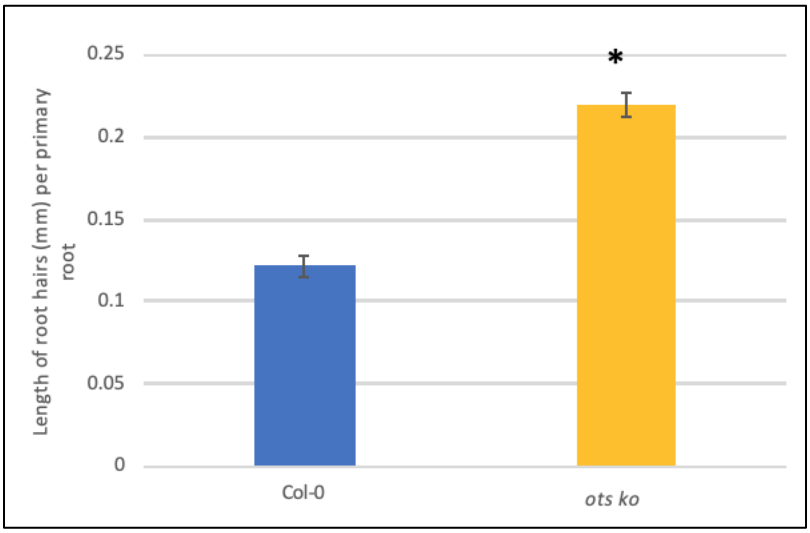

Figure 5.3 Quantification of the length of root hairs in ots ko and Col-0 grown on 0.1% sucrose. *Seedlings were germinated on 1/2MS and 0.8% phytoagar plates supplemented with 0.1% sucrose. Seedlings were then grown under long day light conditions for 7 days before the length of root hairs were counted. Data are means ± se (n = 20 roots). A one tailed T-test determined a statistical significance between Col-0 (122.3 ± 6.86) and ots ko (220.6 ± 7.27) root length hairs (t(99)= -9.84 p=0.00001). * indicates a statistically significant difference (p<0.05). Two repeats conducted.*

As the *ots ko* mutant has a root hair phenotype, a fusion of OTS1-VENUS driven by the native OTS1 promoter, kindly provided by Dr Jason Banda, was examined to determine if OTS1 was expressed in root hair cells. The seeds were grown on 1/2MS agar plates in long day conditions, supplemented with 0.1% sucrose. Five day old seedlings were examined using a fluorescence microscope (Zeiss LSM 880 Airyscan). It has already been reported that OTS1 and OTS2 are only expressed in the nucleus (Conti et al., 2008). As can be seen from figure 5.4 expression of VENUS-tagged OTS1 under its own promoter potentially results in weak expression of OTS1 in the nucleus of root hair cells. However it should be noted that the nucleus was not stained with a nuclear staining dye such as DAPI, for this experiment to be considered robust it should be repeated using a nuclear staining dye.

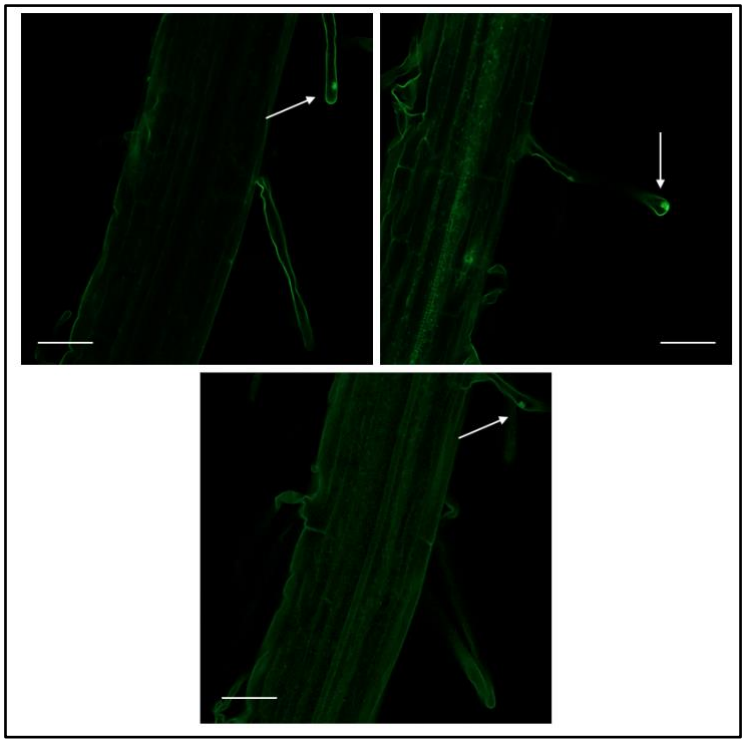

Figure 5.4 VENUS tagged OTS1 protein localises in the nuclei of root hair cells when stably expressed in Arabidopsis under its own promoter. *Localisation of own promoter driven OTS1-VENUS fusion protein stably transformed in 5 day old ots ko background Arabidopsis roots (kindly donated by Dr Banda) was analysed by confocal laser scanning microscopy. The green signal indicates VENUS. Weak expression of OTS1 can be seen in the nuclei of root hair cells (white arrows). Scale bar= 50 µm.*

5.3 RSL4 has SUMO sites

The *ots ko* mutant root hair phenotype of fewer and longer root hairs, and the localisation data of OTS1 in root hair nuclei prompted us to analyse several key proteins in root hair development for potential SUMO binding sites using in-house bioinformatic software, HyperSUMO (Nelis, PhD thesis 2014). The proteins that showed the strongest and most conserved putative SUMO sites were the transcription factors RSL2, RSL4 and RHD6.

Three SUMO sites were identified in RSL4 (K25, K171 and K205), two SUMO sites were identified in RSL2 (K252 and K305) and one SUMO site was identified in RHD6 (K233). One of the SUMO sites in RSL2, RSL4 and RHD6 (K305, K205 and K233 respectively) is conserved amongst the three transcription factors and is located within the bHLH region of the protein (figure 5.5). The bHLH domain of the protein is a structural motif typical in transcription factors, it is composed of an N-terminal basic end, involved in DNA-binding (Murre et al., 1989; Ferre-D'Amare et al., 1994), the C-terminal HLH region functions as a dimerisation domain (Nair and Burley, 2000). In addition to this SUMO site being conserved in RSL2, RSL4 and RHD6, it is also conserved in the RSL4 in other plant species (figure 5.6) (following the method in Orosa et al, (2018), Verma et al, (2021) and Srivastava et al, (2020)). The two other SUMO sites identified in RSL4, K25 and K171 are not conserved in RSL2 and RHD6, however they are conserved in RSL4 proteins found in *C. sativa, B. rapa* and *E. salsugineu*, which indicates an evolutionary conserved functional relationship.

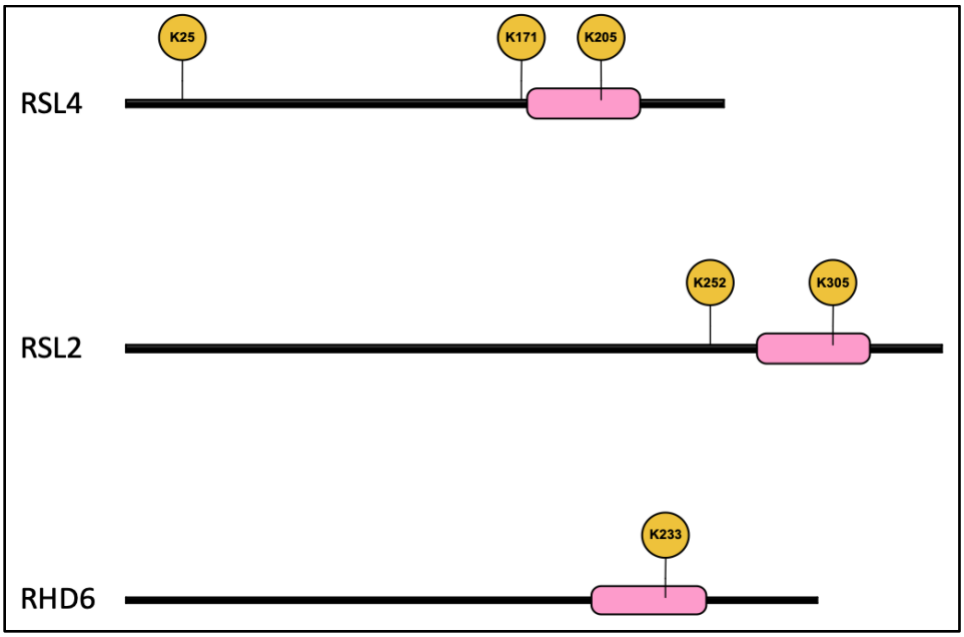

Figure 5.5 Schematic diagram of RSL2, RSL4 and RHD6 protein identifying the predicted SUMO sites (yellow circles) identified using in-house software. *The amino acid sequences, from TAIR, were used as the query sequence for the in-house plant SUMO site prediction software. Two SUMO sites were predicted in RSL2, three SUMO sites were predicted in RSL4 and one SUMO site in RHD6. SUMO sites denoted by yellow circles, containing the lysine residue*

SUMO binds too. One of the predicted SUMO sites, K205 in RSL4 is conserved in RSL2 at K305 and in RHD6 at K233 in the bHLH region (pink cylinders).

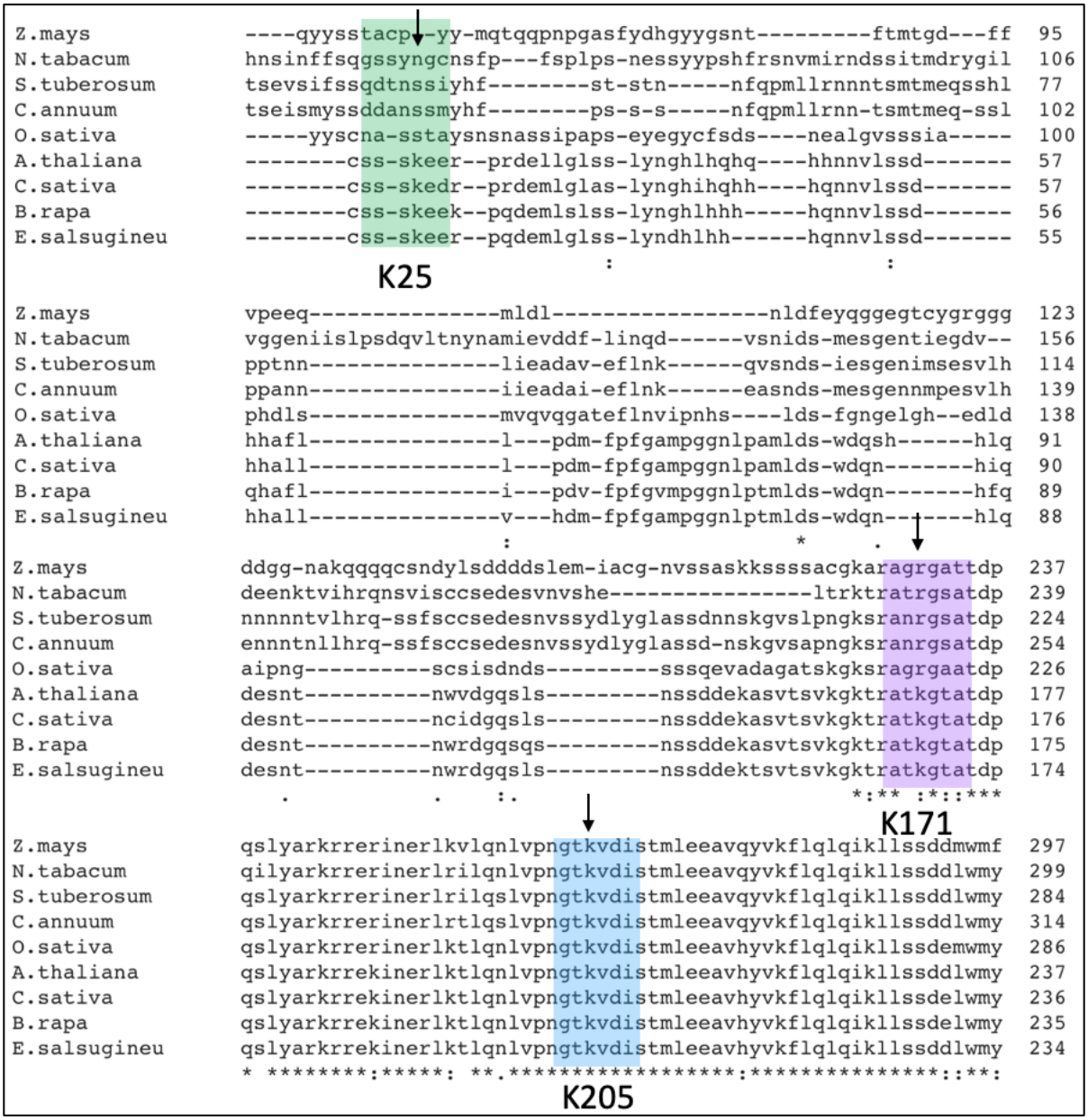

Figure 5.6 Location of the three predicted SUMO sites in RSL4, from different species. *Alignment of RSL4 from different plant species depicting the SUMO sites present in AtRSL4. The amino acid sequences, from Uniprot, of RSL4 from different plant species were aligned using the Clustal Omega website. The K205 SUMO site, highlighted by the blue box, is highly conserved in RSL4 from different plant species. The second and third predicted SUMO sites, K171 and K25, highlighted by the purple and green boxes, respectively, are not conserved amongst all the species that are aligned. The black arrows indicate the SUMOylatable lysine (K).*

For further investigation of the putative SUMO sites in RSL4, the full length *At*RSL4 (777 bp) was amplified (figure 5.7) from Col-0 cDNA, generated from 10 day old Col-0 seedlings, using oligonucleotides (appendix table 5.1) and cloned into the entry clone *pENTR/Dual Selection* (Sigma) using restriction sites enzymes NotI and XhoI. The constructs were transformed into *E. coli* DH5α and the colonies screened for successful clones by PCR (figure 5.8). Sequenced clones were transferred via recombination into the 35S N-terminal GFP-tag Gateway destination vector pEARLYGATE104 and transformed into *Agrobacterium* for plant expression.

Mutation PCRs were then carried out on RSL4^{WT} to generate the triple mutant RSL4$^{3K/R}$ by mutating each lysine in the predicted SUMO sites to an arginine. This was done using specially designed overlapping mismatch primers by amplifying first the RSL4^{WT} pENTR/Dual Selection, to generate first the single mutation RSL4^{K25R}, then this plasmid was used as the template to generate RSL4$^{2K/R}$, this plasmid was then used as the template to generate the triple mutation, RSL4$^{3K/R}$ using the proofreading DNA polymerase Q5 (NEB). The mutated clones were transferred to pEARLYGATE104 and transformed into *Agrobacterium* for plant expression.

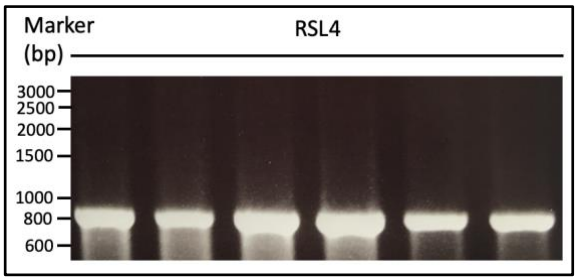

Figure 5.7 Cloning of Arabidopsis RSL4 from cDNA. *Image of DNA gel showing PCR amplification of full length RSL4 (777 bp) from cDNA extracted from Col-0.*

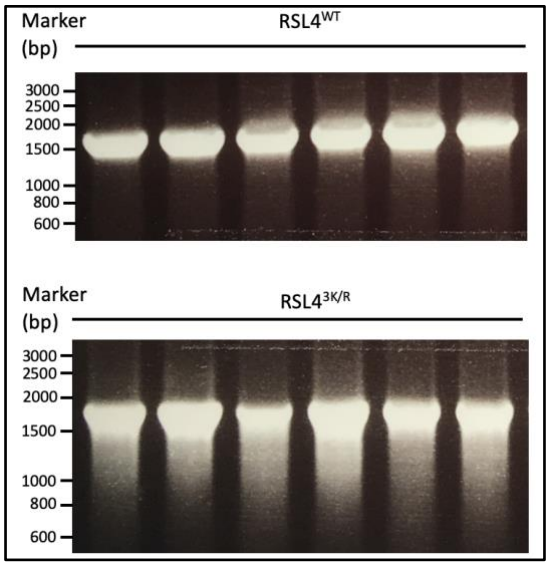

Figure 5.8 RSL4 genes transformed into plant expression vector pEG104. *Image of a DNA gel showing PCR amplification of plasmid DNA, extracted from E. coli, using an internal pEG104 primer and an RSL4 primer to confirm the presence of RSL4 in the pEG104 vector (1680 bp).*

A transient assay in *N. benthamiana* using 35S:GFP:RSL4^{WT} and 35S:GFP:RSL4$^{3K/R}$ co-infiltrated with 35S:SUMO:Ha was conducted to investigate the SUMOylation status of RSL4, along with a GFP control (figure 5.9). RSL4 was expressed with GFP fused to the N-terminus of RSL4 to replicate the construct made in Yi et al., 2010. In both RSL4^{WT} and RSL4$^{3K/R}$ extracts the detected protein was the expected size of RSL4 plus GFP (29kDa + 26kDa) in the IP lane, however they were not detected in the input. This confirms that in *N. benthamiana* both proteins are equally expressed, however some GFP breakdown is observed in the RSL4 IP lanes. The SUMO blot confirms that the SUMO 'smear' seen in RSL4^{WT} is not present in RSL4$^{3K/R}$ and GFP. However two faint bands are present in the RSL4$^{3K/R}$ SUMO blot, which may be due to cross reactivity, for confirmation SUMO cannot bind to RSL4$^{3K/R}$ a SUMO IP should be conducted again, involving more wash steps.

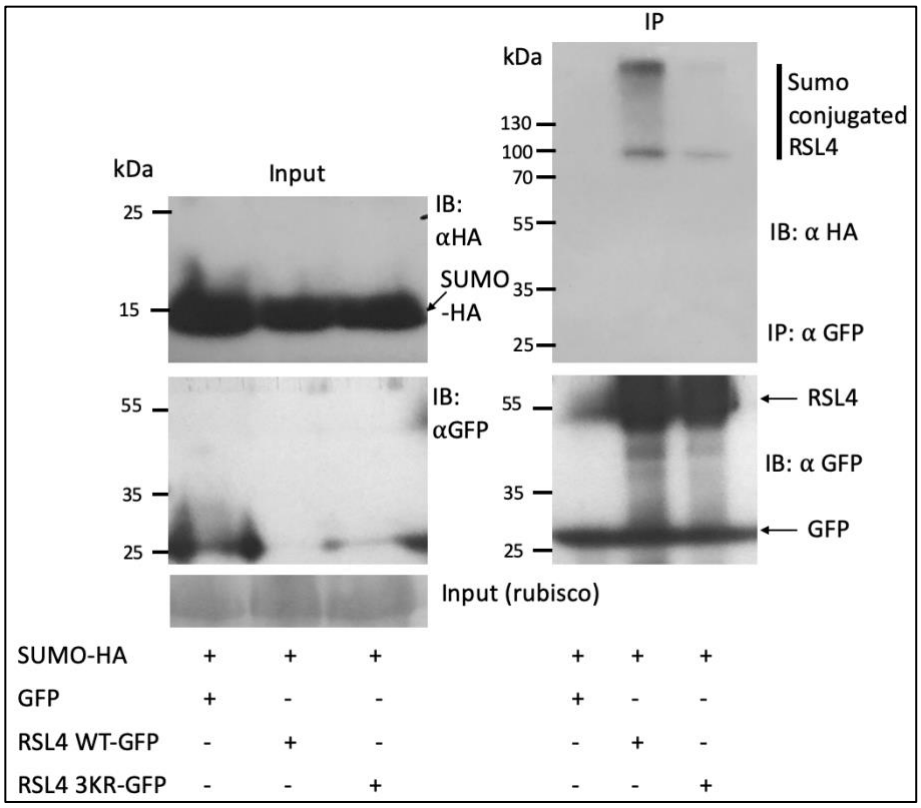

Figure 5.9 Immunoblot analysis shows mutation of the three lysines to arginines in RSL4$^{3K/R}$ reduces SUMOylation. *Transient expression was performed in Nicotiana benthamiana leaves co-expressing RSL4^{WT}-GFP, RSL4$^{3K/R}$-GFP, or GFP with SUMO1-HA. Total protein (input) was subjected to immunoprecipitation (IP: α-GFP) with α-GFP immunoaffinity beads followed by immunoblot analysis anti-GFP (IB: α-GFP) antibodies to detect GFP/RSL4^{WT}/RSL4$^{3K/R}$-GFP and anti-HA (IB: α-HA) antibodies to detect SUMO1-HA. Total protein of all samples (input) was probed with anti-GFP antibodies and anti-HA antibodies to determine GFP/RSL4^{WT}/RSL4$^{3K/R}$ and SUMO1 protein levels. Below the input is the ponceau-s stained rubisco loading control. Arrow indicates SUMO1-HA (14 kDa), RSL4-GFP (54 kDa) and GFP (25kDa). These western blots were repeated thrice, this figure is a representative of outcome of those experiments.*

5.4 Generation of stably transformed lines.

The two DNA constructs mentioned above, RSL4^{WT} and RSL4$^{3K/R}$ that are over-expressed via the 35S promoter in the pEarleyGate104 vector were transformed into *Agrobacterium* and floral dipped into Col-0, to replicate an experiment by Yi et al., 2010, that showed that overexpressing RSL4 in Col-0 plants resulted in longer root hairs due to constitutively expressed RSL4. The transgenics were grown to the T3 homozygous generation containing a single copy insertion of the transgene. The independent transgenic lines were analysed for expression levels of the transgene by real-time qPCR. In order to ensure the T3 transgenics were selected that had similar transgene expression levels to each other the expression levels of a minimum of 3 independent transgenic lines were analysed by real-time qPCR (figure 5.10) A minimum of two transgenic lines per construct that showed similar levels of

transgene expression to the other transgenics were selected for further analysis. Figure 5.10 shows expression of *GFP* relative to *ACTIN2* in different transgenic lines of RSL4^{WT} and RSL4$^{3K/R}$ in the Col-0 background. The primers used are in appendix table 5.2. Whilst this experiment was conducted to identify transgenics with similar expression levels these RT-qPCRs should be repeated as it was only conducted with technical repeats not biological repeats, additionally the expression of the *RSL4* transcript should be analysed in Col-0, in addition to *rsl ko* and the respective transgenics as the current experiment only account for transgene expressed *RSL4* not *RSL4* expression in Col-0.

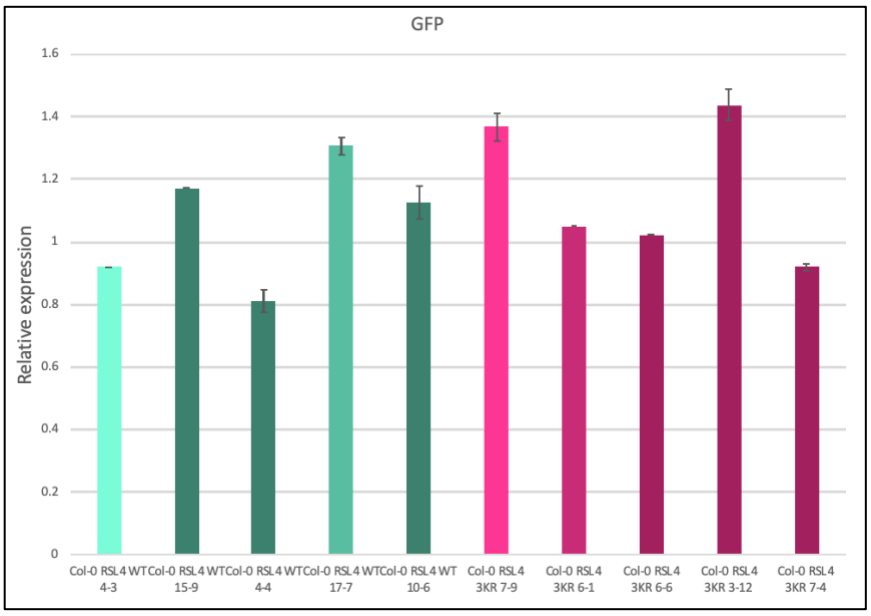

Figure 5.10 Analysis of GFP expression levels in Col-0 transgenic lines*. Expression levels of different transgenic plant lines in the Col-0 background expressing RSL4^{WT} and RSL4$^{3K/R}$ analysed by RT-qPCR. Relative GFP expression levels in 10 days old seedlings relative to ACTIN2. Error bars represent SD of expression.*

To analyse the abundance of the protein produced by the transgenic seedlings, western blot analyses were performed to analyse RSL4 protein levels. Protein was extracted from seedlings from the two independent transgenic lines of RSL4^{WT} and RSL4$^{3K/R}$ in the Col-0 background, that had been selected due to equal transgene expression. Figure 5.11 shows the lines selected are expressing RSL4 protein with a GFP tag. The RSL4 protein cannot be detected in the total protein, only cross reactivity was detected, it can only be detected after immunoprecipitation with αGFP beads. In both RSL4^{WT} and RSL4$^{3K/R}$ extracts, protein of the expected size of the RSL4 protein plus GFP was detected which is 55kDa. However there is a smaller abundance of RSL4$^{3K/R}$ lines compared to RSL4^{WT}. Potentially it may be suggested that RSL4$^{3K/R}$ is less stable than RSL4^{WT}, suggesting that at least one of the SUMO sites in RSL4 may protect the protein from degradation. However this could not be conclusively proved until the seedlings are treated with CHX (a protein synthesis inhibitor) or MG132 (a proteasome inhibitor) to determine

if these chemicals promote the degradation of or stabilise RSL4$^{3K/R}$ respectively. As expected no bands were seen in the Col-0 lane.

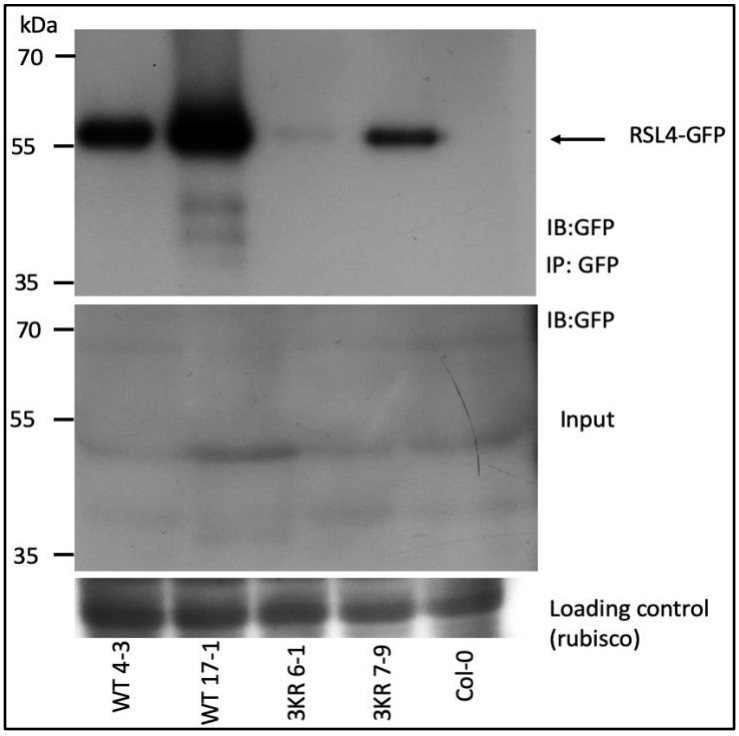

Figure 5.11 Immunoblot analysis shows that RSL4^{WT} protein is more abundant compared to RSL4$^{3K/R}$. *The protein levels of RSL4^{WT}-GFP (4-3 and 17-1) and RSL4$^{3K/R}$-GFP (6-1 and 7-9) in different transgenic lines (Col-0 backgrounds) were analysed by extracting total protein from each different line of transgenic Arabidopsis. Protein was also extracted from Col-0 as a negative control. Total protein (input) was immunoprecipitated (IP: α-GFP) with α-GFP immunoaffinity beads followed by immunoblot analysis with anti-GFP (IB: α-GFP) antibodies to detect RSL4-GFP. Total protein of all samples (input) was probed with anti-GFP antibodies to determine RSL4 protein levels, which was not detected however there was cross reactivity with non-specific proteins. Arrow indicates RSL4-GFP (54 kDa). Below each blot is the ponceau-s stained rubisco loading control.*

5.5 Analysis of transgenics

Initially the two independent transgenic lines each of RSL4^{WT} and RSL4$^{3K/R}$ in the Col-0 background seedlings were grown on a number of different 1/2 MS plates supplemented with either 0.1% sucrose, 10 nm IAA, high (312 µM) and low (3 µM) phosphate. These different treatments were selected as IAA and low phosphate have been reported to increase root hair growth (Zhang et al., 2016), conversely high phosphate has been reported to reduce root hair growth (Bhosale et al., 2018), due to surplus nutrient availability. To determine if SUMO controls root hair development via SUMOylating the RSL4 protein the root hair length and number of root hairs per mm was examined

between RSL4^{WT} and RSL4$^{3K/R}$ grown on these different mediums. However, the root hairs that formed on these different mediums were very stunted compared to Col-0 and did not form uniformly down the roots, making measuring the root hairs difficult (figure 5.12, 5.13, 5.14, 5.15, 5.16). Due to time constraints these different mediums were not measured or statistically analysed.

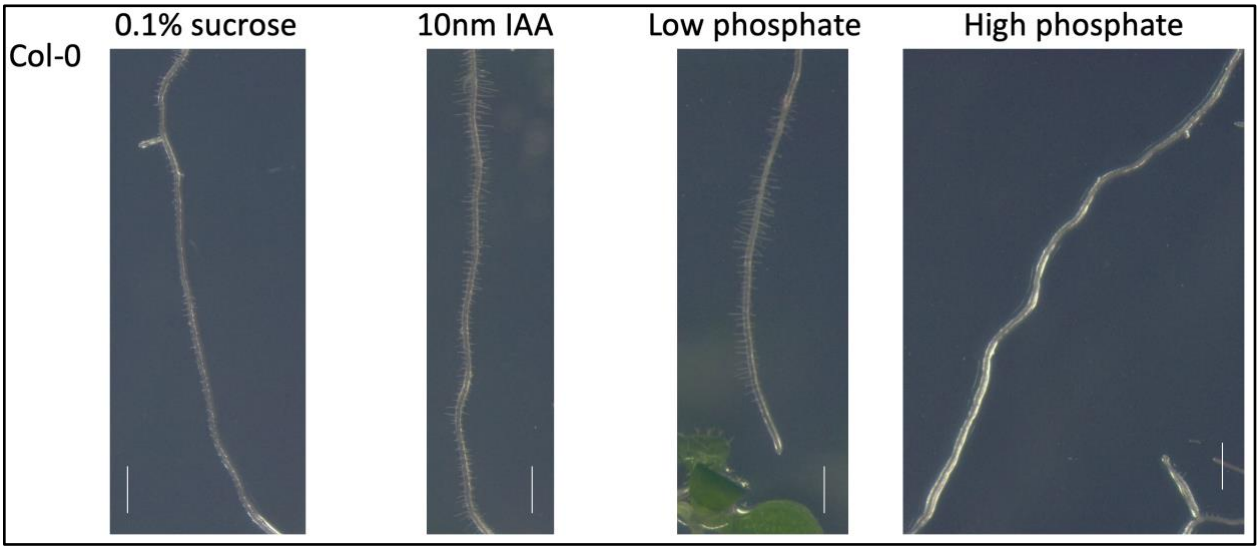

Figure 5.12 Col-0 shows the expected root hair phenotype when grown on 0.1% sucrose, 10nm IAA, low phosphate and high phosphate. *A representative white light image of 10 day old Col-0 seedling root grown on 0.1% sucrose, 10nm IAA, low phosphate and high phosphate. The seedlings were germinated of 1/2MS and 0.8% phyto agar plates for 3 days before being transferred to given plates. Scale 1mm.*

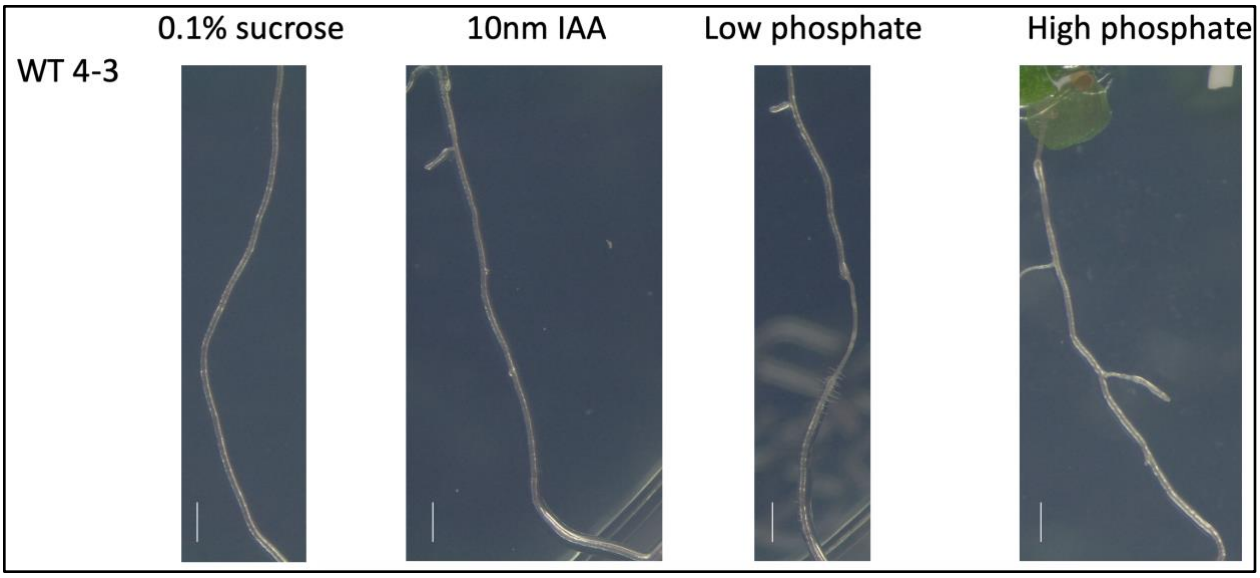

Figure 5.13 Root hair phenotype of Col-0 RSL4^{WT} 4-3 when grown on 0.1% sucrose, 10nm IAA, low phosphate and high phosphate. *A representative white light image of 10 day old Col-0 RSL4^{WT} 4-3 seedling root grown on 0.1% sucrose, 10nm IAA, low phosphate and high phosphate. The seedlings were germinated of 1/2MS and 0.8% phyto agar plates for 3 days before being transferred to given plates. Scale 1mm.*

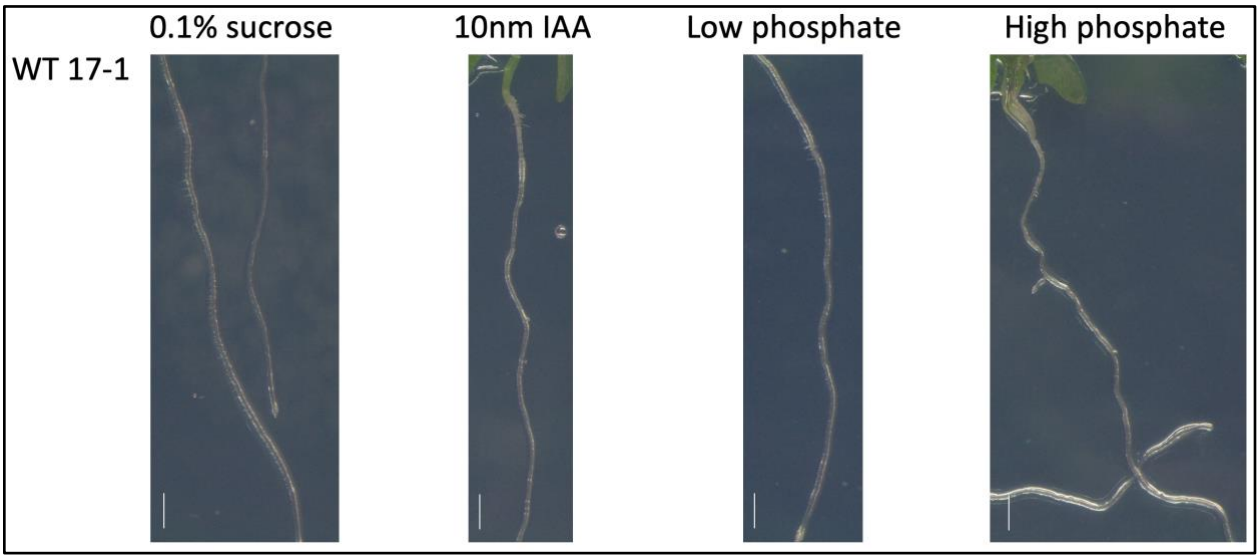

Figure 5.14 Root hair phenotype of Col-0 RSL4^{WT} 17-1 when grown on 0.1% sucrose, 10nm IAA, low phosphate and high phosphate. *A representative white light image of 10 day old Col-0 RSL4^{WT} 17-1 seedling root grown on 0.1% sucrose, 10nm IAA, low phosphate and high phosphate. The seedlings were germinated of 1/2MS and 0.8% phyto agar plates for 3 days before being transferred to given plates. Scale 1mm.*

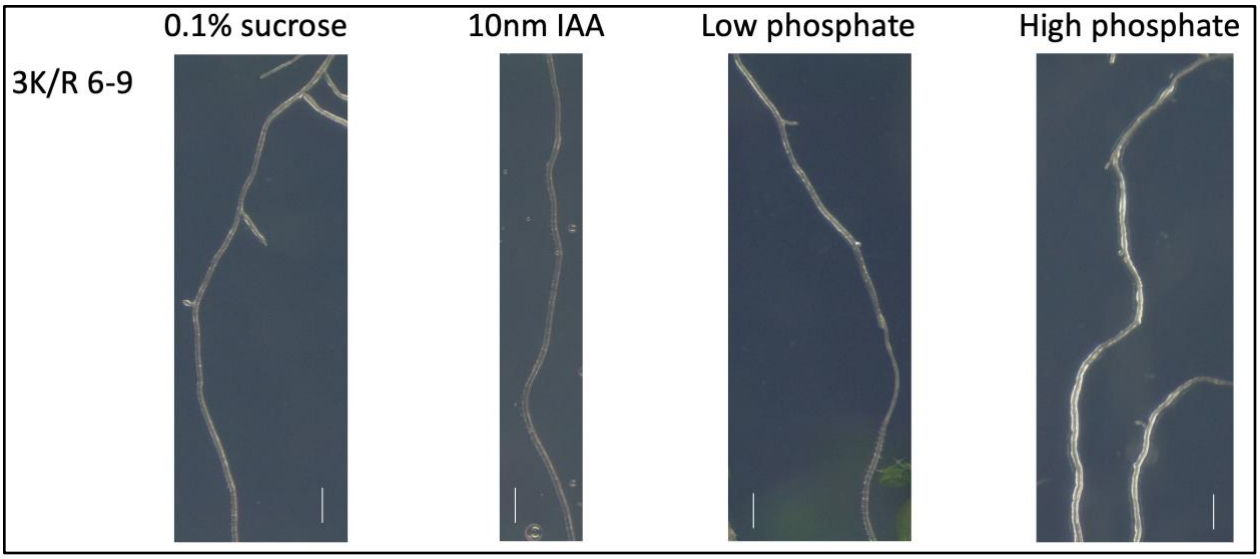

Figure 5.15 Root hair phenotype of Col-0 RSL4$^{3K/R}$ 6-9 when grown on 0.1% sucrose, 10nm IAA, low phosphate and high phosphate. *A representative white light image of 10 day old Col-0 RSL4^{WT} 6-9 seedling root grown on 0.1% sucrose, 10nm IAA, low phosphate and high phosphate. The seedlings were germinated of 1/2MS and 0.8% phyto agar plates for 3 days before being transferred to given plates. Scale 1mm.*

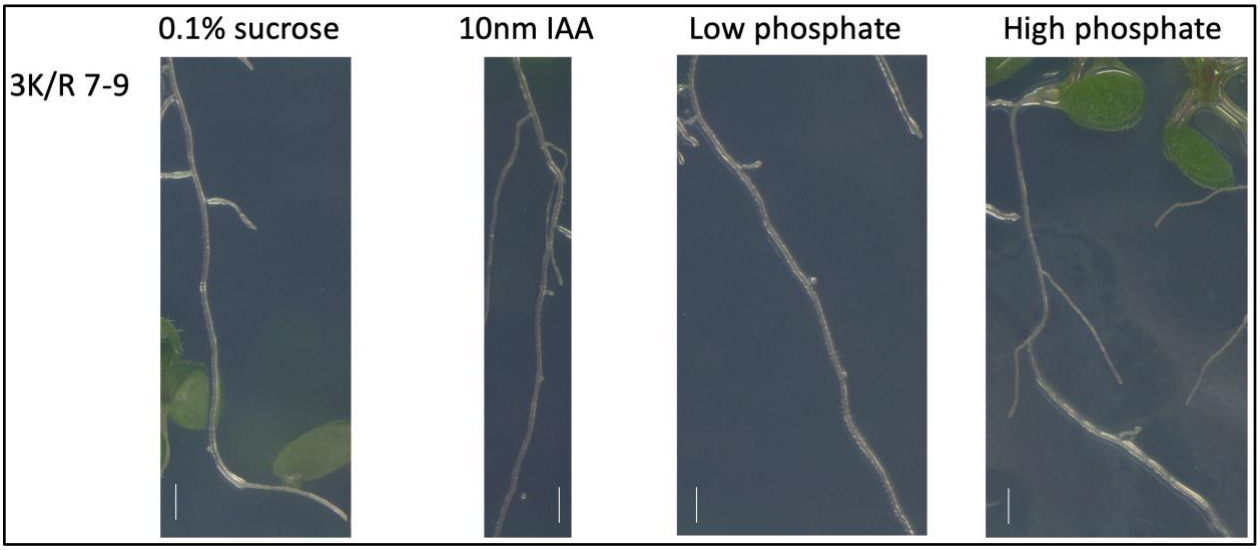

Figure 5.16 Root hair phenotype of Col-0 RSL4$^{3K/R}$ 7-9 when grown on 0.1% sucrose, 10nm IAA, low phosphate and high phosphate. *A representative white light image of 10 day old Col-0 RSL4^{WT} 7-9 seedling root grown on 0.1% sucrose, 10nm IAA, low phosphate and high phosphate. The seedlings were germinated of 1/2MS and 0.8% phyto agar plates for 3 days before being transferred to given plates. Scale 1mm.*

This was unexpected as the T2 generation, consisting of homozygous and heterozygous transgenics had root hair length and number comparable to Col-0 (figure 5.17). It was also unexpected as these transgenics were in the Col-0 background, which had normal root hair formation, suggesting overexpression of RSL4 was suppressing the growth of the root hairs. Additionally this data conflicts with Yi et al., 2010 which demonstrated that overexpressing RSL4, driven by the 35S promoter resulted in longer root hairs, than Col-0. Potentially this could be the result of an unknown negative feedback loop.

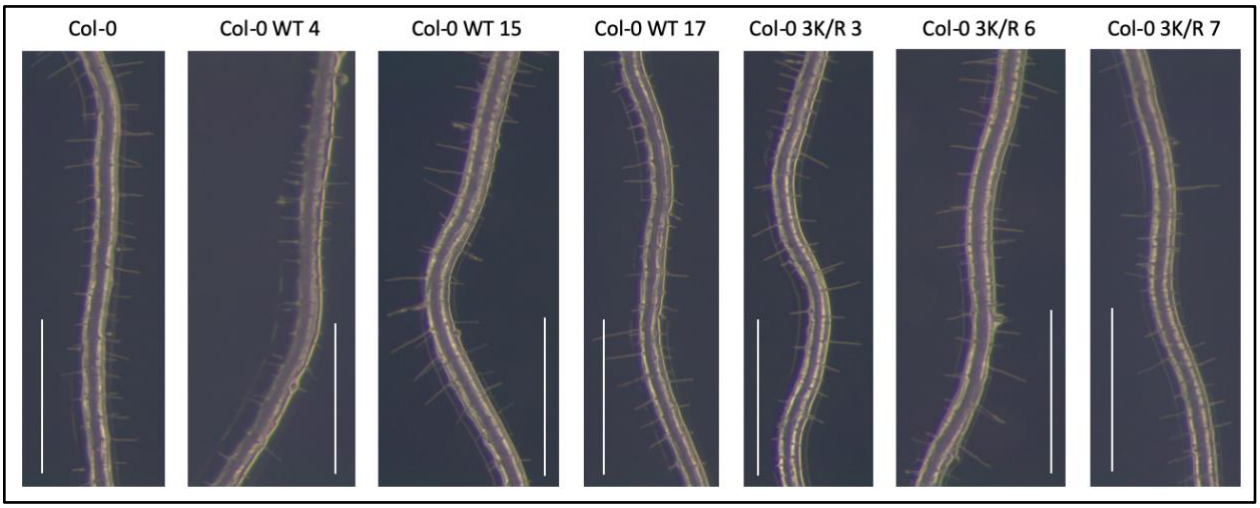

Figure 5.17 T2 Col-0 RLS4^{WT} and Col-0 RSL4$^{3K/R}$ root hair development is similar to Col-0. *A representative white light image of the roots of Col-0, 3 independent T2 transgenics lines of RSL4^{WT} and 3 independent T2 transgenics lines of RSL4$^{3K/R}$. Scale bar = 1 mm.*

Despite the stunted root hair formation, described above, the transgenic root hairs formed uniformly in seedlings grown for 10 days on 100nm ACC. The root hairs in the transgenics were much smaller, compared to Col-0 (figure 5.18 and 5.19), however they were long enough to measure and analyse. So Col-0, two independent transgenic lines of Col-0 overexpressing RSL4^{WT} (4-3 and 17-1) and two independent transgenic lines of Col-0 overexpressing RSL4$^{3K/R}$ (7-9 and 6-9) were grown on 1/2 MS media supplemented with 100nm ACC to determine if there was a phenotypic different between the RSL4^{WT} and RSL4$^{3K/R}$ (figure 5.18, 5.19 and 5.20).

RSL4$^{3K/R}$ showed longer and more root hairs on 100nm ACC, compared to RSL4^{WT} (figure 5.18 and 5.19). This was surprising, as the protein abundance data (figure 5.11) indicated that RSL4$^{3K/R}$ may be less stable than RSL4^{WT}, and was less abundant, which should result in shorter root hairs (Yi et al., 2010). It was speculated that one of the other SUMO sites in RSL4^{WT} may block the activity of RSL4, for example it may block RSL4 binding to the DNA. One of the SUMO sites in RSL4 (that was conserved in RSL2 and RHD6) was located in the bHLH domain of RSL4. Potentially SUMO binding at this region may block RSL4 binding to DNA, blocking RSL4 controlled expression of genes that

encode proteins affecting cell growth. Additionally SUMO may also block RSL4 interaction with proteins required in a protein complex for transcription.

There was not such a clear phenotypic difference in the number of root hairs formed between $RSL4^{WT}$ and $RSL4^{3K/R}$ (figure 5.20). Whilst $RSL4^{WT}$ 4-3 has significantly fewer root hairs, $RSL4^{3K/R}$ 6-1, $RSL4^{WT}$ 17-1 and $RSL4^{3K/R}$ 7-9 did not have a significantly different number of root hairs, compared to any of the other genotypes, suggesting that SUMO modified RSL4 may not play a role in determining the number of root hairs.

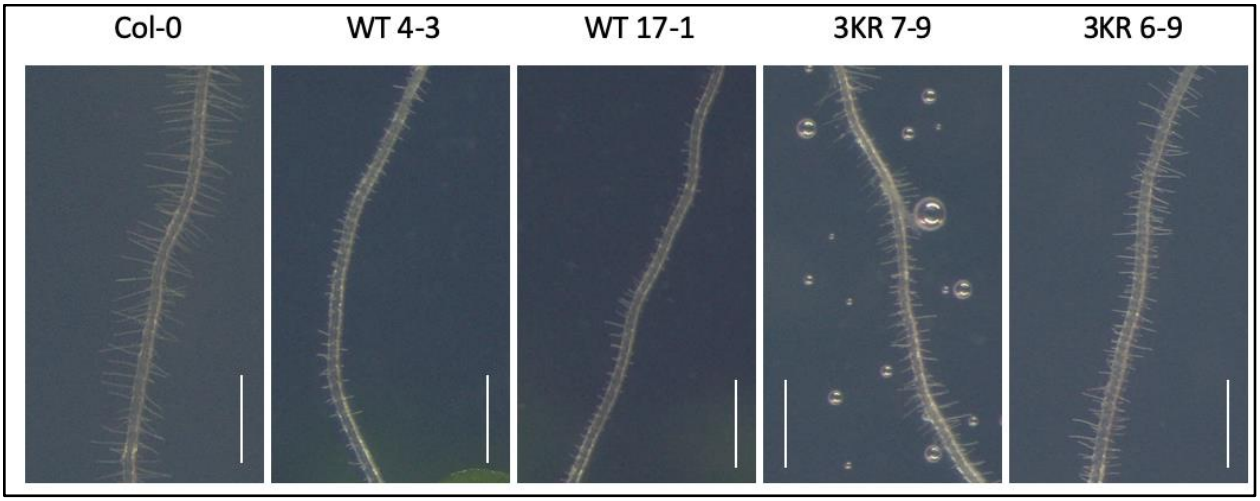

Figure 5.18 The Col-0 transgenics overexpressing $RSL4^{3K/R}$ have longer root hairs compared to $RSL4^{WT}$ when grown on 100nm ACC. *A representative white light image of the roots of 10-day-old Col-0, 2 independent transgenic lines overexpressing $RSL4^{WT}$ (4-3 and 17-1) in the Col-0 background and 2 independent transgenic lines overexpressing $RSL4^{3K/R}$ (7-9 and 6-9) in the Col-0 background. The seedlings were germinated of 1/2MS and 0.8% phyto agar plates supplemented with 100nm ACC. The seedlings were grown for 10 days before the number and length of root hairs were counted. Scale 1mm.*

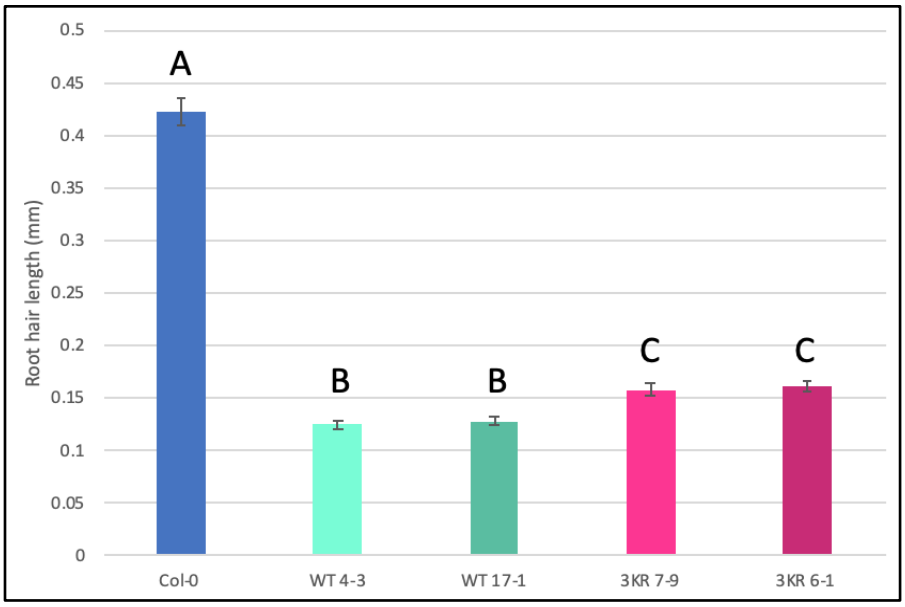

Figure 5.19 Quantification of Col-0 RSL4$^{3K/R}$ root hair length in comparison to Col-0 RLS4^{WT} on 100 nm ACC. *Analysis of average root hair length of 10-day old Col-0, 2 independent transgenic lines of Col-0 RSL4^{WT} (4-3 and 17-1) and 2 independent transgenic lines of Col-0 RSL4$^{3K/R}$ (7-9 and 6-1) in the Col-0 background. Seedlings were germinated on 1/2 MS and 0.8% phyto agar plates supplemented with 100nm ACC and grown for 10 days before the length of the root hairs were measured. Data are means ± sem (n = 120-399 each). A one-way ANOVA determined a statistical significance between the groups (F(5,1507) = 532 P < 0.00001). A Tukey post hoc test revealed that the only root hair length that was not statistically significant was between WT 4-3 (0.125 ± 0.0038) and WT 17-1 (0.128 ± 0.0045) and between 3KR 7-9 (0.158 ± 0.0058) and 3KR 6-1 (0.161 ± 0.0055). Bars with different letters were significantly different from others; p<0.01; one-way ANOVA with post hoc Tukey test.*

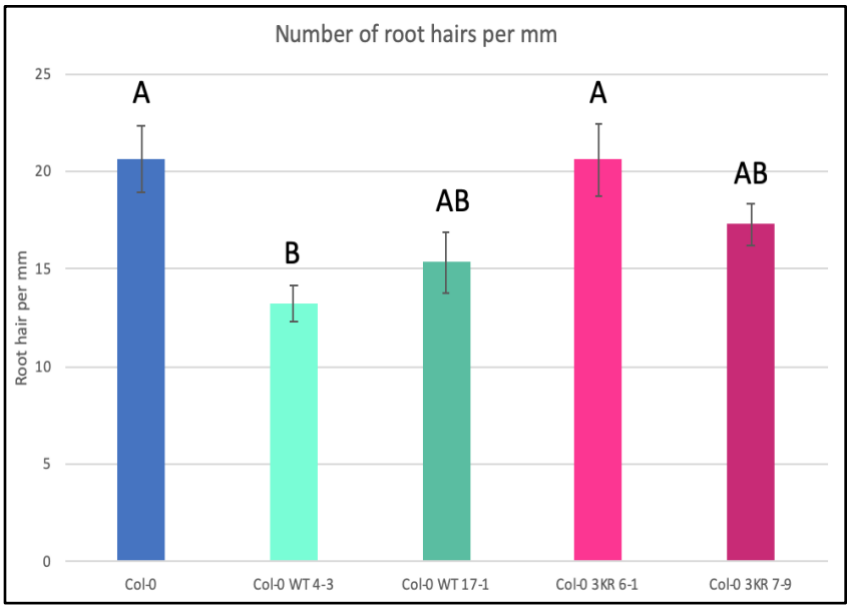

Figure 5.20 Quantification of number of root hairs per mm in Col-0, Col-0 RLS4^{WT} and RSL4$^{3K/R}$ on 100nm ACC. *Analysis of average number of root hairs per mm of 10-day old Col-0, 2 independent transgenic lines of Col-0 RSL4^{WT} (4-3 and 17-1) and 2 independent transgenic lines of Col-0 RSL4$^{3K/R}$ (6-1 and 7-9). Seedlings were germinated on 1/2 MS and 0.8% phyto agar plates supplemented with 100nm ACC and grown for 10 days before the length of the root hairs were measured. Data are means ± sem (n = 5-21 each). A one-way ANOVA determined a statistical significance between the groups (F(4,61) = 5.616 P < 0.0006). A Tukey post hoc test revealed only Col-0 RSL4^{WT} 4-3 had significantly fewer root hairs per mm, compared to Col-0 and Col-0 RSL4^{WT} 6-1, all other genotypes revealed no significant difference. Bars with different letters were significantly different from others; p<0.01; one-way ANOVA with post hoc Tukey test.*

As RSL4^{WT} had shorter root hairs, compared to RSL4$^{3K/R}$, we speculated that SUMO binding to the SUMO site located in the bHLH region of the protein may block RSL4 binding to DNA, preventing RSL4 from promoting transcription. The transcript levels of RSL4 regulated genes (Yi et al., 2010) was determined using qRT-PCR using primers in appendix table 5.3. Plants were grown for 10 days on 1/2 MS media supplemented with 100 nm ACC, samples were taken and frozen for processing. The qRT-PCR was conducted on seedlings grown in 100 nm ACC as this is when root hair formation was observed. The qRT-PCR was normalised using primers for the *ACTIN*2 housekeeping transcript. Several RSL4 targeted downstream genes were chosen, based on reduced transcript levels in *rsl4-1* mutants and increased transcript levels in overexpressed 35S RSL4 plants (Yi et al., 2010).

The transcript levels of *CAN OF WORMS1* (*COW1), EXPANSIN A7 (EXPA7), MORPHOGENISIS OF ROOT HAIR 3 (MRH3)* and *MORPHOGENISIS OF ROOT HAIR 6 (MRH6)* (identified in Yi et al., 2010 as being regulated by RSL4) were significantly up-regulated (relative to housekeeping gene-*ACTIN2*) in RSL4^{WT} compared to RSL4$^{3K/R}$ (figure 5.21). This does not fit the observed root hair length phenotype, a greater expression of genes that promote cell growth should result in longer root hairs. However, the qPCR data suggests that SUMO may aid RSL4 promotion of genes that promote cell growth. To be considered robust this RT-qPCR should be conducted with biological repeats.

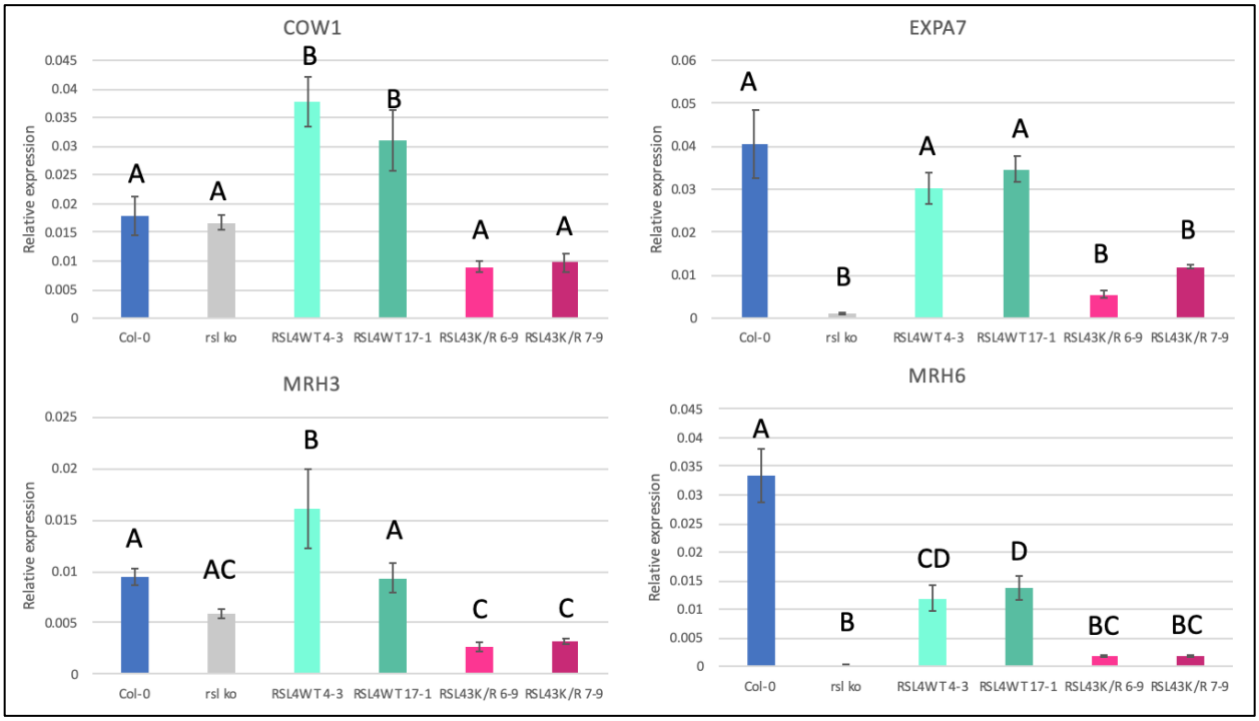

Figure 5.21 Genes required for root hair growth are upregulated in Col-0 RSL4^{WT}, compared to Col-0 RSL4$^{3K/R}$ in presence of 100 nm ACC. *Expression analysis of RSL4 regulated genes in Col-0, rsl ko, RSL4^{WT} 4-3, RSL4^{WT} 17-1, RSL4$^{3K/R}$ 6-9 and RSL4$^{3K/R}$ 7-9 when grown for days on 100 nm ACC. Seedlings were germinated and grown for 10 days on 1/2MS plates, 0.8% phyto agar plates supplemented with 100nm ACC. Total RNA was extracted, quality control checks were performed and cDNA synthesised. ACTIN2 transcript was analysed as the internal control, expression of COW1, EXPA7, MRH3 and MRH6 was analysed. Error bars represent ±SE of 3 technical repeats. Bars with different letters were significantly different from others; p > 0.05; one-way ANOVA with post-hoc Tukey test.*

To ensure that under the 35S promoter RSL4 was being expressed in the root hairs the transgenics were observed under confocal microscopy. Strong expression of both RSL4^{WT} and RSL4$^{3K/R}$ was seen in the root hair nuclei of the transgenics figure 5.22. However the nucleus was not stained with a nuclear staining dye such as DAPI, for this experiment to be considered robust it should be repeated using a nuclear staining dye.

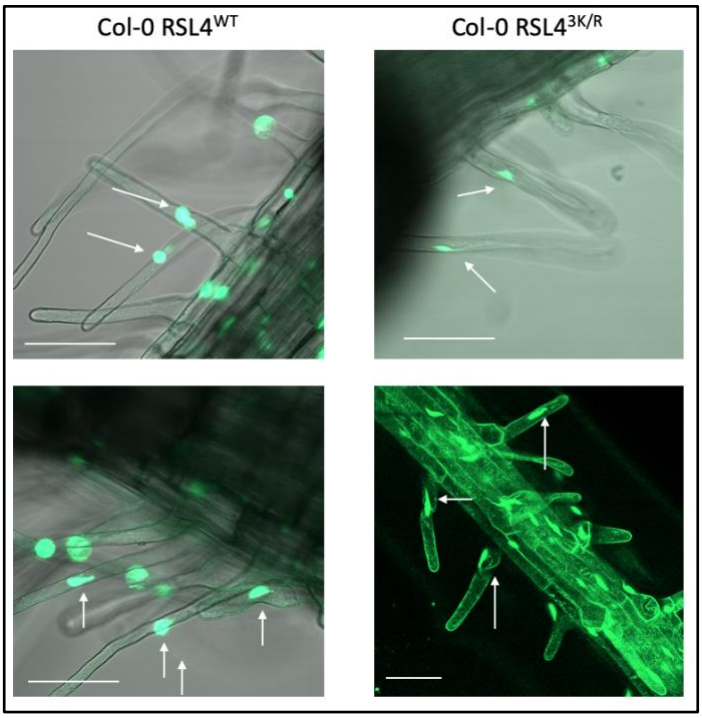

Figure 5.22 GFP tagged RSL4^{WT} and RSL4$^{3K/R}$ proteins localise in the nucleus of root hair cells in T2 Col-0 RSL4 Arabidopsis transgenics. *Localisation of RSL4^{WT}-GFP and RSL4$^{3K/R}$-GFP fusion proteins in stably transformed 5 day old Arabidopsis roots was analysed by confocal laser scanning microscopy. The localisation pattern does not alter after mutation of lysine to arginine. The green signal indicates GFP. Strong expression of both RSL4^{WT} and RSL4$^{3K/R}$ can be seen in the nucleus of the cells (white arrow). Scale bar= 100 µm*

Finally, in addition to generating RSL4^{WT} and RSL4$^{3K/R}$ overexpression lines in Col-0, the same GFP-tagged 35S overexpressing constructs were used to transform the *rsl ko* background to generate complementation lines. Using the same method as for generating the Col-0 transgenics the RSL4 constructs were floral dipped into the *rsl ko* background, the plants were grown to maturity and seeds collected. As the *rsl ko* already contained BASTA resistance, transgenic seedlings were identified by root hair growth, as the *rsl ko* background mutants are root hairless. Seedlings that developed root hairs grew to a similar size to Col-0, they were allowed to mature and seeds collected for segregation assays. These seedlings, T2 stage, were grown and plants that produced root hairs at a 1:3 (1:2:1) ratio were grown to maturity and seeds collected.

However as was also observed in RSL4 overexpression in Col-0 the T1 generation produced normal looking root hairs that did not need to be viewed under a microscope. In the second T2 generation overexpression of RSL4 in the *rsl ko* mutant background resulted in root hairs that were much smaller than Col-0. As was the same for the Col-0 transgenics (albeit a generation later) the root hairs, in the T2 generation, could only be viewed under a light microscope, when grown on 1/2MS supplemented with 100 nm ACC (figure 5.23). This may be due to weak expression of RSL4 in the required hair cells, in Col-0 native RSL4 is still present to enable root hair growth.

Additionally it may be due to RSL2 playing an important initial role in root hair formation, or elongation, which is not present in the *rsl ko* transgenics. However, due to the *rsl ko* RSL4 overexpression transgenics having such small root hairs and due to a lack of time it was decided not to proceed analysing the transgenics.

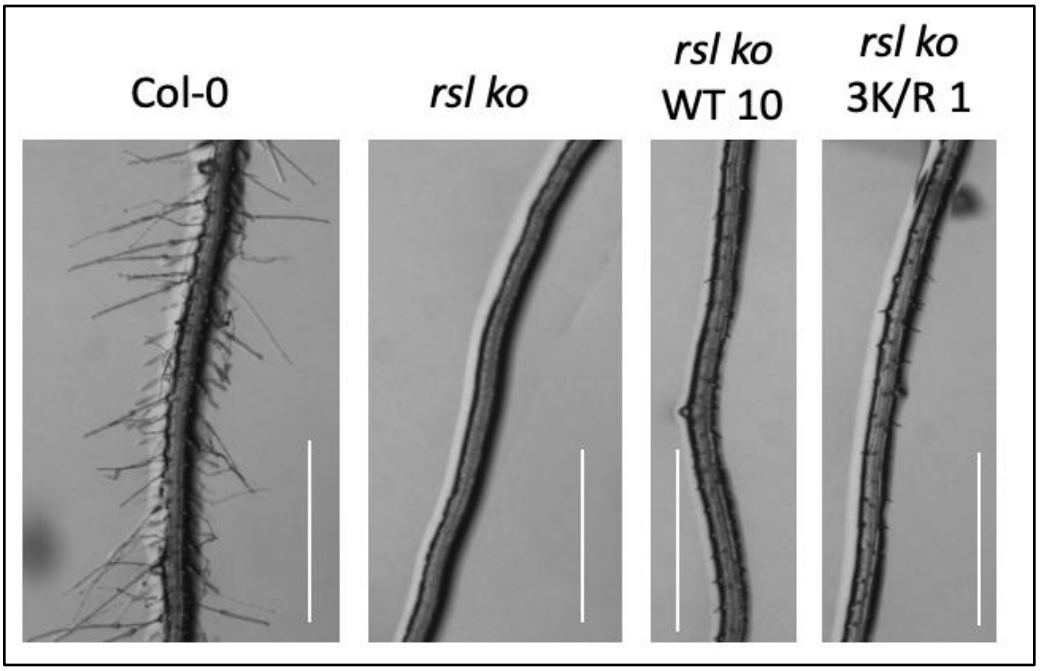

Figure 5.23 The T2 rsl ko RLS4^{WT} and rsl ko RSL4$^{3K/R}$ grew very short root hairs on 100 nm ACC. *Seedlings were germinated on 1/2MS and 0.8% phytoagar plates supplemented with 0.1% sucrose. Seedlings were then grown under long day light conditions for 7 days before the number of root hairs were counted. The white line denotes 1 mm.*

5.6 Discussion

This chapter has explored the role of SUMOylation of the bHLH transcription factor RSL4, that promotes post mitotic cell growth in *Arabidopsis* root hair cells. The protein has been demonstrated to be SUMOylated in *N. benthamiana* and mutating the three identified SUMO sites reduces this SUMOylation from occurring. These SUMO sites are conserved in RSL4 proteins from different plant species suggesting that the SUMO site may be functional and has been evolutionary conserved. Additionally these SUMO sites are also conserved among two bHLH transcription factors involved in root hair formation, RHD6 and RSL2 in *Arabidopsis*. Whilst the SUMO status of these proteins was not analysed, it is likely these proteins are also SUMOylated at these conserved sites.

Transgenics were generated by overexpressing RSL4^{WT} and RSL4$^{3K/R}$, in these transgenics RSL4^{WT} had a greater abundance of protein, compared to RSL4$^{3K/R}$, potentially suggesting the latter is less stable and more readily degraded. One of the SUMO sites in RSL4 may for example, block ubiquitin E3 ligases interacting and degrading the protein via the 26S proteasome (Datta et al., 2015). Yi et al., 2010 demonstrated that increased presence of RSL4, in root hairs, results in longer root hairs, so it was expected that RSL4^{WT} would harbour longer root hairs, than RSL4$^{3K/R}$, due to RSL4^{WT} protein increased abundance. However the length of the root hairs, when grown on 100 nm ACC, conflicted with this, as RSL4$^{3K/R}$ harboured longer root hairs, compared to RSL4^{WT}. Additionally whilst the protein stability was suggested to be more stable in RSL4^{WT}, exposing the seedlings to CHX and MG132 would be required to determine if RSL4^{WT} was more resistant to degradation via the 26S proteasome than RSL4$^{3K/R}$.

It was hypothesised, that despite RSL4^{WT} potential increased stability, RSL4$^{3K/R}$ may harbour increased activity. As a transcription factor RSL4 promotes expression of downstream genes that affect cell growth. The RT-qPCR data examining the transcript levels of genes RSL4 promotes expression of was increased in the RSL4^{WT} transgenics, as opposed to the RSL4$^{3K/R}$ transgenics, suggesting that SUMO may enhance RSL4 gene promoting activity.

The work completed in this chapter has hinted at the roles SUMO may play in the RSL4 protein; potentially increasing stability and increasing promotion of genes required for cell growth. These roles can be further elucidated in further experiments. Analysing RSL4^{WT} and RSL4$^{3K/R}$ protein-DNA interaction via a ChIP (chromatin immunoprecipitation) assay would help to test if the SUMO site mutations affect RSL4 binding to DNA. Additionally SUMO may aid transcriptional regulation in RSL4 potentially by increasing interaction with other proteins, required in the transcription complex, that harbour a SIM site. Furthermore conducting additional stability assays, pre-treating the seedlings with biosynthesis inhibitors and proteasome inhibitors could determine if RSL4$^{3K/R}$ is degraded faster than RSL4^{WT}.

The work conducted on RSL4 can also be further supported by examining the phenotype of SUMOylatable RSL2 and RHD6, which harbour the same SUMO sites. Using these proteins, that have 2 and 1 SUMO site(s) respectively, may shed further light on the role of each SUMO site in the proteins.

Finally interaction IPs should be conducted to determine which SUMO protease interacts with RSL4. Understanding under which conditions the SUMO protease deSUMOylates RSL4, will shed light on which conditions SUMOylation of RSL4 is required. This may help elucidate the effect SUMOylation of RSL4 has on the RSL4 protein. This can also be achieved by determining when there is increased or decreased SUMOylation of RSL4. The SUMOylation status of RSL4^{WT} can be determined by growing the transgenics on different media, immunoprecipitation of RSL4 and probing with αSUMO antibodies, the levels of SUMOylation of RSL4 can be determined.

In conclusion, this chapter has found some interesting, albeit contradictory results suggesting potentially SUMO may protect RSL4 from degradation and may help promote expression of downstream targets. This is however in conflict

with phenotypic data that demonstrates SUMO binding to RSL4 may decrease root hair length. A lot more research is required to fully understand the role of SUMOylation of RSL4, which unfortunately was not able to be completed due to time restraints.

Chapter 6

Does SUMO play a novel role in regulating the DELLA interactome?

6.1 Introduction

SUMO has been identified to modify several transcription factors including RSL4, as discussed in chapter 5. In addition to modifying transcription factors SUMO also modifies transcriptional activator DELLA (Conti et al., 2014), which is a key negative regulator of the gibberellin (GA) signalling pathway. DELLA proteins have been shown to mediate cross-talk with other hormone signalling pathways, coordinating plant growth in response to different stimuli by modulating the activity of transcription factors and transcriptional regulators (Blanco-Tourinan et al., 2020).

As has already been mentioned the DELLA proteins are post-translationally modified by phosphorylation (Hussain et al., 2005), *O*-GlcNAcylation (Zentella et al., 2016) and *O*-fucosylation (Zentella et al., 2017). As had already been mentioned another post-translational modification that DELLA is subjected to is SUMOylation (Conti et al., 2014). The fraction of SUMOylated DELLA determines the overall DELLA levels independent of GA due to GID1 (via its SIM site) binding to SUMOylated DELLA independent of GA. The levels of SUMOylated DELLA increase during stress sequestering GID1 from non-SUMO-DELLA enabling DELLA build up to restrain growth (Conti et al., 2014).

As has also been mentioned the single rice DELLA protein, SLR1, has been identified to be SUMOylated at a different residue than the K65 residue which Conti et al., 2014 identified in *Arabidopsis.* Instead SLR1 is SUMOylated at the

second residue in the protein K2 and not at K60, the residue counterpart to the *Arabidopsis* K65. Constitutively overexpressing SUMOylated SLR1 shows reduced stress to salt treatment. Gene expression analysis of constitutively overexpressed SUMOylated SLR1 transgenics revealed increased expression of *GA20ox2* and *GA2ox3,* key dioxygenases that regulate GA. SUMOylation of SLR1 also blocked interaction with growth regulator YAB4. Furthermore the interactions of six other transcription factors was found to be disrupted or reduced, demonstrating that SUMO represents a novel mechanism to disrupt interaction with several transcription factor families and modulate DELLA activity (Gonçalves et al., 2020).

When the *Arabidopsis* DELLA protein GAI was scanned for potential SUMO binding sites using in-house bioinformatic software, HyperSUMO (Nelis, PhD thesis 2014) that predicts SUMO sites, a second SUMO site was identified. In addition to K49, which was already identified by Conti et al., 2014, a second SUMO site was identified at K392 in the PFYRE GRAS domain. This SUMO site, K392, is not as well conserved as K49, it is not present in *Arabidopsis* RGL1, nor is it found in GAI in different plant species, *Z. mays* or *S. tuberosum* (figure 6.1 and 6.2), however, K392 conserved in six different plant species.

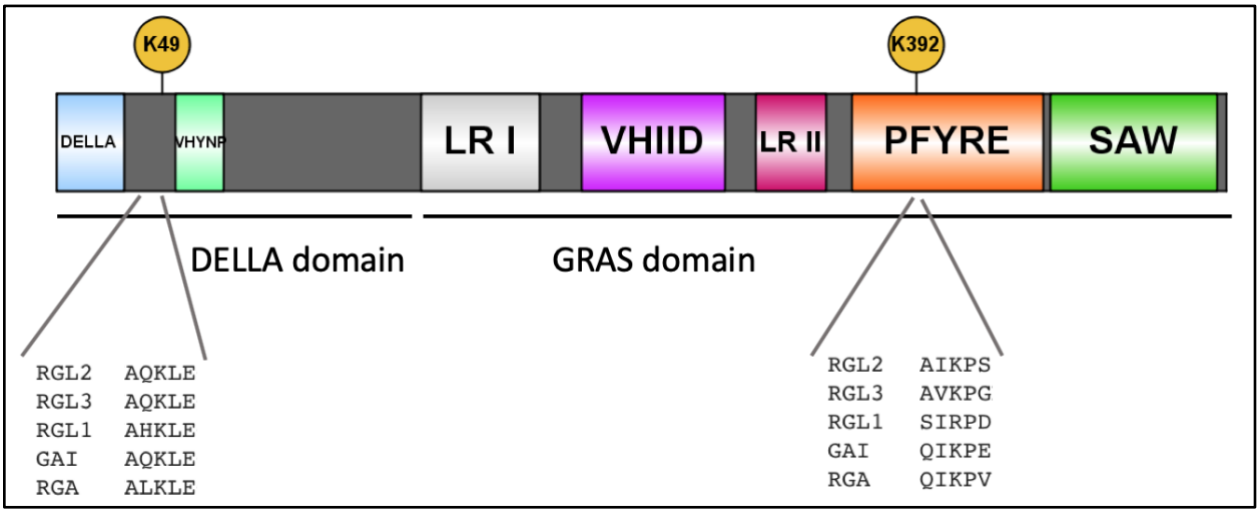

Figure 6.1 Schematic diagram of Arabidopsis GAI protein depicting the conserved protein domains and the location of the SUMO sites (yellow circles) predicted using in-house software. *The above panel shows the different domains present in the DELLA proteins including the DELLA domain (blue box) and VHYNP (light green box) regions which make up the DELLA domain and is required for GID1 binding. Additionally the LR I domain (grey box), VHIID (purple box), LR II (pink box), PFYRE (orange box) and SAW region (green box) make up the GRAS domain which is required for interaction with transcription factors. The amino acid sequence, from TAIR, was used as the query sequence for the in-house plant SUMO site prediction software, the predicted SUMO sites are shown in yellow circles containing the lysine residue SUMO binds too. The alignments below show the SUMO sites of the five DELLAs in Arabidopsis. Whilst all the Arabidopsis DELLAs share the K49 SUMO site, the K392 SUMO site is conserved amongst all the DELLAs, except RGL1.*

Figure 6.2 The location of the two predicted SUMO sites in GAI, across different plant species. *Alignment of different plant species of GAI, depicting the SUMO sites present in AtGAI. The amino acid sequences, from Uniprot, of GAI from different plant species were aligned using the Clustal Omega website. The K49 SUMO site, highlighted by the red box, is highly conserved in all GAI proteins from different plant species. The second predicted SUMO site, K392 highlighted by the blue box, is conserved amongst all the species, other than Z. mays and S. tuberosum. The black arrows indicate the position of the SUMOylated lysine (K).*

Previous work, conducted by project collaborator Dr Vivek Verma (University of Durham), had examined the interaction of GAI^{WT} and GRAS-domain mutated GAI^{K392R} with the different transcription factors GAI is known to sequester and transactivate. Using a transient assay conducted in *N. benthamiana* Dr Vivek Verma showed that PIF4 had a weaker interaction with GAI^{K392R}, compared to GAI^{WT}. Another transient assay conducted by Dr Vivek Verma using *N. benthamiana* established JAZ9 interacts more with GAI^{K392R} as opposed to GAI^{WT}.

6.2 PIF4 has a SIM site

Dr Vivek Verma's experiment had demonstrated that PIF4 interacts more with GAI^{WT} than GAI^{K392R}, we speculated this may be due to PIF4 harbouring a SIM site. PIF4 was scanned with HyperSUMO software (Nelis, PhD thesis 2014)

to predict potential SIM sites, which aid interaction with SUMOylated partners. A SIM site was identified and was found to be conserved amongst the PIFs (figure 6.3), on the C-terminus of the bHLH (helix-loop-helix) region which is involved in DNA binding. Using Phyre2 (http://www.sbg.bio.ic.ac.uk/phyre2/html/page.cgi?id=index) to predict the 3D structure of PIF4 I examined if the SIM site is exposed to the external environment to enable interaction, and is located on a beta sheet as the beta sheet enables interaction with the groove in the SUMO protein. However, Phyre2 was only able to predict a small region of the protein containing the bHLH, as the structure prediction is based on sequence homology to other proteins, no other structures of the protein were identified. However the HyperSUMO software predicted a strong confidence value for the identified SIM and there is strong conservation amongst the PIFs so this SIM site was further analysed. A month after the submission of this thesis Alphafold (https://alphafold.ebi.ac.uk/) 3D prediction software became available for public use, which uses artificial intelligence and has revolutionised protein structure production due to its accuracy at predicting 3D structures. Future work should determine the 3D structure of PIF4 using Alphafold to determine the location of the SIM site in the 3D structure of PIF4.

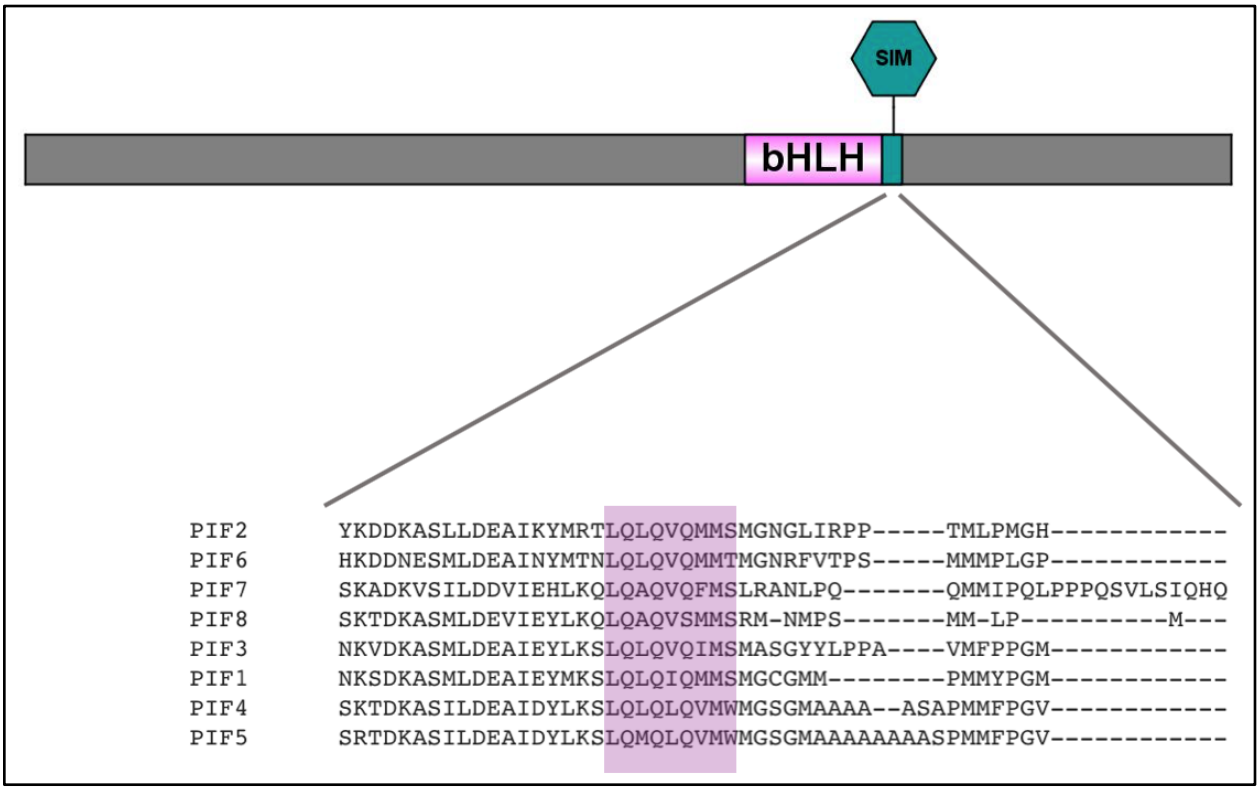

Figure 6.3 Schematic of PIF4 depicting the bHLH region of the protein (pink box) and predicted SIM site (green hexagon). *The above panel shows the location of the bHLH domains (pink box) present in the PIF proteins, and the location of the SIM site (green hexagon). The below alignment shows the alignment of the amino acid sequences,*

from Uniprot, of Arabidopsis PIF proteins, aligned using the Clustal Omega website. The purple box highlights the SIM site located in the PIFs.

In order to test whether if PIF4 contained a SIM site, full length PIF4 was amplified (figure 6.4, appendix table 6.1) from Col-0 cDNA and cloned into the entry clone *pENTR/D-TOPO* (Sigma). The constructs were transformed into *E. coli* DH5α and the colonies screened for successful clones by PCR. A mutation PCR was then carried out on $PIF4^{WT}$ to generate a SIM mutation $PIF4^{VM/AA}$ by mutating the hydrophobic residues to less charged alanine residues using overlapping mismatch primers amplifying $PIF4^{WT}$ pENTR4/D-TOPO, to generate $PIF4^{VM/AA}$. Mutant clones were identified through sequencing by DBS Genomics, both $PIF4^{WT}$ and $PIF4^{VM/AA}$ were transferred via recombination into the 35S N-terminal GFP-tag Gateway destination vector pEARLYGATE104. Confirmed PIF4 clones in pEG104, identified via colony PCR (figure 6.5, appendix table 6.1) from *E. coli* DH5α and transformed into the *Agrobacterium* strain GV3101 for transient expression.

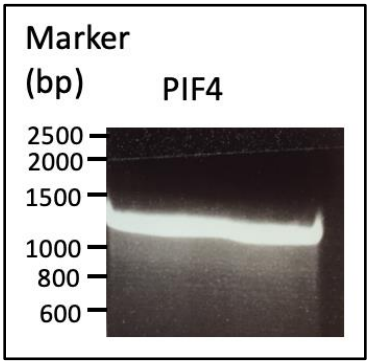

Figure 6.4 Cloning of Arabidopsis PIF4 from cDNA. *Image of DNA gel showing PCR amplification of full length PIF4 from cDNA extracted from Col-0, PCR product (1293 bp).*

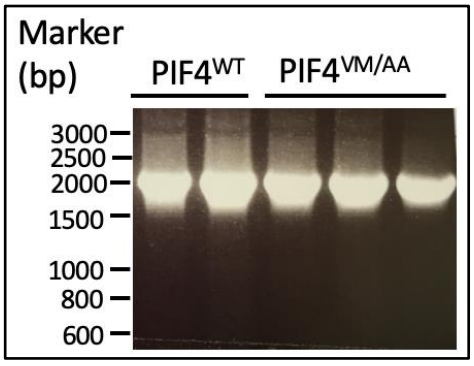

Figure 6.5 PIF4 genes transformed into plant expression vector pEG104. *Image of a DNA gel showing PCR amplification of plasmid DNA, extracted from E.coli, using an internal pEG104 primer and a PIF4 primer to confirm the presence of PIF4 in the pEG104 vector (2196 bp).*

A transient assay in *N. benthamiana* using 35S:GFP-PIF4^{WT} and 35S:GFP-PIF4$^{VM/AA}$ was conducted to test whether PIF4^{WT} contained a SIM site, and the mutation PCR removed the SIM site. Two bands observed in the IP sample were due to phosphorylated and non-phosphorylated PIF4 (Bernardo-Garcia et al., 2014). The non-phosphorylated band (lower band) is 73 kDa (48 kDa plus 25 kDa GFP). The SIM site present in PIF4^{WT} may prevent the accumulation of non-phosphorylated PIF4, as PIF4$^{VM/AA}$ had a greater accumulation of non-phosphorylated PIF4$^{VM/AA}$, compared to PIF4^{WT} (figure 6.6). The presence of a SIM site was shown via western blotting with α-HA antibodies (Sigma). A single band of apparent relative molecular mass at ~15kDa indicates that SUMO was bound to PIF4^{WT} via a non-covalent interaction. SUMO was only observed in PIF4^{WT} immunoprecipitates, suggesting that PIF4^{WT} harbours a SIM site, which has been mutated and removed in PIF4$^{VM/AA}$.

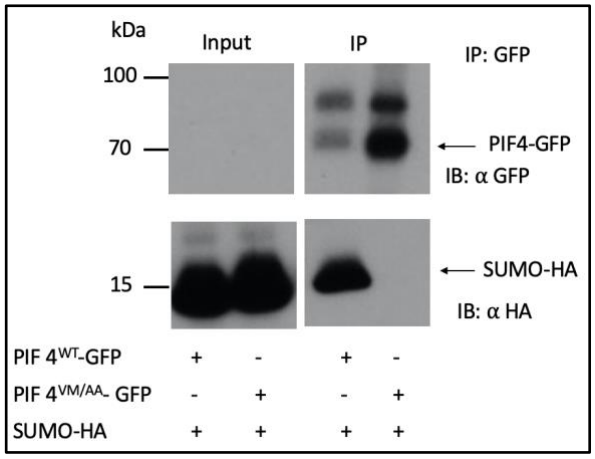

Figure 6.6 Immunoblot analysis shows PIF4 contains a SIM site, mutation of the PIF4 SIM site prevents SUMO interaction. *Transient expression was performed in Nicotiana benthamiana leaves co-expressing PIF4^{WT}-GFP or PIF$^{VM/AA}$-GFP with SUMO1-HA. Total protein (input) was subjected to immunoprecipitation (IP: α-GFP) with α-GFP immunoaffinity beads followed by immunoblot analysis anti-GFP (IB: α-GFP) antibodies to detect PIF4^{WT}/PIF$^{VM/AA}$-GFP and anti-HA (IB: α-HA) antibodies to detect SUMO1-HA. Total protein of all samples (input) was probed with anti-GFP antibodies and anti-HA antibodies to determine PIF4 and SUMO protein levels. Arrows indicate PIF4-GFP (73 kDa) and SUMO1-HA (14 kDa). These western blots were repeated twice, this figure is a representative of outcome of those experiments.*

In order to elucidate further the role of the SIM site in PIF4, transgenics were generated by stably transforming PIF4 into a quadruple PIF mutant background comprised of *pif1-1 pif3-3 pif4-2 pif5-3* (Leivar et al., 2008b), here in called *pifq*. *pif1-1* is a T-DNA insertion line that deletes the bHLH domain (Huq et al., 2004), *pif3-3* contains a 2.5 kbp

deletion that produces no detectable *PIF3* transcript (Monte et al., 2004), *pif4-2* is a T-DNA insertion in the sixth intron (Leivar et al., 2008a), *pif5-3* a T-DNA insertion mutant (SALK_087012), RNA transcript of *PIF5* could not be detected by northern blot hybridisation (Fujimori et al., 2004). *pifq* mutants have resistance to BASTA, due to the presence of the SAIL resistance cassette. This meant that the pEG104 vector could not be used to transform the plants, as it would not be possible to select for transformants containing the PIF4 gene. Instead the $PIF4^{WT}$ and $PIF4^{VM/AA}$ genes were transferred into a destination vector with appropriate resistance, pGWB14, which harbours resistance to hygromycin, a resistance cassette not present in *pifq*. In addition to the hygromycin resistance cassette, pGWB14 has an N-terminal 3X HA tag and is driven by the 35S promoter. The $PIF4^{WT}$ and $PIF4^{VM/AA}$ genes in the pGWB14 vectors were transformed into *Agrobacterium*, the positive *Agrobacterium* colonies were checked by PCR (figure 6.7, appendix table 6.1).

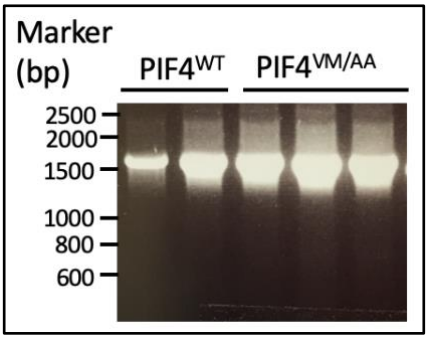

Figure 6.7 PIF4 genes transformed into plant expression vector pGWB14. *Image of a DNA gel showing PCR amplification of plasmid DNA, extracted from Agrobacterium, using an internal pGWB14 primer and a PIF4 primer to confirm the presence of PIF4 in the pGWB14 vector (1785 bp).*

Once positive *Agrobacterium* colonies were identified, the floral dip method was used to insert the wild type and SIM site mutated PIF4 constructs back into the *pifq* background. The presence of the PIF4 transgene was confirmed via PCR (figure 6.8).

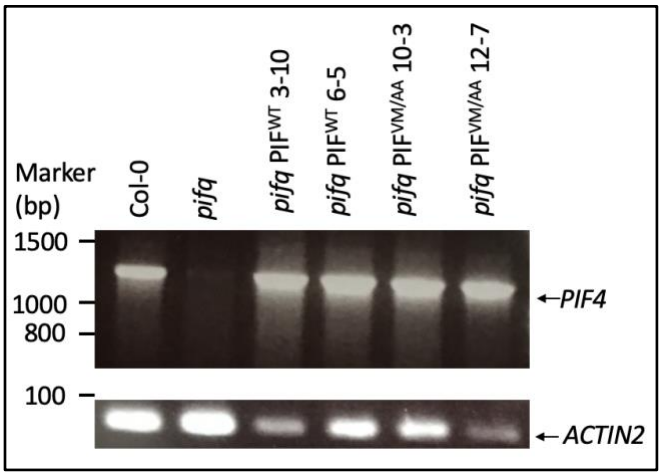

Figure 6.8 PIF4 transcript detected by PCR in Arabidopsis transgenics cDNA. *Image of a DNA gel showing PCR amplification of PIF4 transgene and ACTIN2 (extraction control) (68 bp) from cDNA from Col-0, pifq, pifq PIF4^{WT} 3-10, pifq PIF4^{WT} 6-5, pifq PIF4$^{VM/AA}$ 10-3 and pifq PIF4$^{VM/AA}$ 12-7. Full length PIF4 (1293 bp) was amplified to confirm the presence of the transgene in the transgenics and the absence of PIF4 in the quadruple PIF knock-out background, pifq.*

The transgenics were grown to the T3 homozygous generation containing a single copy insertion of the transgene. The independent transgenic lines were analysed for expression levels of the transgene by real-time qPCR. In order to ensure the T3 transgenics were selected that had similar transgene expression levels to each other the expression levels of a minimum of 3 independent transgenic lines were analysed by real-time qPCR (figure 6.9) A minimum of two transgenic lines per construct that showed similar levels of transgene expression to the other transgenics were selected for further analysis. Figure 6.9 shows expression of *PIF4* relative to *ACTIN2* in different transgenic lines of PIF4^{WT} and PIF4$^{3K/R}$ in the *pifq* background. PIF4^{WT} 3-10 had a similar expression level to PIF4$^{VM/AA}$ 10-3, whilst with a lower expression, PIF4^{WT} 6-5 had a similar expression level to PIF4$^{VM/AA}$ 12-7 (figure 6.10). Whilst this experiment was conducted to identify transgenics with similar expression levels these RT-qPCRs should be repeated as it was only conducted with technical repeats not biological repeats. Additionally the expression of the *PIF4* transcript should be analysed in Col-0, in addition to *pifq* and the respective transgenics as the current experiment only identified expression levels amongst the transgenics and did not take account of *PIF4* expression in Col-0 or *pifq*.

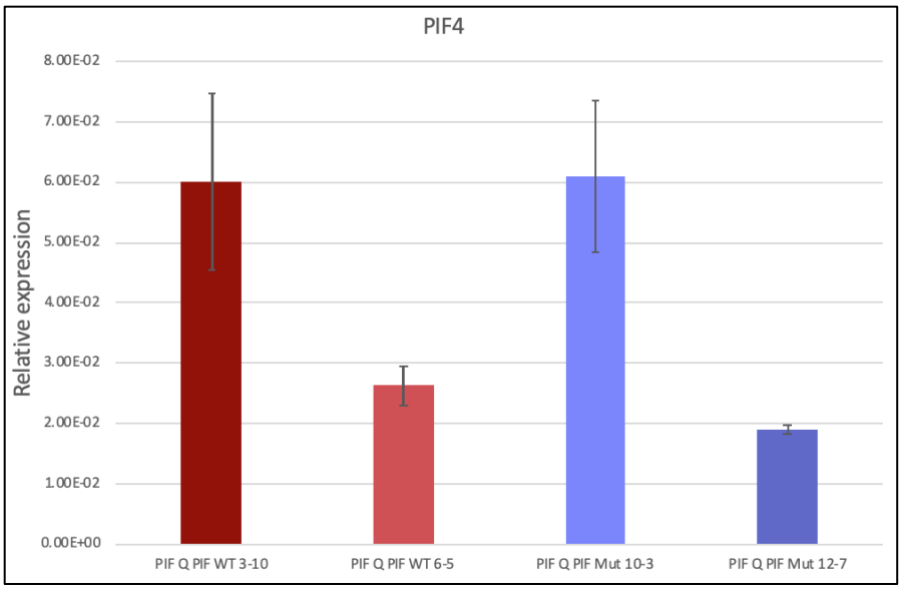

Figure 6.9 Analysis of PIF4 expression levels in pifq transgenic lines. *Expression levels of PIF4 in different transgenic plant lines in the pifq background expressing PIF4^{WT} (3-10 and 6-5) and PIF4$^{VM/AA}$ (10-3 and 12-7) analysed by RT-qPCR. Relative PIF4 expression levels in 10 days old seedlings relative to ACTIN2. Error bars represent ±SE of 3 technical repeats.*

Typically the total protein would be extracted from the *Arabidopsis* transgenics, immunoprecipitated and analysed by immunoblotting to determine the stability of PIF4^{WT} and PIF4$^{VM/AA}$ in the transgenics. However this was not able to be completed, due to time constraints. Unfortunately due to time constraints, these PIF expressing transgenics were not able to be analysed for PIF4 phenotypes.

6.3 Analysis of GAI transgenics

To ascertain the function of the second SUMO site in the GRAS domain of DELLA, GAI^{WT}, GAI$^{2K/R}$, GAI^{K392R} and GAI^{K49R} were expressed in *Arabidopsis* under a constitutive 35S promoter. The transgenics were generated by Dr Vivek Verma in the double DELLA mutant background *rga-24 gai-t6* (Dill and Sun, 2001) (herein called *della ko)*, which generated from the *Ler* wildtype. The *rga-24* mutant is a null allele due to a deletion spanning the *RGA* locus (Silverstone et al., 1998) and *gai-t6* is a null allele due to a Ds insertion in the *GAI* coding region (Peng et al., 1997). In this background Dr Vivek Verma dipped the pGWB14 expression vector expressing 35S:GAI^{WT}-3XHA, 35S:GAI^{K49R}-3XHA, 35S:GAI^{K392R}-3XHA and 35S:GAI$^{2K/R}$-3XHA (Clough and Bent 1998). These homozygous T3 stage seeds were generated and kindly donated by Dr Vivek Verma. The presence of the transgene was confirmed via PCR (figure 6.10).

Whilst Dr Vivek Verma generated multiple T3 stage lines of GAI^{WT}, GAI$^{2K/R}$ and GAI^{K392R}, which were studied in this thesis, only one independent transgenic line of 35S:GAI^{K49R}-3XHA was generated by Dr Vivek Verma. For this thesis I took T0 stage 35S:GAI^{K49R}-3XHA seeds (dipped and collected by Dr Vivek Verma) and grew this through several generations to generate several lines of T3 stable transgenic GAI^{K49R}.

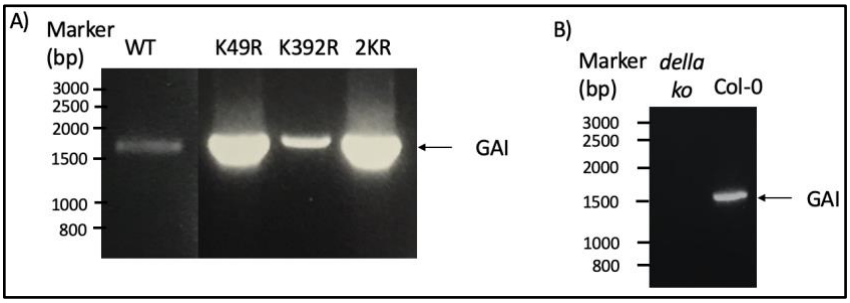

Figure 6.10 GAI transcript detected by PCR in Arabidopsis transgenics cDNA. *Images of DNA gels showing PCR amplification of PIF4 transgene from cDNA from* ***A)*** *della ko GAI^{WT}, della ko GAI^{K49R}, della ko GAI^{K392R} and della ko GAI$^{2K/R}$ and* ***B)*** *Col-0 and della ko. Full length GAI (1602 bp) was amplified to confirm the presence of the transgene in the transgenics and the absence of GAI in the double DELLA knock-out background, della ko.*

The transgenics were grown to the T3 homozygous generation containing a single copy insertion of the transgene. The independent transgenic lines were analysed for expression levels of the transgene by real-time qPCR. In order to ensure the T3 transgenics were selected that had similar transgene expression levels to each other the expression levels of a minimum of 3 independent transgenic lines were analysed by real-time qPCR (figure 6.11) A minimum of two transgenic lines per construct that showed similar levels of transgene expression to the other transgenics were selected for further analysis. Figure 6.11 shows expression of *GAI* relative to *ACTIN2* in different transgenic lines of GAI^{WT}, GAI^{K49R}, GAI^{K392R} and GAI$^{2K/R}$ in the *della ko* background. Whilst this experiment was conducted to identify transgenics with similar expression levels these RT-qPCRs should be repeated as it was only conducted with technical repeats not biological repeats. Additionally the expression of the *GAI* transcript should be analysed in Col-0, in addition to *della ko* and the respective transgenics as the current experiment only identified expression levels amongst the transgenics and did not take account of *GAI* expression in Col-0 or *della ko*.

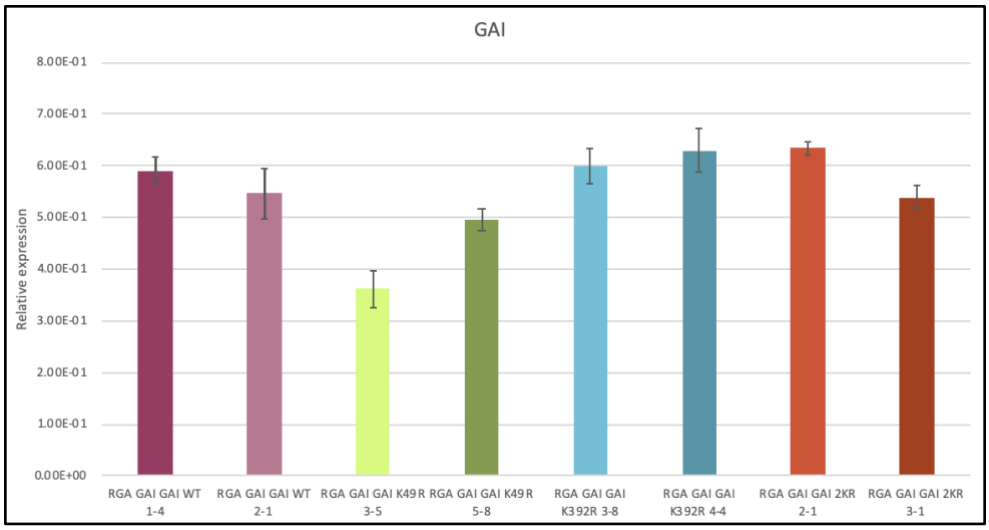

Figure 6.11 Analysis of GAI expression levels in della ko transgenic lines. *Expression levels of GAI in different transgenic plant lines in the della ko background expressing GAI^{WT} (1-4 and 2-1), GAI^{K49R} (3-5 and 5-8), GAI^{K392R} (3-8 and 4-4) and GAI$^{2K/R}$ (2-1 and 3-1) analysed by RT-qPCR. Relative GAI expression levels in 10 days old seedlings relative to ACTIN2. Error bars represent ±SE of 3 technical repeats.*

Furthermore to ensure the expressed proteins have a similar abundance the proteins were analysed by western blot (figure 6.12). GAI$^{2K/R}$ 2-1 despite expressing the *GAI* transcript, does not produce protein that can be seen via western blotting. Project co-collaborator Dr Alberto Campanaro developed a different extraction buffer for extracting GAI and used a different GAI$^{2K/R}$ line to GAI$^{2K/R}$ 2-1, which showed no protein, data kindly provided by Dr Alberto Campanaro (figure 6.13).

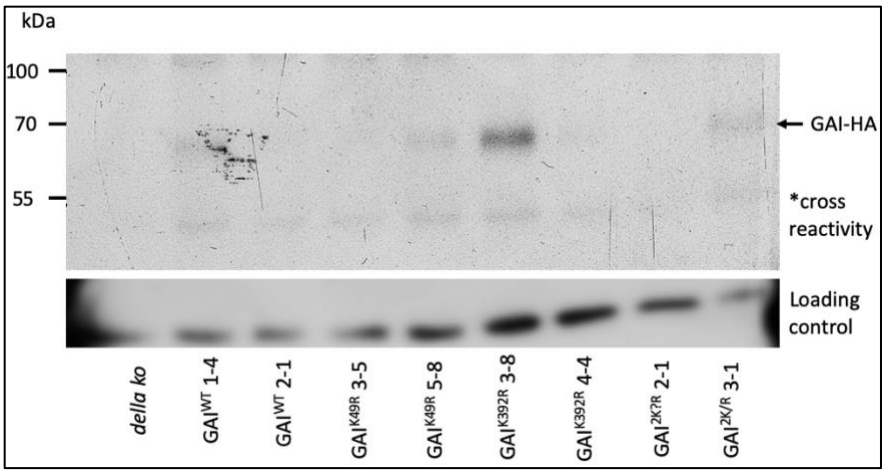

Figure 6.12 Immunoblot analysis of the stability of GAI-HA transgenics in della ko background. *The protein levels of GAI^{WT}-HA (1-4 and 2-1), GAI^{K49R}-HA (3-5 and 5-8), GAI^{K392R}-HA (3-8 and 4-4) and GAI$^{2K/R}$-HA (2-1 and 3-1)in different transgenic lines (della ko backgrounds) were analysed by extracting total protein from each different line of transgenic Arabidopsis. Protein was also extracted from della ko as a negative control. Total protein (input) was immunoprecipitated (IP: α-HA) with α-HA immunoaffinity beads followed by immunoblot analysis with anti-HA (IB: α-HA) antibodies to detect GAI-HA. Arrow indicates GAI-HA (62 kDa). Below the blot is the loading control. * denotes cross reactivity bands.*

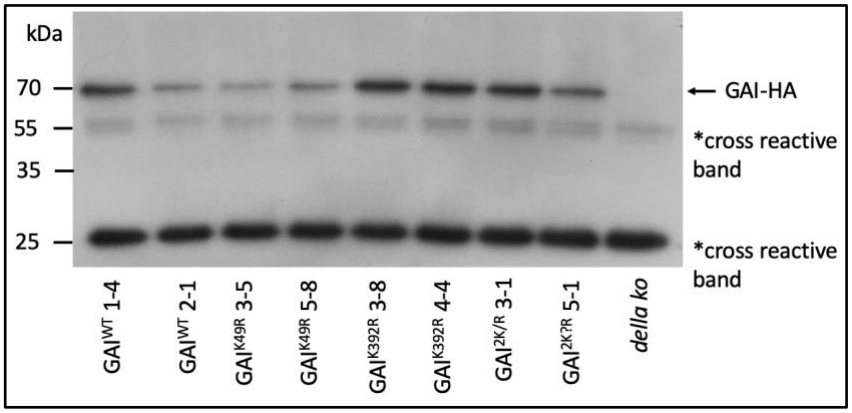

Figure 6.13 Immunoblot analysis of the stability of GAI-HA transgenics in della ko background. *The protein levels of GAI^{WT}-HA (1-4 and 2-1), GAI^{K49R}-HA (3-5 and 5-8), GAI^{K392R}-HA (3-8 and 4-4) and GAI$^{2K/R}$-HA (2-1 and 5-1)in different transgenic lines (della ko backgrounds) were analysed by extracting total protein from each different line of transgenic Arabidopsis. Protein was also extracted from della ko as a negative control. Total protein (input) was immunoprecipitated (IP: α-HA) with α-HA immunoaffinity beads followed by immunoblot analysis with anti-HA (IB: α-HA) antibodies to detect GAI-HA. Arrow indicates GAI-HA (62 kDa). * denotes cross reactivity bands. Figure kindly donated by Dr Alberto Campanaro.*

As JAZ9 had been demonstrated to interact less with GAI^{WT} and more with GAI^{K392R} (work completed by Dr Vivek Verma) the sensitivity of the transgenics to jasmonic acid was analysed to determine if there was a phenotype in the transgenics overexpressing GAI^{WT}, GAI^{K49R}, GAI^{K392R} and $GAI^{2K/R}$. To test if the SUMO site mutations in GAI affected the interactions with JAZ9, the transgenics were germinated on 1/2 MS then 3 days later transferred to 1/2 MS alone or 1/2 MS supplemented with 10 µM JA, and the length of the root lengths were measured 6 days later.

It has previously been reported that the *della ko* mutants have longer roots, when grown on JA than GA deficient mutants (Hou et al., 2010). Hou et al., 2010 found that the *della ko* mutants had 33% relative root length on JA, compared to root length on non-JA media after 8 days, comparable to (figure 6.14). Overexpressing GAI^{WT} did not result in greater root inhibition on JA, compared to *della ko*, which was unexpected as it had been hypothesised that GAI^{WT} would have shorter roots compared to *della ko* due to the increased presence of DELLA, which would bind to JAZ9 liberating MYC2 to promote JA responses. However the experiment was repeated three times finding the same result every time that the overexpressing GAI transgenics had reduced JA mediated root length inhibition, compared to *della ko.*

It had also been predicted that GAI^{K392R} would have shorter roots, compared to GAI^{WT}, as GAI^{K392R} would bind more to JAZ9, leaving MYC2 to promote transcription of JA responsive genes. However as can be seen in (figure 6.14) there was no significant difference in JA mediated root length inhibition between the transgenics grown on 10 µM JA. These transgenics are in the *Ler* background and typically this experiment should be conducted with *Ler* as a control, however due to time pressure, these seeds could not be obtained in time and this was not conducted, however future experiments should repeat this experiment, with *Ler* seedlings.

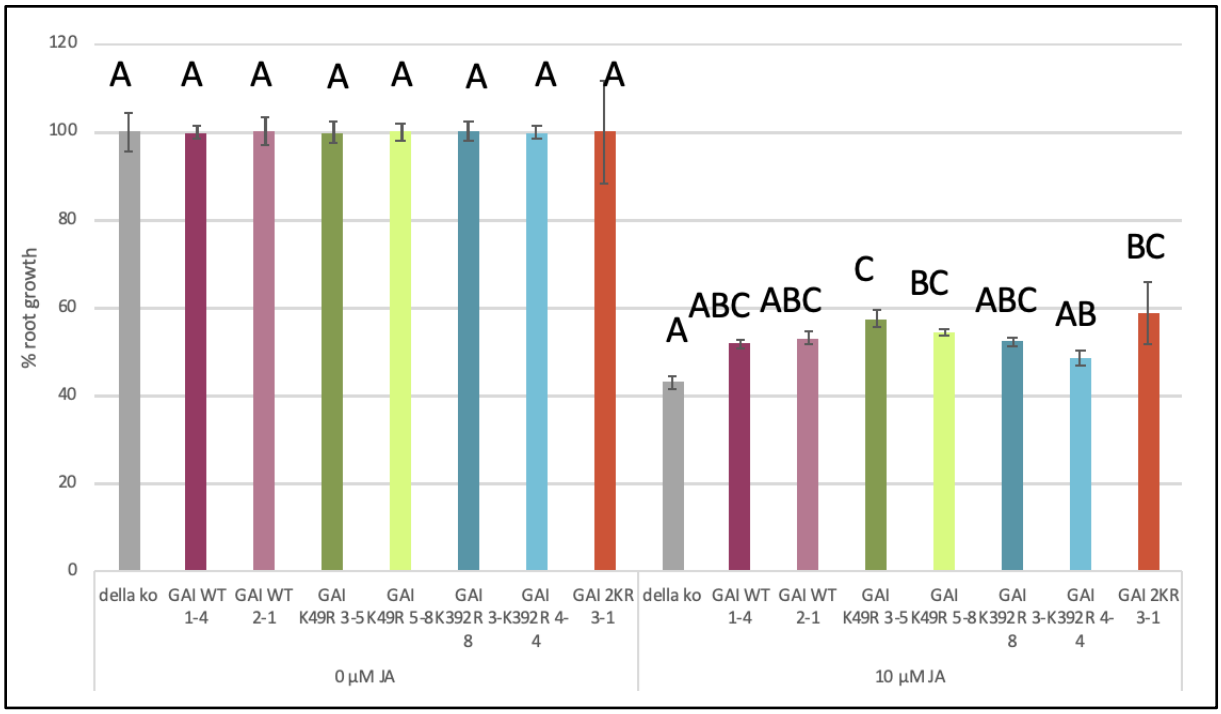

Figure 6.14 Quantification of JA-mediated root growth inhibition of della ko, 2 independent lines of GAI^{WT}, 2 independent lines of GAI^{K49R}, 2 independent lines of GAI^{K392R} and 2 independent lines of GAI$^{2K/R}$. *Seedlings were germinated on 1/2MS at 3 days old, the seedlings were transferred to the prepared assay plates: 1/2MS supplemented with either 10 µM JA or no hormone treatment (control). Seedlings were grown for a further 6 days before the root length was measured. Data is relative to growth of 0µM JA. Data are means ± sem (n = 18-60 each). Bars with different letters, in each treatment were significantly different from others P>0.05; two-way ANOVA with post hoc Tukey test.*

Primers were designed and tested to determine downstream expression of JA responsive genes to analyse transcript levels of *BASIC CHITINASE (B-CHI), PLANT DEFENSIN 1.2 (PDF1.2), LIPOXYGENASE (LOX3)* and *TYROSINE AMINOTRANSFERASE (TAT1).* However due to a lack of time these JA responsive genes were not able to be analysed. Completing a time course of gene expression in response to exogenous JA may elucidate the role of SUMOylated DELLA in JA signalling.

Due to the identification of a SIM site in PIF4 and its weakened interaction with GAI^{K392R}, the role of DELLA PIF interaction was examined. DELLAs are known to inhibit PIFs by sequestering their DNA recognition regions (de Lucas et al., 2008; Feng et al., 2008). PIFs accumulate in the dark to maintain skotomorphogenesis. Conversely, in the absence of GA DELLAs inhibit PIFs, degrading the PIFs, resulting in shorter hypocotyls (Li et al., 2016).

To test if the SUMO site mutations in GAI affected the interactions with PIFs the transgenics were germinated on 1/2 MS alone or 1/2 MS supplemented with 5 µM GA_3 and grown in far red to examine the hypocotyl elongation

growth. The transgenics were grown in far red light as PIF4 induces hypocotyl elongation in shade avoidance, detected by a reduction of far red light.

As can be seen in figure 6.15 the hypocotyl length did not change in *della ko*, this is due to the absence of the two DELLA proteins, in the presence of GA the DELLAs are degraded, resulting in PIF4 promoting gene expression. As the DELLAs are absent in the *della ko* the presence or absence of GA does not affect PIF4 promoting gene expression. The GAI$^{2K/R}$ and GAI^{K49R} have similar % hypocotyl elongation on GA compared to *della ko,* conversely GAI^{K392R} has increased % hypocotyl elongation, similar to GAI^{WT} 1-4.

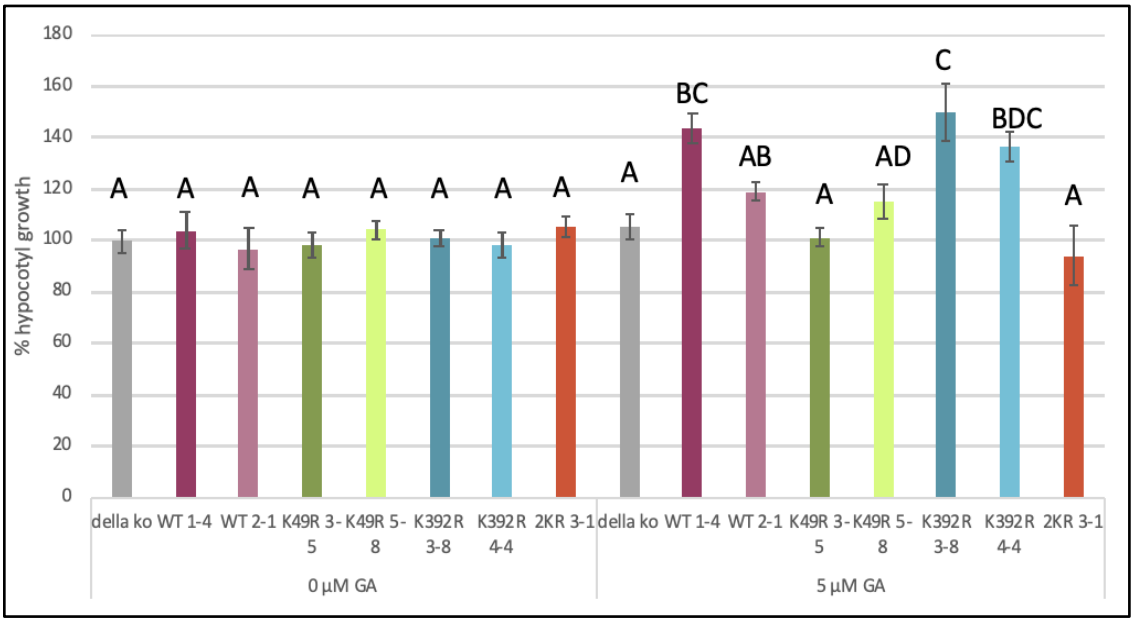

Figure 6.15 Quantification of GA-mediated hypocotyl elongation in far red light of della ko, 2 independent lines of GAI^{WT}, 2 independent lines of GAI^{K49R}, 2 independent lines of GAI^{K392R} and 2 independent lines of GAI$^{2K/R}$. *Analysis of % hypocotyl elongation on 5 µM GA, compared to growth on 1/2 MS of 4-day old della ko, 2 independent transgenic lines of della ko GAI^{WT}, 2 independent transgenic lines of della ko GAI^{K49R}, 2 independent transgenic lines of della ko GAI^{K392R} and 2 independent transgenic lines of della ko GAI$^{2K/R}$. Seedlings were germinated on either 1/2 MS and 0.8% or 1/2 MS plates supplemented with 5 µM JA. They were grown for 4 days in far-red light before the hypocotyl length was measured. Data are means ± sem (n = 20 each). A one-way ANOVA determined the statistical difference between the genotypes. Bars with different letters in each treatment were significantly different from others; p > 0.05; one-way ANOVA with post-hoc Tukey test.*

The results of the hypocotyl elongation assay were very unclear as to the role of SUMO in DELLA PIF interaction in hypocotyl elongation, the assay should be repeated, including using the PIF4^{WT} and PIF4$^{VM/AA}$ transgenics that were generated, to determine further the phenotype.

To try to understand better as well the role of SUMO primers were designed and tested to analyse transcript levels of *ARABIDOPSIS THALIAN HOMEOBOX PROTEIN 2 (ATHB2), EXPANSIN 8 (EXP8), LIPID TRANSFER PROTEIN 3 (LTP3)* and *XYLOGLUCAN ENDOTRANSGLYCOSYLASE 7 (XTR7)* which are PIF4 activated genes. However due to a lack of time these PIF4 activated genes were not able to be analysed. Future work could establish if in the presence/absence of GA there is difference in expression of these genes in the transgenics.

6.4 Discussion

The DELLA proteins are important regulatory proteins that mediate the crosstalk with many hormone pathways in the plant via a complicated coordination of many transcription factors and regulatory proteins that the DELLAs sequester or transactivate. This can make trying to elucidate the role of post-translational modification (PTM) difficult as the PTM could have many different functions, such as affecting stability of the DELLA, altering its interaction with a wide variety of different interacting partners or altering subsequent PTMs of DELLA.

This chapter has attempted to shed further light on the role of the SUMO site in the GRAS domain of GAI. Previous work conducted in the lab had indicated via interaction IPs that SUMOylation of GAI in the GRAS domain increased interaction with PIF4 and decreased interaction with JAZ9. To further examine this PIF4 was mutated at its SIM site and $PIF4^{WT}$ and $PIF4^{VM/AA}$ SUMO interaction was examined. The $PIF4^{VM/AA}$ mutation abolished PIF4s interaction with SUMO. Additionally it was observed that $PIF4^{VM/AA}$ had a greater accumulation of non-phosphorylated PIF4, compared to $PIF4^{WT}$. PIF4 is known to be phosphorylated by BIN2, the negative regulator of brassinosteroid signalling. Upon PIF4 phosphorylation via BIN2 PIF4 is degraded via the proteasome (Bernardo-Garcia, 2014), potentially mutating the SIM site of PIF4 may reduce interaction with BIN2, resulting in increased accumulation of non-phosphorylated PIF4. To determine if $PIF4^{WT}$ and $PIF4^{VM/AA}$ have different levels of phosphorylation $PIF4^{WT}$ and $PIF4^{VM/AA}$ protein should be analysed via a phos-tag gel which increases the separation of phosphorylated proteins.

In order to better understand the role of the SIM site present in PIF4, transgenic *Arabidopsis* was generated overexpressing both $PIF4^{WT}$ and $PIF4^{VM/AA}$ in the *pifq* mutant background. However unfortunately due to time constraints these transgenics were not able to be analysed prior to completion of this thesis. However the experiments that had been planned included examining the hypocotyl length of the transgenics when grown under far-red light, in response to PAC (an inhibitor of GA biosynthesis) and GA_3. It was hypothesised that the $PIF4^{VM/AA}$ transgenics would have had increased hypocotyl elongation, compared to $PIF4^{WT}$, as $PIF4^{VM/AA}$ would be less likely to bind to GAI, due to the abolition of the SIM site, resulting in accumulation of free PIF4 capable of promoting PIF4-

activated gene expression. This phenotype could be further explored by conducting qRT-PCR on downstream genes promoted by PIF4 such as *ATHB2*, *LTP3*, *EXP8* and *XTR7*.

As part of this hypothesis it would also be predicted that the GRAS domain mutated GAI^{K392R} would also result in longer hypocotyl length, compared to GAI^{WT}, as GAI^{K392R} would interact less with PIF4, leaving PIF4 free to promote PIF4-activated gene expression. Whilst hypocotyl elongation in response to GA resulted in longer hypocotyl elongation in GAI^{K392R} compared to GAI^{K49R} and GAI$^{2K/R}$ the hypocotyl elongation was similar to GAI^{WT}.

Whilst the phenotype of hypocotyl elongation, in response to GA did not produce a clear phenotypic difference between the various GAI mutants it may be due to SUMO not playing a role in the DELLA PIF4 interaction during hypocotyl elongation. PIF4 functions in a wide range of developmental and environmental responses including hypocotyl gravitropism, phototropism, leaf senescence, stomatal development and thermosensory growth (Casson et al., 2009; Lorrain et al., 2008; Choi et al., 2016; Sun et al, 2013; Sakuraba et al., 2014; Song et al., 2014; Lau et al., 2018; Gangappa et al., 2017). The different GAI mutated transgenics need to be examined when subjected to these different environmental and developmental stresses to determine the role of SUMO in the DELLA PIF4 interaction.

A promising phenotype to examine is PIF4 interaction with DELLA in response to heat, when a plant is heat stressed PIF4 positively regulates growth and negatively regulates immunity (Gangappa et al., 2017). It has already been reported that heat shock results in increasing SUMOylation of proteins (Miller and Vierstra, 2011), potentially SUMOylation of DELLA may mediate its subsequent interactions with PIFs and other transcription factors providing a balance between temperature-resilience and disease resistance. Recent work by project collaborator Dr Alberto Campanaro has indicated that the GAI transgenics have a thermosensory phenotype, with GAI^{WT} and GAI^{K49R} showing shorter hypocotyl lengths when grown in elevated heat of 28˚C. The data indicates that SUMOylation of GAI at K392R increases GAI interaction with PIF4, suppressing growth, conversely GAI^{K392R} and GAI$^{2K/R}$ have longer hypocotyl, when grown in elevated heat.

Finally the role of the SUMO site in the GRAS domain of DELLA was examined to determine if it altered the interactions with JAZ9 leading to an altered JA response. The lengths of the roots of the various GAI mutation transgenics, grown on 10 µM JA was examined. None of the examined transgenics showed a clear phenotype, this suggests that SUMO may not play a role in DELLA JAZ9 interaction when seedlings are applied to exogenous JA. The JAZ proteins interact with transcription factors that have a wide range of effects in plants ranging from development, JA synthesis, defence against pathogens and secondary metabolite synthesis (Ruan et al., 2017). The biotic and/or abiotic stress that triggers SUMOylation of GAI should be explored, to determine if this alters interactions with JAZ9.

This project has attempted to understand if the second SUMO site in the GRAS domain of DELLA alters interactions with transcription factors. Whilst it has identified a SIM site in PIF4, due to a lack of time the PIF4 transgenics were not able to be analysed. However the work has suggested that SUMO may not play a role in PIF-GAI interaction in

hypocotyl elongation. Preliminary data has also indicated that the second SUMO site in the GRAS domain of DELLA may also not play a role in JAZ9-GAI interaction in exogenous application of JA. Due to a lack of time further phenotypes could not be examined, however, due to the large number of transcription factors DELLA interacts with there are many potential stresses that could be examined.

Chapter 7

Final discussion

7.1 Summary

The aim of this thesis was to provide insights into the role of SUMO in various hormone pathways and root hair development in *Arabidopsis*. Over the course of this research analysis of the role of SUMO in root hair development has led to discovery of three SUMO sites in RSL4, a bHLH transcription factor that promotes root hair cell growth. Analysis of the role of SUMO in the ABA hormone pathway has discovered two SUMO sites in PP2CA, the negative regulator in the ABA pathway and a hypothesised SIM site in the ABA co-receptor PYL8. Lastly initial analysis has been carried out on *Arabidopsis* transgenics overexpressing SUMO site mutations in GAI, identifying a SIM site in PIF4. Each topic will be discussed separately below.

7.2 SUMOylation of PP2CA

Results in chapter 3 identified the location of two SUMO sites in PP2CA. Transient expression and immunoprecipitation of $PP2CA^{WT}$ and $PP2CA^{2K/R}$ showed SUMO1 attachment to $PP2CA^{WT}$, which was not present in $PP2CA^{2K/R}$. These SUMO sites were also predicted to be conserved amongst the *Arabidopsis* PP2Cs and conserved amongst PP2Cs from different plant species, although the SUMO status of these proteins (determined by a SUMO IP) was not tested. The ABA sensitivity of various SUMO proteases was analysed, including *ots ko* and *spf ko*. Both

knockout lines showed increased ABA sensitivity in root length inhibition by ABA. However subsequent transient expression and co-immunoprecipitation of OTS1, SPF1 and SPF2 failed to identify interactions with PP2CA. However other methods to test protein interaction, such as bimolecular fluorescence complementation (BiFC) or yeast two hybrid were not tested. Whilst these mutants demonstrate ABA sensitivity, it seems unlikely this sensitivity is due to interaction with PP2CA and likely due to deSUMOylation of other components of the ABA pathway. These proteases may deSUMOylate the ABA transcription factors that are already known to be SUMOylated (Miura et al., 2009; Zheng et al., 2012). A final transient expression and co-immunoprecipitation of PP2CA with recently identified SUMO proteases Desi3B and Desi4A indicated these proteases may interact with PP2CA. This co-immunoprecipitation should be repeated to confirm the results, ideally expressing Desi3B with a tag that is not shared with PP2CA. Additionally these interactions should be further confirmed by determining co-localisation in *N. benthamiana* for example by fluorescently tagging each protein with a different tag and overlaying the images to determine if they are localising in the same region of the cell. Additionally the proteins could be tagged with a split fluorophore, which upon interaction of the two proteins re-forms the fluorescent protein, resulting in fluorescence. The ABA sensitivity of *Arabidopsis* knockout plant lines of the two SUMO proteases in question should be analysed. Lastly the SUMO protease stability should be determined upon application of ABA.

The results in chapter 4 continued analysis of SUMOylated PP2CA by generating transgenic *Arabidopsis* that expressed PP2CA^{WT} and PP2CA$^{2K/R}$ under its own promoter to determine if the ABA sensitivity was altered within the two sets of transgenics. Root length inhibition assays determined in two different PP2C knockout backgrounds (*p3* and *pp2ca-1*) that PP2CA$^{2K/R}$ was less sensitive to ABA compared to PP2CA^{WT}. The expression of ABA responsive genes was analysed and showed increased expression in PP2CA^{WT} transgenics, compared to PP2CA$^{2K/R}$. The proteins showed similar levels of abundance, however the protein stability should be examined in future work, additionally looking at stability in response to ABA. Future work should also establish if SUMOylation of PP2CA increases or decreases in the presence of ABA and should also confirm the result from transient expression that in *Arabidopsis* PP2CA$^{2K/R}$ is not SUMOylated.

Based on this data, it was hypothesised that PP2CA^{WT} may show greater disease resistance to *Pst* when dip inoculated in the pathogen, as Lim et al., 2014 had demonstrated that the ABA hypersensitive mutant *pp2ca-1* is more resistant to *Pst*, compared to Col-0 in a *Pst* dipping assay. Lim et al., 2014 showed this was due to the ABA hypersensitive mutant having a greater number of closed stomata in response to *Pst,* resulting in reduced infection. As SUMO is generally regarded as a rapid response PTM, it was hypothesised SUMO may have a role in ABA induced rapid stomatal closure upon detection of pathogens. A pathotest was conducted examining the bacterial growth in leaves dipped in *Pst*, comparing PP2CA^{WT} and PP2CA$^{2K/R}$. Surprisingly, conflicting with the data already discussed, PP2CA$^{2K/R}$ showed greater pathogen resistance, compared to PP2CA^{WT}. This experiment, due to time constraints, was only conducted once and should be repeated. The phenotype should be further examined by comparing the resistance of PP2CA^{WT} and PP2CA$^{2K/R}$ in *Pst* infiltration assays in addition to dipping assays, as based on the initial

pathotest data it would be hypothesised PP2CA$^{2K/R}$ would have greater *Pst* susceptibility, compared to PP2CA^{WT} in a *Pst* infiltration assay. This is because once the pathogen has bypassed the stomata the increased ABA sensitivity would aid pathogen susceptibility. Once the pathogen is present in the cell, increased ABA signalling becomes disadvantageous in pathogen resistance, as ABA signalling blocks SA and JA signalling. Furthermore the bacterial growth in the transgenics, after both dipping and infiltration, should be monitored over several days, because, as mentioned, ABA signalling has differing advantages and disadvantages, at different stages of pathogen infection. Additionally the phenotype should be further examined by determining the stomatal size of PP2CA^{WT} and PP2CA$^{2K/R}$ transgenics. The plants should be treated with Coronatine, Flg22 and ABA to determine if upon treatment with Flg22 and ABA PP2CA$^{2K/R}$ stomata close quicker or stay closed for longer.

Although conflicting with the pathotest data, based on the increased ABA root length sensitivity and increased expression of ABA responsive genes in PP2CA^{WT}, compared to PP2CA$^{2K/R}$ it was hypothesised that PP2CA^{WT} may aid interaction with ABA co-receptor PYLs, which would increase ABA sensitivity. SIM site prediction software predicted a SIM site in PYL3 to PYL13. Transient expression and co-immunoprecipitation of PYL1 and PYL8 showed SUMO1 interaction with PYL8 and not PYL1, as the software had predicted. Whilst PYL13 was also tested, expression was too low to determine if PYL13 harbours a SIM site. Due to time restrictions a planned transient expression and co-immunoprecipitation assay using tagged SUMO1, tagged PYL8^{WT} and SIM site mutated PYL8$^{VM/AA}$ was not completed. If SUMO1 immunoprecipitated with PYL8^{WT} and not with PYL8$^{VM/AA}$ this would have validated the SIM prediction site and proved the PYL8 SIM site had been removed. However as this data is missing, only speculation can be provided to fill in the blanks, a hydrophobicity plot has indicated that hydrophobicity has been reduced at the intended location.

Transgenic *Arabidopsis* overexpressing PYL8^{WT} and the hypothetically removed SIM site PYL8$^{VM/AA}$ was generated in the *pyl458* background and briefly analysed to determine the ABA sensitivity. Due to time constraints the experiment was only conducted once, the brief analysis of the PYL8 transgenics root length inhibition on ABA did not provide conclusive results to determine if the transgenics are more or less sensitive to ABA, as one PYL8$^{VM/AA}$ line showed increased sensitivity to ABA, whereas the other line had the same sensitivity as the two PYL8^{WT} lines. This experiment should be repeated at least twice more, in addition a seedling establishment assay should be conducted. Furthermore the expression of downstream ABA responsive genes should also be analysed. However the most important experiment still required is analysing the PYL8 SIM site as mentioned above, namely determining if the PYL8$^{VM/AA}$ mutation removes the SIM site and interaction IPs, establishing the interactions between PP2CA^{WT}, PP2CA$^{2K/R}$, PYL8^{WT} and PYL8$^{VM/AA}$.

Whilst significantly more research is required to fully understand the mechanism of PP2CA SUMOylation based on the data generated so far figure 7.1 shows a hypothesised model for the influence of SUMO on ABA signalling. Whilst SUMO is not critical for ABA signalling the phenotype demonstrated by PP2CA$^{2K/R}$ suggests that SUMO may aid ABA

signal transduction resulting in a stronger ABA response. Figure 7.1 shows how in the presence of ABA SUMOylated PP2CA results in an ABA response. NonSUMOylated PP2CA whilst still interacting with ABA, resulting in some ABA signalling seems to result in weaker signal transduction, potentially some active PP2CA is still inhibiting the SnRK2s. This model is based on the $PP2CA^{WT}$ and $PP2CA^{2K/R}$ phenotype, however the dynamics of PYL PP2CA interaction has not been tested so this model may prove to be incorrect. These interactions should be tested using co-IPs testing the interactions of $PP2CA^{WT}$ and $PP2CA^{2K/R}$ with $PYL8^{WT}$ and $PYL8^{VM/AA}$. Additionally if SUMOylated PP2CA is generated the phosphatase activity in the presence of a PYL can be analysed and compared to nonSUMOylated PP2CA. Whilst SUMO may alter interactions with PYLs, due to SUMO site K179 being located near the active site of PP2CA, SUMOylated PP2CA activity may also be reduced due to SUMO blocking of the ABA active site. This could be determined by x-ray crystallography of SUMOylated PP2CA.

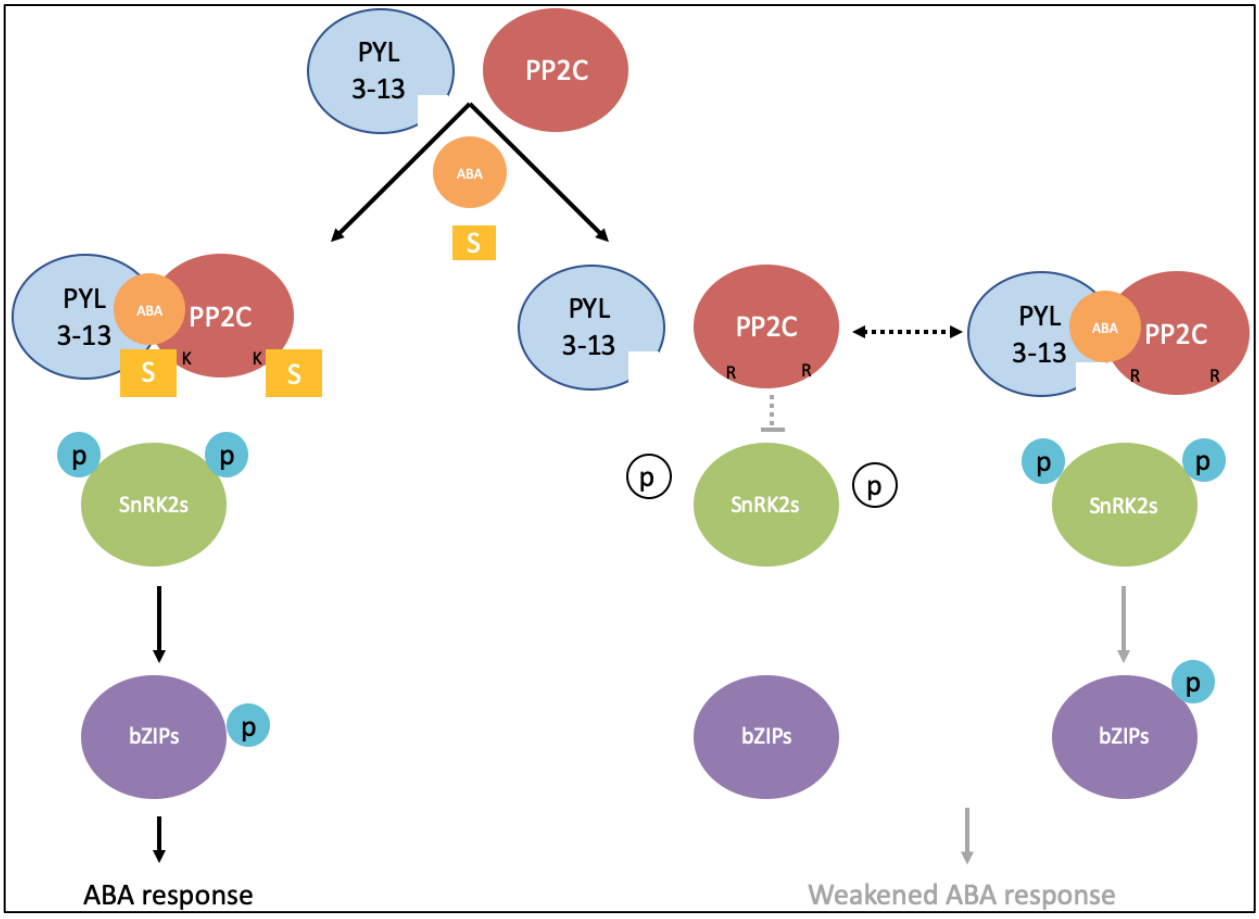

Figure 7.1 Hypothesised model of the influence of SUMO on ABA signalling. *SUMOylated PP2C (containing two SUMOylatable K's) becomes SUMOylated and with ABA interacts with PYL3-13 harbouring a SIM site, potentially SUMO blocks the active site of the PP2Cs. This results in SnRK2s rephosphorylating and phosphorylating bZIPs resulting in an ABA response. Whereas nonSUMOylated PP2CA (containing two mutated K>R residues which cannot be SUMOylated) interacts with PYL3-13 in the presence of ABA resulting in ABA signal transduction it also may have*

reduced interaction with PYL3-13 resulting in active PP2C capable of dephosphorylating SnRK2s resulting in a weakened ABA response.

The data suggests that SUMO may provide an additional level of control to ABA signalling. It is also interesting to note that the PYLs which were identified to contain SIM sites, other than PYL3 and PYL4 are capable of inhibiting PP2Cs in the absence of ABA (PYL5-PYL12) and PYL13 which is irresponsive to ABA (Li et al., 2013). If the SIM sites predicted are true this suggests that potentially SUMO may provide a mechanism to control PYL/PP2C interaction in the absence of ABA. Proteins typically become SUMOylated under rapid stresses such as heat shock. We have speculated that PP2CA may become SUMOylated upon detection of pathogen MAMPs/PAMPs, as when detected stomata need to rapidly close to prevent disease. Due to the rapid response required the PP2Cs can be quickly SUMOylated resulting in PYL interaction prior to ABA presence and resulting in downstream ABA response. The pathotest conducted in this thesis found the opposite phenotype, however it was only conducted once and the results were not statistically significant. This theory could be tested by measuring stomatal aperture in $PP2CA^{WT}$ and $PP2CA^{2K/R}$ in response to pathogens. Additionally the SUMO status of PP2CA in response to pathogens could also be determined.

In conclusion the data generated in chapter 3 and 4 of this thesis has suggested that PP2CA SUMOylation may result in stronger signal transduction than $PP2CA^{2K/R}$. Whilst the mechanism behind this has not been sufficiently researched it has been hypothesised this could be due to PYLs harbouring SIM sites and may also be due to the location of SUMO near the active site of PP2CA. If this hypothesis proves to be correct it could be speculated that PP2CA may be SUMOylated in stress responses resulting in rapid stronger ABA signalling than in the absence of SUMO.

7.3 SUMOylation of RSL4

The results in chapter 5 investigated the role of SUMO in root hair development. Initially the root hair phenotype of double SUMO protease knockout mutant *ots ko* was characterised. The *ots ko* mutant was found to have fewer, longer root hairs compared to Col-0 and expression of OTS1 was established in the nuclei of root hairs. This prompted us to scan a selection of proteins required for root hair growth, to determine if the OTS SUMO proteases target a root hair development protein and to establish if the root hair phenotype of *ots ko* is caused by hyperSUMOylation of this protein. Three bHLH Root Hair Defective-Six like (RSL) Class II family of transcription factors RSL2, RSL4 and RHD6 were identified as containing SUMO sites. Whilst the three transcription factors contained a conserved SUMO

site in the bHLH domain, RSL2 and RSL4 contained an additional one and two SUMO site(s), respectively. Before I joined the project RSL4 had been selected as the transcription factor to study. Phylogenetic analysis determined that the three SUMO sites present in *Arabidopsis* RSL4 was also present in RSL4 proteins from different plant species. However the SUMOylation status of *Arabidopsis* RSL2 and RHD6 were not tested, nor were the RSL4 proteins from different plant species, these can only be hypothesised.

The three SUMO sites in RSL4 were mutated to arginine, which maintains the structural environment of the surrounding protein structure, due to both amino acids having similar biochemical properties (Grantham, 1974), however it prevents SUMO binding. Transient expression and immunoprecipitation of $RSL4^{WT}$ and $RSL4^{3K/R}$ showed SUMO1 attachment to $RSL4^{WT}$ and greatly reduced SUMO1 attachment to $RSL4^{3K/R}$. Whilst the transient assay did not show complete removal of SUMO1 from $RSL4^{3K/R}$ the SUMOylation status of RSL4 in the transgenic *Arabidopsis* should be analysed to determine if $RSL4^{3K/R}$ shows SUMOylation. Unfortunately due to time constraints this was not completed. Furthermore future work also needs to establish, via transient expression and co-immunoprecipitation of RSL4 and OTS1, if OTS1 interacts with RSL4.

Transgenic *Arabidopsis* that overexpressed $RSL4^{WT}$ and $RSL4^{3K/R}$ was generated to explore the root hair phenotype and to attempt to decipher the roles of SUMO in RSL4. However the transgenics produced showed a disagreement in the phenotype observed, in conflict with gene expression data and protein abundance. It has been reported by Yi et al., 2010 that overexpressing RSL4 in the Col-0 background results in longer root hairs, compared to Col-0, due to constitutive RSL4 expression resulting in constitutive cell growth. Whilst the T2 stage *Arabidopsis* overexpressing RSL4 in the Col-0 background had comparable root hair length compared to Col-0, by the T3 homozygous stage the transgenics overexpressing RSL4 had considerably smaller root hairs, compared to Col-0. It had been planned to determine the root hair phenotype in a variety of environments including high and low phosphate, in addition to 1/2 MS supplemented with sucrose and 1/2 MS supplemented with IAA. Unfortunately there were too few root hairs to be analysed so the root hair length and number were only analysed in plants grown on ACC. The transgenics had much smaller root hairs than Col-0 but showed a clear phenotypic difference of longer root hairs in $RSL4^{3K/R}$ compared to $RSL4^{WT}$. This was unexpected as protein abundance data had indicated that $RSL4^{WT}$ was more abundant than $RSL4^{3K/R}$, based on Yi et al., 2010 research this should have meant $RSL4^{WT}$ should have had longer root hairs due to increased amount of RSL4. However future research should determine the protein stability of $RSL4^{WT}$ and $RSL4^{3K/R}$ when grown in ACC. Protein stability should be assayed by treating samples with protein synthesis inhibitors. Additionally based on the increased presence of $RSL4^{WT}$, compared to $RSL4^{3K/R}$, despite similar expression levels it was assumed that $RSL4^{3K/R}$ may be degraded more quickly by the proteasome. However this was not tested and is only speculative. In the future this could be analysed by treating plants a proteasome inhibitor to determine if this increases $RSL4^{3K/R}$ stability. If it does it could be hypothesised that SUMO protects RSL4 from degradation.

Additional data that conflicted with the observed increased root hair length of RSL4$^{3K/R}$ was increased expression of genes in RSL4^{WT} compared to RSL4$^{3K/R}$ of RSL4 targeted downstream genes. Genes were chosen, based on reduced transcript levels in *rsl4-1* mutants and increased transcript levels in overexpressed 35S RSL4 plants (Yi et al., 2010). This experiment was conducted as it was speculated that despite increased presence of RSL4^{WT} over RSL4$^{3K/R}$ the short root hair phenotype in RSL4^{WT} may be due to RSL4$^{3K/R}$ being more active. As a transcription factor determining expression levels of genes RSL4 targets would help elucidate if RSL4$^{3K/R}$ was more active, however the data suggested that RSL$^{3K/R}$ is not more active than RSL4^{WT}, as there was reduced expression of RSL4 targeted genes in RSL4$^{3K/R}$. However it is also worth noting that the activity levels between RSL4^{WT} and RSL4$^{3K/R}$ may not differ, the increased expression of RSL4 targeted genes in RSL4^{WT} may be due to greater RSl4^{WT} protein abundance. However the expression analysis could not explain the observed phenotype. Future work to determine if SUMO affects the activity of the proteins should conduct a CHIP-seq assay, comparing RSL4^{WT} and RSL4$^{3K/R}$.

Due to the contradictory data generated in chapter 5 it is difficult to determine a mechanism of action. Figure 7.2 demonstrates how based on the phenotypic data RSL4$^{3K/R}$ results in longer root hairs however the mechanism of this is not known. Due to RSL4 harbouring three SUMO sites it's possible that each SUMO site may provide a different function. As SUMO site K205 is located in the bHLH domain of RSL4 it is possible that SUMOylation at this lysine may block RSL4 binding to DNA preventing downstream transcription of genes promoting cell growth. Additionally one of the other lysines in RSL4 may also be ubiquitinated, SUMOylation may block ubiquitination preventing RSL4 from being degraded resulting in more protein abundance. Due to the contradictory phenotype and gene expression it seems unlikely that the true phenotype has been determined which means it is not possible to provide real life examples of when this SUMOylation would be biologically relevant. It may prove easier to decipher this with RHD6 and RSL2 which harbour fewer SUMO sites and may provide more clear phenotypes. Ultimately the biological relevance of the SUMO sites may be determined by deciphering when these proteins are SUMOylated, this may be easier to deduce when the proteins are expressed under native promoters.

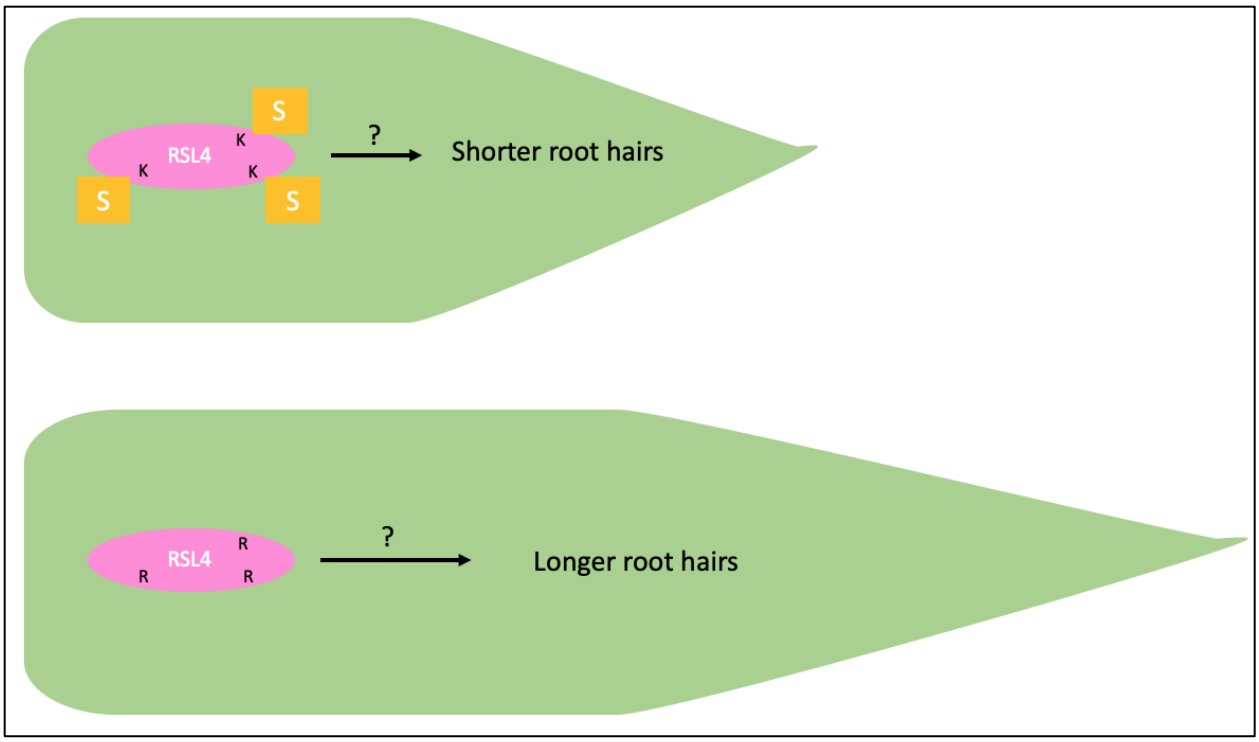

Figure 7.2 Hypothesised model of the influence of SUMO of SUMO on root hair length. *SUMOylatable RSL4 (containing 3 SUMOylatable Ks) results via an unknown mechanism (denoted by ?) in shorter root hairs. Conversely nonSUMOylatable RSL4 (containing three mutated K>R residues which cannot be SUMOylated) results via an unknown mechanism (denoted by ?) in longer root hairs.*

7.4 SUMOylation of GAI

The final project that was worked on is detailed in chapter 6 examining the role of the SUMO site in the GRAS domain of DELLA. This project was continuing work produced by Dr Vivek Verma, who had determined that a second SUMO site in the GRAS domain in DELLA proteins altered interactions with transcription factors DELLA sequesters and transactivates. The GRAS domain SUMO site is conserved in all but one *Arabidopsis* DELLA protein and is conserved amongst GAI proteins from different plant species. Work completed by Dr Vivek Verma had determined that the GRAS domain SUMO site increased interaction with PIF4, a bHLH transcription factor that is involved in hypocotyl gravitropism, phototropism, leaf senescence, stomatal development and thermosensory growth (Casson et al., 2009; Lorrain et al., 2008; Choi et al., 2016; Sun et al, 2013; Sakuraba et al., 2014;Song et al., 2014; Lau et al., 2018; Gangappa et al., 2017). In addition the GAI GRAS domain SUMO site decreased interaction with JAZ9, the negative regulator of JA signalling (Chini et al., 2007).

Using in-house HyperSUMO software (Nelis, PhD thesis 2014) to predict SIM sites the PIFs were found to harbour a SIM site next to the bHLH motif. This motif was mutated to generate a $PIF4^{VM/AA}$ protein that was transiently expressed and co-immunoprecipitated with SUMO1 in addition to PIF^{WT}, this showed $PIF4^{WT}$ interacting with SUMO1 and $PIF4^{VM/AA}$ not interacting with SUMO1, demonstrating the SIM site has been removed. Transgenic *Arabidopsis* overexpressing PIF4 in the *pifq* background was generated, however unfortunately due to time constraints these transgenics were not able to be analysed. Planned experiments however included determining if there was a hypocotyl elongation phenotype when grown under far-red light and in response to GA or PAC or had a thermosensory response.

Transgenic *Arabidopsis* kindly provided by Dr Vivek Verma overexpressing GAI^{WT}, GAI^{K49R}, GAI^{K392R} and $GAI^{2K/R}$ in the *della ko* background were analysed after generating two independent lines of GAI^{K49R} from Dr Vivek Vermas original T1 seed. Despite gene transcript expression one of the $GAI^{2K/R}$ lines provided did not produce protein that could be detected by immunoblotting, so due to a lack of time, analysis continued with one line of $GAI^{2K/R}$. The transgenics were first analysed for JA mediated root inhibition. No clear phenotypic differences could be observed between the different GAI mutations analysed. Primers had been designed and tested to examine expression of JA responsive genes, unfortunately this experiment was not able to be carried out due to time constraints but may elucidate the role of SUMOylated DELLA in JAZ9 interaction. Additionally whilst a phenotype was not observed in root growth in response to exogenous JA the disease phenotype of the transgenics could be examined in response to necrotrophic infection. The SUMO status of GAI should be determined in different environmental stresses such as biotic stress this may help elucidate the role of SUMO in DELLA JAZ9 interaction.

Finally the hypocotyl elongation phenotype of the transgenics when exposed to exogenous GA was examined in far red light. Again no clear phenotype was observed, primers had been designed and tested to examine expression of PIF4 targeted genes, unfortunately this experiment was not able to carried out due to time constraints but may elucidate the role of SUMOylated DELLA in PIF4 interaction. Further work undertaken by Dr Alberto Campanaro has subsequently found a thermosensory phenotype with GAI^{WT} and GAI^{K49R} showing shorter hypocotyl lengths when grown in elevated heat of 28˚C. The data indicates that SUMOylation of GAI at K392R increases GAI interaction with PIF4, suppressing growth, conversely GAI^{K392R} and $GAI^{2K/R}$ have longer hypocotyl, when grown in elevated heat. This suggests that SUMO may not have a role in DELLA PIF4 interaction in hypocotyl elongation. The thermosensory experiments should be repeated with the PIF4 transgenics. Additionally the SUMO status of GAI should be examined in thermosensory stress.

Figure 7.3 demonstrates how SUMOylated DELLA preferentially binds to PIF4 via the SIM site located in PIF4, leaving JAZ9 active to negatively regulate the JA pathway. Conversely non-SUMOylated DELLA preferentially binds JAZ9 leaving PIF4 active to mediate gene expression. The biological relevance of DELLA sequestering JAZ9 has not been determined in this thesis as no phenotypic difference was determined when GAI^{WT}, GAI^{K49R}, GAI^{K392R} and $GAI^{2K/R}$ was

grown on exogenous JA. As JAZ9 blocks immunity and promotes growth it is possible to hypothesis that JAZ9 may bind and be sequestered by DELLA in response to pathogen attack. Whilst a phenotype was not established in exogenous JA other experiments could determine if GAI^{WT}, GAI^{K49R}, GAI^{K392R} and $GAI^{2K/R}$ has a phenotype in pathogen infection, when it would be beneficial for JAZ9 to be sequestered to enable JA signalling.

In this thesis no phenotypic difference was identified when GAI^{WT}, GAI^{K49R}, GAI^{K392R} and $GAI^{2K/R}$ was grown on exogenous GA. However project collaborator Dr Alberto Campanaro identified a thermosensory phenotype with GAI^{WT} and GAI^{K49R} showing shorter hypocotyl lengths when grown in elevated heat of 28˚C, compared to GAI^{K392R} and $GAI^{2K/R}$. This suggests that in elevated heat stress wildtype DELLA is SUMOylated sequestering PIF4 preventing downstream gene expression resulting in hypocotyl elongation. This may be due growth immunity trade-off PIF4 helps regulate, PIF4 positively regulates growth and development and negatively regulates immunity (Gangappa et al., 2017). SUMOylation of DELLA during elevated heat may help balance the trade-off ensuring plant defence is not compromised. In conclusion this is a complex mechanism to deduce as DELLA is regulated by many posttranslational modifications and interacts with many transcription factors. Determining the biological conditions under which DELLA is SUMOylated and when PIF4 and JAZ9 bind will help determine the biological relevance of SUMOylation of DELLA.

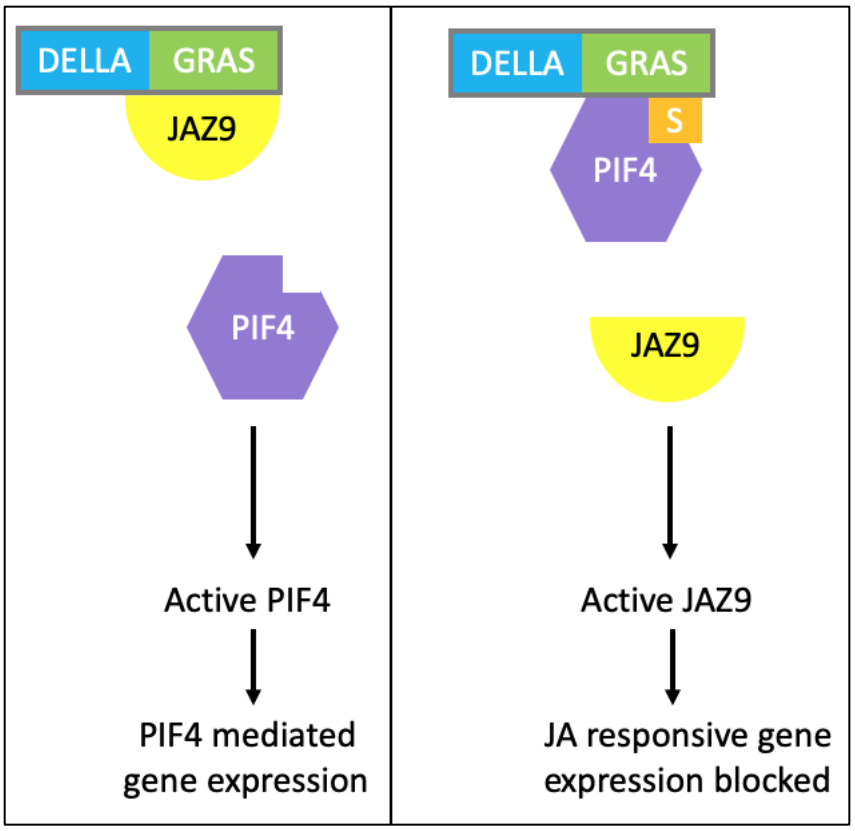

Figure 7.3 Hypothesised model showing the effect of SUMOylation at the GRAS domain of the DELLA protein altering interactions with JAZ9 and PIF4. *When the DELLA protein is not SUMOylated JAZ9 preferentially binds leaving PIF4 active to regulate gene expression. When the DELLA protein is SUMOylated PIF4 preferentially binds due to its SIM site leaving JAZ9 active to negatively regulate the JA pathway.*

7.5 Concluding remarks

This thesis has provided a broad overview of SUMOs involvement in two different hormone pathways, ABA and GA and SUMOs involvement in root hair development. The research conducted has provided insights into the role of SUMO in each individual research strand and has aimed to provide insights into additional experiments that are required. The varied effects SUMO can have on its substrates has been examined further by identifying SUMO and SIM sites in a number of different proteins. The thesis highlights the importance of carefully analysing SUMO phenotypes, which as has been shown in this thesis, can result in complex and in some cases seemingly contradictory phenotypes. Potentially, as with GAI it may prove useful to analyse each SUMO site in PP2CA and RSL4 separately as it is possible each SUMO site may have a different role and alter the respective protein in different ways. Overall it has demonstrated the importance of SUMO in both plant hormone signalling and root hair development.

Appendix

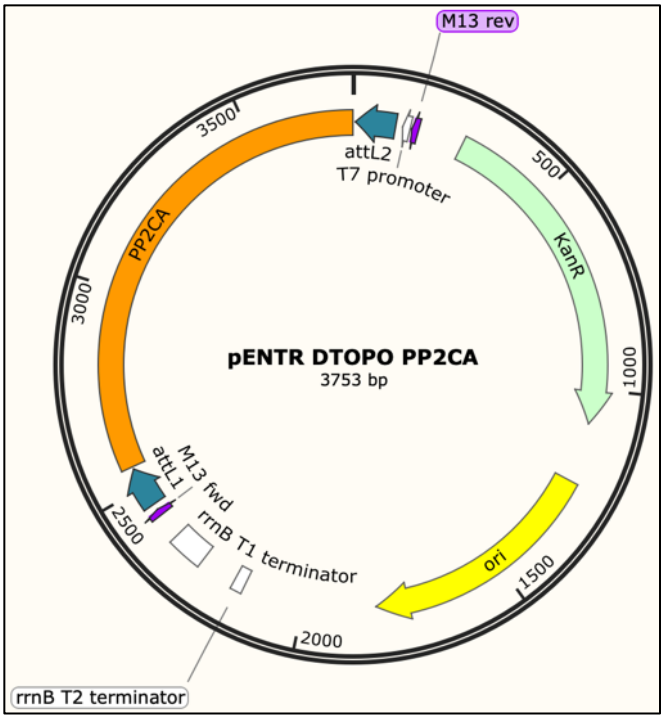

Figure A.2.1 Plasmid map of entry vector pENTR DTOPO PP2CA

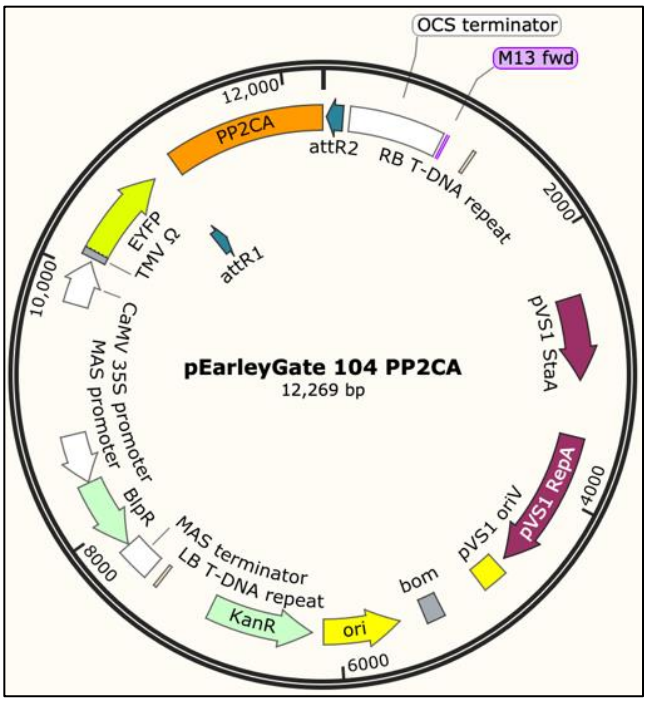

Figure A.2.2 Plasmid map of plant expression vector pEG104 PP2CA

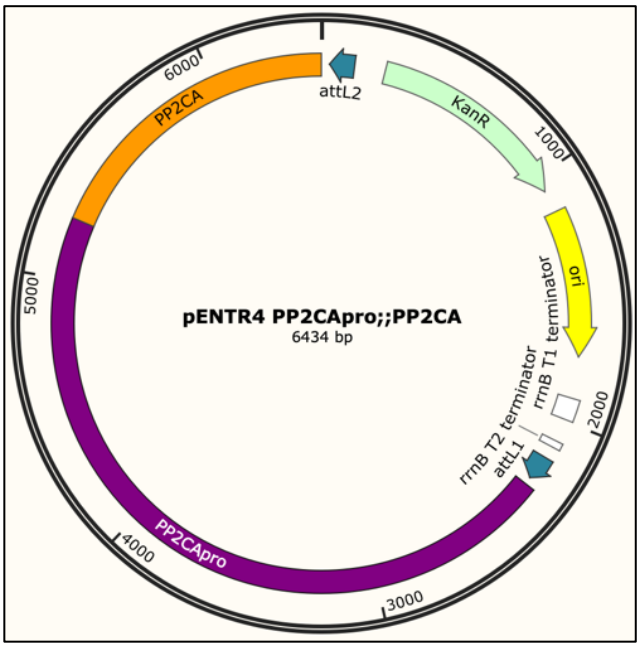

Figure A.2.3 Plasmid map of entry vector pENTR4 PP2CA$_{pro}$;;PP2CA

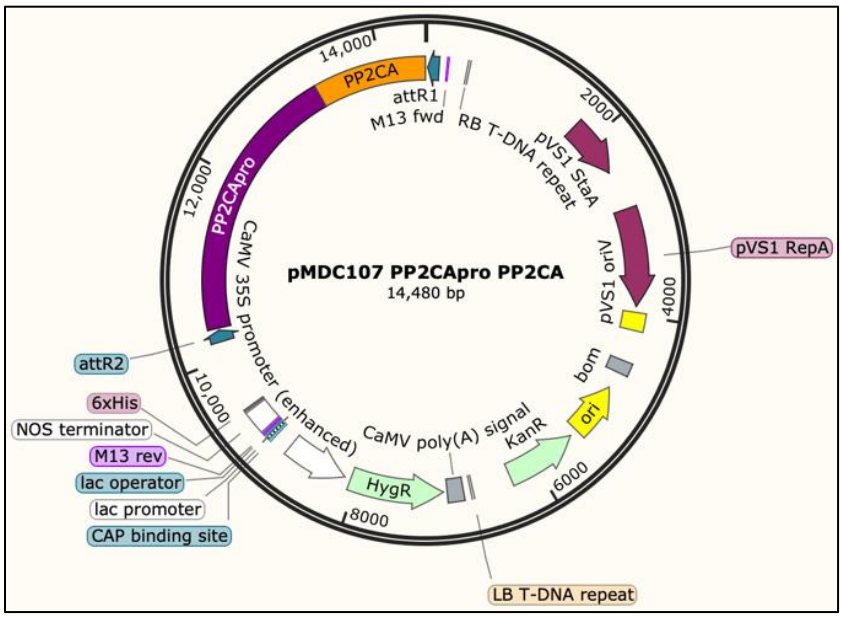

Figure A.2.4 Plasmid map of plant expression vector pMDC107 PP2CA$_{Pro}$;;PP2CA

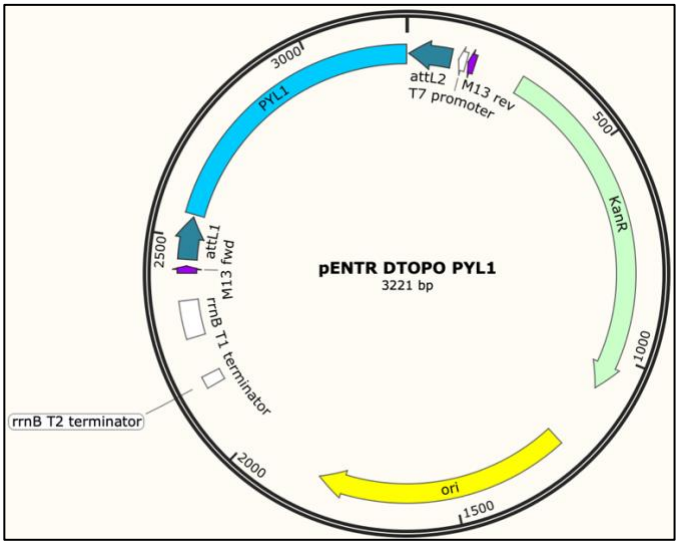

Figure A.2.5 Plasmid map of entry vector pENTR DTOPO PYL1

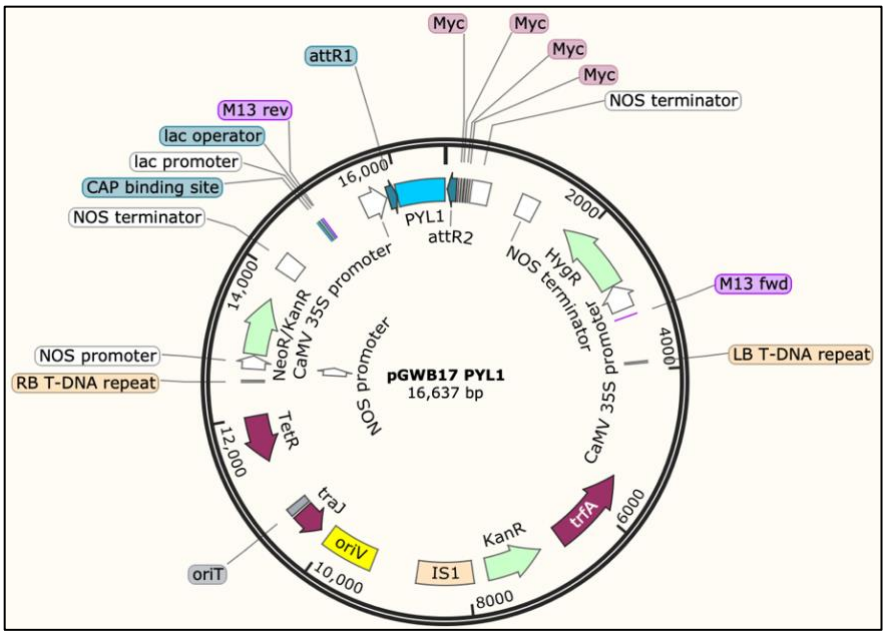

Figure A.2.6 Plasmid map of plant expression vector pGWB17 PYL1

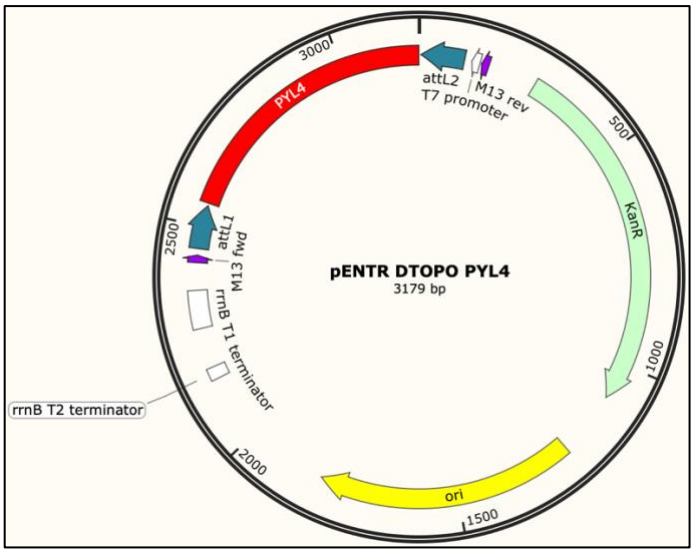

Figure A.2.7 Plasmid map of entry vector pENTR DTOPO PYL4

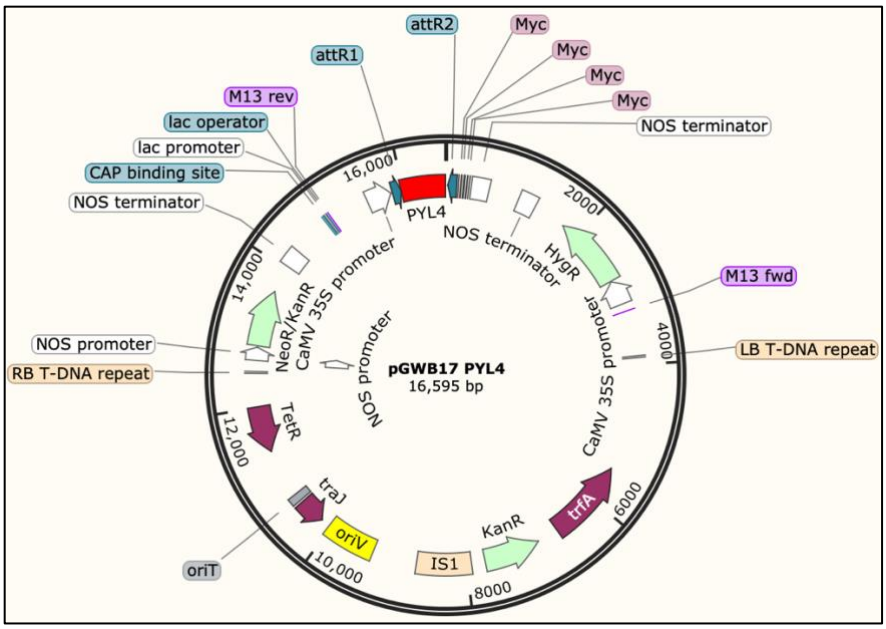

Figure A.2.8 Plasmid map of plant expression vector pGWB17 PYL4

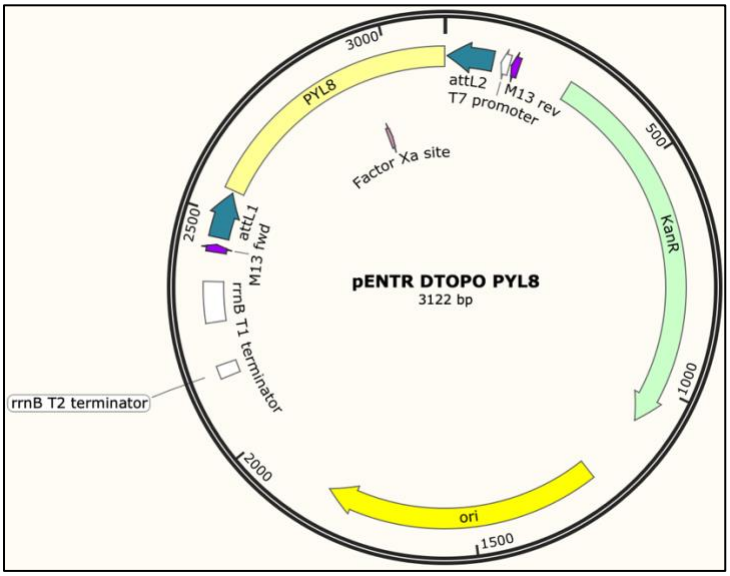

Figure A.2.9 Plasmid map of entry vector pENTR DTOPO PYL8

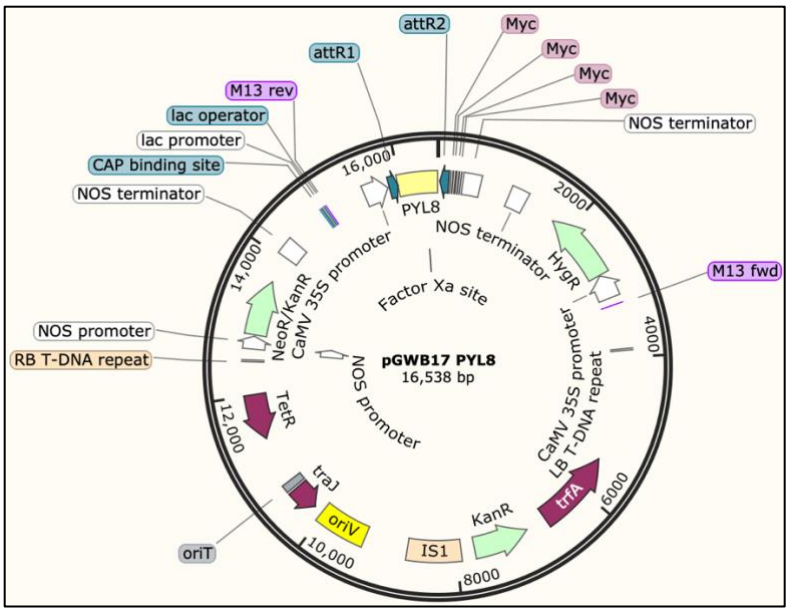

Figure A.2.10 Plasmid map of plant expression vector pGWB17 PYL8

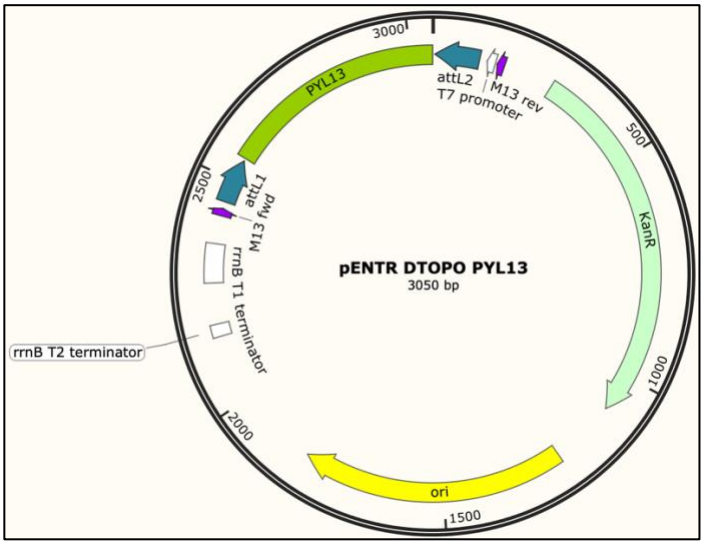

Figure A.2.11 Plasmid map of entry vector pENTR DTOPO PYL13

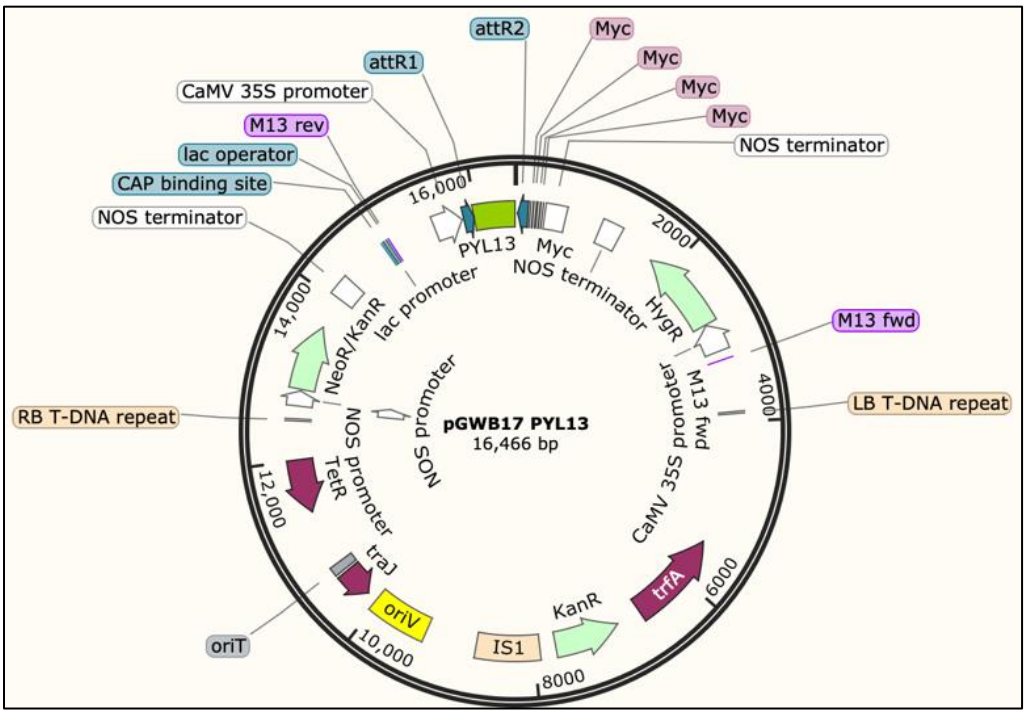

Figure A.2.12 Plasmid map of plant expression vector pGWB17 PYL13

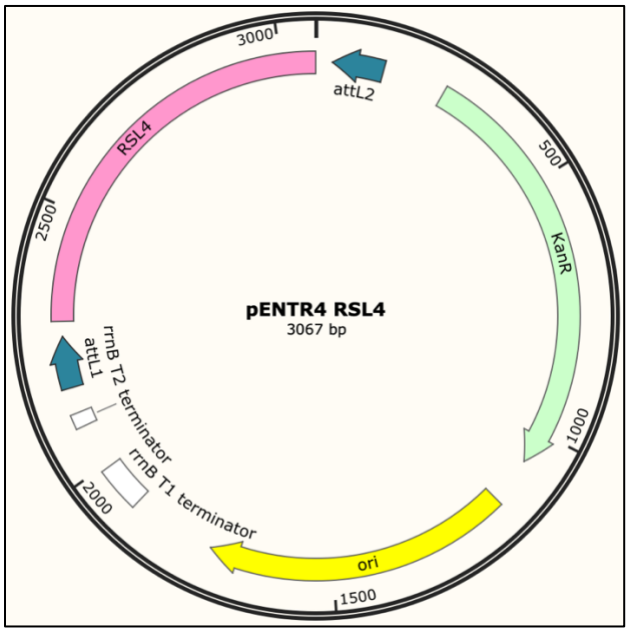

Figure A.2.13 Plasmid map of entry vector pENTR4 RSL4

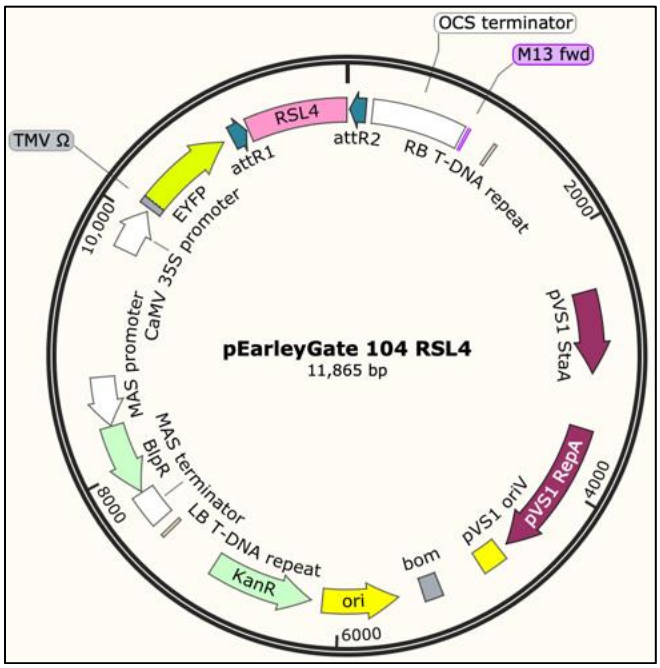

Figure A.2.14 Plasmid map of plant expression vector pEG104 RSL4

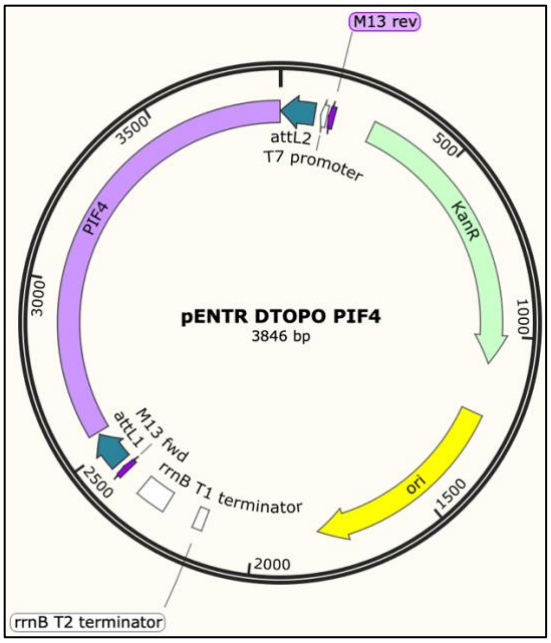

Figure A.2.15 Plasmid map of entry vector pENTR DTOPO PIF4

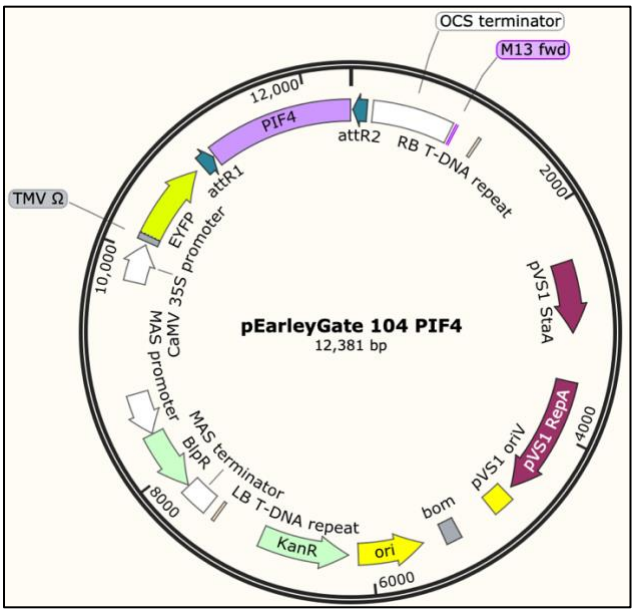

Figure A.2.16 Plasmid map of plant expression vector pEG104 PIF4

Table A.3.1 List of primers used for cloning PP2CA, colony PCR and mutating the gene. *The cloning primers used for PP2CA contain a primer sequence homologous to the start sequence of the gene and a reverse complement of the end sequence of the gene. The forward primer also contains CACC required for cloning in dTOPO cloning vectors. The colony PCR primer sets include one gene primer and one vector sequence. This includes a forward primer sequence from pEG104 (35S promoter) and the reverse primer was homologous to the reverse complement of the end sequence of the gene. The mutation PCR primers spanned the same region of the PP2CA, differing the forward and reverse direction of the primers. Each primer contained approximately 1-3 bp changes from the WT DNA, located in the middle of the primer to aid annealing of the primer to the DNA.*

Gene name	Forward sequence	Reverse sequence	Expected fragment size (bp)
PP2CA	CACCATGGCTGGGATTTGTTGC	CACCGCGGCCGCAAAGACGACGCTTGATTATTCCTCC	1197
PP2CA K179R	GAGACGATGGTTAGGAGTTTTCA	TGAAAACTCCTAACCATCGTCTC	~3500
PP2CA K260R	GATCACAGGCCGGATCGAC	GTCGATCCGGCCTGTGATC	~3500
GFP F + PP2CA R	ATGGGCAAGGGCGAGGAGC	CACCGCGGCCGCAAAGACGACGCTTGATTATTCCTCC	~2100

Table A.3.2 Primer sequences used for qPCR analysis of downstream gene expression*. RT-qpcr primers used for checking the expression of genes in the ABA biosynthetic pathway and genes expressed downstream in the ABA pathway in Arabidopsis transgenics. Each primer contains a sequence homologous to a portion of the gene, which was checked against the Arabidopsis genome, to ensure it would not bind to other non-specific sequences. Before being used in the qPCR reaction the primers were run in a standard PCR and analysed on an agarose gel by electrophoresis size separation to ensure the primers only generated one product of the expected size.*

Gene name	Forward sequence	Reverse sequence	Expected fragment size (bp)
Actin	CTTGCACCAAGCAGCATGAA	CCGATCCAGACACTGTACTTCCTT	68
ABA1	GGCATTTGGTCTAAGGT	CAGACTCGATATCCGCTGGTA	112
AAO3	GGAGTCAGCGAGG	TGCTCCTTCGGTCT	125
NCED3	CGGTGGTTTACGACAAGAACAA	CAGAAGCAATCTGGAGCATCAA	103
RD22	GGTTCGGAAGAAGCGGAGAT	GTGGAAACAGCCCTGACGTG	155
RD29A	GGAAGTGAAAGGAGGAGGAGGAA	CACCACCAAACCAGCCAGATG	134
RD29B	ATGAGACAAAACCAAGCACCTACA	CTGCCCGTAAGCAGTAACAGAT	185
RAB18	CGGGACTGAAGGCTTTGGAA	TCCTCCTCCCTCCTTGTCCA	155

Table A.4.1 List of primers used for cloning PP2CA promoter and generating the fused PP2CA coding region and promoter. *The cloning primers used for amplification of the PP2CA promoter region, a primer sequence homologous to the start sequence of the promoter region and a reverse complement of the end sequence of the promoter region. The overlap primers each binding to the forward and reverse regions of DNA consist of a complement to the end region of the promoter and forward region of the gene. It also consists of primer sequence homologous to the start sequence of the promoter containing the SalI restriction site, for entry in pENTR4 plasmid and primer sequence homologous to the end sequence of PP2CA containing the NotI restriction site, for entry in pENTR4 plasmid.*

Gene name	Forward sequence	Reverse sequence	Expected fragment size (bp)	Restriction enzymes used
PP2CA promoter	CACCGTCGACCACA GCTGGATGCGATGG	TTGATCTCTAACAAA ACTTCTCC	2947	
PP2CA overlap primers	GTAAATTGGAGAAG TTTTGTTAGAGATCA AATGGCTGGGATTT GTTGCGGTG	CCAACAACACCGCA ACAAATCCCAGCCAT TTGATCTCTAACAAA ACTTCTCC	4144	
	CACCGTCGACCACA GCTGGATGCGATGG	CACCGCGGCCGCAA AGACGACGCTTGAT TATTCCTCC	4144	SalI and NotI

Table A.4.2 List of primers used for cloning the PYLs and conducting colony PCR. *The cloning primers used for the PYLs contain a primer sequence homologous to the start sequence of the gene and a reverse complement of the end sequence of the gene. The forward primer also contains CACC required for cloning in dTOPO cloning vectors. The colony PCR primer sets include one gene primer and one vector sequence. This includes a forward primer sequence from pDTOPO (Attb1) and the reverse primer was homologous to the reverse complement of the end sequence of the gene. The mutation PCR primers spanned the same region of the PYL8, differing the forward and reverse direction of the primers. Each primer contained approximately 1-3 bp changes from the WT DNA, located in the middle of the primer to aid annealing of the primer to the DNA.*

Gene name	Forward sequence	Reverse sequence	Expected fragment size (bp)
PYL1	CACCATGGCGAATTCAGAGTCCTCC	CCTAACCTGAGAAGAGTTGTTGTTG	666
PYL8	CACCATGGAAGCTAACGGGATTGAG	GACTCTCGATTCTGTCGTGTC	567
PYL13	CACCATGGAAAGTTCTAAGCAAAAACGATG	CTTCATCATTTTCTTTGTGAGCTTAGC	495
AttB1 + PYL1 R	ACAAGTTTGTACAAAAAAGCAGGCT	CCTAACCTGAGAAGAGTTGTTGTTG	~791
AttB1 + PYL8 R	ACAAGTTTGTACAAAAAAGCAGGCT	GACTCTCGATTCTGTCGTGTC	~692
AttB1 + PYL13 R	ACAAGTTTGTACAAAAAAGCAGGCT	CTTCATCATTTTCTTTGTGAGCTTAGC	~620
PYL8$^{VM/AA}$	GGAAGAATAGGAACAGCTGCGATTGAGTCATTTGTGG	CCACAAATGACTCAATCGCAGCTGTTCCTATTCTTCC	~2867

Table A.5.1 List of primers used for cloning RSL4, colony PCR and mutating the cDNA. *The cloning primers used for RSL4 contain a primer sequence homologous to the start sequence of the gene and a reverse complement of the end sequence of the gene, they also contain restriction sites for entry into the entry vector. The colony PCR primer sets include one gene primer and one vector sequence. This includes a forward primer sequence from pENTR4 (Attb1) and a forward primer sequence from pEG104 (35S promoter) and the reverse primer was homologous to the reverse complement of the end sequence of the gene. The mutation PCR primers spanned the same region of the RSL4, differing the forward and reverse direction of the primers. Each primer contained approximately 1-3 bp changes from the WT DNA, located in the middle of the primer to aid annealing of the primer to the DNA.*

Gene name	Forward sequence	Reverse sequence	Expected fragment size (bp)
RSL4	CACCGCGGCCGCATGGACGTTTTTGTTGATGG	CACCCTCGAGTGCATAAGCCGAGACAAAAGG	777

AttB1 + RSL4 R	ACAAGTTTGTACAAAAAAG CAGGCT	CACCCTCGAGTGCATAAGC CGAGACAAAAGG	~790
35S promoter F + RSL4 R	CTATCCTTCGCAAGACCCT TC	CACCCTCGAGTGCATAAGC CGAGACAAAAGG	~1820
K25R mutation	GTTCATCATCTAGAGAGGA GAGACC	GGTCTCTCCTCTCTAGATG ATGAAC	~3000
K171R mutation	CTAGAGCCACCAGAGGGA CAGCCAC	GTGGCTGTCCCTCTGGTGG CTCTAG	~3000
K205R mutation	GCCAAACGGGACAAGAGT CGATATAAGC	GCTTATATCGACTCTTGTC CCGTTTGGC	~3000

Table A.5.2 Primer sequences used for qPCR analysis of gene expression. *RT-qpcr primers used for checking the expression of GFP and RSL4 in Arabidopsis transgenics. Each primer contains a sequence homologous to a portion of the gene, which was checked against the Arabidopsis genome, to ensure it would not bind to other non-specific sequences. Before being used in the qPCR reaction the primers were run in a standard PCR and analysed on an agarose gel by electrophoresis size separation to ensure the primers only generated one product of the expected size.*

Gene name	Forward sequence	Reverse sequence	Expected fragment size (bp)
Actin 7	CTTGCACCAAGCAGCATGA A	CCGATCCAGACACTGTACT TCCTT	68
GFP	ATGGGCAAGGGCGAGGA GC	GGACTTGAAGAAGTCGTG CTGC	258

Table A.5.3 Primer sequences used for qPCR analysis of downstream gene expression. *RT-qpcr primers used for checking the expression of genes expressed downstream of RSL4 in Arabidopsis transgenics. Each primer contains a sequence homologous to a portion of the gene, which was checked against the Arabidopsis genome, to ensure it would not bind to other non-specific sequences. Before being used in the qPCR reaction the primers were ran in a standard PCR and analysed on an agarose gel by electrophoresis size separation to ensure the primers only generated one product of the expected size.*

Gene name	Forward sequence	Reverse sequence	Expected fragment size (bp)
COW1	ATGCTTCGATTTTTGAGAGCA	TTGTCAATCTTGCAAAGCCTT	437
EXPA7	ATCCCAGTTGCATACCGAAG	TATCCAATTCGTCCGGCTAC	159

EXPA18	GCATGCGGTCAATGTTTCCA	AGAGGTGAGCCGGAACGAGA	447
MRH3	GATGACCTAGACCACCACTAT	GCCTTCAATTCCAGGACTTGAC	141
MRH4	CGAGGGTTGGCTCTGTCC	GGTGGTGATTGTTGTGTTGAC	103
MRH6	TGGTTGTTGTGGACACAACTTC	GCCAAGAGCCAGAAATCTTTG	493
PRP3	CGTCTCCTCCTCTCTCCATACG	CCGTATGATGCTGGGTCGGAAC	175
RHS4	CCTCCTCCTAGAGACTCCACC	GCTTGTTCTTTCCGAAGCCAGG	193
RHS18	GTTACTCTTGCAAGCGGAGG	GGCGCTTAGTTCTTCGACC	294
RSL4	GTGCCAAACGGGACAAAAGT	TTGTGATGGAACCCCATGTC	158

Table A.6.1 List of primers used for PIF4 cloning. *The gene names corresponding to the gene of interest coding DNA. Primer sets consisted of one gene primer and one vector sequence. The PIF4 forward cloning primer starts with CACC, required for cloning in dTOPO cloning vectors. For PIF4 the forward primer was taken from the GFP sequence of pEG104 and reverse complement of PIF4. The forward primer of the 35S promoter was taken from pGWB14 sequence.*

Gene name	Forward sequence	Reverse sequence	Expected fragment size (bp)
PIF4	CACCATGGAACACCAAGGTTGGAGTTTTG	CTAGTGGTCCAAACGAGAACCG	1293
35S promoter F + PIF4 R	CTATCCTTCGCAAGACCCTTC	CTAGTGGTCCAAACGAGAACCG	1785
GFP F + PIF4 R	ATGGGCAAGGGCGAGGAGC	CTAGTGGTCCAAACGAGAACCG	2196
GAI F + GAI R	ATGAAGAGAGATCATCATCATCATCATC	CTAATTGGTGGAGAGTTTCCAAGC	1602

Table A.6.2 Primer sequences used for qPCR analysis of downstream GA and JA gene expression*. RT-qpcr primers used for checking the expression of gene expressed in the downstream pathways of GA and JA. Each primer contains a sequence homologous to a portion of the gene, which was checked against the Arabidopsis genome, to ensure it would not bind to other non-specific sequences. Before being used in the qPCR reaction the primers were ran in a standard PCR and analysed on an agarose gel by electrophoresis size separation to ensure the primers only generated one product of the expected size.*

Gene name	Forward sequence	Reverse sequence	Expected

			fragment size (bp)
ATHB2	CAAATCCATCTGTTTCTGTTACTCC	TGTGACGAATCTGAGTTTGGA	109
EXP8	CGCGTGCTATGAGATGAAGT	AAGAGGAGGATTGCACCAAC	136
LTP3	GTGGGTTGGTGCCACCTTCA	TCACTTGATGTTGTTGCAGT	218
XTR7	AAGGAGCAACACATGACGAG	GGGTCTCCAGACAATGGAGT	173
B-CHI	CCATGCGCATCTGGCAAACG	GGTTTGGGAGGCTGAGCAGTC	188
LOX2	AATGAGCCTGTTATCAATGC	CATACTTAACAACACCAGCTCC	130
PDF1.2	ACCCTTATCTTCGCTGCTC	TCCTTCAAGGTTAATGCACTG	153
TAT1	CTTGAACTCGTTGAAGAACTCTTCG	AGAGATTCAGCTTAACCATCATTGC	119

References

An F, Zhang X, Zhu Z, Ji Y, He W, Jiang Z, Li M, Guo H. (2012). Coordinated regulation of apical hook development by gibberellins and ethylene in etiolated Arabidopsis seedlings. Cell Res. 22, 915-927.

Antoni R, Gonzalez-Guzman M, Rodriguez L, Rodrigues A, Pizzio G A, Rodriguez P L. (2012). selective inhibition of clade A phosphatases type 2C by PYR/PYL/RCAR abscisic acid receptors. Plant Physiol. 158, 970–980. doi: 10.1104/pp.111.188623.

Augustine RC, York SL, Rytz TC, Vierstra RD. (2016). Defining the SUMO system in maize: SUMOylation is up-regulated during endosperm development and rapidly induced by stress. Plant Physiology 171, 2191–2210.

Bai MY, Shang JX, Oh E, Fan M, Bai Y, Zentella R, Sun TP, Wang ZY. (2012). Brassinosteroid, gibberellin and phytochrome impinge on a common transcription module in Arabidopsis. Nature Cell Biology 14, 810–817.

Bailey M, Srivastava A, Conti L, Nelis S, Zhang C, Florance H., et al. (2016). Stability of small ubiquitin-like modifier (SUMO) proteases OVERLY TOLERANT TO SALT1 and -2 modulates salicylic acid signalling and SUMO1/2 conjugation in Arabidopsis thaliana. J. Exp. Bot. 67, 353–363. doi: 10.1093/jxb/erv468.

Balcerowicz D, Schoenaers S, Vissenberg K. (2015) Cell Fate Determination and the Switch from Diffuse Growth to Planar Polarity in Arabidopsis Root Epidermal Cells. Front Plant Sci. 6:1163.

Baluška F, Salaj J, Mathur J, Braun M, Jasper F, Šamaj J, Chua N-H, Barlow PW, Volkmann D. (2000). Root hair formation: F-actin-dependent tip growth is initiated by local assembly of profiling-supported F-actin meshworks accumulated within expansin-enriched bulges. Dev Biol. 227: 618-632. 10.1006/dbio.2000.9908.

Barrero JM, Millar AA, Griffiths J, Czechowski T, Scheible WR, Udvardi M, Reid JB, Ross J, Jacobsen JV, Gubler F. (2010). Gene expression profiling identifies two regulatory genes controlling dormancy and ABA sensitivity in Arabidopsis seeds. Plant J. 61:611–622.

Bartetzko V, Sonnewald S, Vogel F, Hartner K, Stadler R, Hammes UZ, et al. (2009). The Xanthomonas campestris pv. Mol. Plant Microbe Interact. 22 (6), 655–664. doi: 10.1094/MPMI-22-6-0655.

Bates T and Lynch J (2000). Plant growth and phosphorus accumulation of wild type and two root hair mutants of Arabidopsis thaliana (Brassicaceae).Amer. J. Bot. 87, 958–963.

Bates T R and Lynch J P (1996). Stimulation of root hair elongation in Arabidopsis thaliana by low phosphorus availability.Plant Cell Environ. 19, 529–538.

Belin C, De Franco PO, Bourbousse C, Chaignepain S, Schmitter JM, Vavasseur A, et al. (2006). Identification of features regulating OST1 kinase activity and OST1 function in guard cells. Plant Physiol. 141:1316–1327.

Benlloch R, Lois LM. (2018). Sumoylation in plants: mechanistic insights and its role in drought stress. J. Exp. Bot. 69, 4539–4554. doi: 10.1093/jxb/ery233.

Bergendahl V, Glaser BT, Burgess RR. (2003). A fast Western blot procedure improved for quantitative analysis by direct fluorescence labeling of primary antibodies. Journal of immunological methods. 277(1–2):117–125.

Berger F, Haseloff J, Schiefelbein J, Dolan L. (1998b). Positional information in root epidermis is defined during embryogenesis and acts in domains with strict boundaries. Curr. Biol. 81(1):421–430.

Berger F, Hung CY, Dolan L, Schiefelbein J. (1998a). Control of cell division in the root epidermis of Arabidopsis thaliana. Dev. Biol. 194, 235-245. doi:10.1006/dbio.1997.8813.

Bernardo-García S, de Lucas M, Martínez C, Espinosa-Ruiz A, Davière JM, Prat S. (2014). BR-dependent phosphorylation modulates PIF4 transcriptional activity and shapes diurnal hypocotyl growth. Genes Dev 28: 1681–1694.

Bernhardt C, Lee MM, Gonzalez A, Zhang F, Lloyd A, Schiefelbein J. (2003). The bHLH genes GLABRA3 (GL3) and ENHANCER OF GLABRA3 (EGL3) specify epidermal cell fate in the Arabidopsis root. Development 130,6431 -6439.

Bhaskara GB, Nguyen TT, Verslues PE. (2012). Unique drought resistance functions of the highly ABA-induced clade A protein phosphatase 2Cs. Plant Physiol. 160:379–395.

Bhosale R, et al. (2018). A mechanistic framework for auxin dependent Arabidopsis root hair elongation to low external phosphate. Nat. Commun. https://doi.org/10.1038/s41467-018-03851-3.

Bibikova TN, Jacob T, Dahse I, Gilroy S. (1998). Localised changes in apoplastic and cytoplasmic pH are associates with root hair development in Arabidopsis thaliana. Development. 125: 2925-2934.

Blanco-Tourinan N, Serrano-Mislata A, Alabadi D. (2020). Regulation of DELLA proteins by post-translational modifications. Plant Cell Phys. 61(11):1891-1901.

Bolle C. (2004). The role of GRAS proteins in plant signal transduction and development. Planta 218: 683–692.

Brandt B, Brodsky DE, Xue S, Negi J, Iba K, Kangasjärvi J, Ghassemian M, Stephan AB, Hu H, Schroeder JI. (2012). Reconstitution of abscisic acid activation of SLAC1 anion channel by CPK6 and OST1 kinases and branched ABI1 PP2C phosphatase action. Proceedings of the National Academy of Sciences of USA. 109:10593–10598. doi: 10.1073/pnas.1116590109.

Brown LK, George TS, Dupuy LX, White PJ. (2013). A conceptual model of root hair ideotypes for future agricultural environments: what combination of traits should be targeted to cope with limited P availability? Ann Bot. 112(2): 317-330.

Camut L, Davière JM, Achard P. (2017). Dynamic Regulation of DELLA Protein Activity: SPINDLY and SECRET AGENT Unmasked! Mol Plant 10, 785–787.

Cao XF, Linstead P, Berger F, Kieber J, Dolan L. (1999). Differential ethylene sensitivity of epidermal cells is involved in the establishment of cell pattern in the Arabidopsis root. Physiol. Plant. 106:311–317.

Caro E, Castellano MM, and Gutierrez C. (2007). A chromatin link that couples cell division to root epidermis patterning in Arabidopsis. Nature 447, 213–217. doi: 10.1038/nature05763.

Carol RJ, Dolan L. (2002). Building a hair: tip growth in Arabidopsis thaliana root hairs. Philosophical Transactions of the Royal Society of London Series B: Biological Sciences 357: 815–821.

Casson SA, et al. (2009). Phytochrome B and PIF4 regulate stomatal development in response to light quantity. Curr. Biol. 19, 229–234.

Castaño-Miquel L, Mas A, Teixeira I, et al. (2017). SUMOylation inhibition mediated by disruption of SUMO E1–E2 interactions confers plant susceptibility to necrotrophic fungal pathogens. Molecular Plant 10, 709–720.

Castaño-Miquel L, Seguí J, Lois LM. (2011). Distinctive properties of Arabidopsis SUMO paralogues support the in vivo predominant role of AtSUMO1/2 isoforms. Biochem. J. 436:581–590. doi: 10.1042/BJ20101446.

Castro PH, Bachmair A, Bejarano ER, Coupland G, Lois LM, Sadanandom A, et al. (2018). Revised nomenclature and functional overview of the ULP gene family of plant deSUMOylating proteases. J. Exp. Bot. 69 (19), 4505–4509. doi: 10.1093/jxb/ery301.

Castro PH, Couto D, Freitas S, Verde N, Macho AP, Huguet S, et al. (2016). SUMO proteases ULP1c and ULP1d are required for development and osmotic stress responses in Arabidopsis thaliana. Plant Mol. Biol. 92, 143–159. doi: 10.1007/s11103-016-0500-9.

Cherel I, Michard E, Platet N, Mouline K, Alcon C, Sentenac H, Thibaud JB (2002). Physical and functional interaction of the Arabidopsis K(+) channel AKT2 and phosphatase AtPP2CA. Plant Cell 14: 1133–1146.

Chini A, Fonseca S, Fernandez G, Adie B, Chico JM, Lorenzo O, Garcia-Casado G, Lopez-Vidriero I, Lozano FM, Ponce MR, Micol JL, Solano R. (2007). The JAZ family of repressors is the missing link in jasmonate signalling. Nature 448 666–671.

Choi H., Oh E. (2016). PIF4 integrates multiple environmental and hormonal signals for plant growth regulation in Arabidopsis. Mol. Cells 39, 587–593.

Chosed R, Mukherjee S, Lois LM, Orth K. (2006). Evolution of a signalling system that incorporates both redundancy and diversity: Arabidopsis SUMOylation. Biochem. J. 398, 521–529. doi: 10.1042/BJ20060426.

Clough SJ, Bent AF, (1998). Floral dip: a simplified method for Agrobacterium-mediated transformation of Arabidopsis thaliana. Plant J, 16(6), pp. 735-743.

Clowes L. (2000). Pattern in root meristem development in angiosperms. New Phytologist 146,83 –94.

Colby T, Matthäi A, Boeckelmann A, Stuible HP. (2006). SUMO-conjugating and SUMO-deconjugating enzymes from Arabidopsis. Plant Physiol. 142 (1), 318–332. doi: 10.1104/pp.106.085415.

Conibear AC. (2020) Deciphering protein post-translational modifications using chemical biology tools. Nat Rev Chem. 4 674-695.

Conti L, Nelis S, Zhang C, Woodcock A, Swarup R, Galbiati M, et al. (2014). Small ubiquitin-like modifier protein SUMO enables plants to control growth independently of the phytohormone gibberellin. Dev. Cell 28, 102–110. doi: 10.1016/j.devcel.2013.12.004.

Conti L, Price G, O'Donnell E, Schwessinger B, Dominy P, Sadanandom A. (2008). Small ubiquitin-like modifier proteases OVERLY TOLERANT TO SALT1 and -2 regulate salt stress responses in Arabidopsis. Plant Cell 20 (10), 2894–2908. doi: 10.1105/tpc.108.058669.

Costa S, Dolan L. (2003). Epidermal patterning genes are active during embryogenesis in Arabidopsis. Development 130, 2893–2901.

Costa S, Shaw P. (2006). Chromatin organization and cell fate switch respond to positional information in Arabidopsis. Nature 439: 493–496.

Cutler SR, Rodriguez PL, Finkelstein RR, Abrams SR. (2010) Abscisic acid: Emergence of a core signaling network. Ann. Rev. Plant Biol. 61:651–679.

Datta SP, Prescott H, Dolan L. (2015). Intensity of a pulse of RSL4 transcription factor synthesis determines Arabidopsis root hair cell size. Nat. Plants 1, 15138. doi:10.1038/nplants.2015.138.

Davière JM, Achard P (2016). A pivotal role of DELLAs in regulating multiple hormone signals. Mol Plant 9:10–20.

de la Torre C, Diez JL, Lopez-Saez JF, Gimenez Martin G. (1972). Eịect of abscisic acid on the cytological components of the root growth. Cytologia 37, 197^205.

de Lucas M, Davière JM, Rodríguez-Falcón M, Pontin M, Iglesias-Pedraz JM, Lorrain S, Fankhauser C, Blázquez MA, Titarenko E, Prat S. (2008). A molecular framework for light and gibberellin control of cell elongation. Nature 451: 480–484.

Deslandes L, Olivier J, Peeters N, Feng DX, Khounlotham M, Boucher C, et al. (2003). Physical interaction between RRS1-R, a protein conferring resistance to bacterial wilt, and PopP2, a type III effector targeted to the plant nucleus. Proc. Natl. Acad. Sci. 100, 8024–8029. doi: 10.1073/pnas.1230660100.

Dharmasiri N, Dharmasiri S, Weijers D, Lechner E, Yamada M, Hobbie L, Ehrismann J, Jürgens G, Estelle M. (2005). Plant development is regulated by a family of auxin receptor F box proteins. Dev. Cell 9 109–119.

Di Cristina M, Sessa G, Dolan L et al. (1996). The Arabidopsis Athb-10 (GLABRA2) is an HD-Zip protein required for regulation of root hair development. Plant J 10:393–402. https://doi.org/10.1046/j.1365-313X.1996.10030393.x.

Dill A, Sun T-P. (2001). Synergistic derepression of Gibberellin signalling by removing RGA and GAI function in *Arabidopsis thaliana*. Genetics 159 (2): 777-785.

Dolan L. (1996). Pattern in the root epidermis: an interplay of diffusible signals and cellular geometry. Annals of Botany 77, 547–553.

Dolan L, Costa S. (2001). Evolution and genetics of root hair stripes in the root epidermis. J. Exp. Bot. 52, 413-417. doi:10.1093/jexbot/52.suppl_1.413.

Dolan L, Duckett CM, Grierson C, Linstead P, Schneider K, Lawson E, Dean C, Poethig S, Roberts K. (1994). Clonal relationships and cell patterning in the root epidermis of Arabidopsis. Development 120, 2465-2474.

Drabikowski K, Ferralli J, Kistowski M, Oledzki J, Dadlez M, Chiquet-Ehrismann R. (2018). Comprehensive list of SUMO targets in Caenorhabditis elegans and its implication for evolutionary conservation of SUMO signaling. Sci. Rep. 8 (1), 1139. doi: 10.1038/s41598-018-19424-9.

Duda DM, et al. (2007). Structure of a SUMO-binding-motif mimic bound to Smt3p-Ubc9p: conservation of a non-covalent ubiquitin-like protein-E2 complex as a platform for selective interactions within a SUMO pathway. J Mol Biol. 369:619–630.

Elrouby N, Bonequi MV, Porri A, Coupland G. (2013). Identification of Arabidopsis SUMO-interacting proteins that regulate chromatin activity and developmental transitions. Proc. Natl. Acad. Sci. 110, 19956–19961. doi: 10.1073/pnas.1319985110

Feng S, Martínez C, Gusmaroli G, Wang Y, Zhou J, Wang F, Chen L, Yu L, Iglesias-Pedraz JM, Kircher S et al. (2008). Coordinated regulation of Arabidopsis thaliana development by light and gibberellins. Nature 451: 475–479.

Ferre-D'Amare AR, Pognonec P, Roeder RG, Burley SK. (1994). Structure and function of the b/HLH/Z domain of USF. EMBO J. 13, 180–189.

Finkelstein R. (2013). Abscisic acid synthesis and response. Arabidopsis Book 11: e0166.

Fohse D, Jungk A. (1983). Influence of phosphate and nitrate supply on root hair formation of rape, spinach and tomato plants. Plant Soil 74, 359–368.

Foreman J, Dolan L. (2001). Root hairs as a model system for studying plant cell growth. Ann. Bot. 88, 1–7.

Franciosini A, Rymen B, Shibata M, Favero DS, Sugimoto K. (2017). Molecular networks orchestrating plant cell growth. Curr. Opin. Plant Biol. 35, 98–104.

Freshour G, Clay RP, Fuller MS, Albersheim P, Darvill AG, Hahn MG. (1996). Developmental and tissue-specific structural alterations of the cell-wall polysaccharides of Arabidopsis thaliana roots. Plant Physiol. 110:1413–1429.

Fuchs S, Tischer SV, Wunschel C, Christmann A, Grill E. (2014). Abscisic acid sensor RCAR7/PYL13, specific regulator of protein phosphatase coreceptors. Proc. Natl. Acad. Sci. U.S.A. 111, 5741–5746. 10.1073/pnas.1322085111.

Fujii H, Verslues PE, Zhu JK. (2011) Arabidopsis decuple mutant reveals the importance of SnRK2 kinases in osmotic stress responses in vivo, Proceedings of the National Academy of Sciences, USA, vol. 108 (pg. 1717-1722).

Fujii H, Zhu JK. (2009) Arabidopsis mutant deficient in 3 abscisic acid-activated protein kinases reveals critical roles in growth, reproduction, and stress. Proc. Natl. Acad. Sci. USA, 106, 8380–8385.

Fujimori T, Yamashino T, Kato T, Mizuno T. (2004). Circadian-controlled basic/helix-loop-helix factor, PIL6, implicated in light-signal transduction in Arabidopsis thaliana. Plant Cell Physiol. 45 : 1078–1086.

Fujita Y, Fujita M, Shinozaki K, Yamaguchi-Shinozaki K. (2011). ABA-mediated transcriptional regulation in response to osmotic stress in plants. J. Plant. Res. 124, 509–525.

Fujita Y, Nakashima K, Yoshida T, Katagiri T, Kidokoro S, Kanamori N, Umezawa T, et al (2009). Three SnRK2 protein kinases are the main positive regulators of abscisic acid signaling in response to water stress in Arabidopsis. Plant Cell Physiol. 50, 2123–2132.

Fukazawa J, Mori M, Watanabe S, Miyamoto C, Ito T, Takahashi Y. (2017). DELLA-GAF1 complex is a main component in gibberellin feedback regulation of GA 20-oxidase2. Plant Physiol. 175: 1395–1406.

Gahoonia T S, Nielsen N E. (2003). Phosphorus (P) uptake and growth of root hairless barley mutant (bald root barley, brb) and wild type in low-and high-P soils. Plant Cell Environ 26:1759–1766.

Gahoonia T S, Care D, Nielsen N E. (1997). Root hairs and acquisition of phosphorus by wheat and barley cultivars. Plant Soil 191, 181-188.

Galway ME, Masucci JD, Lloyd AM, Walbot V, Davis RW, Schiefelbein JW. (1994). The TTG gene is required to specify epidermal cell fate and cell patterning in the Arabidopsis root. Dev Biol 166: 740–754.

Gangappa SN, Berriri S, Kumar SV. (2017). PIF4 coordinates thermosensory growth and immunity in Arabidopsis. Curr. Biol. 27:243–249.

Gareau JR, Lima CD. (2010). The SUMO pathway: emerging mechanisms that shape specificity, conjugation and recognition. Nature Reviews in Molecular Cell Biology. 11:861–871.

Geer LY, Marchler-Bauer A, Geer RC, Han L, He J, He S, Liu C, Shi W, Bryant SH. (2010). The NCBI BioSystems database. Nucleic. Acids Res. 38(Database Issue):D492–D496.

Ghassemian M, Nambara E, Cutler S, Kawaide H, Kamiya Y, McCourt P. (2000). Regulation of abscisic acid signaling by the ethylene response pathway in Arabidopsis. Plant Cell 12, 1117–2000. 10.1105/tpc.12.7.1117.

Ghimire S, Tang N, Liu W, Qi X, Fu X, Si H. (2020). Genomic Analysis of the SUMO-Conjugating Enzyme and Genes under Abiotic Stress in Potato (Solanum tuberosum L.) Int J Genomics un 24;2020:9703638. doi: 10.1155/2020/9703638. eCollection 2020.

Giaever G., Chu AM, Ni L, Connelly C, Riles L, Veronneau S, et al. (2002). Functional profiling of the Saccharomyces cerevisiae genome. Nature 418, 387–391. doi: 10.1038/nature00935.

Gillies J, Hochstrasser MA. (2012). New class of SUMO proteases. EMBO Rep. 13, 284–285. doi: 10.1038/embor.2012.34.

Gish W, States DJ. (1993). Identification of Protein Coding Regions by Database Similarity Search. Nat. Genet. 3:266–272. doi: 10.1038/ng0393-266.

Gonçalves NM, Fernandes T, Nunes C, Rosa MTG, Matiolli CC, Rodrigues MAA, Barros PM, Oliveira MM, Abreu IA. (2020). SUMOylation of rice DELLA SLR1 modulates transcriptional responses and improves yield under salt stress. Mar 12 bioRxiv DOI: 10.1101/2020.03.10.986224 PPR: PPR117032.

Gou M, Huang Q, Qian W, Zhang Z, Jia Z, Hua J. (2017). Sumoylation E3 ligase SIZ1 modulates plant immunity partly through the immune receptor gene SNC1 in Arabidopsis Mol. Plant Microbe Interact., 30, pp. 334-342.

Grantham R. (1974). Amino acid difference formula to help explain protein evolution. Science 185: 862–864.

Grierson C, Nielsen E, Ketelaarc T, Schiefelbein J. (2014). Root hairs. Arabidopsis Book. https://doi.org/10.1199/tab.0172.

Grierson C, Schiefelbein J. (2002). Root hairs. Arabidopsis Book. 1:e0060. doi: 10.1199/tab.0060.

Griffiths J, Murase K, Rieu I, Zentella R, Zhang ZL, Powers SJ, Gong F, Phillips AL, Hedden P, Sun TP, Thomas SG. (2006). Genetic characterization and functional analysis of the GID1 gibberellin receptors in Arabidopsis. Plant Cell 18: 3399–3414.

Hao Q, Yin P, Li W, Wang L, Yan C, Lin Z, Wu JZ et al. (2011). The molecular basis of ABA-independent inhibition of PP2Cs by a subclass of PYL proteins. Mol. Cell, 42, 662–672.

Hassan H, Scheres B, Blilou I. (2010). JACKDAW controls epidermal patterning in the Arabidopsis root meristem through a non-cell-autonomous mechanism. Development 137, 1523-1529. doi:10.1242/dev.048777.

Hay RT. (2005). SUMO: a history of modification. Mol. Cell 18, 1–12. doi: 10.1016/j.molcel.2005.03.012.

Hecker CM, Rabiller M, Haglund K, Bayer P, Dikic I. (2006). Specification of SUMO1- and SUMO2-interacting motifs. J Biol Chem 281: 16117–16127.

Hedden P. (2003). The genes of the Green Revolution. Trends Genet. 19:5–9. doi: 10.1016/S0168-9525(02)00009-4.

Hermkes R, Fu YF, Nürrenberg K, Budhiraja R, Schmelzer E, Elrouby N, et al. (2011). Distinct roles for Arabidopsis SUMO protease ESD4 and its closest homolog ELS1 . Planta 233 (1), 63–73. doi: 10.1007/s00425-010-1281-z.

Hickey CM, Wilson NR, Hochstrasser M. (2012). Function and regulation of SUMO proteases. Nat. Rev. Mol. Cell Biol. 13, 755–766. doi: 10.1038/nrm3478.

Himmelbach A, Hoffmann T, Leube M, Hohener B, Grill E. (2002). Homeodomain protein ATHB6 is a target of the protein phosphatase ABI1 and regulates hormone responses in Arabidopsis. EMBO J. 21, 3029–3038.

Høgh-Jensen H, Pedersen MB. (2003). Morphological plasticity by crop plants and their potassium use efficiency. Journal of Plant Nutrition 26, 969–984.

Hooper CM, Castleden I, Tanz SK, Aryamanesh, Millar AH. (2017). SUBA4: the interactive data analysis centre for Arabidopsis subcellular protein locations Nucleic Acids Res. Jan 4;45(D1):D1064-D1074. doi: 10.1093/nar/gkw1041.

Hotson A, Chosed R, Shu H, Orth K, Mudgett MB. (2003). Xanthomonas type III effector XopD targets SUMO-conjugated proteins in planta. Mol. Microbiol. 50, 377–389. doi: 10.1046/j.1365-2958.2003.03730.x.

Hotson A, Mudgett MB. (2004). Cysteine proteases in phytopathogenic bacteria: identification of plant targets and activation of innate immunity. Curr. Opin. Plant Biol. 7, 384–390. doi: 10.1016/j.pbi.2004.05.003.

Hou X, Lee LYC, Xia K, Yan Y, Yu H. (2010). DELLAs modulate jasmonate signaling via competitive binding to JAZs. Dev. Cell 19 884–894. 10.1016/j.devcel.2010.10.024.

Huang L, Yang S, Zhang S, Liu M, Lai J, et al. (2009). The Arabidopsis SUMO E3 ligase AtMMS21, a homologue of NSE2/MMS21, regulates cell proliferation in the root. Plant J 60: 666–678.

Huq E, Al-Sady B, Hudson M, Kim C, Apel K, Quail PH. (2004). Phytochrome-interacting factor 1 is a critical bHLH regulator of chlorophyll biosynthesis. Science, 305: 1937-1941.

Hussain A, Cao DN, Cheng H, Wen ZL, Peng JR (2005). Identification of conserved Ser/Thr residues important for gibberellin-sensitivity of Arabidopsis RGL2 protein. Plant J 44: 88–99.

Jacobsen SE, Olszewski NE. (1993). Mutations at the SPINDLY locus of Arabidopsis alter gibberellin signal transduction. Plant Cell. Aug;5(8):887–896.

Jin JB, Jin YH, Lee J, Miura K, Yoo CY, Kim WY, et al. (2008). The SUMO E3 ligase, AtSIZ1, regulates flowering by controlling a salicylic acid-mediated floral promotion pathway and through effects on FLC chromatin structure, Plant J., vol. 53 (pg. 530-540).

Johnson ES. (2004). Protein modification by SUMO. Annu. Rev. Biochem. 73, 355–382. doi: 10.1146/annurev.biochem.73.011303.074118.

Kang YH, Kirik V, Hulskamp M, Nam KH, Hagely K, Lee MM, Schiefelbein J. (2009). The MYB23 gene provides a positive feedback loop for cell fate specification in the Arabidopsis root epidermis. Plant Cell 21, 1080-1094. doi:10.1105/tpc.108.063180.

Karssen CM, Brinkhorst-van der Swan DLC, Breekland AE, Koornneef M. (1983). Induction of dormancy during seed development by endogenous abscisic acid: studies on abscisic acid deficient genotypes of Arabidopsis thaliana (L.) Heynh. Planta 157, 158-165.

Kasuga M, Miura S, Shinozaki K, Yamaguchi-Shinozaki K. (2004) A combination of the Arabidopsis DREB1A gene and stress-inducible rd29A promoter improved drought- and low-temperature stress tolerance in tobacco by gene transfer. Plant Cell Physiol 45: 346–350.

Katagiri F, Thilmony R, He SY. (2002). The Arabidopsis Thaliana Pseudomonas Syringae Interaction. The Arabidopsis Book, 20(1):e0039.

Ketelaar T, Faivre-Moskalenko C, Esseling JJ, De Ruijter NCA, Grierson CS, Dogterom M, Emons AMC. (2002). Positioning of nuclei in Arabidopsis root hairs: an actin-regulated process of tip growth. Plant Cell. 14:2941–2955.

Kieber JJ, Rothenberg M, Roman G, Feldman KA, Ecker JR. (1993). CTR1, a negative regulator of the ethylene response pathway in Arabidopsis, encodes a member of the Raf family of protein kinases. Cell. 72:427–441.

Kim JG, Stork W, Mudgett MB. (2013). Xanthomonas type III effector XopD desumoylates tomato transcription factor SlERF4 to suppress ethylene responses and promote pathogen growth. Cell Host Microbe 13, 143–154. doi: 10.1016/j.chom.2013.01.006.

Kirik V, Simon M, Huelskamp M, Schiefelbein J. (2004). The ENHANCER OF TRY AND CPC1 gene acts redundantly with TRIPTYCHON and CAPRICE in trichome and root hair cell patterning in Arabidopsis. Dev. Biol. 268:506–513.

Kong L, Cheng J, Zhu Y. et al. (2015). Degradation of the ABA co-receptor ABI1 by PUB12/13 U-box E3 ligases. Nat. Commun. 6, 8630.

Kong, X., Luo, X., Qu, G. P., Liu, P., Jin, J. B. (2017). Arabidopsis SUMO protease ASP1 positively regulates flowering time partially through regulating FLC stability. *J. Integr. Plant Biol.* 59, 15–29. doi: 10.1111/jipb.12509

Koornneef M, Reuling G, Karssen CM. (1984). The isolation and characterization of abscisic acid–insensitive mutants of Arabidopsis thaliana. Physiol. Plant. 61, 377–383.

Kurepa J, Walker JM, Smalle J, Gosink MM, Davis SJ, Durham TL, et al. (2003). The small ubiquitn-like modifier (SUMO) protein modification system in Arabidopsis. J. Biol. Chem. 278, 6862–6872. doi: 10.1074/jbc.M209694200.

Kwak SH, Schiefelbein J. (2007). The role of the SCRAMBLED receptor-like kinase in patterning the Arabidopsis root epidermis. Dev. Biol. 302, 118–131 10.1016/j.ydbio.2006.09.009.

Kwak SH, Schiefelbein J. (2008). A feedback mechanism controlling SCRAMBLED receptor accumulation and cell-type pattern in Arabidopsis. Curr. Biol. 18, 1949-1954. doi:10.1016/j.cub.2008.10.064.

Kwak SH, Schiefelbein J. (2014). TRIPTYCHON, not CAPRICE, participates in feedback regulation of SCM expression in the Arabidopsis root epidermis. Plant Signal. Behav. 9, e973815. doi:10.4161/15592324.2014.973815.

Kwak SH, Shen R, Schiefelbein J. (2005). Positional signaling mediated by a receptor-like kinase in Arabidopsis. Science 307, 1111-1113. doi:10.1126/science.1105373.

Lang V, Palva ET. (1992). The expression of a rab-related gene rabl8 is included by abscisic acid during the cold acclimation process of Arabidopsis thaliana (L) Heynh. Plant Mo1 Biol20 951-962.

Lau OS, et al. (2018). Direct control of SPEECHLESS by PIF4 in the high-temperature response of stomatal development. Curr. Biol. 28, 1273–1280 e1273.

Lee J, Nam J, Park HC, Na G, Miura K, Jin JB, Yoo CY, Baek D, Kim DH, Jeong JC, et al. (2007). Salicylic acid-mediated innate immunity in Arabidopsis is regulated by SIZ1 SUMO E3 ligase. Plant J.

Lee MM, Schiefelbein J. (1999). WEREWOLF, a MYB-related protein in Arabidopsis, is a position-dependent regulator of epidermal cell patterning. Cell 99:473–483. https://doi.org/10.1016/S0092-8674(00)81536-6.

Leivar P, Monte E, Al-Sady B, Carle C, Storer A, Alonso JM, Ecker JR, Quail PH. (2008a). The Arabidopsis phytochrome-interacting factor PIF7, together with PIF3 and PIF4, regulates responses to prolonged red light by modulating phyB levels. Plant Cell 20, 337-352

Leivar P, Monte E, Oka Y, Liu T, Carle C, Castillon A, Huq E, Quail PH. (2008b) Multiple phytochrome-interacting bHLH transcription factors repress premature seedling photomorphogenesis in darkness. Curr Biol. 18(23): 1815-1823.

Leung J, Bouvier-Durand M, Morris PC, Guerrier D, Chefdor F, Giraudat J. (1994). Arabidopsis ABA-response gene ABI1: Features of a calcium-modulated protein phosphatase. Science 264, 1448–1452.

Leung J, Merlot S, Giraudat J. (1997). The Arabidopsis ABSCISIC ACID–INSENSITIVE 2 (ABI2) and ABI1 genes encode redundant protein phosphatases 2C involved in abscisic acid signal transduction. Plant Cell 9, 759–771.

Li D, Li Y, Zhang L, Wang X, Zhao Z, Tao Z, Wang J, Wang J, Lin M, Li X, Yang Y. (2014). Arabidopsis ABA receptor RCAR1/PYL9 interacts with an R2R3-type MYB transcription factor, AtMYB44. Int J Mol Sci. 13;15(5):8473-90.

Li K, Yu R, Fan LM, Wei N, Chen H, Deng XW. (2016). DELLA-mediated PIF degradation contributes to coordination of light and gibberellin signalling in Arabidopsis. Nat Commun 7: 11868.

Li W, Wang L, Sheng X, Yan C, Zhou R, Hang J, et al. (2013). Molecular basis for the selective and ABA-independent inhibition of PP2CA by PYL13. Cell Res. 23, 1369–1379. 10.1038/cr.2013.143.

Lim CW, Luan S, Lee SC. (2014). A prominent role for RCAR3-mediated ABA signaling in response to Pseudomonas syringae pv. tomato DC3000 infection in Arabidopsis. Plant Cell Physiol 55:1691–1703.

Lin DY, Huang YS, Jeng JC, Kuo HY, Chang CC, Chao TT, Ho CC, Chen YC, Lin TP, Fang TP, et al. (2006). Role of SUMO-interacting motif in Daxx SUMO modification, subnuclear localization, and repression of sumoylated transcription factors Mol. Cell, 24, pp. 341-354.

Liu, L., Jiang, Y., Zhang, X., Wang, X., Wang, Y., Han, Y., et al. (2017a). Two SUMO proteases SUMO PROTEASE RELATED TO FERTILITY1 and 2 are required for fertility in Arabidopsis. *Plant Physiol.* 175 (4), 1703–1719. doi: 10.1104/pp.17.00021

Locascio A, Blázquez MA, Alabadí D. (2013). Genomic analysis of DELLA protein activity. Plant Cell Physiol 54: 1229–1237.

Lois LM, Lima CD, Chua NH. (2003). Small ubiquitin-like modifier modulates abscisic acid signaling in Arabidopsis. Plant Cell 15 1347–1359.

Lois LM. (2010). Diversity of the SUMOylation machinery in plants. Biochem. Soc. Trans. 38, 60–64. doi: 10.1042/BST0380060.

Lorrain S, Allen T, Duek PD, Whitelam GC, Fankhauser C. (2008). Phytochrome-mediated inhibition of shade avoidance involves degradation of growth-promoting bHLH transcription factors. Plant J. 53, 312–323.

Ludwig SR, Habera LF, Dellaporta SL, Wessler SR. (1989). Lc, a member of the maize R gene family responsible for tissue-specific anthocyanin production, encodes a protein similar to transcriptional activators and contains the myc-homology region. Proc. Natl. Acad. Sci. USA. 861(1):7092–7096.

Ma Y, Szostkiewicz I, Korte A, Moes DI, Yang Y, Christmann A, Grill E. (2009). Regulators of PP2C phosphatase activity function as abscisic acid sensors. Science. 324:1064–1068.

Ma Z, Bielenberg DG, Brown KM, Lynch JP. (2001). Regulation of root hair density by phosphorus availability in Arabidopsis thaliana. Plant Cell Environ. 24, 459-467. doi:10.1046/j.1365-3040.2001.00695.x.

Masucci JD, Schiefelbein JW. (1996). Hormones act downstream of TTG and GL2 to promote root hair outgrowth during epidermis development in the Arabidopsis root. Plant Cell. 8:1505–1517.

Masucci JD, Rerie WG, Foreman DR, Zhang M, Galway ME, Marks MD, Schiefelbein JW (1996). The homeobox gene GLABRA2 is required for position-dependent cell differentiation in the root epidermis of Arabidopsis thaliana. Development 122: 1253–1260.

Masucci JD, Schiefelbein JW (1994). The rhd6 mutation of Arabidopsis thaliana alters root-hair initiation through an auxin- and ethylene-associated process. Plant Physiol 106:1335–1346. https://doi.org/10.1104/pp.106.4.1335.

Melcher K, Ng L M, Zhou X E, Soon F F, Xu Y, Suino-Powell K M, Park S Y, Weiner J J, Fujii H, Chinnusamy V, Kovach A, Li J, Wang Y, Li J, Peterson F C, Jensen D R, Yong E L, Volkman B F, Cutler S R, Zhu J K, Xu H E. (2009). A gate-latch-lock mechanism for hormone signalling by abscisic acid receptors Nature. Dec 3;462(7273):602-8. doi: 10.1038/nature08613.

Melotto M, et al. (2006). Plant stomata function in innate immunity against bacterial invasion. Cell 126, 969–980.

Meluh PB, Koshland D. (1995). Evidence that the MIF2 gene of Saccharomyces cerevisiae encodes a centromere protein with homology to the mammalian centromere protein CENP-C. Mol. Biol. Cell 6, 793–807. doi: 10.1091/mbc.6.7.793.

Menand B, Yi K, Jouannic S, Hoffmann L, Ryan E, Linstead P, et al. (2007). An ancient mechanism controls the development of cells with a rooting function in land plants. Science 316, 1477–1480.

Merlot S, Gosti F, Guerrier D, Vavasseur A, Giraudat J. (2001). The ABI1 and ABI2 protein phosphatases 2C act in a negative feedback regulatory loop of the abscisic acid signalling pathway. Plant J 25 295–303.

Meyer K, Leube MP, Grill E. (1994). A protein phosphatase 2C involved in ABA signal transduction in Arabidopsis thaliana. Science 264, 1452–1455.

Millar AH, Heazlewood JL, Giglione C, Holdsworth MJ, Bachmair A, Schulze WX. (2019). The scope, functions, and dynamics of posttranslational protein modifications. Annu. Rev. Plant Biol. 70, 119–151. doi: 10.1146/annurev-arplant-050718-100211.

Miller MJ, Vierstra RD. (2011). Mass spectrometric identification of SUMO substrates provides insights into heat stress-induced SUMOylation in plants. Plant. Signal. Behav. 6:130–133. doi: 10.4161/psb.6.1.14256.

Minty A, Dumont X, Kaghad M, Caput D. (2000). J. Biol. Chem. 275, 36316–36323.

Miura K, Hasegawa PM. (2009). Sumoylation and abscisic acid signaling. Plant Signal Behav. 4:1176–1178. doi: 10.4161/psb.4.12.1004.

Miura K, Rus A, Sharkhuu A, Yokoi S, Karthikeyan AS, Raghothama KG, Baek D, Koo YD, Jin JB, Bressan RA, et al. (2005). The Arabidopsis SUMO E3 ligase SIZ1 controls phosphate deficiency responses. Proc Natl Acad Sci USA 102: 7760–7765.

Miura K, Jin JB, Lee J, Yoo CY, Stirm V, Miura T, et al. (2007). SIZ1-mediated sumoylation of ICE1 controls CBF3/DREB1A expression and freezing tolerance in Arabidopsis. Plant Cell 19, 1403–1414. doi: 10.1105/tpc.106.048397.

Miyazono K, Miyakawa T, Sawano Y, Kubota K, Kang HJ, Asano A, Miyauchi Y. et al (2009). Structural basis of abscisic acid signalling. Nature, 462, 609–614.

Mizra JI, Olsen GM, Iversen TH, Maher EP. (1984). The growth and gravitropic responses of wild-type and auxin resistant mutants of Arabidopsis thaliana. Physiol. Plant. 1984;60:516–522.

Molendijk AJ, Bischoff F, Rajendrakumar CSV, Friml J, Braun M, Gilroy S, Palme K. (2001). Arabidopsis thaliana Rop GTPases are localized to tips of root hairs and control polar growth. EM BO J. 2001;20:2779–2788.

Monte E, Tepperman JM, Al-Sady B, Kaczorowski KA, Alonso JM, Ecker JR, Li X, Zhang Y, Quail PH. (2004). The phytochrome-interacting transcription factor, PIF3, acts early, selectively, and positively in light-induced chloroplast development. Proc. Natl. Acad. Sci. USA, 101: 16091-16098.

Morrell R, Sadanandom A. (2019a). Dealing with stress: A Review of plant SUMO proteases. Front. Plant. Sci. 10:1122. doi: 10.3389/fpls.2019.01122.

Morrell R, Sadanandom A. (2019b). Keeping Up With the Pathogens: The Role of SUMOylation in Plant Immunity 2019b SUMOylation and Ubiquitination: Current and Emerging Concepts (Edited by: Van G. Wilson). Caister Academic Press, U.K. Pages: 489-500.

Mukhopadhyay D, Dasso M. (2007). Modification in reverse: the SUMO proteases. Trends Biochem. Sci. 32, 286–295. doi: 10.1016/j.tibs.2007.05.002.

Mulkey T, Evans M, Kuzmanoff K. (1983). The kinetics of abscisic acid action on root growth and gravitropism. Planta 157:150–157. doi:10.1007/bf00393649.

Müller M, Schmidt W. (2004). Environmentally induced plasticity of root hair development in Arabidopsis. Plant Physiol. 134, 409-419. doi:10.1104/pp.103.029066.

Murase K. Hirano Y, Sun TP, Hakoshima T. (2008). Gibberellin-induced DELLA recognition by the gibberellin receptor GID1. Nature 456: 459–463.

Murre C, Schonleber McCaw P, Vässin H, Caudy M, Jan L Y, Jan L N, Cabrera C V, Buskin J N, Hauschka S D, Lassar A B, Weintraub H, Baltimore D. (1989). Interactions between heterologous helix-loop-helix proteins generate complexes that bind specifically to a common DNA sequence Cell, 58, pp. 537-544.

Murtas G, Reeves PH, Fu YF, Bancroft I, Dean C, Coupland G. (2003). A nuclear protease required for flowering-time regulation in Arabidopsis reduces the abundance of SMALL UBIQUITIN-RELATED MODIFIER conjugates. Plant Cell 15: 2308–2319.

Nagpal P, Walker LM, Young JC, Sonawala A, Timpte C, Estelle M, Reed JW. (2000). AXR2 encodes a member of the Aux/ IAA protein family. Plant Physiol. 123:563–573.

Nair SK, Burley SK. (2000). Recognizing DNA in the library. Nature 404: 715–, 717–718.

Nakashima K, Fujita Y, Kanamori N, Katagiri T, Umezawa T, Kidokoro S, Maruyama K, Yoshida T, lshiyama K, Kobayashi M, Shinozaki K, Yamaguchi-Shinozaki K. (2009). Three Arabidopsis SnRK2 protein kinases, SRK2D/SnRK2.2, SRK2E/SnRK2.6/OST1 and SRK2I/ SnRK2.3, involved in ABA signaling are essential for the control of seed development and dormancy. Plant Cell Physiol. 50:1345–1363.

Narang RA, Bruene A, Altmann T. (2000). Analysis of phosphate acquisition efficiency in different arabidopsis accessions. Plant Physiol. 124: 1786-1799.

Nelis S. (2014). An investigation into the role and mechanism of action of small ubiquitin-like modifier interacting motifs in Arabidopsis thaliana proteins (Unpublished PhD Thesis, University of Warwick).

Nemhauser J L, Hong F, Chory J. (2006). Different plant hormones regulate similar processes through largely nonoverlapping transcriptional responses. Cell, 126, 467–475.

Ng LM, Soon FF, Zhou XE, West GM, Kovach A, Suino-Powell KM, Chalmers MJ. et al (2011). Structural basis for basal activity and autoactivation of abscisic acid (ABA) signaling SnRK2 kinases. Proc. Natl. Acad. Sci. USA, 108, 21259–21264.

Novatchkova M, Budhiraja R, Coupland G, Eisenhaber F, Bachmair A. (2004). SUMO conjugation in plants. Planta 220, 1–8. doi: 10.1007/s00425-004-1370-y.

Novatchkova M, Tomanov K, Hofmann K, Stuible HP, Bachmair A. (2012). Update on sumoylation: defining core components of the plant SUMO conjugation system by phylogenetic comparison. New Phytol. 195, 23–31. doi: 10.1111/j.1469-8137.2012.04135.x.

Ohta M, Guo Y, Halfter U, Zhu JK. (2003). A novel domain in the protein kinase SOS2 mediates interaction with the protein phosphatase 2C ABI2. Proc. Natl. Acad. Sci. USA 100, 11771–11776.

Okada S, Nagabuchi M, Takamura Y, Nakagawa T, Shinmyozu K, Nakayama J, Tanaka K. (2009). Reconstitution of Arabidopsis thaliana SUMO Pathways in E. coli: Functional Evaluation of SUMO Machinery Proteins and Mapping of SUMOylation Sites by Mass Spectrometry. Plant Cell Physiol; 50 (6): 1049-1061. doi: 10.1093/pcp/pcp056.

Oldroyd GED, Dixon R. (2014). Biotechnological solutions to the nitrogen problem. Curr. Opin. Biotechnol. 26, 19-24. doi:10.1016/j.copbio.2013.08.006.

Oldroyd GED Downie JM. (2008). Coordinating nodule morphogenesis with rhizobial infection in legumes. Annu. Rev. Plant Biol. 59:519-546.

Orosa-Puente B, Leftley N, von Wangenheim D, Banda J, Srivastava AK, Hill K, et al. (2018). Root branching toward water involves posttranslational modification of transcription factor ARF7 . Science 362 (6421), 1407–1410. doi: 10.1126/science.aau3956.

Orosa B, Yates G, Verma V, Srivastava AK, Srivastava M, Campanaro A, et al. (2018). SUMO conjugation to the pattern recognition receptor FLS2 triggers intracellular signalling in plant innate immunity. Nat. Commun. 9 (1), 5185. doi: 10.1038/s41467-018-07696-8.

Orth K, Palmer LE, Bao ZQ, Stewart S, Rudolph AE, Bliska JB, et al. (1999). Inhibition of the mitogen-activated protein kinase kinase superfamily by a Yersinia effector. Science 285 (5435), 1920–1923. doi: 10.1126/science.285.5435.1920.

Orth K, Xu Z, Mudgett MB, Bao ZQ, Palmer LE, Bliska JB, et al. (2000). Disruption of signaling by Yersinia effector YopJ, a ubiquitin-like protein protease. Science 290, 1594–1597. doi: 10.1126/science.290.5496.1594.

Park S Y, Fung P, Nishimura N, Jensen D R, Fujii H, Zhao Y, Lumba S, Santiago J, Rodrigues A, Chow T F. (2009). Abscisic acid inhibits type 2C protein phosphatases via the PYR/PYL family of START proteins. Science; 324:1068–1071.

Peek J, Harvey C, Gray D, Rosenberg D, Kolla L, Levy-Myers R, Yin R, McMurry JL, Kerscher O. (2018). SUMO targeting of a stress-tolerant Ulp1 SUMO protease. PLoS ONE 13, e0191391.

Pemberton LMS, Tsai SL, Lovell PH, Harris PJ. (2001). Epidermal patterning in seedling roots of eudicotyledons. Ann. Bot. 87, 649-654. doi:10.1006/anbo.2001.1385.

Peng J, Carol P, Richards D E, King K E, Cowling R J et al. , (1997). The Arabidopsis GAI gene defines a signalling pathway that negatively regulates gibberellin responses. Genes Dev. 11: 3194–3205.

Pettersen EF. et al. (2004). UCSF Chimera−a visualization system for exploratory research and analysis. J. Comput. Chem. 25, 1605–1612.

Pitts RJ, Cernac A, Estelle M. (1998). Auxin and ethylene promote root hair elongation in Arabidopsis. Plant J 16:553–560. https://doi.org/10.1046/j.1365-313x.1998.00321.x.

Rawlings ND, Morton FR, Kok CY, Kong J, Barrett AJ. (2008). MEROPS: the peptidase database. Nucleic Acids Res. 36, D320–D325. doi: 10.1093/nar/gkm954.

Rerie WG, Feldmann KA, Marks MD. (1994). The GLABRA2 gene encodes a homeodomain protein required for normal trichome development in Arabidopsis. Genes Dev. 8:1388–1399.

Roden J, Eardley L, Hotson A, Cao Y, Mudgett MB. (2004). Characterization of the Xanthomonas AvrXv4 effector, a SUMO protease translocated into plant cells. Mol. Plant Microbe Interact. 17, 633–643. doi: 10.1094/MPMI.2004.17.6.633.

Rodríguez-Gacio Mdel C, Matilla-Vázquez M A, Matilla AJ. (2009). Seed dormancy and ABA signaling: the breakthrough goes on. Plant Signal. Behav. 4 1035–1049. 10.4161/psb.4.11.9902.

Rodriguez L, Gonzalez-Guzman M, Diaz M, Rodrigues A, Izquierdo-Garcia A C, Peirats-Llobet M, Fernandez M A, Antoni R, Fernandez D, Marquez J A, Mulet J M, Albert A, Rodriguez P L. (2014) C2-Domain Abscisic Acid-Related

Proteins Mediate the Interaction of PYR/PYL/RCAR Abscisic Acid Receptors with the Plasma Membrane and Regulate Abscisic Acid Sensitivity in Arabidopsis. Plant Cell. 26(12): 4802-4820.

Rodriguez PL, Benning G, Grill E. (1998). ABI2, a second protein phosphatase 2C involved in abscisic acid signal transduction in Arabidopsis. FEBS Lett. 421, 185–190.

Rubio S, Rodrigues A, Saez A, Dizon MB, Galle A, Kim TH, Santiago J. et al (2009) Triple loss of function of protein phosphatases type 2C leads to partial constitutive response to endogenous abscisic acid. Plant Physiol. 150, 1345–1355.

Rymen B, Kawamura A, Schäfer S, Breuer C, Iwase A, Shibata M, et al. (2017). ABA suppresses root hair growth via the obp4 transcriptional regulator. Plant Physiol. 173, 1710–1762.

Sadanandom A, Adam E, Orosa B, Viczian A, Klose C, Zhang C, et al. (2015). SUMOylation of phytochrome-B negatively regulates light-induced signaling in Arabidopsis thaliana. Proc. Natl. Acad. Sci. U.S.A. 112, 11108–11113. doi: 10.1073/pnas.1415260112.

Saez A, Apostolova N, Gonzalez-Guzman M, Gonzalez-Garcia MP, Nicolas C, Lorenzo O, Rodriguez PL. (2004). Gain-of-function and loss-of-function phenotypes of the protein phosphatase 2C HAB1 reveal its role as a negative regulator of abscisic acid signalling. Plant J. 37, 354–369.

Saez A, Robert N, Maktabi MH, Schroeder JI, Serrano R, Rodriguez PL. (2006). Enhancement of abscisic acid sensitivity and reduction of water consumption in Arabidopsis by combined inactivation of the protein phosphatases type 2C ABI1 and HAB1. Plant Physiol. 141, 1389–1399.

Saez A, Rodrigues A, Santiago J, Rubio S, Rodriguez PL. (2008). HAB1-SWI3B interaction reveals a link between abscisic acid signaling and putative SWI/SNF chromatin-remodeling complexes in Arabidopsis. Plant Cell, 20, 2972–2988.

Saitoh H, Hinchey J. (2000). Functional heterogeneity of small ubiquitin-related protein modifier SUMO-1 versus SUMO-2/3. J. Biol. Chem. 275, 6252–6258. doi: 10.1074/jbc.275.9.6252.

Sakuraba, Y. et al. (2014). Phytochrome-interacting transcription factors PIF4 and PIF5 induce leaf senescence in Arabidopsis. Nat. Commun. 5, 4636.

Salazar-Henao JE, Vélez-Bermúdez IC, Schmidt W. (2016). The regulation and plasticity of root hair patterning and morphogenesis. Development 143: 1848–1858.

Santiago J, Dupeuxb F, Betzb K, Antonia R, Gonzalez-Guzmana M, Rodrigueza L, Marquezb JA, Rodriguez PL. (2012). Structural insights into PYR/PYL/RCAR ABA receptors and PP2Cs. Plant Sci 182:3–11.

Santiago J, Rodrigues A, Saez A, Rubio S, Antoni R, Dupeux F, Park SY. et al. (2009). Modulation of drought resistance by the abscisic acid receptor PYL5 through inhibition of clade A PP2Cs. Plant J. 60, 575–588.

Saracco SA, Miller MJ, Kurepa J, Vierstra RD. (2007). Genetic analysis of sumoylation in Arabidopsis: Heat-induced conjugation of SUMO1 and 2 is essential. Plant Physiol. 145 (1), 119–134. doi: 10.1104/pp.107.102285.

Schellmann S, Schnittger A, Kirik V et al. (2002). TRIPTYCHON and CAPRICE mediate lateral inhibition during trichome and root hair patterning in Arabidopsis. EMBO J 21:5036–5046. https://doi.org/10.1093/emboj/cdf524.

Schiefelbein J W, Shipley A, Rowse P. (1992). Calcium influx at the tip of growing root-hair cells of Arabidopsis thaliana. Planta. 187:455–459.

Schiefelbein J, Huang L, Zheng X. (2014). Regulation of epidermal cell fate in Arabidopsis roots: the importance of multiple feedback loops. Front. Plant Sci. 5, 47. doi:10.3389/fpls.2014.00047.

Schmidt W, Schikora A. (2001). Different pathways are involved in phosphate and iron stress- induced alterations of root epidermal cell development. Plant Physiol. 125:2078–2084.

Schmidt W, Tittel J, Schikora A. (2000). Role of hormones in the induction of iron deficiency responses in Arabidopsis roots. Plant Physiol. 122: 1109-1118.

Schulz S, Chachami G, Kozaczkiewicz L, Winter U, Stankovic-Valentin N, Haas P, et al. (2012). Ubiquitin-specific protease-like 1 (USPL1) is a SUMO isopeptidase with essential, non-catalytic functions. EMBO Rep. 13, 930–938. doi: 10.1038/embor.2012.125.

Schwechheimer C. (2012). Gibberellin signaling in plants—the extended version. Front. Plant Sci. 2:107.

Shin EJ, Shin HM, Nam E, Kim WS, Kim JH, Oh BH, et al. (2012). DeSUMOylating isopeptidase: a second class of SUMO protease. EMBO Rep. 13, 339–346. doi: 10.1038/embor.2012.3.

Shinozawa A, Otake R, Takezawa D, Umezawa T, Komatsu K, Tanaka K, Amagai A, Ishikawa S, Hara Y, Kamisugi Y, Cuming AC, Hori K, Ohta H, Takahashi F, Shinozaki K, Hayashi T, Taji T, Sakata Y. (2019). SnRK2 protein kinases represent an ancient system in plants for adaptation to a terrestrial environment. CommunBiol. 2:1–13.

Sievers F, Wilm A, Dineen D, Gibson TJ, Karplus K, Li W, Higgins DG. (2011). Fast, scalable generation of high-quality protein multiple sequence alignments using Clustal Omega. Mol. Syst. Biol. 7(1):539. doi: 10.1038/msb.2011.75.

Silverstone A L, Ciampaglio C N, Sun T-P. (1998). The Arabidopsis RGA gene encodes a transcriptional regulator repressing the gibberellin signal transduction pathway. Plant Cell 10: 155–169.

Simon M, Lee MM, Lin Y, Gish L, Schiefelbein J. (2007). Distinct and overlapping roles of single-repeat MYB genes in root epidermal patterning. Dev Biol. 311:566–78.

Son GH, Park BS, Song JT, Seo HS. (2014). FLC-mediated flowering repression is positively regulated by sumoylation. J. Exp. Bot. 65, 339–351. doi: 10.1093/jxb/ert383.

Song J, Durrin LK, Wilkinson TA, Krontiris TG, Chen Y. (2004). Identification of a SUMO-binding motif that recognizes SUMO-modified proteins. Proc Natl Acad Sci USA 101: 14373–14378.

Song L, Yu H, Dong J, Che X, Jiao Y, Liu D. (2016). The molecular mechanism of ethylene-mediated root hair development induced by phosphate starvation. PLoS Genet. 12:e1006194.

Song Y. et al. (2014). Age-triggered and dark-induced leaf senescence require the bHLH transcription factors PIF3, 4, and 5. Mol. Plant 7, 1776–1787.

Soon FF, Ng LM, Zhou XE, West GM, Kovach A, Tan MH, Suino-Powell KM. et al. (2012). Molecular mimicry regulates ABA signaling by SnRK2 kinases and PP2C phosphatases. Science, 335, 85–88.

Srivastava AK, Zhang C, Caine RS, Gray J, Sadanandom A. (2017). Rice SUMO protease Overly Tolerant to Salt 1 targets the transcription factor, Osb ZIP 23 to promote drought tolerance in rice. Plant J 92(6):1031–1043.

Srivastava M, Srivastava AK, Orosa-Puente B, Campanaro A, Zhang C, Sadanandom A. (2020). SUMO conjugation to BZR1 enables brassinosteroid signaling to integrate environmental cues to shape plant growth. Curr. Biol. 30, 1410–1423.e1413. 10.1016/j.cub.2020.01.089.

Srivastava A, Orosa B, Singh P, et al. (2018). SUMO Suppresses the Activity of the Jasmonic Acid Receptor CORONATINE INSENSITIVE 1. Plant Cell. 30 (9), 2099–2115. doi: 10.1105/tpc.18.00036.

Suh HY, Kim JH, Woo J S, Ku B, Shin EJ, Yun Y, et al. (2012). Crystal structure of DeSI-1, a novel deSUMOylase belonging to a putative isopeptidase superfamily. Proteins 80, 2099–2104. doi: 10.1002/prot.24093.

Sun TP. (2011). The molecular mechanism and evolution of the GA-GID1-DELLA signaling module in plants. Curr. Biol. 21: R338–R345.

Sun J, Qi L, Li Y, Zhai Q, Li C. (2013). PIF4 and PIF5 transcription factors link blue light and auxin to regulate the phototropic response in Arabidopsis. Plant Cell 25, 2102–2114.

Takahashi Y, Zhang J, Hsu PK, Ceciliato PHO, Zhang L, Dubeaux G, Munemasa S, Ge C, Zhao Y, Hauser F, et al. (2020). MAP3Kinase-dependent SnRK2-kinase activation is required for abscisic acid signal transduction and rapid osmotic stress response. Nat Commun 11, 12.

Tanimoto M, Roberts K, Dolan L. (1995). Ethylene is a positive regulator of root-hair development in Arabidopsis thaliana. Plant J. 8:943–948.

Tomanov K, Zeschmann A, Hermkes R, Eifler K, Ziba I, Grieco M, Novatchkova M, Hofmann K, Hesse H, Bachmair A (2014). *Arabidopsis* PIAL1 and 2 promote SUMO chain formation as E4-type SUMO ligases and are involved in stress responses and sulfur metabolism. *Plant Cell* 26, 4547–4560. doi: 10.1105/tpc.114.131300

Ton J, Flors V, Mauch-Mani B. (2009). The multifaceted role of ABA in disease resistance. Plant cell, Jun; 14(6): 310-317.

Ueguchi-Tanaka M, Ashikari M, Nakajima M, Itoh H, Katoh E, Kobayashi M, Chow TY, Hsing YI, Kitano H, Yamaguchi I, Matsuoka M. (2005). GIBBERELLIN INSENSITIVE DWARF1 encodes a soluble receptor for gibberellin. Nature 437: 693–698.

Underwood W, Melotto M, He SY. (2007). Role of plant stomata in bacterial invasion, Cell. Microbiol., vol. 9 (pg. 1621-1629).

Vahisalu T, Kollist H, Wang YF, Nishimura N, Chan WY, Valerio G, Lamminmaki A, Brosche M, Moldau H, Desikan R, Schroeder JI, Kangasjarvi J. (2008). SLAC1 is required for plant guard cell S type anion channel function in stomatal signalling. Nature. 452:487–491.

van den Burg HA, Kini RK, Schuurink RC, Takken FL. (2010). Arabidopsis small ubiquitin-like modifier paralogs have distinct functions in development and defense. Plant Cell 22, 1998–2016. doi: 10.1105/tpc.109.070961.

Van Hengel AJ, Barber C, Roberts K. (2004). The expression patterns of arabinogalactan-protein AtAGP30 and GLABRA2 reveal a role for abscisic acid in the early stages of root epidermal patterning. The Plant Journal: for Cell and Molecular Biology 39:70–83. doi: 10.1111/j.1365-313X.2004.02104.

Verma V, Srivastava A K, Gough C, Campanaro A, Srivastava M, Morrell R, Joyce J, Bailey M, Zhang C, Krysan P J, Sadanandom A. (2021). SUMO enables substrate selectivity by mitogen-activated protein kinases to regulate immunity in plants. PNAS 9;118(10):e2021351118. doi: 10.1073/pnas.2021351118.

Very AA, Davies JM. (2000). Hyperpolarization-activated calcium channels at the tip of Arabidopsis root hairs. Proc. Natl. Acad. Sci. USA. 97:9801–9806.

Villajuana-Bonequi M, Elrouby N, Nordström K, Griebel T, Bachmair A, Coupland G. (2014). Elevated salicylic acid levels conferred by increased expression of ISOCHORISMATE SYNTHASE 1 contribute to hyperaccumulation of SUMO1 conjugates in the Arabidopsis mutant early in short days 4. Plant J. 79, 206–219. doi: 10.1111/tpj.12549.

Vishwakarma K, Upadhyay N, Kumar N, Yadav G, Singh J, Mishra RK, et al. (2017). Abscisic acid signaling and abiotic stress tolerance in plants: a review on current knowledge and future prospects. Front. Plant Sci. 8:161. 10.3389/fpls.2017.00161.

Wada T, Tachibana T, Shimura Y, Okada K. (1997). Epidermal cell differentiation in Arabidopsis determined by a Myb homolog, CPC. Science. 277:1113–1116.

Walker AR, Davison PA, Bolognesi-Winfield AC, James CM, Srinivasan N, Blundell TL, Esch JJ, Marks MD, Gray JC. (1999). The TRANSPARENT TESTA GLABRA1 locus, which regulates trichome differentiation and anthocyanin biosynthesis in Arabidopsis, encodes a WD40 repeat protein. Plant Cell. 11:1337–1349.

Walsh C. The role of SUMOylation in the Auxin Response Pathway. (Unpublished PhD Thesis, University of Durham).

Wang F, Liu Y, Lai J, Yang C, Shi Y. Han D, Wu Y, Ye W, Yang H, Li G, et al. (2020). SUMOylation stabilizes the transcription factor DREB2A to improve plant thermotolerance. Plant. Physiol. 183:41–50. doi: 10.1104/pp.20.00080.

Wang H, Makeen K, Yan Y, Cao Y, Sun S, Xu G. (2011). OsSIZ1 regulates the vegetative growth and reproductive development in rice. Plant Mol. Biol. Rep.29: 411–417.

Wang Q, Qu GP, Kong X, Yan Y, Li J, Jin JB. (2018). Arabidopsis SUMO protease ASP1 positively regulates ABA signaling during early seedling development. J. Integr. Plant Biol. 60 (10), 924–937. doi: 10.1111/jipb.12669.

Warton K, Foster NC, Gold WA, Stanley KK. (2004). A novel gene family induced by acute inflammation in endothelial cells. Gene 342, 85–95.

Wilkinson KA, Henley JM. (2010). Mechanisms, regulation and consequences of protein SUMOylation. Biochem J 428(2): 133-145.

Willige BC, Ghosh S, Nill C, Zourelidou M, Dohmann EM, Maier A, Schwechheimer C. (2007). The DELLA domain of GA INSENSITIVE mediates the interaction with the GA INSENSITIVE DWARF1A gibberellin receptor of Arabidopsis. Plant Cell 19: 1209–1220.

Wilson A, Pickett FB, Turner JC, Estelle M. (1990). A dominant mutation in Arabidopsis confers resistance to auxin, ethylene, and abscisic acid. Mol. Gen. Genet. 222:377–383.

Winter D, Vinegar B, Nahal H, Ammar R, Wilson GV, Provart NJ. (2007). An "Electronic Fluorescent Pictograph" browser for exploring and analyzing large-scale biological data sets. PLoS One 2:e718. 10.1371/journal.pone.0000718.

Wu Q, Zhang X, Peirats-Llobet M, Belda-Palazon B, Wang X, Cui S, Yu X, Rodriguez PL, An C. (2016). Ubiquitin Ligases RGLG1 and RGLG5 regulate abscisic acid signaling by controlling the turnover of phosphatase PP2CA. Plant Cell, 28, 2178–2196.

Wymer CL, Bibikova TN, Gilroy S. (1997). Cytoplasmic free calcium distributions during the development of root hairs of Arabidopsis thaliana. Plant J. 12:427–439.

Xing L, Zhao Y, Gao J, Xiang C, Zhu JK. (2016). The ABA receptor PYL9 together with PYL8 plays an important role in regulating lateral root growth. Sci Rep 6: 27177.

Xu H, Liu Q, Yao T, Fu X. (2014). Shedding light on integrative GA signaling. Curr Opin Plant Biol 21: 89–95.

Yamaguchi-Shinozaki K, Shinozaki K. (1993). Characterization of the expression of a desiccation-responsive rd29 gene of Arabidopsis thaliana and analysis of its promoter in transgenic plants. Mol Gen Genet 236(2):331–340.

YAN X, LIAO H, BEEBE SE, BLAIR MW, LYNCH JP. (2004) QTL mapping of root hair and acid exudation traits and their relationship to phosphorus uptake in common bean. Plant and Soil, v.265, p.17-29.

Yang SH, Sharrocks AD. (2010). The SUMO E3 ligase activity of Pc2 is coordinated through a SUMO interaction motif Mol. Cell. Biol., 30, pp. 2193-2205.

Yang Y, Sulpice R, Himmelbach A, Meinhard M, Christmann A, Grill E. (2006) Fibrillin expression is regulated by abscisic acid response regulators and is involved in abscisic acid-mediated photoprotection. Proc. Natl Acad. Sci. USA, 103, 6061–6066.

Yates G, Srivastava AK, Sadanandom A. (2016). SUMO proteases: Uncovering the roles of deSUMOylation in plants. J. Exp. Bot. 67 (9), 2541–2548. doi: 10.1093/jxb/erw092.

Yi K, Menand B, Bell E, Dolan L. (2010). A basic helix-loop-helix transcription factor controls cell growth and size in root hairs. Nat Genet 42:264–267. https://doi.org/10.1038/ng.529.

Yin P, Fan H, Hao Q, Yuan X, Wu D, Pang Y, Yan C, Li W, Wang J, Yan N. (2009). Structural insights into the mechanism of abscisic acid signaling by PYL proteins. Nat. Struct. Mol. Biol. 16, 1230–1236.

Yoshida T, Nishimura N, Kitahata N, Kuromori T, lto T, Asami T, Shinozaki K, Hirayama T. (2006). ABA-hypersensitive germination3 encodes a protein phosphatase 2C (AtPP2CA) that strongly regulates abscisic acid signaling during germination among Arabidopsis protein phosphatase 2Cs. Plant Physiol. 140:115–126.

Yu Z, Zhang D, Xu Y, Jin S, Zhang L, Zhang S, Yang G, Huang J, Yan K, Wu C, Zheng C. (2019). CEPR2 phosphorylates and accelerates the degradation of PYR/PYLs in Arabidopsis. J Exp Bot. 70(19): 5457-5469.

Yunta C, Martinez-Ripoll M, Albert A. (2011). SnRK2.6/OST1 from Arabidopsis thaliana: cloning, expression, purification, crystallization and preliminary X-ray analysis of K50N and D160A mutants. Acta Crystallogr F Struct Biol Crystallizat Commun. 67:364–368.

Zeevaart JAD, Creelman RA. (1988). Metabolism and physiology of abscisic acid. Annu Rev Plant Physiol Plant Mol Biol 39 439–473.

Zentella R, Hu J, Hsieh WP, Matsumoto PA, Dawdy A, Barnhill B, et al. (2016). O-GlcNAcylation of master growth repressor DELLA by SECRET AGENT modulates multiple signaling pathways in Arabidopsis. Genes Dev. 30: 164–176.

Zentella R, Sui N, Barnhill B, Hsieh WP, Hu J, Shabanowitz J, et al. (2017). The Arabidopsis O-fucosyltransferase SPINDLY activates nuclear growth repressor DELLA. Nat. Chem. Biol. 13: 479–485.

Zhang S, Zhuang K, Wang S, Lv J, Ma N, Meng Q. (2017). A novel tomato SUMO E3 ligase, SlSIZ1, confers drought tolerance in transgenic tobacco. J. Integr. Plant Biol. 59 102–117. 10.1111/jipb.12514.

Zhang F, Gonzalez A, Zhao M, Payne CT, Lloyd A. (2003). A network of redundant bHLH proteins functions in all TTG1-dependent pathways of Arabidopsis. Development 130, 4859–4869.

Zhang S, Huang L, Yan A, Liu Y, Liu B, Yu C, et al. (2016). Multiple phytohormones promote root hair elongation by regulating a similar set of genes in the root epidermis in Arabidopsis. J. Exp. Bot. 67, 6363–6372. doi: 10.1093/jxb/erw400.

Zhang ZL, Ogawa M, Fleet CM, Zentella R, Hu J, Heo JO, et al. (2011). Scarecrow-like 3 promotes gibberellin signaling by antagonizing master growth repressor DELLA in Arabidopsis. Proc. Natl. Acad. Sci. U.S.A. 108, 2160–2165. doi: 10.1073/pnas.1012232108.

Zhao Y, Chan Z, Xing L, Liu X, Hou YJ, Chinnusamy V, et al. (2013). The unique mode of action of a divergent member of the ABA-receptor protein family in ABA and stress signaling. Cell Res. 23, 1380–1395. 10.1038/cr.2013.149.

Zhao Y, Xing L, Wang X, Hou YJ, Gao J, Wang P, et al. (2014). The ABA receptor PYL8 promotes lateral root growth by enhancing MYB77-dependent transcription of auxin-responsive genes. Sci. Signal. 7, ra53. 10.1126/scisignal.200505.

Zhao Y. et al. (2018). Arabidopsis duodecuple mutant of PYL ABA receptors reveals PYL repression of ABA-independent SnRK2 activity. Cell Rep. 23, 3340–3351. e5.

Zheng Y, Schumaker KS, Guo Y. (2012). Sumoylation of transcription factor MYB30 by the small ubiquitin-like modifier E3 ligase SIZ1 mediates abscisic acid response in Arabidopsis thaliana. Proc Natl Acad Sci USA. 109:12822–12827. doi: 10.1073/pnas.1202630109

Zhu C, Gan L, Shen Z, Xia K. (2006). Interactions between jasmonates and ethylene in the regulation of root hair development in Arabidopsis. Journal of Experimental Botany 57:1299–1308. doi: 10.1093/jxb/erj103.